THESIS REPORT

Master's Degree

Development of an Optical-Based Vision System for Surface Finish Assessment Using Fractal Geometry

by M.J. Jung IV
Advisor: G.M. Zhang

M.S. 96 -8

Sponsored by
the National Science Foundation
Engineering Research Center Program,
the University of Maryland,
Harvard University,
and Industry

Abstract

Title of Thesis:	Development of an Optical-Based Vision System for Surface Finish Assessment Using Fractal Geometry
Name of degree candidate:	Melvin Joseph Jung IV
Degree and Year:	Master of Science, 1996
Thesis directed by:	Dr. Guangming Zhang, Associate Professor, Department of Mechanical Engineering, and Institute for Systems Research

Assessment of finish quality of machined components has been a major concern of the machine tool industry in an effort to improve quality and productivity. The research presented in this thesis focuses on assessing the finish quality of machined parts. A new approach is formulated to apply fractal geometry to characterize the surface texture formed during machining.

Research efforts have been devoted to understanding the need and importance of moving fractal geometry from a purely mathematical domain into a manufacturing domain. In addition to using fractal dimension, a second fractal parameter called lacunarity is introduced to characterize the space filling, or the slope distribution of surface texture. This addition represents a unique contribution of this thesis research for improving the precision of surface characterization.

A vision system, in which optical devices are employed, is designed and built to implement the surface finish assessment using fractal geometry. The developed prototype serves as a testbed for this thesis research. The testbed employs a CCD (Charged Coupled Device) camera to capture the image of a machined surface. A computer software tool is developed and implemented to process the image data and extract information characterizing the surface condition by using the proposed fractal geometry approach. The system provides 3-D visualization of surface topography and displays numerical values of the surface characterization indices including the fractal dimension and the lacunarity for the purpose of performing diagnostics.

Special efforts have been made to investigate effects of the reflectivity of part material on the optical area-based surface characterization technique. Significant findings include the effectiveness of using light filters in image data acquisition and the utilization of light filters to facilitate the system calibration for machining a variety of materials through compensation.

Development of an Optical-Based Vision System for Surface Finish Assessment Using Fractal Geometry

by

Melvin Joseph Jung IV

Thesis submitted to the Faculty of the Graduate School
of The University of Maryland in partial fulfillment
of the requirement for the degree of
Master of Science
1996

Advisory Committee:

Associate Professor Guangming Zhang, Chairman/Advisor
Assistant Professor Balakumar Balachandran
Associate Professor K. J. Ray Liu

Acknowledgments

I am indebted to my thesis advisor, Dr. Guangming Zhang, for his never ending guidance and support. Without Dr. Zhang's suggestions and dedication this work would not have been possible. I feel extremely honored to have been able to work with Dr. Zhang at the Advanced Design and Manufacturing Laboratory, which has provided me with untold benefits.

I would like to extend my sincere gratitude to Dr. Liu and Dr. Balachandran for serving on my thesis committee and providing suggestions for improvements in this research. This work has been conducted under the support of the Mechanical Engineering Department and the Institute for Systems Research. Sincere appreciation also goes to Thompson Industries for kindly supplying a powerslide and controller for the system.

I am grateful to have had the opportunity to be a Graduate Advisor for an ME480 Senior Experimentation Project. This has given me the opportunity to work with undergraduate students, Allen Au, Michael Johnson, Paul Lee, Jonathan White and Kevin Wooden, and I would like to thank them for their help with performing experiments. I would also like to thank Zhen Ding, a Computer Science student, for his help in converting the Vision Program to a Microsoft Windows based program.

Finally, I would like to thank the following graduate students in the Advanced Design and Manufacturing Laboratory for their support and encouragement: Charles Clinton, Adrian Hood, Lenox Job, DT Le, Huynh Luu, Stanley Ng, Mark Richardson, and Rena Surana.

Table of Contents

List of Figures vii

List of Tables xii

1 Introduction....1

1.1 Requirement for Surface Finish Quality Assessment....1

1.2 Scope of Thesis....3

1.3 Organization of Thesis....4

2 Survey of Salient Literature....7

2.1 Surface Texture Parameter....7

2.2 Traditional Methods of Surface Characterization....10

2.2.1 Surface Roughness Measurements and Applications....10

2.2.2 Traditional Approach for Characterization of Rough Surfaces....11

2.2.3 Traditional Surface Characterization System....13

2.3 Utilization of Digitization for Statistical Parameters....15

2.3.1 Shape Parameters Machining....16

2.3.2 Hybrid Parameters Machining....16

2.3.3 Statistical Functions Machining....16

2.4 Approach Using Fractal Geometry....18

2.4.1 Fractal Dimension....20

2.4.2 Methods of Determining Fractal Dimension....21
2.4.3 Previous Work in Surface Characterization....22
2.4.4 Limitations of Fractal Dimension....23
2.4.5 Three Dimensional Non-Contact Optical Method....24
2.5 Current Status of Research....25
2.5.1 Scattering Theory of Electromagnetic Waves....25
2.5.1.1 Beckmann's Scattering Theory....25
2.5.1.2 Surface Facet Model....28
3 Fractal Geometry Approach....30
3.1 Algorithms Formulation....30
3.1.1 Fractal Dimension....30
3.1.2 Lacunarity....33
3.2 Feasibility Study/ Preliminary Experiments....34
3.2.1 Simulation and Evaluation of Surfaces with Fractal Dimension....34
3.2.2 Preliminary Experiments with System Correlations....36
3.2.3 Case Study....38
3.2.4 Simulation and Evaluation of Surfaces with Lacunarity....39
3.3 Factorial Design Experiment....49
3.4 Summary Experiment....50
4 Design and Implementation of Optical-Based Vision System....52

4.1 Theory of Vision System Based on Scattering Theory.....52

4.2 Components of Surface Monitoring and Characterization System.....55

4.3 Description of Off-Line System.....58

4.3.1 Height Adjustment System.....59

4.3.2 Light Enclosure.....60

4.3.3 Selection of Light Source.....62

4.3.4 Design of Enclosure.....66

4.3.4.1 Light Enclosures: Basic Lighting Techniques.....66

4.3.5 Powerslide.....74

4.3.6 Reasoning Behind Off-Line System.....75

4.4 Software.....76

5 Experimental Setup and Results.....78

5.1 Experimental Procedure.....78

5.2 Factors Affecting First System.....79

5.3 Factors Affecting New System.....82

5.4 Factors Affecting Correlation of System.....85

5.4.1 Machine Tool.....86

5.4.2 Magnification.....87

5.4.3 Filters.....89

5.4.4 Material.....90

5.4.5 Decreased Roughness Range.....95

5.5 Repeatability....99

5.6 Alternate Parameters....99

5.7 Velocity Tests....100

5.8 Experiments with Lacunarity on Machined Surfaces....103

5.8.1 Evaluation of Machined Surfaces with Lacunarity....102

5.8.2 Reconstruction of Surfaces Using Fractal Dimension and Lacunarity....106

6 Conclusions and Future Work....109

6.1 Conclusions....109

6.2 Future Work....111

Appendix A Experimental Data....114

Appendix B Hardware Specifications....145

Appendix C Surface Assessment Devices....146

Appendix D Software Listing....152

References....180

List of Figures

Figure 2.1 Surface Texture....7

Figure 2.2 Surface Profile....11

Figure 2.3 Stylus Profilometer....13

Figure 2.4 Soft Surface Showing Scratches from Profilometer....14

Figure 2.5 Koch Curve....20

Figure 2.6 Scattering Geometry....26

Figure 2.7 Transition from Specular Reflection to Diffuse Scattering....28

Figure 2.8 Surface Facet Model....29

Figure 3.1 Box Size vs. Number of Boxes....31

Figure 3.2 Histogram of Machined Surface.... 32

Figure 3.3 Lacunarity....34

Figure 3.4 Fractal Dimensions From Generated Surfaces....36

(a) Sin Function....35

(b) Radial Sin Function....35

(c) Sin and Cos Function.... 35

(d) Random Function....35

(e) All Surfaces....36

Figure 3.5 Surface Plots With Same Ra But Different FD1....37

(a) Surface Plot....37

(b) Surface Plot....37

Figure 3.6 Correlation of 30 Samples....38

Figure 3.7 Plots of Surfaces Having Same FD But Different Lacunarity....40

(a) Sin Generated Surface.... 40

(b) Radial Sin Surface....40

(c) Sin and Cos Surface....40

(d) Random Surface....40

Figure 3.8 Frequency vs. Lacunarity of a Periodic Function....44

Figure 3.9 Calculation of Lac for Sin Function with Added Noise....45

Figure 3.10 Calculation of Lac for Saw Tooth Function with Added Noise....45

Figure 3.11 Two Surfaces with Same Ra and FD1....46

(a) Original Surface Plot....46

(b) Surface Plot of Re-distributed Points....46

Figure 3.12 High FD1, Low Lac(3)....47

Figure 3.13 Low FD1, High Lac(3)....47

Figure 3.14 High FD1, Low Lac(3)....48

Figure 3.15 Low FD1, Low Lac(3)....48

Figure 3.16 Factorial Design....50

Figure 4.1 Picture of Entire Off-Line Setup....55

Figure 4.2 CAD Model of Components for Off-line System....56

Figure 4.3 Picture of Off-line Hardware....57

Figure 4.4 Camera Height Adjustment System....59
Figure 4.5 Camera Location on the Adjustment System....60
Figure 4.6 Enclosure with Top....61
Figure 4.7 Enclosure without Top....61
Figure 4.8 Picture of Light Enclosure....62
Figure 4.9 Diffuse Front Lighting....67
Figure 4.10 Directional Front Illumination....67
Figure 4.11 Light Tent....68
Figure 4.12 Collimated Back Lighting....68
Figure 4.13 Dark Field Illumination....69
Figure 4.14 Diffused Backlighting....69
Figure 4.15 Low Angle Illumination....70
Figure 4.16 Polarized Front Illumination....70
Figure 4.17 Polarized Backlighting....71
Figure 4.18 Strobed Illumination....71
Figure 4.19 Structured Light....72
Figure 4.20 Coaxial Lighting....73
Figure 4.21 Filters....74
Figure 4.22 Base....75
Figure 5.1 Surface Plot of Roughness Values....85
Figure 5.2 FD1 vs. Ra Two Flutes Endmill....87

Figure 5.3 FD1 vs. Ra Four Flutes Endmill....87

Figure 5.4 FD1 vs. Ra Magnification = 15x....88

Figure 5.5 Reflectance of Light from Aluminum....90

Figure 5.6 FD1 vs. Ra White Diffuser Filters....90

Figure 5.7 Correlation for Copper Samples....93

Figure 5.8 Reflection of Light from Copper....94

Figure 5.9 Cu and Al with Red and White Filters....95

Figure 5.10 Model for Selecting Machining Conditions....96

Figure 5.11 Surface Plot of Roughness Values....97

Figure 5.12 Correlation....98

Figure 5.13 Feed = 0.02 in/min....100

Figure 5.14 Feed = 0.1 in/min....101

Figure 5.15 Feed = 1.0 in/min....101

Figure 5.16 Feed = 5.0 in/min....101

Figure 5.17 Feed = 10.0 in/min....101

Figure 5.18 Feed = 25 in/min....102

Figure 5.19 Feed = 50 in/min....102

Figure 5.20 Feed = 80 in/min....102

Figure 5.21 Frequency vs. Lacunarity of Machined Surfaces....103

Figure 5.22 Speed=1000 rpm, Feed=1.2 in/min, Lac=-0.00857,
Lac(3)=0.2879....103

Figure 5.23 Speed=1000 rpm, Feed=2.4 in/min, Lac=0.010375, Lac(3)=0.2988 104
Figure 5.24 Speed=1000 rpm, Feed=4.0 in/min, Lac=0.02085, Lac(3)=0.2776 104
Figure 5.25 Speed=1000 rpm, Feed=7.0 in/min, Lac=0.0248, Lac(3)=0.3178 104
Figure 5.26 Speed=1000 rpm, Feed=10.0 in/min, Lac=0.0453, Lac(3)=0.3389 105
Figure 5.27 Speed=1000 RPM, Feed=15.7 in/min, Lac=0.0419, Lac(3)=0.3084 105
Figure 5.28 Speed=1000 RPM, Feed=19.7 in/min, Lac=0.04365, Lac(3)=0.3377 105
Figure 5.29 Lac = .01375 FD1 = 2.79 107
Figure 5.30 1000 rpm, 2.4 in/min 107
Figure 5.31 Lac = .04485, FD1 = 2.82 107
Figure 5.32 1000 rpm, 7.0 in/min 108

List of Tables

Table 3.1 Test Conditions....49

Table 5.1 Variables....79

Table 5.2 Factorial Design Grid....80

Table 5.3 Significant Effects....80

Table 5.4 Variables....83

Table 5.5 Design Matrix....83

Table 5.6 Two Flutes Endmill Ra Measurements....86

Table 5.7 Four Flutes Endmill Ra Measurements....86

Table 5.8 Correlation Coefficients....88

Table 5.9 Correlation Coefficients....89

Table 5.10 Ra Values for Copper....91

Table 5.11 Slope and Intercept Values of Correlation Curves for Aluminum....94

Table 5.12 Aluminum Samples with Filter....95

Table 5.13 Roughness Values....97

Table 5.14 Correlation Coefficients....98

Table 5.15 Repeatability Error....99

Chapter 1

Introduction

1.1 Requirement for Surface Finish Quality Assessment

American companies must be able to manufacture products of superior quality at competitive costs to compete effectively in the global economy. The ability to produce quality products hinges on four key factors: modeling of process form and precision levels, design tolerancing of parts and products, selecting production processes that match part specifications, and applying quantitative measurement methods for inspection and process control. The research conducted in this thesis emphasizes the assessment of surface finish quality of machined parts.

The surfaces of a component are important. They affect product performance, assembly, fit, and esthetic appeal that a product must present to a potential customer. Surface quality is mainly determined by the production process that created the surface texture. Surface roughness, or texture, is the "fingerprint" left on a machined workpiece after a manufacturing process. Inspection and mensuration of surface roughness, to ensure that the finish quality of a machined part meets specifications, have been essential parts of the manufacturing practice. As computer integrated manufacturing matures, sensing devices will be used increasingly to enhance production automation. To assure product quality in such highly automated manufacturing environments, on-line and in-process monitoring of surface roughness during machining has become a focused area to certify production

automation. In this research, the vision system is designed for adaptation to an in-process device.

Traditional methods for controlling finish quality rely on off-line measurements. Most of these measurements use the stylus instrumentation. In general, profiles, or traces, are taken from a machined surface of the machined part. A decision on surface quality is made based on the measured data, e.g., roughness average values, RMS values, and peak-to-valley values. However, these methods are not applicable in on-line monitoring systems because they require direct contact with the surface. They limit measurement speed, require navigation around surface discontinuities, and degrade measurement accuracy in the presence of environmental vibration. As mentioned later, the stylus can degrade work surfaces.

Research activities in developing systems to perform on-line extraction of information from remote sensing devices have received great attention in recent years. Most of them concentrate on optical measurement methods. The non-contact measurement method proposed by Jansson[1] used laser-based profilometry devices, achieving much faster measurement speeds than stylus profilometers. Gilsonn and Vorburger presented a summary report on roughness measurements of industrial surfaces using optical methods. They categorized all optical measurement methods into profiling and area techniques. They pointed out that profiling techniques suffered from an inability to characterize the entire surface topography. However, area-scattering techniques suffered from high variations in measurements[2].

1.2 Scope of Thesis

In this research, a new approach is formulated to apply fractal geometry to characterize the surface texture formed during machining. Optical devices are incorporated in developing a vision system capable of evaluating the finish quality.

There are two options in the assessment of the surface finish: perform an in-process measurement of the surface roughness or machine the part and then assess the roughness off-line. An in-process measurement is desirable to increase productivity because it avoids producing defects in the first place, instead of identifying the defects after manufacture of the products. If the on-line method is to be used, the main requirements are speed of data acquisition, analysis of the acquired data, and immediate insertion of feedback data into the process. This feedback from the in-process system can be used to alter machining conditions in order to keep the surface finish within required tolerance limits.

This thesis presents a vision system capable of off-line surface analysis. The system's speed of data acquisition and resistance to vibration makes it adaptable to an on-line monitoring system. In this method, an approach based on optical area-scattering is employed. In this technique, two new performance indices using fractal geometry are introduced. These indices characterize surface roughness to achieve high efficiency in signal processing and increase sensitivity in detecting surface irregularities resulting from the machining process. This thesis will present the

design of a prototype system to realize the proposed approach. The prototype comprises a CCD camera, height adjustment lead screw assembly, powerslide with controller for positioning, fluorescent lighted enclosure, and a computer system for signal processing. The computer system consists of a digital frame grabber, a personal computer and a developed Microsoft Windows-based software system. This thesis will discuss the significance of introducing fractal dimension and lacunarity into surface characterization. Initial results from this investigation will be presented to illustrate the effectiveness of, and identify the limitations of, the developed optical area-based surface characterization technique in the realization of on-line monitoring systems.

1.3 Organization of Thesis

Chapter 1: Introduction

This chapter introduces the current requirement for surface finish quality assessment and its role in the manufacturing environment. A brief description of the developed prototype for an area-based vision system for the assessment of surface texture is presented.

Chapter 2: Survey of Salient Literature

The parameters used to describe the characterization of surface finish are outlined and briefly described. The advantages and disadvantages of using traditional approaches are included. A new way of characterizing the surface topography with

fractal geometry is discussed. Justification is given for the benefits of fractal geometry of traditional parameters along with the problems and need for additional measurable parameters. Finally, this paper presents a review of the previous work at the Advanced Design and Manufacturing Lab which has influenced this research.

Chapter 3: Fractal Geometry Approach

The method of using a single parameter, fractal dimension, to describe surface roughness and the implementation of an algorithm for calculating the fractal dimension from image data are discussed. The effectiveness of fractal dimension and the need for a second parameter, lacunarity, to characterize the surface are introduced. A definition and algorithm for evaluating the lacunarity of a surface from image data is included. These two parameters provide a more unique characterization of surface texture than fractal dimension alone. Just as two surfaces with the same surface roughness can have completely different topographies so can two surfaces with the same fractal dimension.

Chapter 4: Design and Implementation of Optical-Based Vision System

Theory of the vision system is presented. A general description of the vision system is presented with additional details given to the hardware and software.

Chapter 5: Experimental Setup and Results

The effect of lighting conditions is tested with the type of light, environment of lighting and filtering of lighting. Correlations are identified with two materials and the effect of different end mills are investigated.

Chapter 6: Conclusions and Recommendations

The effectiveness of the hardware, software and algorithms is assessed. Finally, a summary of recommendations and future work for the project is given.

Chapter 2

Survey of Salient Literature

2.1 Surface Texture Parameters

Surface texture is defined as the characteristics that define the overall surface topography. Thus, it is often confused with roughness. Texture includes all surface geometrical properties, such as roughness, waviness, lay, and flaws[3,4]. Figure 2.1 gives a graphical representation of these parameters.

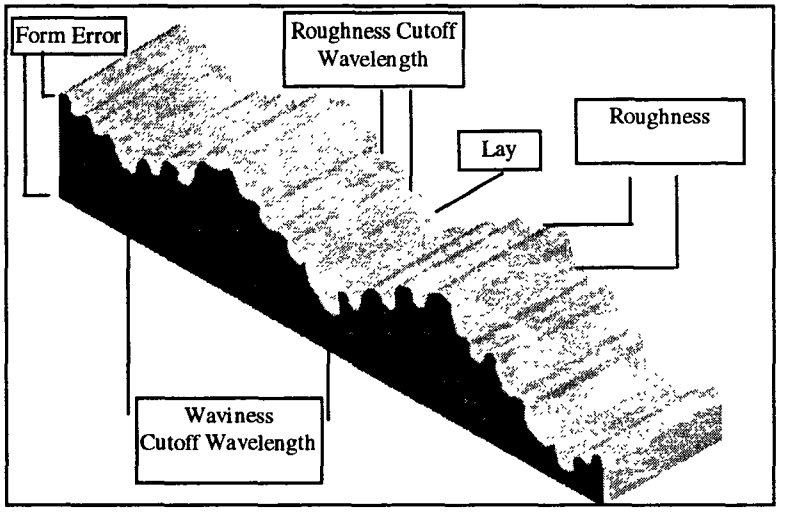

Figure 2.1 Surface Texture

When discussing the parameters that characterize surface topography, roughness is a key feature. Surface roughness is defined as the fine irregularities present on a surface as a result of the action of the production process used to produce the surface, such as traverse feed marks and other irregularities. The

fineness of the irregularities considered to be part of the surface roughness must be defined in terms of a roughness sampling length, or cutoff wavelength. Surface roughness is often referred to as the primary texture. For a machine surface, it is caused primarily by the action of the cutting tool used to produce the surface. Traditionally the evaluation of roughness is performed on a surface produced by a machining operation. However, roughness measurements are also applicable to surfaces which are not created with conventional machine tools. Examples are the surface finish assessment of parts created by the molding process and the stereolithography process[5].

In addition to surface roughness, waviness is a more widely spaced (longer wavelength) component of the surface texture. Waviness includes irregularities with a wavelength greater than the roughness cutoff wavelength, but less than the waviness sampling cutoff wavelength. Typically, the waviness cutoff wavelength is defined by surface irregularities caused by machine tool deflections, vibration, chatter, or heating effects. Waviness is a secondary texture. There is no primary wavelength that can be specified which discerns primary and secondary texture; this is dependent upon the class of work concerned.

Lay is the dominant direction in the surface striations typically directed along the dominant motion of the cutting tool used in the machining operation. For instance, in a milling operation the lay is directed along the radial motion of the milling bit, rather than along the feed direction.

Form error is any surface irregularity that is not included with the surface texture. Form errors may be caused by tool misalignment, improper workpiece mounting, or similar and related errors.

The center line is the line about which the surface roughness is measured. The center line, also called the graphical center line, is measured parallel to the measured profile direction, and is defined within the limits of the roughness cutoff frequency. The center line is found such that the areas between the center line and the roughness height level are equal on each side of the center line.

To better define the parameters used for surface texture characterization, National Standards (BS 1134: 1972) define four orders of geometrical irregularities. The four orders associated with machined surfaces are related to the manufacturing process and they are as follows:

1. First Order. Those arising out of inaccuracies in the machine tool, deformation of the work under the cutting forces or the weight of the material itself.
2. Second Order. Those caused by vibrations of the machine or workpiece (for example, chatter marks).
3. Third Order. Those caused by the machining itself and characteristic of the process.
4. Fourth Order. Those arising from the rupture of the material during chip removal process.

In practice it is accepted that first and second orders of irregularity produce waviness, while the third and fourth orders produce true surface roughness. The surface consists of many different wavelengths, some resulting from the feed of the tool and others caused by the actual cutting action. In addition there may be others produced by vibration[6].

2.2 Traditional Methods of Surface Characterization

2.2.1 Surface Roughness Measurements and Applications

The texture parameter that is of most concern to us in this research is the surface roughness. Surface roughness is routinely used to assess the finish quality of surfaces formed by manufacturing of components. Aesthetics and tolerances of parts are affected by surface finish. The roughness has a strong effect on sealing, accuracy, cleanliness, reflectivity, tool life, electrical resistance, fluid flow, and integrity of joints. The roughness of a part also has the supposed effects of load carrying, creep, and assembly. The only effect waviness has on a part is the load carrying ability. The form and lay do not have a strong effect on any of the aforementioned functions. However, the lay has supposed effects on sealing, reflectivity, tool life, fluid flow, and assembly; the form has a supposed effect on the accuracy of the part. From these examples, clearly the roughness of a machined part is critical to many aspects of a part's functional effectiveness. This is why roughness has been widely used in the shop floor inspection and is the most investigated

surface texture parameter by the manufacturing community. Groups that have an interest in the roughness of solid surfaces range from quality assurance and control in production engineering through tribology, biomechanics and hydrodynamics, to oceanography and selenology. Surface texture influences the tribological performance of metals and non-metals: and this has been not merely in the traditional areas of wear, friction and lubrication, but also in other fields, like sealing, hydrodynamics, and electrical and thermal conduction. The surface textures of parts strongly influence the manner in which they interact with the world around them[6].

2.2.2 Traditional Approach for Characterization of Rough Surfaces

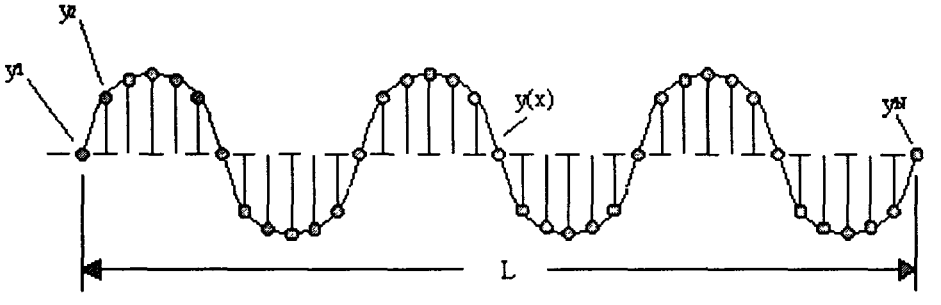

Figure 2.2 Surface Profile

The most common statistical descriptor of surface height is the roughness average, R_a, and the RMS(Root-Mean Squared) surface roughness (also called R_q).

These two parameters are closely related to each other and are given by the following formulas, shown in integral and digitized form:

$$R_a = \frac{1}{L}\int_0^L |y(x)|dx = \frac{1}{N}\sum_{i=1}^{N}|y_i| \tag{2.1}$$

$$R_q = \left[\frac{1}{L}\int_0^L y^2(x)dx\right]^{\frac{1}{2}} = \left[\frac{1}{N}\sum_{i=1}^{N} y_i{}^2\right]^{\frac{1}{2}} \tag{2.2}$$

where y(x) is the surface profile height with respect to the center line which divides two equal areas about itself. It is sampled by the set of N points y_i over the length, L, as shown in Figure 2.2. The parameters R_a and R_q are useful estimators of the average heights and depths of surface profiles. The R_a or center line average is probably the most universally used roughness parameter because of its ease of measurement. The RMS surface roughness is commonly specified for the surfaces of optical components. In general the lower the RMS roughness of an optical component, the less stray scattered light and thus the higher the quality of the component. The RMS surface roughness has almost dropped out of practical usage. For some time prior to this it had attained considerable circulation in theoretical work. It tends to be more sensitive than R_a to large deviations from the center line. Roughness average is used in the automotive and other metalworking industries to specify the surface finish of many types of components, ranging from cylinder bores to brake drums. Another height parameter used is the peak to valley height, which is

the separation of highest peak and lowest valley measurements over a given interval. The peak to valley measurement (PTV) can be expressed as follows:

$$PTV = (y_{\max} - y_{\min}) \qquad (2.3)$$

In Equation 2.3 y_{max} is the highest point of the profile within the given range and y_{min} is the lowest point of the profile within the given range.

2.2.3 Traditional Surface Characterization System

The current national standard for assessing surface roughness is based on the performance of a stylus instrument[6]. The most popular method to measure surface topography is using a profilometer shown in Figure 2.3. This traditional method of measuring surface roughness characteristics is an approach carried out in two-dimensional space.

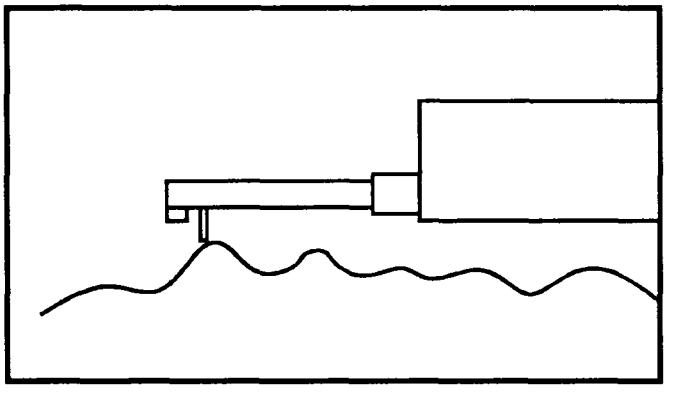

Figure 2.3 Stylus Profilometer

Despite being the base for all national standards, the instrument has several disadvantages. One factor that affects the system is mechanical vibration and this can be due to any vibration in the general vicinity of the stylus. The system is also

subject to electrical noise from its amplifier. Some stylus instruments have a leaf spring that imposes a force on the surface of around 0.001 N and this may cause some permanent damage to the surface being measured as seen in Figure 2.4. Another weakness of the stylus is that it only provides information on a profile for one sweep of the surface[7]. Disadvantages of the stylus instrument can be summarized as follows[8]:

1. It only provides information on a profile, not an area.
2. Pressure of contact between the stylus tip and specimen can cause permanent damage to the surface; this damage is undesirable and invalidate R_a measurements.
3. The stylus instrument is slow, and cannot be used in in-process measurements.

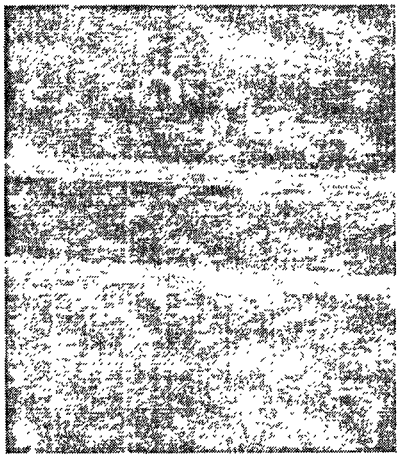

Figure 2.4 Soft Surface Showing Scratches from Profilometer

2.3 Utilization of Digitization for Statistical Parameters

It was noticed in the mid-1960's that many common surface textures possess height distributions that can be accurately described in terms of the Gaussian probability function[3,6]. This triggered a number of theories of surface interaction that make use of the convenient statistical properties of this function to treat the large population of surface asperities involved in contact phenomena. A Gaussian surface is one that has a height distribution relative to the nominal surface. The height distribution satisfies the normal, or Gaussian, probability function. These findings have led to shape parameters, hybrid parameters and more advanced statistical parameters. It has been found that not all surfaces are Gaussian in nature and care should be taken when describing them with the Gaussian model[3,6].

Development of digital systems has increased the flexibility of stylus instruments and other surface characterization devices. It has allowed the access to data points representing the surface topography of a desired part. Some stylus instruments have been adapted to take multiple traces at set distance to simulate an area method and provide a larger quantity of data for the surface.

These digitization techniques, along with advanced statistical analysis, have led to a perceived new direction in surface analysis. These statistical parameters still have not come close to reaching the acceptance and wide use that the roughness average has. The surface roughness can provide a single physical parameter understood by people currently in the industry.

2.3.1 Shape Parameters Machining

Profiles can have the same R_a and wavelength, but have different shapes and thus may perform differently in different applications. It is easy to compare periodic surfaces by looking at their skewness which is a measure of the symmetry of the profile about the mean line. Skewness is defined as:

$$R_{sk} = \frac{1}{NR_q^3} \sum_{i=1}^{N} y_i^3 \tag{2.4}$$

2.3.2 Hybrid Parameters Machining

Slope and curvature are two examples of quantities that combine the concepts of height deviation and lateral displacement and are thus termed hybrid parameters. They can be defined analytically or digitally in several ways.

2.3.3 Statistical Functions Machining

More complete statistical descriptions of the properties of surface profiles can be obtained from statistical functions, such as those used in random process theory and time series analysis. Four important statistical functions are the amplitude density function or height distribution, the bearing area curve, the power spectral density, and the autocorrelation function[6].

The Power Spectral Density (PSD) decomposes the surface profile into its spatial Fourier component wavelengths. It is given analytically by:

$$PSD(F) = \lim_{L\to\infty}\left(\frac{1}{L}\right)\left|\int_0^L y(x)e^{-2i\pi Fx}\right|^2 \tag{2.5}$$

and is estimated in the digitized form by:

$$PSD(k) = \frac{1}{N\Delta}\left|\sum_{j=1}^{N} y(j)e^{-2i\pi kj/N\Delta}\right|^2 \tag{2.6}$$

In the above equations, Δ is the lateral point spacing (sampling interval) of the digitized data points, the total length of the profile, L, is equal to $N\Delta$, and the set of spatial frequencies, F, in the digitized PSD is given by k/L, where k is an integer that ranges from 1 to N/2. Calculation of the digital Fourier transform can be greatly sped up by using Fast Fourier transform (FFT) algorithms.

Autocovariance and Autocorrelation. The complementary function to the power spectral density is its Fourier transform, the autocovariance function, $C(\tau)$:

$$C(\tau) = \int_{-\infty}^{\infty}[PSD(F)]e^{2i\pi F\tau}\,dF \tag{2.7}$$

Alternatively, the autocovariance function can be calculated directly from the profile itself. That formula is given by an overlap integral of shifted and unshifted profiles:

$$C(\tau) = \frac{1}{L}\int_0^L [y(x)][y(x+\tau)]dx \tag{2.8}$$

Where the quantities L and y(x) have been defined previously. The value of the autocovariance function at zero shift ($\tau = 0$) is by definition equal to the mean square roughness, R_q^2, of the profile, provided an appropriate mean line has been subtracted from the profile to calculate y(x). When the autocovariance function is normalized by dividing by zero shift value, the result is known as the autocorrelation function (ACF), $c(\tau)$:

$$c(\tau) = \frac{C(\tau)}{R_q^2} = \frac{\int_0^L [y(x)][y(x+\tau)]dx}{\int_0^L [y^2(x)]dx} \tag{2.9}$$

Note that the overlap between the shifted and unshifted profiles decreases as the shift distance increases for a finite length profile. If this fact is taken into account and the digital formulation is simultaneously used, the ACF can be estimated by:

$$c(\tau) = \left(\frac{1}{N-j}\right)\left(\frac{\sum_{i=1}^{N-j}[y(i)][y(i+j)]}{\sum_{i=1}^{N} y^2(i)}\right) \tag{2.10}$$

The autocovariance and autocorrelation functions are useful for visualizing the relative degrees of periodicity and randomness in surface profiles[9]. The autocovariance function, or its normalized form the autocorrelation function, has been the most popular way of representing spatial variation.

2.4 Approach Using Fractal Geometry

Fractal geometry, as an extension of classical Euclidean geometry, characterizes the average slope of a profile in the two-dimensional space and reflects the space filling ability in the three-dimensional space. Fractals have literally captured the attention, enthusiasm and interest of the manufacturing community to describe the correlation of surface irregularities and the dynamics of the machine tool[10]. Using the power of computer graphics, the incorporation of image processing with fractal geometry offers a new and unique environment in which to effectively implement a surface monitoring system such as the one designed in this research.

2.4.1 Fractal Dimension

As implied earlier, most statistical parameters are scale-dependent and in some cases, not representative of surface characteristics, especially for very fine surfaces. Very often precision manufacturing leads to surfaces that have very fine surface finishes and the scale dependent parameters fail to completely describe these surfaces. However, it is recognized that many engineering surfaces show fractal characteristics, and that some scale-independent parameters may be extracted by using fractal theory and this is a tool that can be used to characterize surface topography[11].

There are several different notions of dimension including: topological dimension, Hausdorff dimension, fractal dimension, self-similarity dimension, box-

counting dimension, capacity dimension, information dimension, Euclidean dimension, etc. These notions of dimension are relevant in some but not necessarily all situations. In some cases, all the notions will make sense and have the same value, but it is important to select the correct dimension for accurate characterization of an object. Of the fractal dimensions, the box-counting dimension has the most applications in science[14].

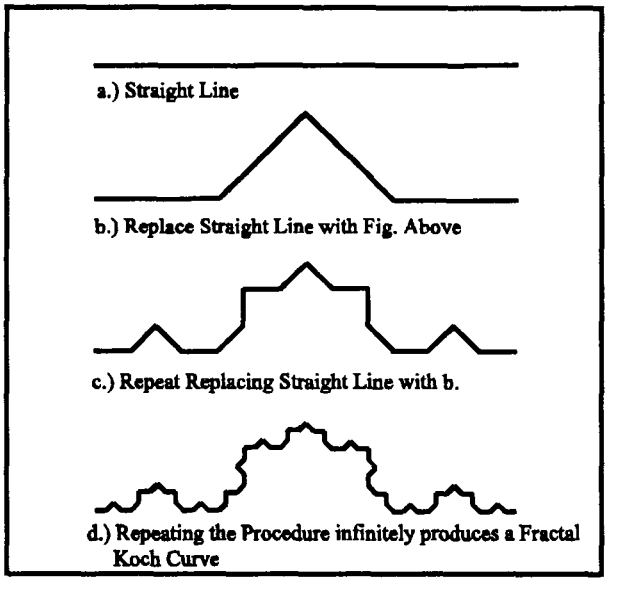

Figure 2.5 Koch Curve

A structure is said to be self-similar if it can be broken down into arbitrarily small pieces, each of which is a small replica of the entire structure. Here it is important that the small piece can in fact be obtained from the entire structure by a similarity transformation. The best way to think of such a transformation is what we obtain from a photocopier with a reduction feature. For example, if we take a Koch curve as seen in Figure 2.5 and put it on a copying machine, set the reduction factor

to 1/3 and produce four copies, then the four copies can be pasted together to give back the Koch curve. However, not all structures that are self similar are fractals and vice versa[14].

If a surface is not self-similar then the self-similarity dimension can not be used to describe that surface. Another form of dimension is required to characterize a non self-similar surface and this can be done using the box-counting dimension. The box-counting dimension proposes a systematic measurement in equation 2.11, which applies to any structure in the plane and can be readily adapted for structures in space.

$$FD = \frac{\log_{10}(N(\varepsilon))}{\log_{10}(1/\varepsilon)} \tag{2.11}$$

2.4.2 Methods of Determining Fractal Dimension

One fractal parameter used in this research is fractal dimension, FD. It is defined as a measure of how densely the fractal occupies the space in which it lies. The box-counting dimension is a special form of the fractal dimension proposed by Mandelbrot and Hausdorff[10]. The reason for choosing the box-counting method is its ease of application to a surface, such as a machined surface, that is not necessarily self-similar. Mathematically, such a parameter can be evaluated by equation 2.11.

This equation is described by Liebovitch and Toth[12]. The algorithm for determining the box counting dimension for a one or two-dimensional structure is

to first lay out a grid of mesh size ε which encloses the surface. The next step is to count the number of boxes which contain any portion of the surface, giving the value of N(ε).

For a three dimensional surface, a cube is needed to cover the entire surface. Cubes of side length ε are used in the three dimensional mesh generation of the box that encloses the surface. The cubes that contain the surface are summed and this value is N(ε). Again equation 2.11 is used to calculate the fractal dimension.

2.4.3 Previous Work in Surface Characterization

Several papers have been written which explore the correlation of surface roughness with fractal dimension[13,14,15,32]. These papers cover all thinkable disciplines and the most relevant works pertain to surfaces created by machining processes. One example is the use of fractals in the mining industry. The surface roughness is compared to the fractal dimension by a study to determine the smoothness of copper samples which have been put through a ball mill. The surfaces are measured with a profilometer to determine the roughness. The fractal dimension of the profilometer traces is measured by the structured walk technique. As the roughness of the samples increases so does the fractal dimension[13]. In another work, fractional Brownian motion(fBm) is studied and the fractal dimension is said to describe the "roughness" of the fBm function at small scales[14]. The Weierstrass-Mandelbrot equation has been used to simulate deterministically both

Brownian and non-Brownian rough surfaces which exhibit statistical resemblance to real surfaces[15].

2.4.4 Limitations of Fractal Dimension

The concept of fractal dimension has inspired scientists to embark on a host of interesting new work and fascinating speculations. Indeed, for a while it seemed as if fractal dimensions would allow us to discover a new order in the world of complex phenomena and structures. This hope, however, has been dampened by some limitations. For one thing, there are several different dimensions that give different answers. We can also imagine that a structure is a mixture of different fractals, each one with a different value of box-counting dimension. What we would desire is something more like a spectrum of numbers which gives information about the distribution of fractal dimensions in a structure. This program has, in fact, been carried out and runs under the theme multifractals[10]. However, the work of investigating multifractals is not undertaken in this research. Another limitation of using a singular parameter such as the fractal dimension or surface roughness, is that one parameter fails to uniquely describe the surface. Adding a second parameter can give a more detailed representation of the surface. If the fractal dimension presents a picture of the amplitude or space filled by a surface, then a second parameter is needed to describe how the space is filled with the surface, and that is why the second parameter, lacunarity, is desirable. In research supporting this thesis a

special effort has been made to study the effects of fractal geometry parameters, fractal dimension and lacunarity, on the surface topography.

2.4.5 Three Dimensional Non-Contact Optical Method

A three dimensional approach to assessing surface roughness, such as the method developed in this research, is well suited to characterization by the box counting method of calculating fractal dimension. Some other methods have been used to develop a three dimensional approach to characterize surface topography and one such method is the assembly of traces using a profilometer. Some advantages of using optical methods over conventional methods are as follows[8]:

1. Aerial data can be obtained.
2. There is no contact with the specimen, therefore no surface damage.
3. Measurements can be taken quickly.

A survey of other surface assessment devices has been conducted on other methods including the following: laser profilometry, microscopy, comparative techniques, and parametric and non-parametric optical devices. Some advantages that the system developed in this research has over these methods are as follows:

1. Measurements can be taken on materials that are not conductive, or magnetic.

2. A vacuum is not required.

3. Specimen preparation is not required.

In Appendix C a description and evaluation of some current systems is included. The requirements for the system are as follows: area based, non-contact, adaptability to in-process system, and real time data acquisition. None of the previous systems contain all of the traits required and furthermore, they cannot be adapted to in-process or on-line monitoring. An attempt to provide all of these criteria into one vision system at a relatively low cost is the drive and goal behind this research.

2.5 Current Status of Research

2.5.1 Scattering Theory of Electromagnetic Waves

2.5.1.1 Beckmann's Scattering Theory

There are several models which have been developed to describe the theory of electromagnetic radiation from rough surfaces[16,17]. These models have led to the development of very general descriptions of the scattering problem while others have led to very specific applications. P. Beckmann put a theory forth in 1963 which provides a general formulation of the scattering problem, while also yielding concrete mathematical relationships between surface parameters and scattering directions and intensities[18]. The fundamental results of Beckmann's theory which

are of interest here are provided in this section, along with the definition of the scattering geometry used by Beckmann.

Consider a light ray incident on a flat, optically rough surface, with an incident angle of θ_1 as measured from the surface normal (which coincides with the z-axis in Figure 2.6). Some of the incident light is scattered away from the specular direction due to the surface roughness. An arbitrary observation is defined by two angles θ_2 and θ_3. θ_2 is measured from the surface normal and θ_3 is the horizontal angle between the projection of the incident light on the surface and the projection of the observation vector on the surface.

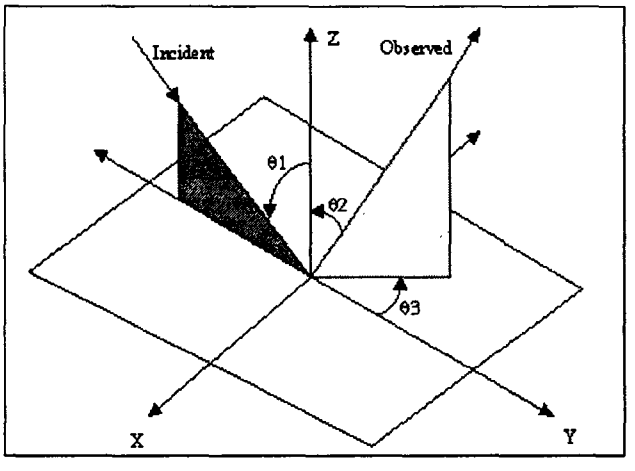

Figure 2.6 Scattering Geometry

Beckmann's scattering theory states that, the mean scattered power (Ψ) of incident light is a function of the surface roughness, incident wavelength, incident angle, observation angles, correlation distance between hills and valleys in the surface, and

planar dimensions of the illuminated surface. Beckmann's equation for this relationship can be stated as follows:

$$\Psi = e^{-g}\left[\rho_o^2 + \frac{\pi F T^2}{A}\sum_{m=1}^{\infty}\frac{g^m}{m!m}\exp\left(\frac{-V_{xy}^2 T^2}{4m}\right)\right] \qquad (2.12)$$

where,

$$\rho_o = \frac{\sin(V_x X_s)\sin(V_y X_s)}{(V_x X_s)(V_y X_s)},$$

$$F = \frac{1+\cos\theta_1\cos\theta_2 - \sin\theta_1\sin\theta_2\cos\theta_3}{\cos\theta_{12}(\cos\theta_1+\cos\theta_2)},$$

$$g = \frac{2\pi\sigma_h}{\lambda}(\cos\theta_1+\cos\theta_2),$$

$$V_x = \frac{2\pi}{\lambda}(\sin\theta_1 - \sin\theta_2\cos\theta_3),\ V_y = \frac{2\pi}{\lambda}(\sin\theta_2\sin\theta_1),\ V_{xy} = \sqrt{V_x^2+V_y^2}$$

The mean scattered power in equation 2.12 represents the intensity of scattered radiation in a given observation direction based solely on the local roughness of the surface. This is based on assuming a small area of interest and assuming a constant incident angle. This theory has been applied to point and line based systems and can be adapted to area-based systems which will describe the local surface roughness[19].

The incident light gradually changes from specular reflection to diffuse scattering as the surface roughness increases, this is shown in equation 2.12. A transition from specular to diffuse reflection can be seen in Figure 2.7. The incident light is reflected entirely in the specular direction from a smooth surface(case 1). In

case (2), there is a strong spike in the specular direction with smaller lobes around the specular direction and the surface exhibits a slightly rough finish. In case (3), a moderately rough surface, the incident radiation is scattered diffusely, but still with a tendency towards the specular direction. In the very rough surface of case (4), the diffuse light has lost the preference for scattering in the specular direction.

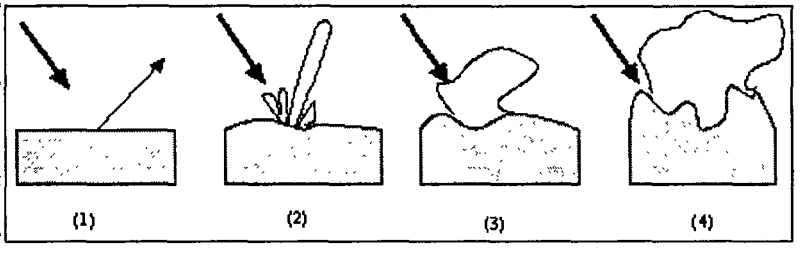

Figure 2.7 Transition from Specular Reflection to Diffuse Scattering

2.5.1.2 Surface Facet Model

The light scattering theory presented by Beckmann considers the statistical properties of the surface under investigation to determine the nature of light reflected from a surface. A much simpler model can be applied to a surface using the surface facet model. In the surface model, the surface is modeled as a set of interconnected flat facets. These facets which make up the surface can only reflect light in a specular fashion. The incident light is modeled by a set of simple light rays with different phases. These light rays are reflected from the surface based on the geometric orientation of the individual facets of the surface. From this assumption based on specular reflection the angle of reflection is equal to the angle of incidence. The resultant reflected light field is simply the sum with respect to the phases of all

rays in a given direction. A two-dimensional representation of the surface facet model can be seen in Figure 2.8. This model provides a starting point for describing some basic aspects of light reflection[20].

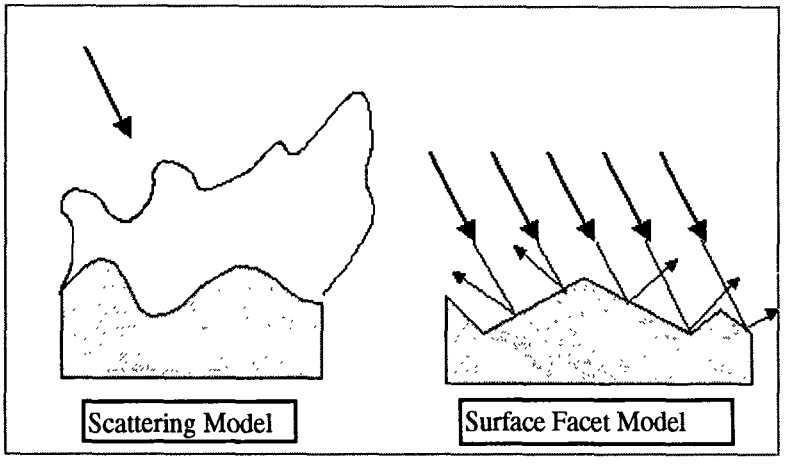

Figure 2.8 Surface Facet Model

Chapter 3

Fractal Geometry Approach

3.1 Algorithms Formulation

3.1.1 Fractal Dimension

The initial method of evaluating the surface roughness was performed using the box-counting method of calculating the fractal dimension described by Liebovitch and Toth[12]. In section 2.4.2, Methods of Determining Fractal Dimension, there is a description of the box-counting method and it is quantified by equation 2.11. A graphical representation of how to estimate the fractal dimension is shown in Figure 3.1. As described earlier, a three dimensional box is needed to cover the entire surface. Cubes of side length ε are used in the three dimensional mesh generation of the box which encloses the surface. The number of cubes which contain the surface are summed and this value is $N(\varepsilon)$. The cube size is originally the largest cube that will enclose the surface and it is gradually reduced while counting the number of boxes that enclose the surface. The smallest box is equal to the size of the smallest data point. The log of $N(\varepsilon)$ is plotted against the log of $1/\varepsilon$ and the slope(α) of this line gives the box-counting dimension. When the slope is evaluated the range is limited by the hardware. The largest cube that encompasses the surface is proportional to the number of pixels captured by the CCD camera[21]. The smallest cube would be a cube with the actual dimensions of the pixel. If the box size is set to its largest value then only one box will encompass the surface and

this will give us little information about the surface. Thus, it is desired to start with a smaller box size usually on the order of 1/4 the maximum size.

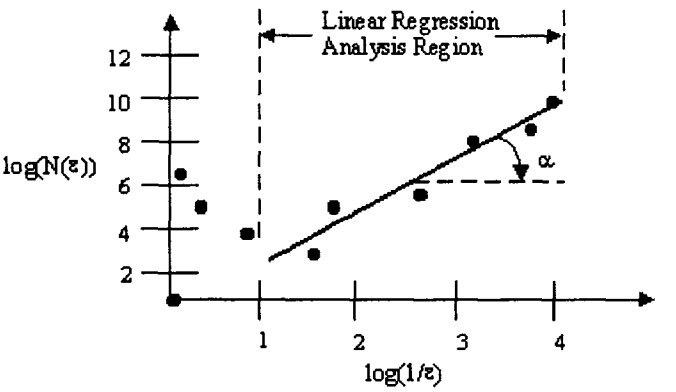

Figure 3.1 Box Size vs. Number of Boxes

In technical reports[22] this method was successfully used to correlate surfaces with the roughness average. The applied range was between 0.185μm and 0.69μm as these reports indicated. When this method was applied to a wider range of roughness values obtained from the vision system, the method was not as efficient as it was when associated with a narrow range of roughness average. For this reason, the method of calculating the fractal dimension via the box-counting method has been revised in this thesis. One of the major revisions made for calculating the fractal dimension is the development of a new algorithm.

The new algorithm is designed to try to minimize the calculation time and adapt the parameter to be more sensitive to the amount of reflected light from an illuminated surface. Although the new method is similar to the original algorithm, one of its unique contributions is that it is applicable to a three dimensional object

that has one unique point for each set of X and Y values, such as a digitized image. When applying the new method, the box size is set equal to the pixel size of the image that is being analyzed. In equation 3.1, FD1 is the fractal dimension, Z_{ij} is the height of a point with coordinates (i,j), and MIN is the minimum value of a point on the surface. The minimum value is not the lowest point but it is determined by a frequency of the histogram in Figure 3.2 and the "MIN" value of the light level is cross referenced from this frequency. The reason for using a "MIN" value is to reduce the sensitivity of the fractal dimension to changes in the amount of light used to illuminate the machined surface. The machined surfaces produced by a CNC milling machine have been shown to follow a normal distribution and this allows the utilization of a histogram to determine a minimum value based on frequency of light levels.

$$FD1 = \frac{\log\left(\sum_{i=0}^{255}\sum_{j=0}^{255}(Z_{ij} - MIN)\right)}{\log(256)} \tag{3.1}$$

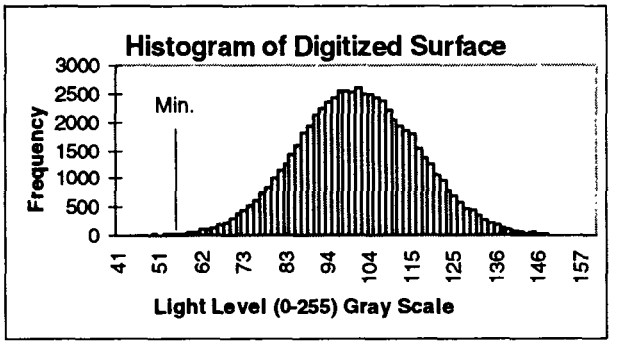

Figure 3.2 Histogram of Machined Surface

3.1.2 Lacunarity

In the theory of fractal geometry, lacunarity is a measure of the difference between the actual mass and the expected mass. This parameter can be used to describe the number of gaps in the surface. The texture of a surface can be described by the lacunarity. As the texture of a surface alters from dense to coarse the lacunarity increases. The lacunarity is a normalized parameter ranging from 0 to 1. A surface that is very dense would have a lacunarity close to zero, while a coarse surface would have a lacunarity close to 1. Following is a definition of lacunarity[23]:

$$\Lambda = E\left[\left(\frac{M}{E(M)} - 1\right)^2\right] \tag{3.2}$$

Mandelbrot has introduced the parameter lacunarity, Λ (lacuna is Latin for gap). Although the qualitative visual effect of changing lacunarity at fixed fractal dimensions is quite striking, to date there have been no quantitative measurements of the lacunarity of various random fractals[14].

The first attempt at defining the lacunarity of a surface was done using the concept put forth by Mandelbrot in equation 3.2. The basic method used for calculating the lacunarity is to look at each point on the surface and examine the points around that point. If the points are greater than or equal to the point in question then a counter is incremented. A representation of this is shown in Figure 3.3. Once the points around the current point have been examined, the counter is

divided by the average number of points. Another option is to divide by the total number of points. This procedure is repeated for every point on the surface and the average value is found.

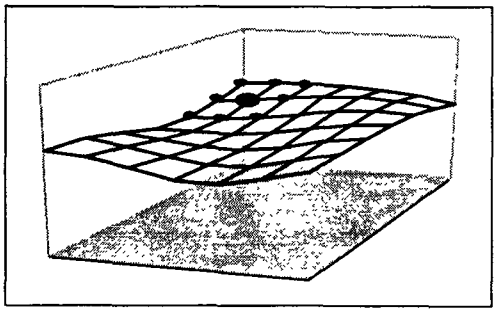

Figure 3.3 Lacunarity

3.2 Feasibility Study/ Preliminary Experiments

3.2.1 Simulation and Evaluation of Surfaces with Fractal Dimension

A periodic surface can be recreated by just its amplitude and frequency. If all surfaces were periodic in nature then it would be simple to reconstruct these surfaces. Unfortunately, patterns of machined surface topographies are irregular and fragmented. Periodic and random surfaces are investigated to determine the role of fractal geometry with respect to surface characterization.

Four surfaces are created for a range of fractal dimensions to investigate the correlation of fractal dimension and roughness average. The range of fractal dimensions is approximately 2.3 to 2.85 and this can be seen in Figure 3.4. The fractal dimension calculated here is done using the parameter FD1. Figure 3.4e shows all of the surfaces on one graph with FD1 correlated to Ra. The correlation

is not as strong when different surfaces are used but it is still present. All of the fractal dimensions of machined surfaces acquired in preliminary experiments from the monitoring system have values between these bounds. Therefore, the range investigated in this thesis work is sufficient. The fractal dimension is varied by changing the amplitude of the function used to generate that fractal dimension. This fractal dimension also shows a direct correlation to the roughness average of the surface.

Two surfaces have been created with the same Ra but different values of FD1. The reason for this is to show that FD1 is more sensitive to valleys in the surface. The sensitivity of FD1 is dependent upon the minimum value on the surface that is selected to calculate FD1. If the absolute minimum point on the surface is used then FD1 will be

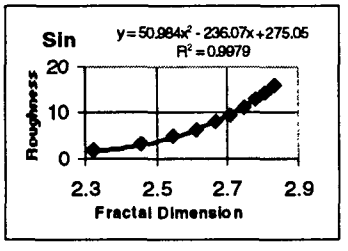

(a) Sin Function

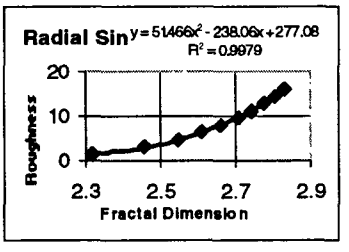

(b) Radial Sin Function

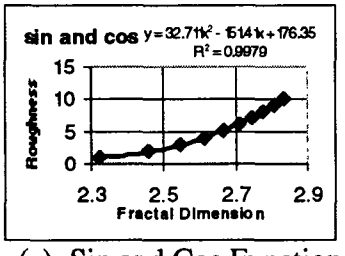

(c) Sin and Cos Function

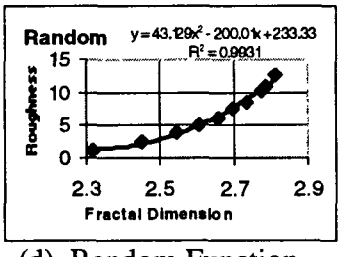

(d) Random Function

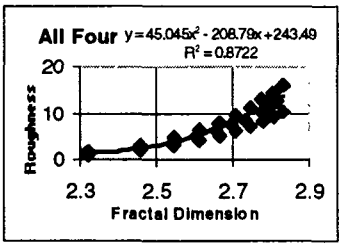

(e) All Surfaces

Figure 3.4 Fractal Dimensions From Generated Surfaces

more sensitive to detecting valleys than Ra. In Figures 3.5a and 3.5b the minimum value used to calculate FD1 has been set to the minimum point on the surface therefore there is a drastic difference in FD1 for the two surfaces. When examining metallic machined surfaces the minimum value used to calculate FD1 is not set to the minimum point on the surface. Rather it is chosen from the histogram of the surface based on 3σ below the mean value of the surface.

3.2.2 Preliminary Experiments with System Correlations

In the previous section of this thesis, it was shown that the fractal dimension correlates with the roughness average of a surface. These surfaces were generated with periodic functions and random noise. In this section of the research, 30 samples were machined out of aluminum with spindle speeds of 500, 900 and 1100 RPM and the feed rates ranged between 1.0 and 4.8 in/min. The roughness average of the samples was found by taking four traces with a surface profilometer and the roughness averages

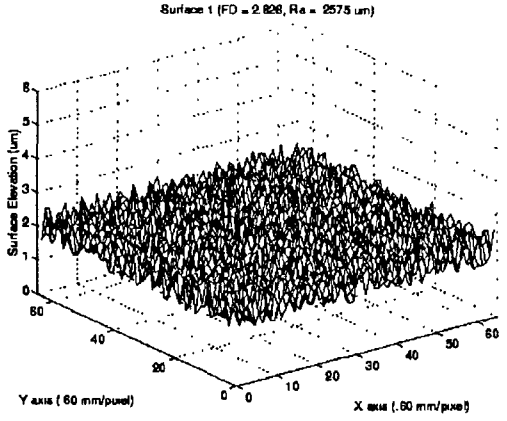

(a) Surface Plot

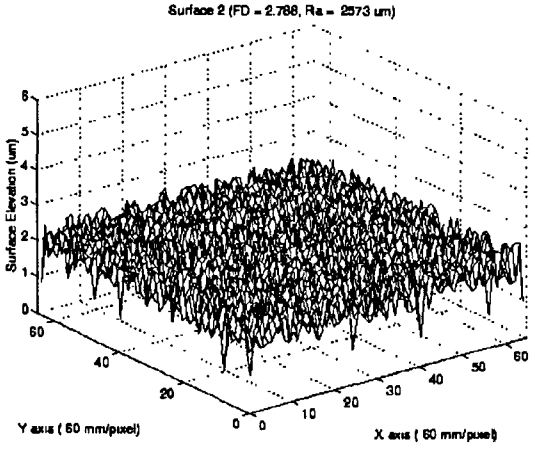

(b) Surface Plot

Figure 3.5 Surface Plots With Same Ra But Different FD1

ranged between 0.16 and 0.594 μm. The fractal dimension, lacunarity and other parameters were found by using the developed surface monitoring system. The fractal dimension correlates with the surface roughness as seen in Figure 3.6. In this figure it can be seen that it is possible that a single Ra value may give two FD values.

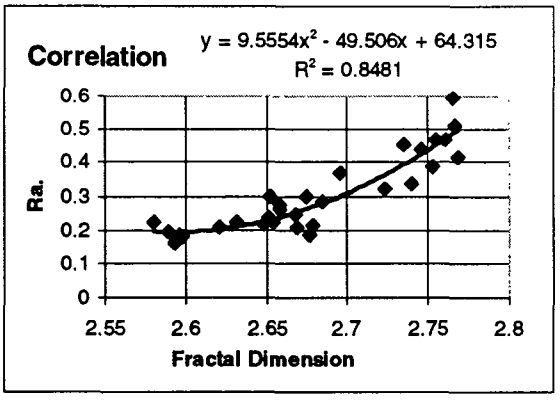

Figure 3.6 Correlation of 30 Samples

3.2.3 Case Study

In order to test the repeatability and accuracy of the developed correlation curve, a sample is machined to have a roughness within the range in which the correlation is defined. The roughness of the specimen is measured using a profilometer prior to examination using the surface monitoring system. Note that all conditions that were used to derive the correlation curve are repeated including the following: the orientation of the external light source, the angle of the external light source, the intensity of the external light source, ambient light, the magnification factor, and the area being examined. Ambient light was present but the level was not monitored, because, as will be shown later it is not significant in the presence of an external light source with sufficient output. The Ra obtained from a profilometer for the surface is 0.222 μm and the Ra obtained from the correlation curve in equation 3.3 is 0.238 μm. The value of the dimension obtained from the monitoring system was FD1 = 2.659. This parameter falls within the range for which the

correlation curve of equation 3.3 is valid. The Ra of the sample also falls within the valid range for which the correlation curve was derived.

$$Ra = 9.56FD^2 - 49.51FD + 64.32 \tag{3.3}$$

3.2.4 Simulation and Evaluation of Surfaces with Lacunarity

An additional parameter to describe the surface topography is desired because two surface the same FD and Ra can have different surface topographies. Mandelbrot stated "distinctly different surfaces can have the same fractal dimension." In order to determine the role of lacunarity in characterizing the surface topography, four surfaces with similar fractal dimensions are created and their lacunarity is compared. The four surfaces are created by the following methods:

1.) $z = A(\sin(\omega x) + 1)$ (3.4)

2.) $z = A[\sin[\omega(x^2 + y^2)^{1/2}]+1]$ (3.5)

3.) $z = A[(\sin(\omega x)+1)+(\cos(\omega y)+1)]$ (3.6)

4.) $z = A(\text{random noise})$ (3.7)

where x, y, z are Cartesian coordinates, A is the amplitude, and ω is the frequency. The plots of these surfaces are shown in Figure 3.7. It can be seen that each of these surfaces has a different value of lacunarity while almost the same fractal dimension based on equation 3.1. In this case the lacunarity is calculated by using Mandelbrot's method.

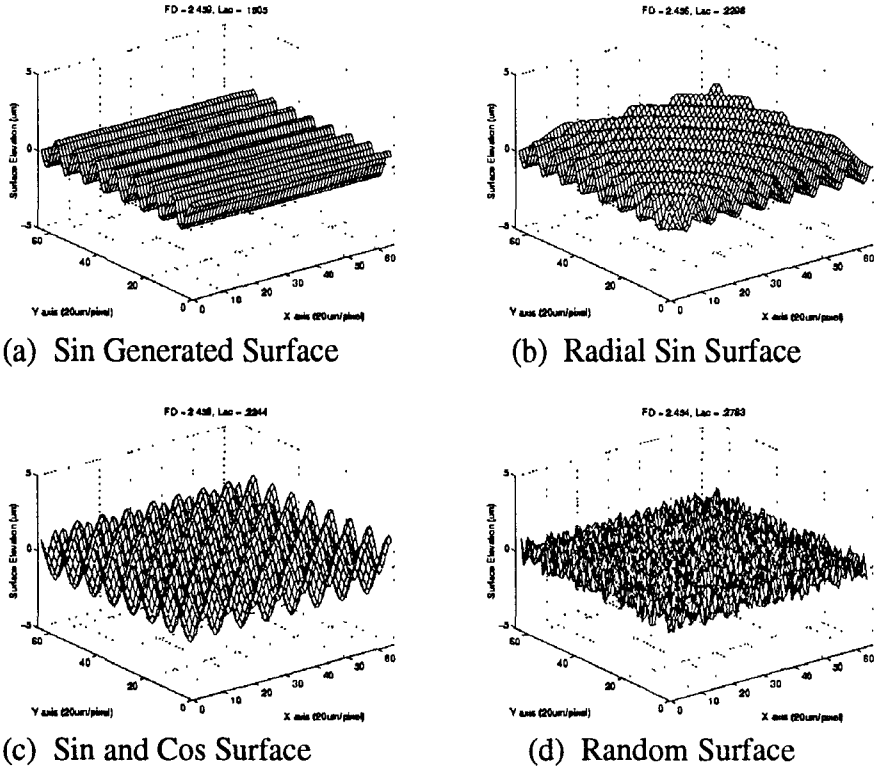

(a) Sin Generated Surface (b) Radial Sin Surface

(c) Sin and Cos Surface (d) Random Surface

Figure 3.7 Plots of Surfaces Having Same FD But Different Lacunarity

In order to investigate further the role of lacunarity, three surfaces are created with a varying range of frequencies. It is observed that for each individual surface with the same frequency the lacunarity is the same. Also, the frequency varies proportionally to the lacunarity and in this case the frequency is a measure of the number of gaps in the surface.

When the fractal dimension is correlated to the roughness average for a group of surfaces with the same pattern the correlation works very well. But, when the fractal dimension is correlated to a group of surfaces created with different patterns the correlation between fractal dimension and roughness average is not as

powerful. As can be seen in Figures 3.20 - 3.23, the lacunarity can be used as an indicator to the existence of drastically different patterns in the surfaces being examined.

From the study of surfaces machined with a milling machine the created surfaces generally followed a normal distribution. If this is truly the case then the simulations with random noise could have more relevance. If the surfaces had been created with a Lathe then a periodic function would have more applications to this method of calculating lacunarity. In order to investigate further, 52 surfaces were analyzed with the new vision system discussed in Chapter 4. Indeed it appeared that the surfaces did follow a normal distribution from the histogram. Furthermore, the lacunarity for each surface showed little deviation from the norm. It also appears that this algorithm is not sensitive enough to separate the noise from the frequency components in a milled surface. However disappointing this method of calculating lacunarity turned out to be there was one positive aspect of this algorithm. It was noticed that if the camera was out of focus the camera could be focused until a peak value of lacunarity was observed to bring the camera into focus. This is analogous to the addition of lacunarity to some work in filmmaking. The addition of irregularities to a surface can be accomplished by continuously increasing the resolution from frame to frame[14]. This increase in irregularities is similar to the increase in irregularities as the surface is brought into focus with the CCD camera.

Since the first method of calculating lacunarity has not taken this research

exactly the desired direction, a second algorithm of calculating lacunarity is investigated. This method is one presented by Voss[24] that suggests calculating the lacunarity from the same probability distribution P(m,L) often used for the estimation of the fractal dimension. The equations describing this method are as follows[14,24]:

$$\Lambda = \frac{\left\langle M^2(L)\right\rangle - \langle M(L)\rangle^2}{\langle M(L)\rangle^2} \text{ where,} \tag{3.8}$$

$$M(L) = \sum_{m=1}^{N} mP(m,L) \tag{3.9}$$

$$M^2(L) = \sum_{m=1}^{N} m^2 P(m,L) \tag{3.10}$$

P(m,L) is the probability that there are m points within a box of size L centered about an arbitrary point on the surface. Λ can be simply represented by the variance of the number of points per box of size L divided by the mean squared of the number of points per box of size L.

This algorithm for calculating lacunarity is similar to the box counting method used to calculate fractal dimension. A three dimensional box is needed to cover the entire surface. Cubes of side length L are used in the three dimensional mesh generation of the box that encloses the surface. The number of points in each individual cube is found and the average value of the number of points in a box of size L is calculated. The variance of the number of points in each cube is found.

The cube size can be originally the largest cube that will enclose the surface and it is gradually reduced while counting the number of boxes which enclose the surface. The smallest box is equivalent to a side length of 3. A graph of the variance divided by the mean squared vs. the box size is created and the slope is equal to the lacunarity. A more practical and intuitive method to calculate the lacunarity is to calculate the lacunarity for one box size. It has been found that a box size of three to calculate lacunarity (lac(3)) has the best correlation to the dominant spatial frequency of a surface profile.

In order to investigate the relationship of lacunarity to the texture of a surface, the frequency of a periodic function is varied in order to show a correlation between the lacunarity and the frequency. The amplitude is kept constant in order to investigate the effects of the frequency alone. In Figure 3.8 there are two graphs: one, with lacunarity vs. spatial frequency, and the other with the lacunarity calculated with a box size of 3 (Lac(3)) vs. spatial frequency. A definitive correlation can be seen between the spatial frequency and the lacunarity as well as Lac(3).

A more meaningful application of lacunarity would be to investigate the effect of the addition of noise to a surface generated with a periodic function. Two functions are used to create the surfaces and they are a sin function and a saw tooth function. The spatial frequency of the surfaces ranges between 2 and 32. Figures 3.9 and 3.10 show the effect of the addition of noise to the signals. The increase in

noise reduces the lacunarity of the surface. Figures 3.9 and 3.10 show that the effect of noise is less for a higher frequency range than the effect for a lower frequency range. It can now be seen that both the frequency and addition of noise to a signal can be used to control the lacunarity.

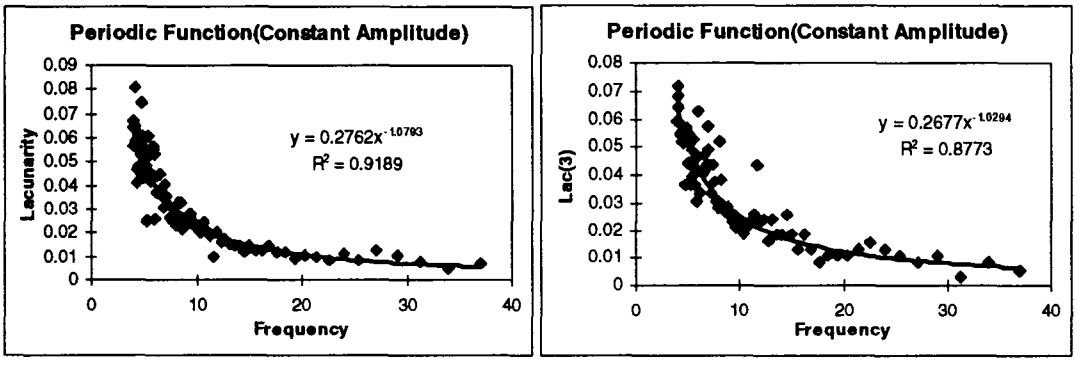

Figure 3.8 Frequency vs. Lacunarity of a Periodic Function

A surface with given values of FD1 and Ra can be rearranged spatially with no effect on either parameter. Lacunarity now comes into the picture to decipher the difference between the spatial arrangement of a surface. A surface is created and part of this surface appears in Figure 3.11a and the values that make up this surface are then randomly assigned to a new surface which is partially shown in Figure 3.11b. The surfaces have the exact same value for Ra and FD1. Lac(3) is different for the two surfaces and the difference is quite noticeable. A more complete picture of surface topography can be created by using the two parameters FD1 and Lac(3) to describe the surface instead of a single parameter.

In order ot uniquely characterize the surface finish using the fractal geometry approach proposed in this thesis work, it is very important to have two paramters

not one.

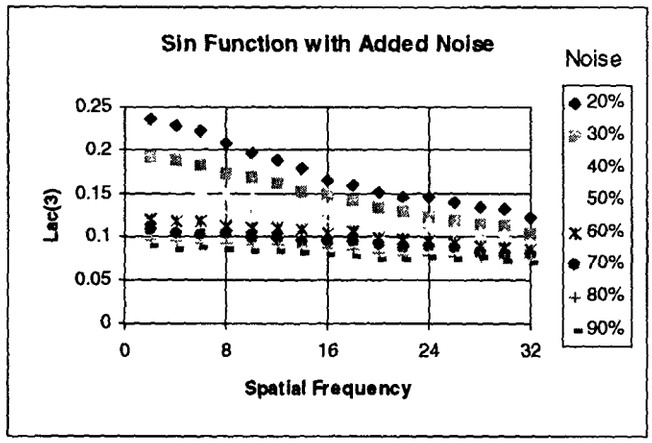

Figure 3.9 Calculation of Lac for Sin Function with Added Noise

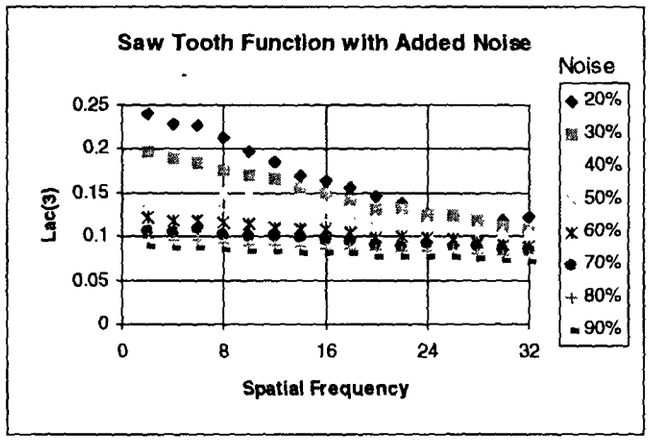

Figure 3.10 Calculation of Lac for Saw Tooth Function with Added Noise

Figures 3.12-3.15 show four surfaces generated with two values of FD1 and two values of Lac(3). The surfaces give a better understanding of the effects of FD1 and Lac(3) on the surface topography. Figure 3.12 shows a high value of FD1 and a low value of Lac(3), Figure 3.13 shows a low value of FD1 and a high value of Lac(3), Figure 3.14 shows a high value of FD1 and a low value of Lac(3), and

Figure 3.15 shows a low value of FD1 and a low value of Lac(3). It is clear from these figures that FD1 describes the height variations while Lac(3) describes the spatial frequency.

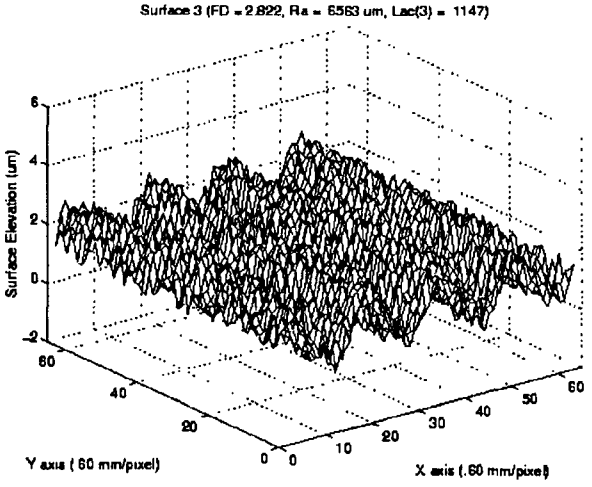

(a) Original Surface Plot

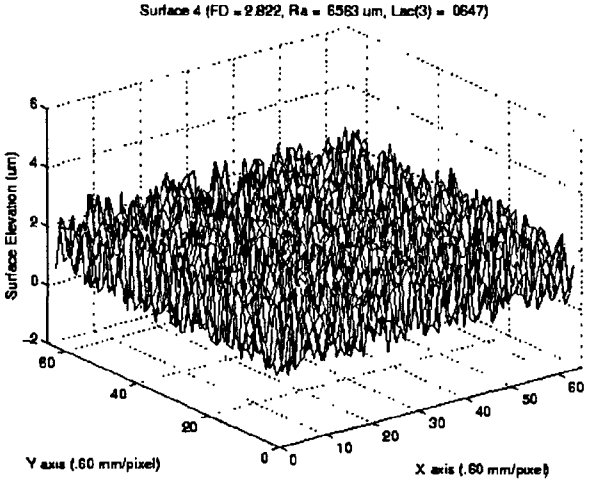

(b) Surface Plot of Re-distributed Points

Figure 3.11 Two Surfaces with Same Ra and FD1

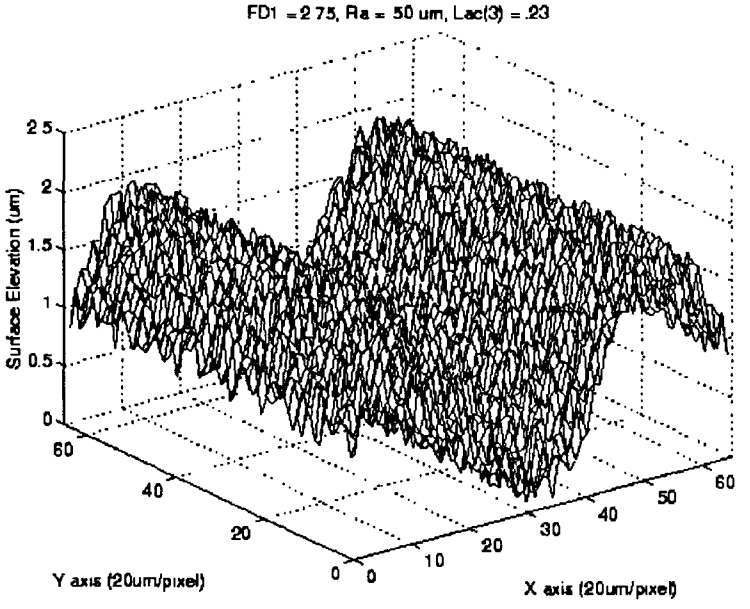

Figure 3.12 High FD1, Low Lac(3)

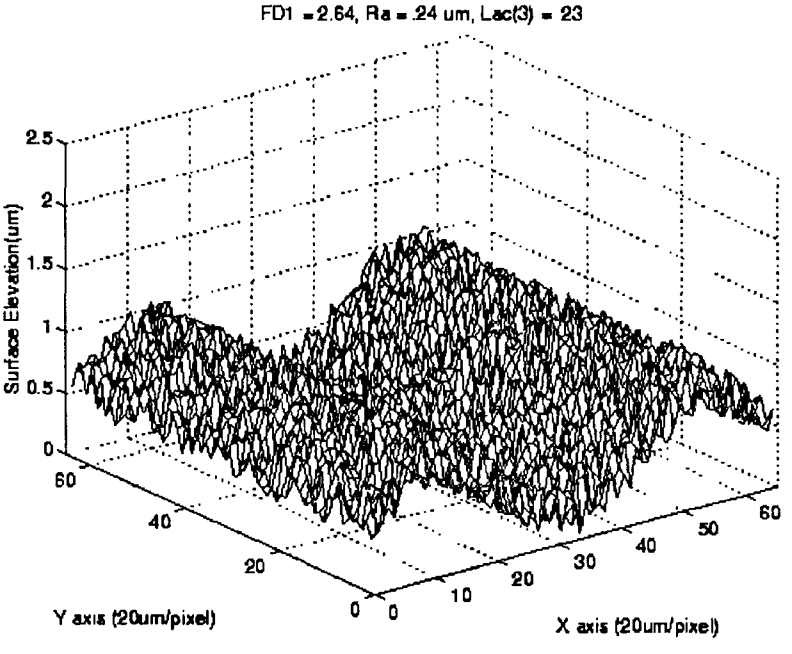

Figure 3.13 Low FD1, High Lac(3)

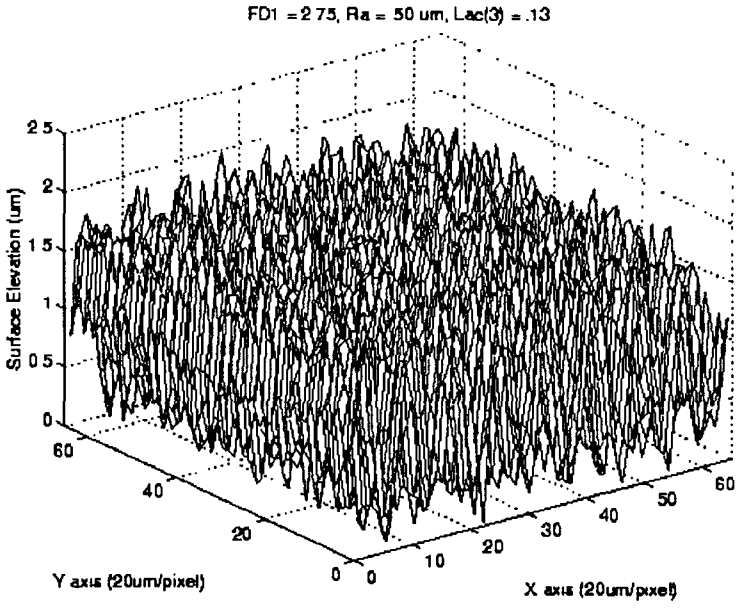

Figure 3.14 High FD1, Low Lac(3)

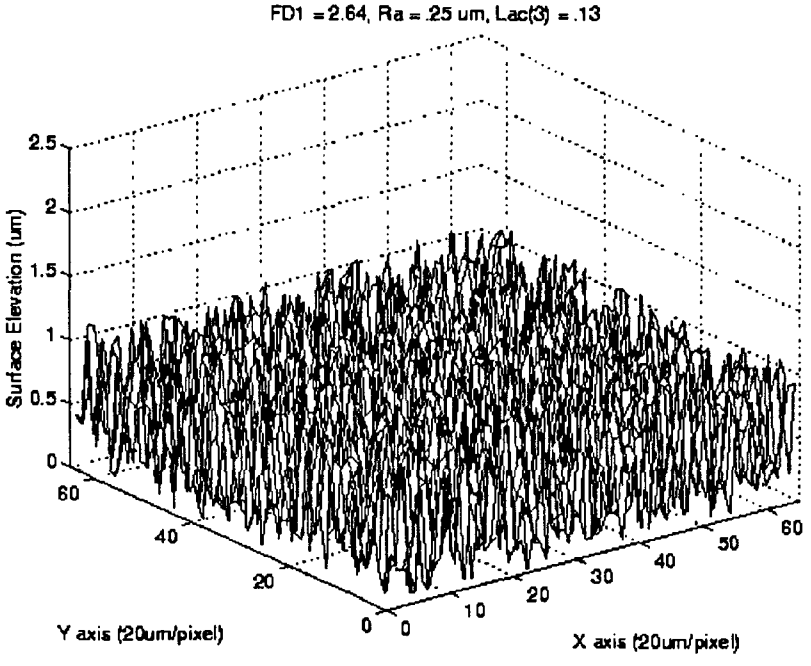

Figure 3.15 Low FD1, Low Lac(3)

3.3 Factorial Design Experiment

Experiments have been carried out to determine which environmental factors affect the characterization of the surface topography. A factorial design experiment[25,26] has been done at two levels with three variables: ambient light, filter for external light source, and grazing angle of external light source. The eight test conditions and the high and low values of the variables are listed in Table 3.1. A physical representation of the factorial design can be seen in Figure 3.16. From the experiments conducted it can be seen that the filter had the most significant effect as seen in equation 3.11. The filter is used to diffuse the light evenly over the machined surface. An external light source is used in conjunction with this light filter. None of the interactive terms were found to be significant. The angle of external light had a small effect on the fractal dimension but the angle can be kept at a fixed value. The final parameter that affected the fractal dimension was the ambient light.

Table 3.1 Test Conditions

Test	1	2	3	12	13	23	123
1	-1	-1	-1	1	1	1	-1
2	1	-1	-1	-1	-1	1	1
3	-1	1	-1	-1	1	-1	1
4	1	1	-1	1	-1	-1	-1
5	-1	-1	1	1	-1	-1	1
6	1	-1	1	-1	1	-1	-1
7	-1	1	1	-1	-1	1	-1
8	1	1	1	1	1	1	1

Test Condition	High (+1)	Low (-1)	
1	on	off	Ambient Light
2	High	Low	Angle of External Light Source
3	on	off	Filter for External Light Source

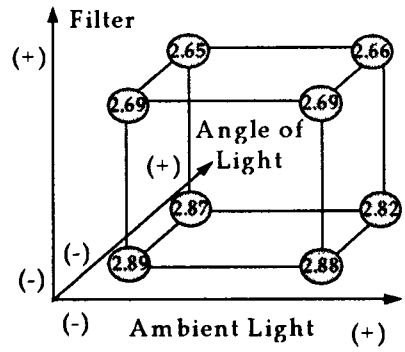

Figure 3.16 Factorial Design

The effect of the ambient light is small because of the external light source used to illuminate the surface. In a separate experiment to investigate ambient light an F-Test was done which showed that the change in ambient light was insignificant in the presence of an external light source with sufficient intensity.

$$FD = 2.77 - \frac{.012}{2}x_1 - \frac{.038}{2}x_2 - \frac{.20}{2}x_3 \qquad (3.11)$$

3.4 Summary Experiment

The goal of this research is to be able to characterize the topography of a machined surface. The realization of this goal has been accomplished using the route of characterizing the surface topography with fractal parameters. Designing a monitoring system and creating visualization software for the system are the next

steps in the research. The current system allows for the correlation of fractal parameters to roughness average. It has been shown that the monitoring system can be used to represent the surface topography of a machined surface using fractal parameters. The fractal dimension correlates very well to the Ra and a second parameter lacunarity can be used to indicate the dominant frequency of a machined surface or as a measure of the gaps in the surface.

Some factors that might keep the monitoring system from accurately describing the surface topography are environmental conditions such as ambient light, external light sources, filters, and angles of the external light sources. It has been found that a filter can be used to diffuse the light evenly over the machined surface. It has also been found that the ambient light is insignificant if there is an external light source with a reasonable intensity. The angle of the external light can have an effect on the outcome of the parameters that the vision system calculates, so it is important but not unreasonable to keep the light source at a fixed angle. The vision system is modified and re-designed to accommodate for shortcomings and environmental factors affecting the system performance.

Chapter 4

Design and Implementation of Optical-Based Vision System

4.1 Theory of Vision System Based on Scattering Theory

The principles behind the operation of the vision system involve both light scattering theory and a basic geometric interpretation of incoherent light reflection. Generally when referring to parameters to characterize a surface the following parameters are used: roughness, average slope, and waviness. Another approach is to define the surface as a set of interconnected facets. These facets are smooth multi-angled facets which make up the surface topography. The surface facet model is described in Section 2.5.1.2.

If a small 'ray cluster'of light is directed at a single facet on the surface then some of the radiation will be reflected in the specular direction corresponding to the incident angle and global orientation of the facet. If the facet has local roughness then some of the incident radiation will be scattered away from the specular direction. As a two-dimensional case, consider a quarter circle illuminated by a distant light source. As an individual light ray hits the surface of the object, much of the incident radiation is reflected away from the surface along the specular direction, which is equal to the incident angle as measured from the surface normal at the point of incidence. A lens collects any reflected light which is directed upwards, and projects it onto an imaging array that displays the intensity of the light reaching these sensors. The projected light intensity gradient does not provide a faithful

reconstruction of the actual surface. The maximum in the projected light intensity gradient occurs at the point where the specular direction is coincident with the upward-directed component of the scattered field, rather than at the top of the circle, while the minimum projected light intensity gradient coincides with the bottom of the circle as expected. This simple case demonstrates that the scattered light intensity does not necessarily correlate directly to the geometry of the illuminated surface. It would be ideal if a direct correlation did exist, but this does not invalidate the potential effectiveness of the optical system. Although it is clear that the scattered field in a given direction over an area of a surface is not proportional to the height variation across the illuminated area, there is a unique relationship between the surface geometry and the scattered field. This relationship takes into the account the slopes of the 'roughness elements' across the surface. In order to quantify this relationship, the integrated scattering/surface facet reflection model can be combined with knowledge of the facet orientations (facet slopes) to provide a mathematical model of the scattered light field.

In order to determine the mean scattered power from a particular facet, the scattering due to each wavelength of incident radiation must be calculated, and the resulting scattered field determined by the superposition of the scattering due to each wavelength. Since the light source used to illuminate the surface does not have constant power across the visual spectrum, a function $C(\lambda)$ is introduced. This

function represents the ratio of power from a particular wavelength to the total spectral power of the incident radiation as shown in equations 4.1 and 4.2.

$$C(\lambda_n) = \frac{P(\lambda_n)}{\int_{\lambda_{min}}^{\lambda_{max}} P(\lambda)d\lambda} \tag{4.1}$$

$$\int_{\lambda_{min}}^{\lambda_{max}} C(\lambda)d\lambda = 1 \tag{4.2}$$

The scattering equation is integrated over the incident spectral range, resulting in

$$\Psi_{i,j,\frac{\pi}{2}} = \int_{\lambda_{min}}^{\lambda_{max}} \left\{ C(\lambda) e^{-g} \left[\rho_o^2 + \frac{\pi F T^2}{A} \sum_{m=1}^{\infty} \frac{g_{i,j}(\lambda)}{m!m} \exp\left(\frac{-V_{xy}^2 T^2}{4m} \right) \right] \right\} d\lambda \tag{4.3}$$

where λmin and λmax are the lower and upper limits of the spectrum to which the optical receiver is sensitive. Note that Equation 4.3 assumes the global incident angle is constant over the full illuminated area, which is not entirely true for the vision system at hand. However, this fact can be overlooked for the current approximation to the scattered field.

Equation 4.3 dictates the scattered power in the observation direction for a given facet defined by the subscripts i and j. This assumes the facets can be identified in terms of a two-dimensional nxm grid. This notation is convenient, as the facets can be set to the size of a pixel. The resolution of the camera is 510x492 pixels. The surface can be modeled as a 510x492 grid of interconnected facets, with each facet scattering the light incident on the facet into a corresponding pixel in the CCD camera. This is reasonable as long as the surface area covered by each facet is

small enough compared to the global roughness of the surface. Therefore the camera magnification and resolution must be sufficient so that the area of the surface which scatters light into an individual CCD pixel is smaller than about ½ the lower cutoff period of the global surface roughness[20].

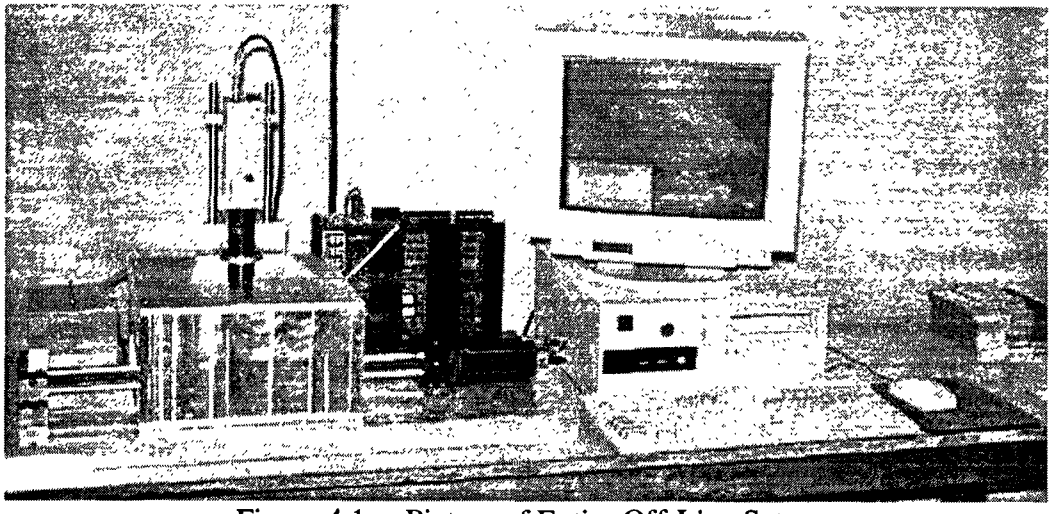

Figure 4.1 Picture of Entire Off-Line Setup

4.2 Components of Surface Monitoring and Characterization System

An important method for determining the roughness of a surface is the visualization of the surface that can be performed using an optical area based method. The current standard for characterizing surface roughness is through a surface profilometer which is a line based contact method. In this research a software package has been developed which is capable of visualizing the surface topography of a machined surface. The software package provides immediate feedback of parameters used to characterize the surface topography, a 3-D reconstruction of the surface, a histogram of the height of the surface, and a live

captured image of the machined surface. The software package is integrated with a hardware system which is developed to optically acquire data from a machined surface.

The main components of the hardware system consist of a CCD camera, a frame grabber, and a personal computer. The CCD camera using a high magnification lens system provides a video signal which a frame grabber converts into an 8-bit gray scale digital image at a rate of 30 frames per second. The frame grabber acquires a 510 x 492 pixel image which represents the activation levels of the CCD elements in the camera. The gray level image is a matrix of values which represent the intensity of each pixel. This image is sent to a microcomputer for signal processing. A computer program is prepared to coordinate the above operational procedure.

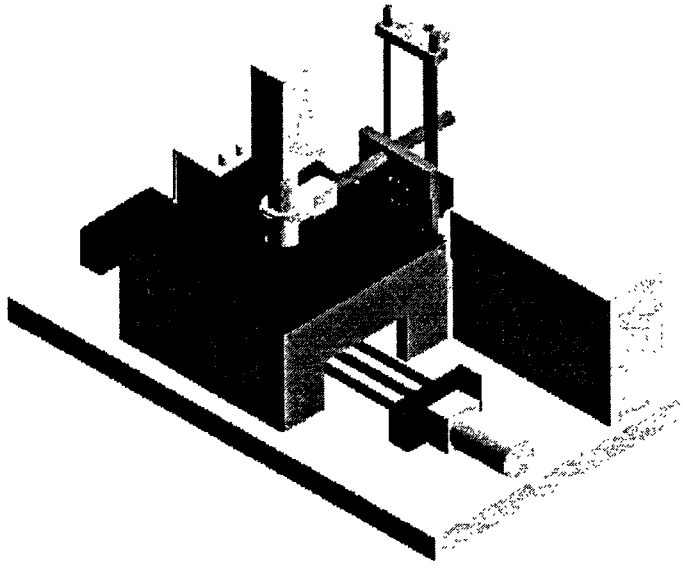

Figure 4.2 CAD Model of Components for Off-Line System

During the signal processing, the captured 2-D image is converted to a 3-D surface topography and displayed on a video monitor using the developed image processing package. The scattered light pattern in the image is examined, and the fractal dimension is calculated and then used as a system performance index for the purpose of monitoring the machined surface.

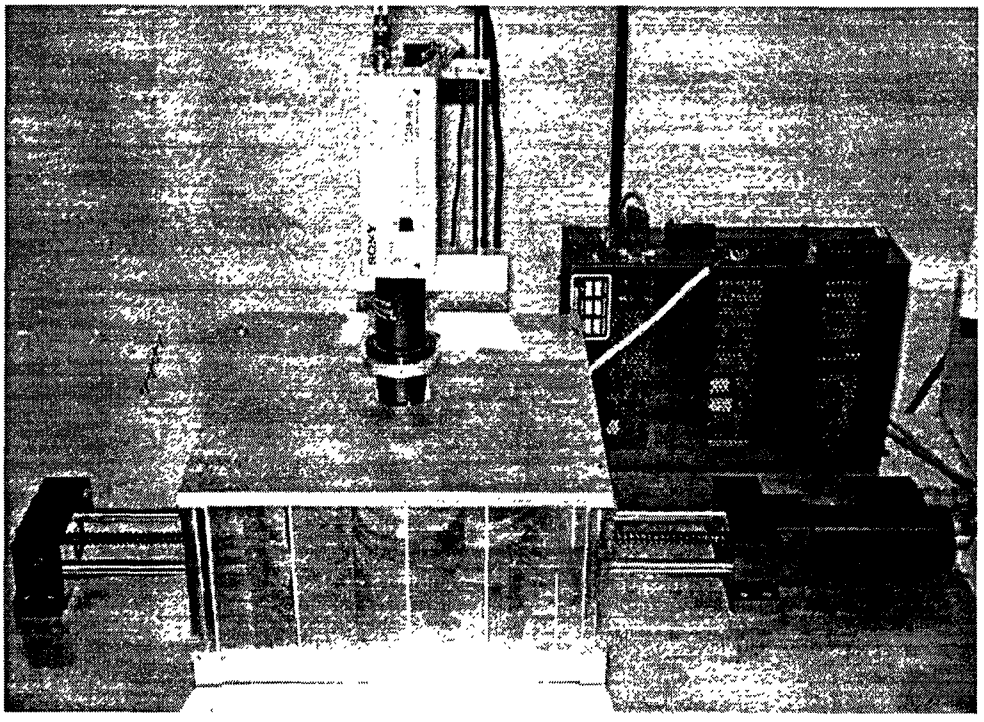

Figure 4.3 Picture of Off-line Hardware

In order for the system to have any meaning, the values obtained from the monitoring system have to be given a physical representation. This is carried out using an external calibration. The fractal dimensions obtained from the system are calibrated to a roughness average obtained from a profilometer. A correlation curve is created for a varying range of fractal dimensions and roughness averages.

The main objective of this investigation is to implement a monitoring system using fractal geometry for an effective estimation of the finish quality of a machined surface. A prototype of this system has been designed and is shown in figures above.

4.3 Description of Off-Line System

In order to determine the feasibility of the surface monitoring system an off-line prototype system has been built to determine the best lighting conditions, the best light source, and the general arrangement of the components. Initial experiments have been done to provide design constraints for the prototype. Some of the requirements that have to be built into the system are repeatability, immunity to environmental effects, and human factors. The repeatability can be controlled by creating an environment with constant lighting conditions. The design chosen used an enclosure around the workpiece with fixed lights. This design eliminates the effects of ambient light and angle of external light source. The system also was designed to provide uniform diffuse lighting in order to remove the effects of light orientation from the system. For example, if the part were illuminated along the feed direction the results would be different than if the part were illuminated 90^0 from the feed direction. The horizontal height adjustment system allows the camera to be focused on different samples by simply turning a leadscrew. The powerslide also provides an automated method of examining the parts. There are several

subsystems which make up the entire system. The subsystems are the camera height adjustment system, the lighting/light enclosure system, and the powerslide.

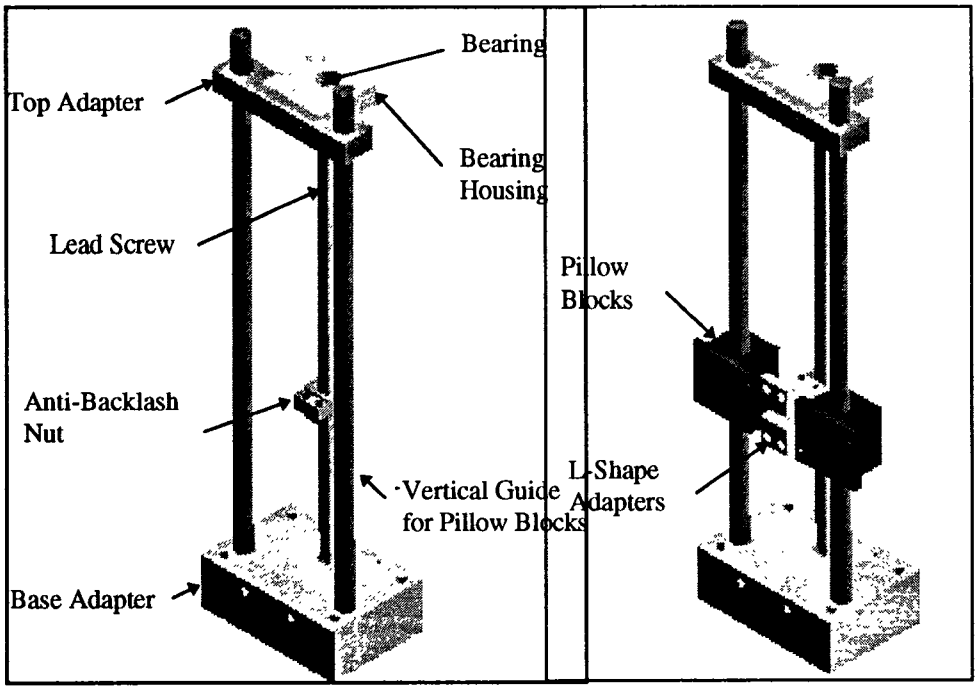

Figure 4.4 Camera Height Adjustment System

4.3.1 Height Adjustment System

The camera height adjustment system consists of a leadscrew, two bearings with bearing housings, an anti-backlash nut, a base, five adapters, two pillow blocks, three guide shafts and a camera holder. The lead screw(50 threads per inch) allows the camera to be manually adjusted for objects of varying size. As the leadscrew

turns, the anti-backlash nut raises the camera assembly. This is also useful for fine-tuning the focus, this apparatus is shown in Figure 4.4.

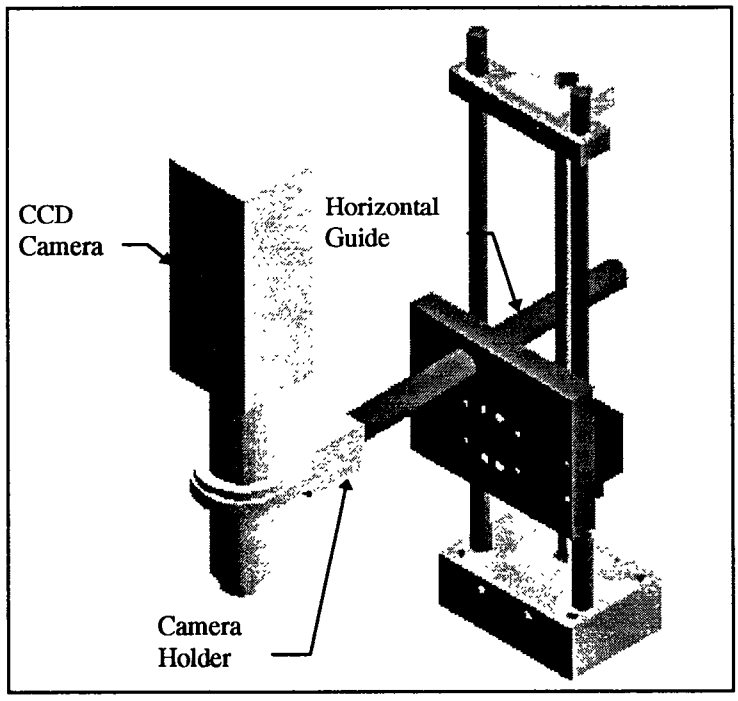

Figure 4.5 Camera Location on the Adjustment System

4.3.2 Light Enclosure

The next assembly is the light enclosure assembly. This assembly consists of four walls, a top, and lights. The inside of the walls are painted white with a flat paint in order to obtain even lighting while reducing glare. The walls are fitted with lights on each side. These lights can be used in any combination with each other. The lighting enclosure can be seen in Figures 4.6 and 4.7, which show the enclosure with and without its top.

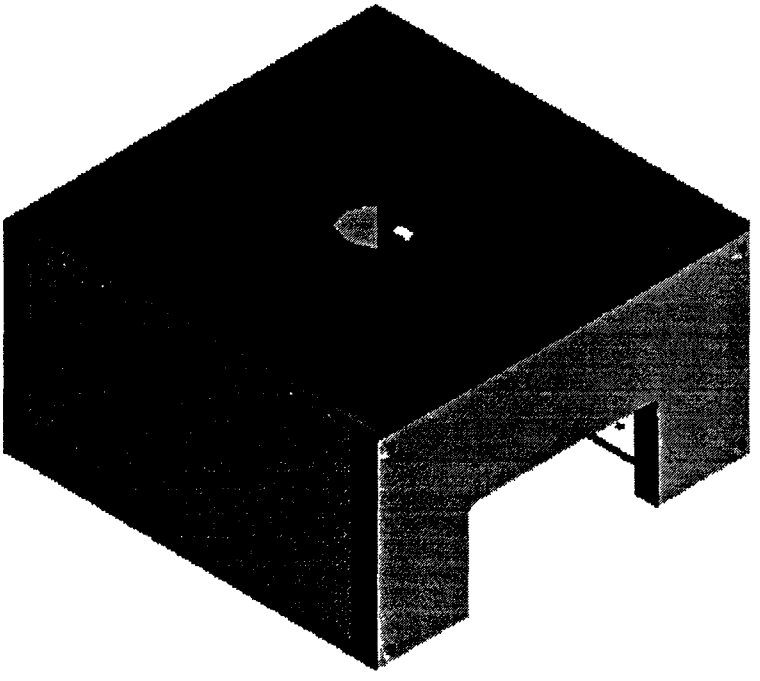

Figure 4.6 Enclosure with Top

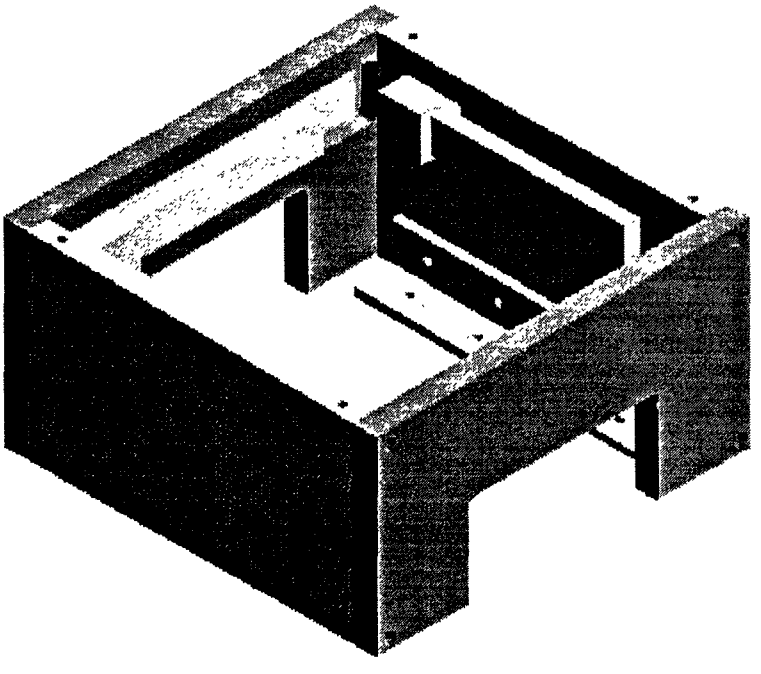

Figure 4.7 Enclosure without Top

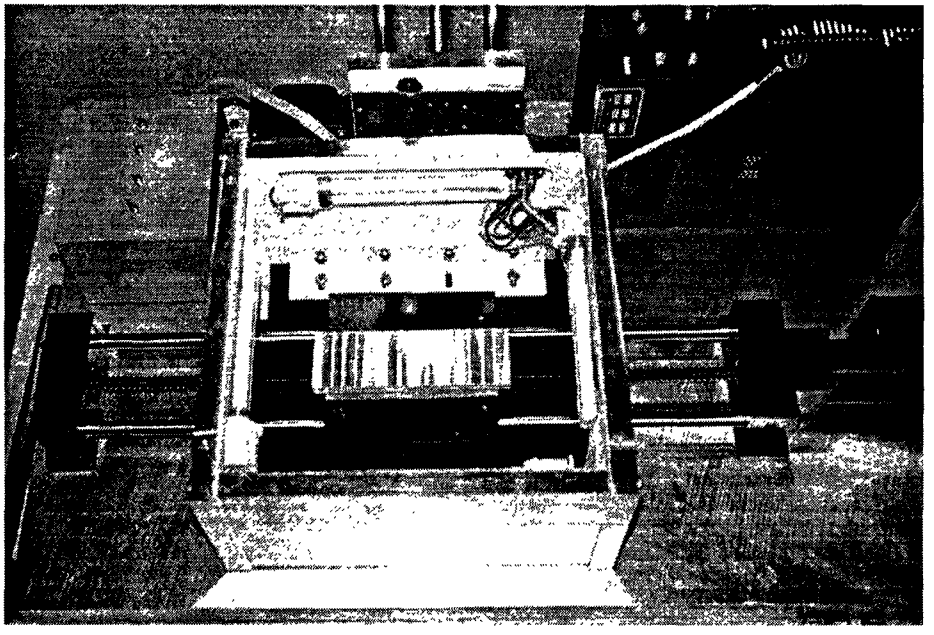

Figure 4.8 Picture of Light Enclosure

4.3.3 Selection of Light Source

In order to illuminate the specimen for data acquisition using the vision system a robust light source is required. The light source must have a minimum decay over time, have a low heat output, be of manageable size, and have relatively diffuse output. A brief description of the advantages and disadvantage of each light source follows:

Incandescent Lamps:

Incandescent lamps are one of most common light sources, having the lowest efficacy(lumens per watt) and shortest life. Its advantages are simplicity, low price for lamp and fixture, does not require a ballast to condition its power supply, light direction and brightness are easily controlled, and light produced has high color

quality. Light is produced in an incandescent lamp when the coiled tungsten filament is heated to incandescence(white light) by its resistance to a flow of electric current. There are many applications where the size, convenience, easy control, color rendering, and relatively low cost of incandescent lamps are suitable for a specific application.

General service incandescent lamps do not have good lumen maintenance throughout their lifetime. This is the result of the tungsten being evaporated off the filament during heating and being deposited on the bulb wall, thus darkening the bulb and reducing the lamp lumen output. The bulb has a lifespan of about 1000 hours. But the life of the bulb is dependent upon the frequency with which it is turned on and off, which places wear on the filament from the surge of current through it. Tungsten **halogen** lamps retain lumen output in excess of 95 percent of initial values throughout their lifetime.

Halogen Lamps:

A variation of the incandescent bulb is the halogen bulb. This is an improvement over incandescent bulbs invented by General Electric in 1958. In a regular incandescent bulb, the tungsten filament evaporates, and over time the inside of the bulb is coated with a fine coat of tungsten from condensed tungsten vapor. This coating will severely limit the light output of the bulb. In a halogen bulb, a small amount of one of the halogens (either Iodine or Bromine are used) is present and combines with the evaporated tungsten. This tungsten iodide or tungsten

bromide molecule has an affinity for the tungsten filament, and returns there and splits. The tungsten from this molecule returns to the filament while the halogen returns to the atmosphere inside the bulb. This process does not work unless the bulb jacket is at least 200 degrees Celsius. This is why halogen lamps are so hot, and must be taken into consideration where heat is a concern. Halogen lamps are 25-30% brighter than regular incandescent bulbs. The halogen cycle, as it is called, takes place in a very small capsule, as it is easier to maintain the high temperature required for the halogen cycle to operate in a smaller space. This capsule is placed inside another glass capsule which serves as the bulb's outer casing and reduces the heat. The life of a halogen bulb is about 2000 hours.

Fluorescent Lamps:

The most common light source is the fluorescent lamp. An electric arc is produced between two electrodes which can be several feet apart depending on the length of the tube. The ultraviolet light produced by the arc activates a phosphor coating on the inside wall of the tube, causing light to be produced. Fluorescent lamps require a ballast to strike the electric arc in the tube initially and to maintain that arc. Proper ballast selection is important for optimum light output and lamp life. Fluorescent lamps are available in a variety of colors but the most common are cool white, warm white and lite white. Fluorescent lamps are linear light sources that have low brightness when compared to point sources(incandescent). While generally good, lumen maintenance throughout the lamp lifetime is a problem for

some fluorescent lamp types. Fluorescent lights undergo an undesirable phenomenon known as "cathode decay" that causes, over time, less energy to be transferred through the mercury vapor. The net effect is that the tube will emit less and less light as it gets older. To all appearances, the tube will put out the same amount of light until it suddenly stops dead; this can take years. The drop off in light output is an exponential decay, the tube should optimally be replaced every six months to avoid the ill effects of cathode decay. Fluorescent lights are expensive to install but cheap to operate. They emit about four times as much light per unit of electricity as incandescent lights.

High Intensity Discharge Lamps:

Four types of lamps fall under this category(mercury vapor, metal halide, high pressure sodium and low pressure sodium). These lamps produce an arc between electrodes like fluorescent lamps but they take several minutes to warm up. Mercury vapor lamps are in limited use in today's lighting systems because fluorescent and other high intensity discharge sources have passed them in both lamp efficacy and system efficiency. Metal halide lamps have distinct drawbacks, including a short life, long restrike time, and tendency to shift colors as the light ages. High pressure sodium lamps have a primary drawback of rendering some colors. The low sodium light has the highest efficacy but it produces an almost pure yellow light. These lamps produce a high light output quite efficiently; however, they can be quite expensive to install initially and may require a fan for cooling in the

housing reflector as they produce phenomenal amounts of heat. HID lamps require a ballast, and almost every bulb requires its own type of ballast. The ballasts are expensive and bulky. HID lamps are built like halogen bulbs. A small capsule contains the vapor that an arc is sent through. This capsule is in turn encased in the much larger outer bulb body. There is a high level of UV generated by the inner capsule that is filtered by the outer capsule[27].

Light Source Chosen:

After weighing the factors for the lights it was decided that fluorescent lighting would prove to be the optimum light source for the vision system. The main reasons were that it had a minimum of heat generated, provided a line source instead of a point source of light, and fitted easily into the enclosure. Another factor for choosing the fluorescent bulbs was that if the bulbs are replaced every six months there is nominal decay. There is also no tungsten buildup with the lights. One problem is that the fluorescent lights are not variable in nature, but this can be overcome by varying the filtering of the light.

4.3.4 Design of Enclosure

4.3.4.1 Light Enclosures:

There are a variety of basic lighting techniques. The Machine Vision Association of the Society of Manufacturing Engineers has compiled a set of basic lighting techniques and light enclosures. This list also appears in "Applied Image

Processing"[28]. These lighting techniques and enclosures are summarized below and each system has been studied to choose the desired characteristics for the vision system lighting enclosure which can be modeled from the existing lighting enclosures.

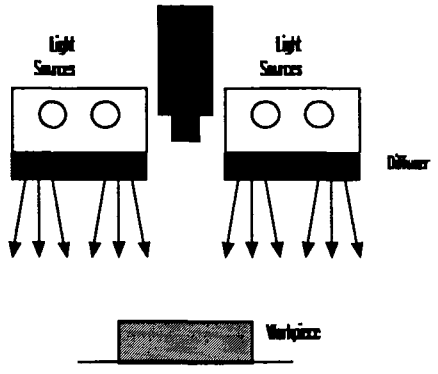

Figure 4.9 Diffuse Front Lighting

1). Diffuse Front Lighting: Used for general top lighting.

The advantages are: soft, fairly non-directional, reduces glare on metallic surfaces, relatively easy to implement. The disadvantages are: edges of parts may be fuzzy, low contrast on monochrome parts.

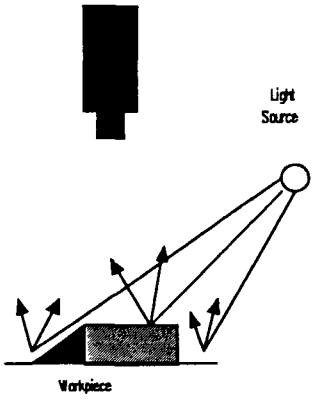

Figure 4.10 Directional Front Illumination

2). **Directional Front Illumination:** Creates shadows and will not reflect into the camera if surface is highly reflective. The advantages are: easy to implement, good for casting shadows, fiber optic delivery in many configurations. The disadvantages are: may create unwanted shadows, illumination is uneven.

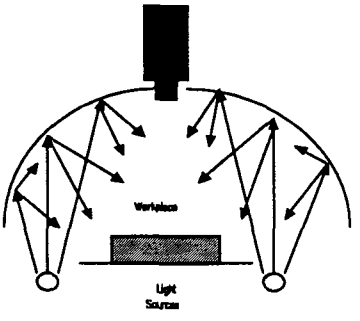

Figure 4.11 Light Tent

3). **Light Tent**(cloudy day effect): Non-directional, totally diffuse top lighting that produces an effect similar to the illumination observed on a cloudy day. Good for metal parts (rivets, ball bearings) and electronic components. The advantages are: eliminates glare, eliminates shadows. The disadvantages are: must surround workpiece, can be costly, size.

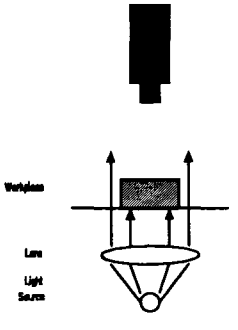

Figure 4.12 Collimated Back Lighting

4). Collimated Back Lighting: Back lighting through a pseudo collimating lens so that the light rays are pseudo parallel. The advantages are: produces very sharp edges for accurate gauging. The disadvantages are: difficult to implement if material handling interferes, may be too bright for camera without neutral density filters.

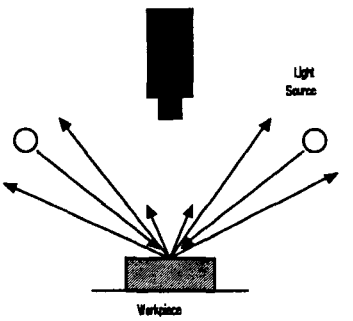

Figure 4.13 Dark Field Illumination

5). Dark Field Illumination: Incident light reflects away from the camera and illumination is created from specular reflections. The advantages are: illuminates defects, provides a high contrast image in some applications. The disadvantages are: does not illuminate flat smooth surfaces.

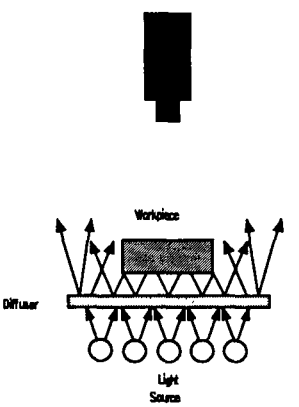

Figure 4.14 Diffuse Backlighting

6). Diffuse Backlighting: Light is on the opposite side of the part as the camera and goes through a diffusing material such as lexan or opal glass. The advantages are: easy to implement, creates silhouette of part, very high contrast image, low cost. The disadvantages are: edges or parts may be fuzzy, difficult to implement if material handling interferes.

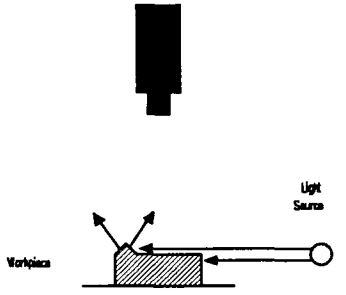

Figure 4.15 Low Angle Illumination

7). Low Angle Illumination: Incident lighting almost horizontal to the surface of the part. The advantages are: shows topological defects. The disadvantages are: single source will produce uneven lighting across surface.

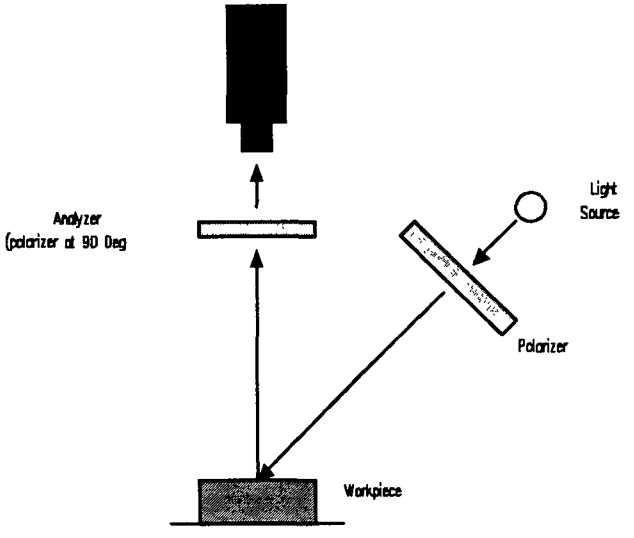

Figure 4.16 Polarized Front Illumination

8). Polarized Front Illumination: Front lighting with a polarizer on the light and a cross-polarizer on the lens. The advantages are: eliminates glare. The disadvantages are: reduces amount of light into the lens significantly.

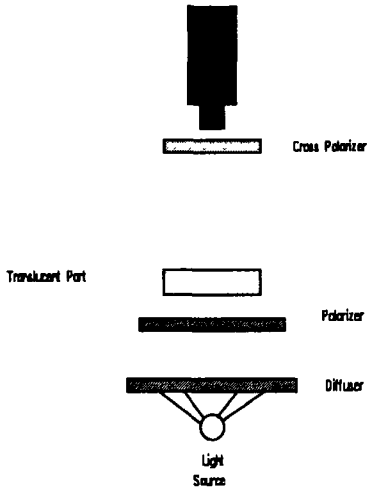

Figure 4.17 Polarized Backlighting

9). Polarized Backlighting: Polarizer and cross-polarizer are on opposite side of the part over some form of backlighting. The advantages are: highlights certain types of features or defects in translucent materials, relatively easy to implement. The disadvantages are: only works for birefringent features, edges of parts may be fuzzy, difficult to implement if material handling interferes.

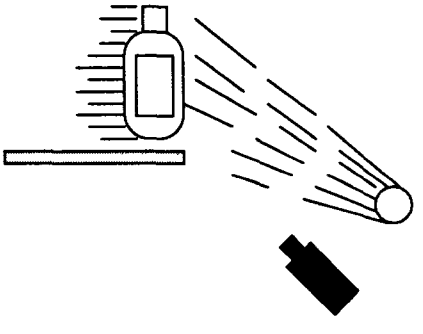

Figure 4.18 Strobed Illumination

10). Strobed Illumination: Microsecond duration lighting used to freeze the motion of moving parts. The advantages are: crisp images with no blurring, can be area, fiber optic or LED, very long lifetime. The disadvantages are: more costly than standard sources, requires accurate timing with camera, must be shielded from personnel.

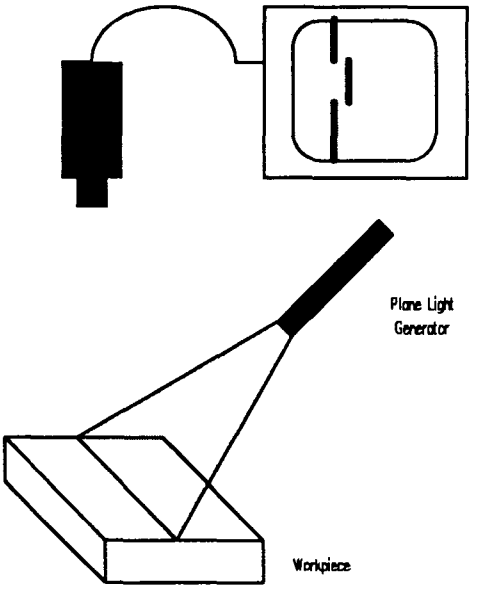

Figure 4.19 Structured Light

11). Structured Light: Plane of light generated via structured white light with focusing optics, or laser line converter, used to show contour/3D information of part. The advantages are: shows 3D information, produces high contrast on most parts, laser frequency can be easily band pass filtered. The disadvantages are: lasers above 5mW pose safety issue, hard to image on some metals and black rubber.

12). Coaxial Lighting: Illumination is along the same path as the camera's viewing path. The advantages are: eliminates shadows, uniform illumination across

FOV. The disadvantages are: complicated to implement, harsh illumination for shiny surfaces.

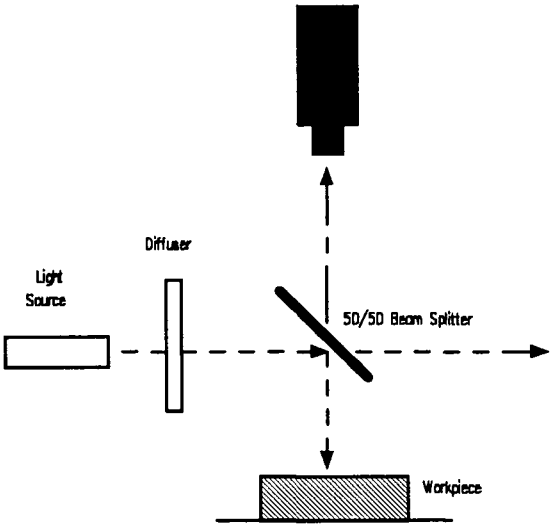

Figure 4.20 Coaxial Lighting

The applicable characteristics of the above enclosures were designed into the enclosure. The three most applicable designs were the Diffuse Front Lighting Illumination, the Dark Field Illumination and the Light Tent. From the factorial design experiments performed previously it was clear that orientation of the light source would directly affect the results obtained from the vision system. In order to overcome this problem the system should be able to remove part orientation bias. The method introduced in this enclosure to provide this requirement was to illuminate the part with diffuse light from all directions. Figure 4.21 illustrates the filters used to diffuse the light before it reached the specimen. The device was

designed to encompass the workpiece in order to provide even and controlled lighting conditions. Also, diffuse lighting without glare from the enclosure was a requirement that was satisfied.

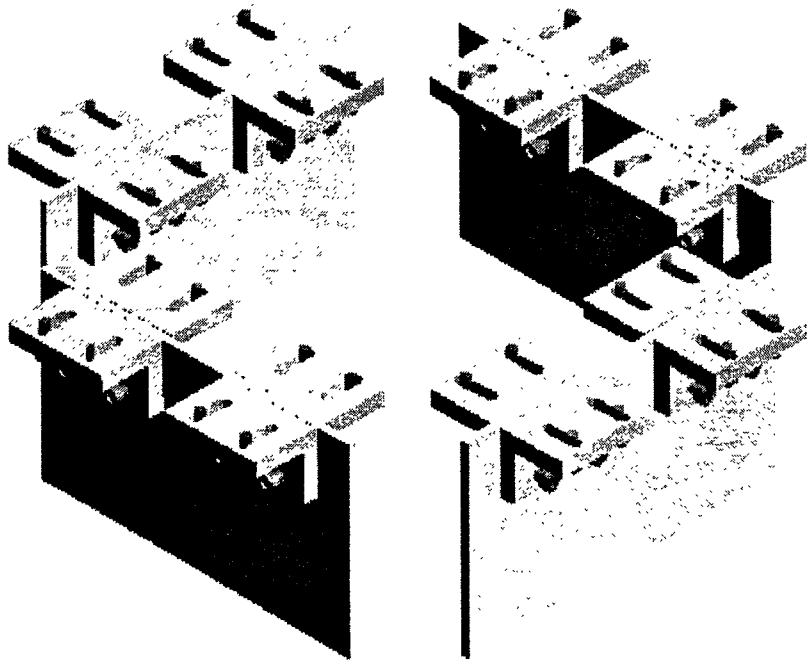

Figure 4.21 Filters

4.3.5 Powerslide

The final assembly is the powerslide which is mounted directly to the base of the system. The powerslide allows horizontal positioning of the machined specimen. The powerslide is also used to determine how fast a feed the specimen can be traveling and still get a clear picture of the workpiece. The Thompson Industry powerslide is translated with a stepper motor which is controlled by a Compumotor

Controller. The controller is programmed with the x programming language which allows relative and absolute motion commands.

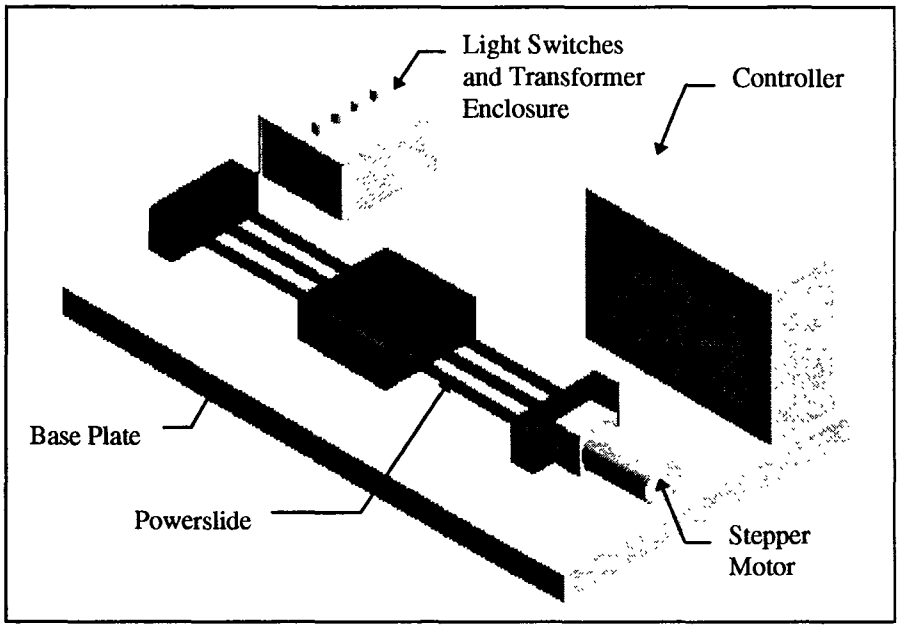

Figure 4.22 Base

4.3.6 Reasoning Behind Off-Line System

In designing an off-line system to measure the surface roughness of a machined surface several factors were kept in mind. The system would eventually be used to model a system which can be implemented on a CNC milling machine for in-process measurement of surface roughness. Two conditions that cannot be modeled by the off-line system are vibration and the interference from coolant and machined chips. Don DeVoe has done factorial design experiments to determine that vibration during machining does not affect the images captured by the CCD camera. The coolant and chips can be removed from the surface before the camera captures an image, by using compressed air. The factors that the system does take

into account are the lighting conditions and the general setup of the apparatus. The off-line system has an additional capability of being able to enclose the specimen and keep out ambient light. The system also can use the powerslide to determine the fastest feed that can be used while machining and still get a recognizable image.

The second major reason for an off-line system is to allow the measurement of the roughness of parts that were not produced using the milling process. Often, a treatment will be performed on a surface if it is going to undergo sliding contact with another solid. Some of these treatments add material and some remove material. The addition of material to a part can be in the form of plating, or coating. The removal of material can be in the form of grinding or etching. Other operations that a surface might undergo are bead blasting, polishing and blasting. An additional way to measure the roughness of these parts is necessary because they no longer have the same roughness as when they were milled. The off-line system is an effective way of assessing the surface texture after the above operations have taken place, or even in between if necessary.

4.4 Software

A PC windows based software package has been developed using Borland C++ 4.0 to acquire and manipulate data for the vision system. The data comes from the frame grabber via the CCD camera. The software package has been designed to present the user with four windows. The windows include a live display of the image from the CCD camera, a 3-D surface plot, a histogram and a section with

data. The live image can be stopped, using the Stop command on the tool bar, this action will also stop the acquisition of data. In order to re-start the acquisition of data, the Acquire command is used. The 3-D surface plot is created using the x-y position of the pixels as the x and y coordinates of the system. The light level for each pixel is used to represent the height of each position on the image. The histogram is created to show that the surface has a normal distribution. Some lighting conditions can affect the histogram. The histogram can be shifted or have additional peaks if the lighting conditions do not illuminate the machined surface evenly. The Idle graph command on the menu bar can be used to stop redrawing the 3-D surface plot and histogram if increased speed is desired. The data that is displayed by the program is updated instantaneously as each image is captured. The data that can be displayed is the fractal dimension, the lacunarity, the mean, the standard deviation, the skewness, the kurtosis, the roughness average, etc. The software has the capability of adding new algorithms to the program. Note an MS-DOS program has also been created which only displays the live image and acquires data. This program can be used for quick and dirty work.

Chapter 5

Experimental Setup and Results

5.1. Experimental Procedure

In order to test the effectiveness of using the vision system to characterize the surface topography, a base standard is needed to compare with the results of the vision system. When the results of the vision system are discussed, the main concern is the fractal dimension which is being used to characterize the surface roughness. Since the current standard and most widely accepted method of determining the surface roughness is by using a stylus profilometer to measure the Ra, the values obtained from the vision system will be correlated to those obtained from the profilometer.

The correlation obtained between the standard method and the vision system parameters can be used to calibrate the vision system. In order to calibrate the system, a number of samples with roughness values between the upper and lower limits for the system are required. In this research the main focus is on the roughness values obtained through the milling process. A set of samples should be machined with the milling machine in order to calibrate the system. The basic procedure for conducting the experiments with the vision system is as follows:

1. Machine samples with CNC milling machine.
2. Take traces with stylus profilometer.
3. Put specimens through vision system.

4. Use regression analysis to fit curve between stylus measurement and optical measurement.

5.2. Factors Affecting First System

The first off-line setup for the vision system consisted of a fiber optic light source used to illuminate the machined surfaces. The system suffered from several environmental factors which included the angle of the light, the orientation of the light, the light intensity and the ambient light. It has already been determined in this research that the effect of ambient light can be insignificant if an external light source is used to illuminate the surface. In order to determine the effect that the remaining factors had on the system performance, a factorial design has been done. Two other factors have been included in the experiment and they are the magnification and the surface roughness. The reason for including the surface roughness is to show that the environmental effects can affect the results as much as the roughness. The magnification is also studied to investigate its effect on the system performance. To test the effect of the aforementioned variables on the system performance, a full factorial design experiment is conducted.

Table 5.1 Variables

	Variable	Low Level	High Level
1	Ra.	0.19μm	7.50μm
2	Grazing Angle	45	55
3	Magnification	15	2.5
4	Light Orientation	Front	Side
5	Light Intensity	25%	50%

Table 5.2 Factorial Design Grid

	R	G	M	O	I																									FD1	FD1
Test	I	1	2	3	4	5	12	13	14	15	23	24	25	34	35	45	123	124	125	134	135	145	234	235	245	345	1234	1235	1245	2345	1345	12345	tnal 1	tnal 2
1	+	-	-	-	-	-	+	+	+	+	+	+	+	+	+	+	-	-	-	-	-	-	-	-	-	-	+	+	+	+	+	-	2.793	2.785
2	+	+	-	-	-	-	-	-	-	-	+	+	+	+	+	+	+	+	+	+	+	+	-	-	-	-	-	-	-	+	-	+	2.879	2.873
3	+	-	+	-	-	-	-	+	+	+	-	-	-	+	+	+	+	+	+	-	-	-	+	+	+	-	-	-	-	-	+	+	2.834	2.837
4	+	+	+	-	-	-	+	-	-	-	-	-	-	+	+	+	-	-	-	+	+	+	+	+	+	-	+	+	+	-	-	-	2.911	2.917
5	+	-	-	+	-	-	+	-	+	+	-	+	+	-	-	+	+	-	-	+	+	-	+	+	-	+	-	-	+	-	-	+	2.688	2.667
6	+	+	-	+	-	-	-	+	-	-	-	+	+	-	-	+	-	+	+	-	-	+	+	+	-	+	+	+	-	-	+	-	2.787	2.764
7	+	-	+	+	-	-	-	-	+	+	+	-	-	-	-	+	-	+	+	+	+	-	-	-	+	+	+	+	-	+	-	-	2.729	2.728
8	+	+	+	+	-	-	+	+	-	-	+	-	-	-	-	+	+	-	-	-	-	+	-	-	+	+	-	-	+	+	+	+	2.807	2.814
9	+	-	-	-	+	-	+	+	-	+	+	-	+	-	+	-	-	+	-	+	-	+	+	-	+	+	-	+	-	-	-	+	2.666	2.661
10	+	+	-	-	+	-	-	-	+	-	+	-	+	-	+	-	+	-	+	-	+	-	+	-	+	+	+	-	+	-	+	-	2.780	2.790
11	+	-	+	-	+	-	-	+	-	+	-	+	-	-	+	-	+	-	+	+	-	+	-	+	-	+	+	-	+	+	-	-	2.675	2.674
12	+	+	+	-	+	-	+	-	+	-	-	+	-	-	+	-	-	+	-	-	+	-	-	+	-	+	-	+	-	+	+	+	2.793	2.787
13	+	-	-	+	+	-	+	-	-	+	-	-	+	+	-	-	+	+	-	-	+	+	-	+	+	-	+	-	-	+	+	-	2.542	2.534
14	+	+	-	+	+	-	-	+	+	-	-	-	+	+	-	-	-	-	+	+	-	-	-	+	+	-	-	+	+	+	-	+	2.668	2.668
15	+	-	+	+	+	-	-	-	-	+	+	+	-	+	-	-	-	+	-	+	+	+	-	-	-	-	-	+	+	-	+	+	2.555	2.540
16	+	+	+	+	+	-	+	+	+	-	+	+	-	+	-	-	+	+	-	+	-	-	+	-	-	-	+	-	-	-	-	-	2.685	2.683
17	+	-	-	-	+	+	+	+	-	+	+	-	+	-	-	-	-	+	-	+	+	-	+	+	+	+	-	-	-	-	-	+	2.824	2.834
18	+	+	-	-	+	-	-	-	+	+	+	-	+	-	-	+	+	-	+	-	-	-	+	+	+	-	+	+	+	-	+	-	2.903	2.920
19	+	-	+	-	-	+	-	+	+	-	-	-	+	+	-	-	+	+	-	-	+	+	+	-	-	+	-	+	+	+	-	-	2.888	2.887
20	+	+	+	-	-	+	+	-	-	+	-	-	+	+	-	-	-	-	+	+	-	-	+	-	-	+	+	-	-	+	+	+	2.953	2.950
21	+	-	-	+	-	+	+	-	+	-	-	+	-	-	+	-	+	+	-	+	+	-	+	-	+	-	-	+	-	+	+	-	2.722	2.713
22	+	+	-	+	-	+	-	+	-	+	-	+	-	-	+	-	-	+	-	-	+	-	+	-	+	-	+	-	+	+	-	+	2.813	2.798
23	+	-	+	+	-	+	-	-	+	-	+	-	+	-	+	-	+	-	+	-	+	-	+	-	-	+	-	+	-	+	-	+	2.777	2.769
24	+	+	+	+	-	+	+	+	-	+	+	-	+	-	+	-	-	+	-	+	-	+	-	+	-	-	-	-	+	-	+	-	2.849	2.841
25	+	-	-	-	+	+	+	+	-	-	+	-	-	-	-	+	-	+	+	+	+	-	+	+	-	-	-	-	+	+	+	-	2.679	2.675
26	+	+	-	-	+	+	-	-	+	+	+	-	-	-	-	+	+	-	-	-	-	+	+	+	-	-	+	+	-	+	-	+	2.788	2.796
27	+	-	+	-	+	+	-	+	-	-	-	+	+	-	-	+	+	-	-	+	+	-	-	-	+	-	+	+	-	-	+	+	2.693	2.689
28	+	+	+	-	+	+	+	-	+	+	-	+	+	-	-	+	-	+	+	-	-	+	-	-	+	-	-	-	+	-	-	-	2.799	2.798
29	+	-	-	+	+	+	+	-	-	-	-	-	-	+	+	+	+	+	+	-	-	-	-	-	-	+	+	+	+	-	-	+	2.559	2.557
30	+	+	-	+	+	+	-	+	+	+	-	-	-	+	+	+	-	-	-	+	+	+	-	-	-	+	-	-	-	-	+	-	2.678	2.689
31	+	-	+	+	+	+	-	-	-	-	+	+	+	+	+	+	-	-	-	-	-	-	+	+	+	+	-	-	-	+	-	-	2.580	2.560
32	+	+	+	+	+	+	+	+	+	+	+	+	+	+	+	+	+	+	+	+	+	+	+	+	+	+	+	+	+	+	+	+	2.700	2.687

Table 5.3 Significant Effects

Effect	Value
Mean	2.748
1	0.102
2	0.028
3	-0.112
4	-0.145
5	0.027
14	0.020
24	-0.018

$$FD1 = 2.748 + \frac{0.102}{2}E_1 + \frac{0.028}{2}E_2 - \frac{0.112}{2}E_3 - \frac{0.145}{2}E_4 + \frac{0.027}{2}E_5 + \frac{0.020}{2}E_{14} - \frac{0.018}{2}E_{24} \qquad (5.1)$$

The main effects are summarized below:

Roughness[c1 = 0.102/2]

The parameter used in this research to characterize the roughness of a surface with the vision system is FD1. The Ra is expected to have a significant effect on FD1. The experiments showed that the roughness had a significant effect on FD1. All other variables must be kept constant in order for a correlation to be valid.

Grazing Angle[c2 = 0.028/2]

The light incident to the surface is varied between 45^0 and 55^0 in order to determine the effect of small variations in the grazing angle on the system performance. An earlier factorial experiment has shown that drastic changes in the angle are significant, therefore, it was desired to test if smaller variations were significant. Smaller variations, on the order of 10^0, continue to affect the system.

Magnification[c3 = -0.112/2]

The magnification was toggled between 15x and 25x to see if a drastic change in magnification would alter the fractal dimension by changing the area examined and the changing the amount of visible irregularities. This factor had a drastic effect not only because of the previous reasons but also because as the magnification increased, the image became considerably darker. This basically would have a similar effect to varying the intensity of the light. The auto-iris function has been turned off in order to reduce variations in measurements. The shutter of the camera stays open the same amount at all times with the auto-iris function disabled.

Light Orientation[c4 = -0.145/2]

The light orientation is expected to have a high significance because of the nature of milled surfaces. Milled surfaces are essentially one-dimensionally rough in the feed direction. The two orientations are along the feed direction and 90^0 from the feed direction. Higher fractal dimension values are obtained when the surfaces are illuminated along the feed direction due to the contrast developed by the peaks and valleys of the surface.

Light Intensity[c5 = 0.027/2]

Of the main effects, the light intensity appears to have the lowest effect. The reason for this is that it is only varied between 25% and 50% of the full intensity of the fiber optic device.

5.3. Factors Affecting New System

In the design of the new vision system, the effects of ambient light, the intensity of the light, the orientation of the light, and the grazing angle of the light were factors that had to be overcome. In order to overcome variation to the system due to ambient light, an enclosure was built around the specimen to shield it from ambient light. In order to negate the variations due to the orientation of the light and the grazing angle, there were several design innovations. The design included using diffuse lighting from all sides of the part. This lighting was created by four fluorescent bulbs which were diffused with white diffusers. The walls of the enclosure were also painted with flat white paint to prevent glare. The result of

these lighting conditions was to create a non-directionally lit environment. The effects of the ambient light and the grazing angle are clearly removed. The effect of the orientation should also be removed but this will be tested in a factorial design experiment. The other two factors that will be varied are the magnification and the roughness which should have a significant effect on the system.

Table 5.4 Variables

	Coded Test Conditions			Actual Test Conditions		
Test	x1	x2	x3	Ra. (μm)	Mag. (x)	Ori.
1	-1	-1	-1	0.19	15	Front
2	1	-1	-1	7.5	15	Front
3	-1	1	-1	0.19	25	Front
4	1	1	-1	7.5	25	Front
5	-1	-1	1	0.19	15	Side
6	1	-1	1	7.5	15	Side
7	-1	1	1	0.19	25	Side
8	1	1	1	7.5	25	Side

Table 5.5 Design Matrix

Test	I	Ra. 1	Mag. 2	Ori. 3	12	13	23	123	Trial 1	Trial 2	Avg.	Diff.	Var.
1	+	-	-	-	+	+	+	-	2.738	2.735	2.737	0.003	0.00000
2	+	+	-	-	-	-	+	+	2.864	2.868	2.866	0.004	0.00001
3	+	-	+	-	-	+	-	+	2.632	2.631	2.631	0.001	0.00000
4	+	+	+	-	+	-	-	-	2.737	2.733	2.735	0.004	0.00001
5	+	-	-	+	+	-	-	+	2.739	2.734	2.736	0.006	0.00002
6	+	+	-	+	-	+	-	-	2.865	2.862	2.863	0.002	0.00000
7	+	-	+	+	-	-	+	-	2.635	2.635	2.635	0.000	0.00000
8	+	+	+	+	+	+	+	+	2.739	2.736	2.737	0.003	0.00000
Effects	2.743	0.116	-0.116	0.001	-0.012	-0.001	0.002	0.000					

$$FD1 = 2.743 + \frac{0.116}{2}E_1 - \frac{0.116}{2}E_2 - \frac{0.012}{2}E_{12} \qquad (5.2)$$

Roughness[c1 = 0.116/2]

As with the previous experiments, in this experiment the roughness had a significant effect on FD1.

Magnification[c2 = -0.116/2]

The magnification was toggled between 15x and 25x to determine if a drastic change in magnification would alter the fractal dimension by changing the area examined and the changing the amount of irregularities that are visible. This factor had a drastic effect not only because of the previous reasons but mainly because as the magnification increased the image became considerably darker.

Light Orientation[c3 = 0.001/2]

The light orientation had almost no effect on the results as was expected. Any variation can be attributed directly to the comparison of the area of interest. The area of interest slightly changed when the part was rotated because of positioning errors.

The factorial design experiments on the two systems show the drastic improvement in reducing the number of variables which affect the system performance. The system takes care of problems relating to grazing angle, light orientation, light intensity, and ambient light. The main variable left that affects the system performance is the magnification and the usefulness of this parameter will be further investigated.

5.4 Factors Affecting Correlation of System

Fifty two samples have been machined with roughness values between 0.15 μm and 8.83 μm. The Ra is measured using a profilometer and three traces of each surface are taken. The traces are taken along the feed direction of the surface. The samples were machined with two endmills with 0.75 in. diameters, the first having two flutes and the second having four flutes. The machining conditions for the two flutes endmill are a depth of cut of 0.05 in., spindle speeds ranging between 400 and 1000 RPM, and feed rates ranging between 1.2 and 19.7 in/min. The machining conditions for the four flutes endmill are a depth of cut of 0.05 in., spindle speeds ranging between 400 and 1000 RPM, and feed rates ranging between 1.2 and 15.7 in/min. The machining conditions along with the average Ra of the three stylus traces for the 52 samples can be seen in Tables 5.6 and 5.7.

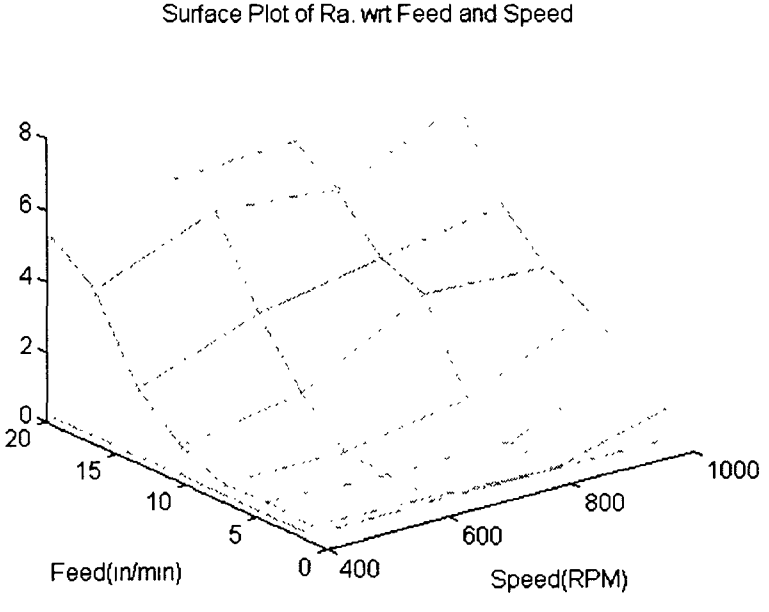

Figure 5.1 Surface Plot of Roughness Values

Table 5.6 Two Flutes Endmill Ra Measurements

	400 RPM (μm)	600 RPM (μm)	800 RPM (μm)	1000 RPM (μm)
0.03 m/min	1.18	0.20	0.33	0.44
0.06 m/min	1.79	0.45	0.40	0.58
0.10 m/min	2.65	1.13	0.53	0.52
0.18 m/min	3.37	3.56	1.64	1.05
0.25 m/min	4.50	3.99	3.38	2.16
0.40 m/min	6.70	5.33	5.70	4.42
0.50 m/min	5.2	6.1	5.98	5.33

Table 5.7 Four Flutes Endmill Ra Measurements

	400 RPM (μm)	600 RPM (μm)	800 RPM (μm)	1000 RPM (μm)
0.03 m/min	0.65	0.35	0.19	0.16
0.06 m/min	2.60	1.39	0.39	0.27
0.10 m/min	3.35	2.55	1.51	0.50
0.18 m/min	7.30	5.37	3.83	2.46
0.25 m/min	8.33	6.37	4.70	3.14
0.40 m/min	8.83	5.85	7.50	5.70

5.4.1 Machine Tool

Two different endmills have been used to machine the surfaces. The reason for using two different endmills is to determine whether surfaces generated using different tools would have an effect on the correlation of Ra to FD1. In all of the experiments the two flutes endmill has had a higher correlation than the four flutes endmill. Both sets of data can be fitted with the same curve and this indicates that the different endmill does not affect the characterization of the surface using the FD1. The four flutes endmill has a higher scatter than the two flute endmill. Figures

5.2 and 5.3 showing the correlation of FD1 to Ra The conditions for these correlations are magnification of 15x and white diffuser filters.

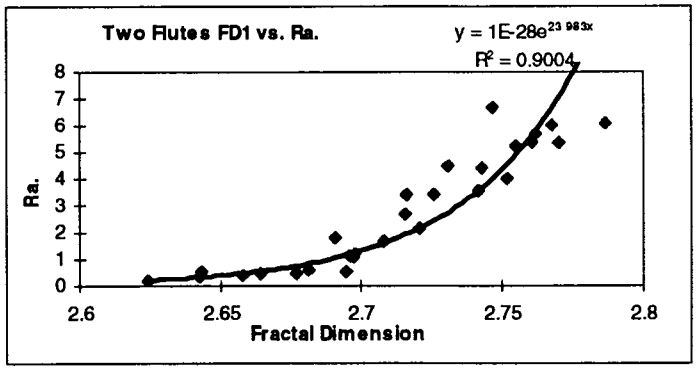

Figure 5.2 FD1 vs. Ra Two Flutes Endmill

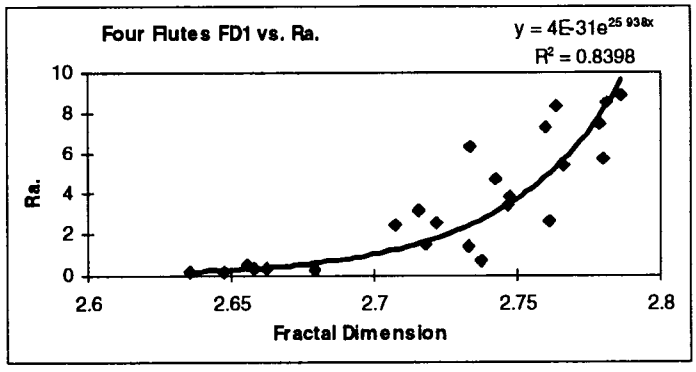

Figure 5.3 FD1 vs. Ra Four Flutes Endmill

5.4.2 Magnification

In order to test the effect of magnification on the effect of the correlation of Ra to the FD1, three tests were conducted with magnification values of 7.5x, 15x, and 30x. The magnification range of the camera is 7.5x to 30x. It was expected that the surfaces with a lower roughness value would require a higher magnification factor than that of surfaces with higher values. It was observed when performing

the experiments that with a magnification of 30x the rougher surfaces were not entirely characterized. This was due to the fact that the area the camera captured might be between two peaks of the surface. Also when a magnification factor of 7.5x was used not all of the roughness details of the finer surfaces could be seen. For the roughness range of 0.15 μm to 8.83 μm the correlation between the Ra and the fractal dimension was the highest with a magnification of 15x. An exponential curve was used to fit the data between the Ra and the fractal dimension. Table 5.8 shows the correlation coefficients for the three magnifications. The correlations were done individually with the two flutes endmills and four flutes endmills, and also with all of the 52 samples. Figure 5.4 shows the correlation between Ra and FD1 for all 52 samples and a magnification of 15x.

Table 5.8 Correlation Coefficients

	R values		
Mag.(x)	All	2 Flutes	4 Flutes
7.5	0.853405	0.959062	0.776981
15	0.926121	0.948894	0.916406
30	0.857205	0.856213	0.865159

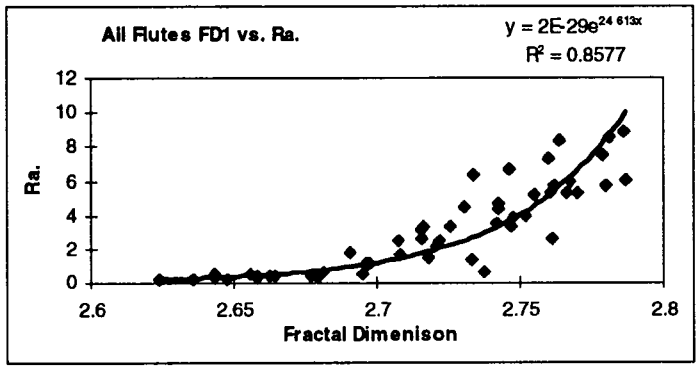

Figure 5.4 FD1 vs. Ra Magnification = 15x

5.4.3 Filters

Different filters are used to filter the light which illuminates the specimens in the lighting enclosure. The purpose of using different filters is to observe the effect on the correlation when electromagnetic radiation when different wavelengths are used to illuminate the surface. This might be useful when different materials are used. The filters can also be altered in order to vary the intensity of light. One of the more important uses for the filters will be to diffuse the light and produce a more uniform light distribution on the part surface. In these experiments the effect on the correlation will be examined when white diffuser filters, blue filters, green filters and red filters are used. There is not expected to be much of a change in the correlation of FD1 to Ra due to the change in wavelength used to illuminate the aluminum samples. The reflectance as seen in Figure 5.5 is nearly uniform for all wavelengths in the visible spectrum. The correlation coefficients for tests with two flute samples, four flute samples and all samples can be seen in Table 5.9. As can be seen from the Table 5.9 there is almost no difference in the correlations but the white diffusers do have the highest correlation as shown in Figure 5.6.

Table 5.9 Correlation Coefficients

	R Values		
Filter	All	2 Flutes	4 Flutes
green	0.8643	0.9301	0.8098
red	0.8875	0.9211	0.8777
white	0.8893	0.9521	0.8701
blue	0.8772	0.9195	0.8429

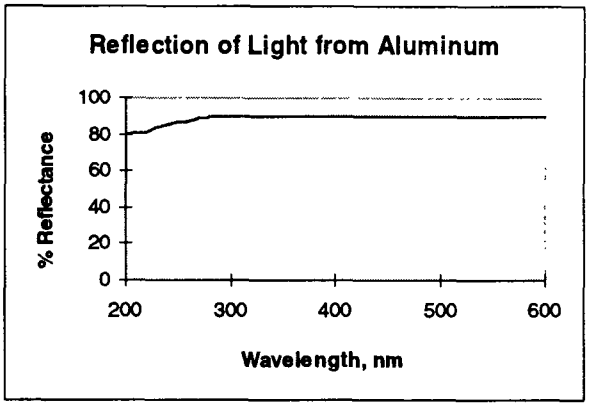

Figure 5.5 Reflectance of Light from Aluminum

	400 RPM (μm)	600 RPM (μm)	800 RPM (μm)	1000 RPM (μm)
0.03 m/min	1.18	0.20	0.33	0.44
0.06 m/min	1.79	0.45	0.40	0.58
0.10 m/min	2.65	1.13	0.53	0.52
0.18 m/min	3.37	3.56	1.64	1.05
0.25 m/min	4.50	3.99	3.38	2.16
0.40 m/min	6.70	5.33	5.70	4.42
0.50 m/min	5.2	6.1	5.98	5.33

Figure 5.6 FD1 vs. Ra White Diffuser Filters

5.4.4 Material

In order to test the adaptability of the system in characterizing different materials, a set of copper specimens were machined. Copper fits into the category of red metals as opposed to aluminum which was classified as a white metal. The samples were machined with a 5/8 in. endmill at a depth of cut equal to 0.05 in, similar to those machining conditions used for preparing aluminum specimens. A procedure, which is used to establish the calibration curve between FD and Ra measurements, is followed to establish the correlation between FD and Ra

measurements for the copper specimens. The feed and speed parameters along with the Ra values obtained are listed in Table 5.10.

Table 5.10 Ra Values for Copper

	500 RPM (μm)	600 RPM (μm)	700 RPM (μm)	800 RPM (μm)	900 RPM (μm)	1000 RPM (μm)
0.02 m/min	0.20	0.26	0.16	0.25	0.16	0.29
0.04 m/min	0.54	0.35	0.39	0.31	0.36	0.23
0.08 m/min	0.45	0.73	0.30	0.36	0.42	0.31
0.10 m/min	0.34	1.47	0.36	0.44	0.45	0.44
0.13 m/min	0.37	0.38	0.40	0.48	0.45	0.46
0.15 m/min	0.79	0.51	0.45	0.48	0.56	0.60
0.18 m/min	0.87	0.58	0.53	0.54	0.56	0.69

The magnification and filters were varied in order to determine their effects on the system correlation. The eight tests conducted were with two magnifications and four filters. Not one of the experiments showed a strong correlation between FD1 and Ra. Other parameters were also used to attempt to describe the surface but they were correspondingly unsuccessful.

In the experiments with copper a 5 μm radius stylus tip was used instead of a 10 μm radius stylus tip. The smaller stylus visibly scratched the surfaces due to their ductile nature. The smaller stylus produced a smaller contact area with the surface thus increasing the stress on the contact area. The stylus scratched the surface of the specimens negating any increase in sensitivity from having a smaller radius. The magnitude of the damage caused by the stylus on the surface finish is not known, because the effect on the Ra results obtained from the stylus measurements is not easily quantifiable. The correlations for copper samples should be viewed with caution. This damage caused by the stylus warrants a non-contact method of

analyzing the surface roughness of the samples. If the depth of the scratch is significant with respect to the height deviations of the surfaces then any results should be disregarded.

In order to establish an accurate correlation between the FD and Ra measurements, special attention was paid to obtaining Ra measurements from the machined surfaces formed on the copper specimens. Recognizing the fact that the hardness of copper material is significantly lower than that of aluminum material, extensive measurements taken from the copper surface may damage the finish condition of the copper specimens. A new type of surface profilometer, called Taylor Hobson Form Talysurf 120L, was used. The profilometer, which is housed at the National Institute of Standards and Technology, utilizes the technique of laser profilometry to avoid direct contact with the specimen being examined. Seven specimens prepared under seven different machining conditions were used. Two traces were taken from each of the seven specimens and a total of fourteen traces were taken. Plots and data obtained from these measurements are included in Appendix A.

The measurements taken on the specimens were at a different location on the specimen than the previous contact measurements. Since the region of measurements was moved on the specimen the seven specimens were analyzed with the vision system approximately at the new locations. The measurements were

taken at a magnification of 30x and using red filters. The correlation of FD1 and Ra can be seen in Figure 5.7.

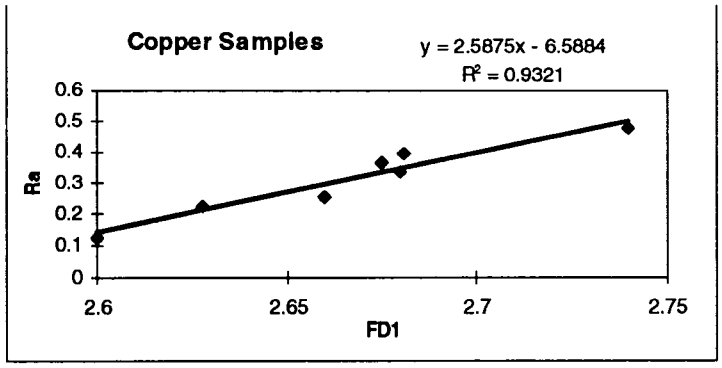

Figure 5.7 Correlation for Copper Samples

A comparison can be made between the copper samples in Figure 5.7 at a magnification of 30x with red filters and a set of aluminum samples in Figure 5.12 at a magnification of 30x with white filters. The Equations relating FD1 to Ra are as follows:

$$Ra = 2.62FD1 - 6.88 \qquad (5.3)$$

$$Ra = 2.59FD1 - 6.59 \qquad (5.4)$$

Equation 5.3 is for aluminum and Equation 5.4 is for copper. As can be seen from the two equations above the Ra obtained from both equations will have similar results.

In the following section a new set of aluminum samples were machined in order to investigate the correlation of Ra and FD1 over a smaller roughness range. These are the samples that are compared to the copper samples. In the next section

the samples are also examined with red, white, blue and green filters. A table follows showing the slopes and intercepts of the correlation of FD1 to Ra.

Table 5.11 Slope and Intercept Values of Correlation Curves for Aluminum

	Slope	Y-Intercept	% Transmission of Light	Wavelength(nm)
Green	2.36	6.25	36	500-570
White	2.62	6.88	28	All
Red	2.89	7.31	12	610-700
Blue	2.96	7.32	5	450-500

Since, aluminum has a uniform reflection for all wavelengths the only factor affecting the slope and intercept values of the correlation curves for aluminum is the transmission of light through the filters. In the case of the copper samples the transmission of light and the wavelength of the light will affect the slope and intercept of the correlation curve for FD1 vs. Ra. Figure 5.8 shows the reflectivity of copper with respect to wavelength of light, it can be seen that the highest reflectivity of copper is around the wavelength of red. If the correct wavelength of light and percent transmission are used in a filter then only one curve will be necessary for characterizing reflective materials. The only adjustment to the system for different reflective materials will be to adjust the filter.

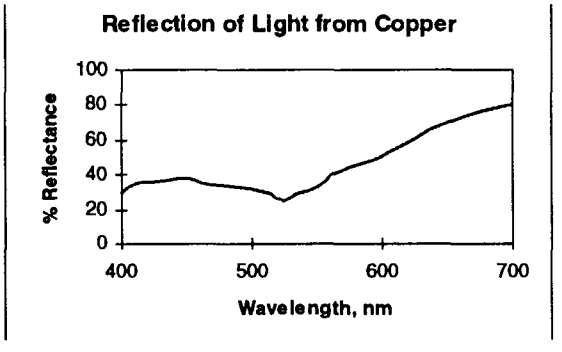

Figure 5.8 Reflection of Light from Copper

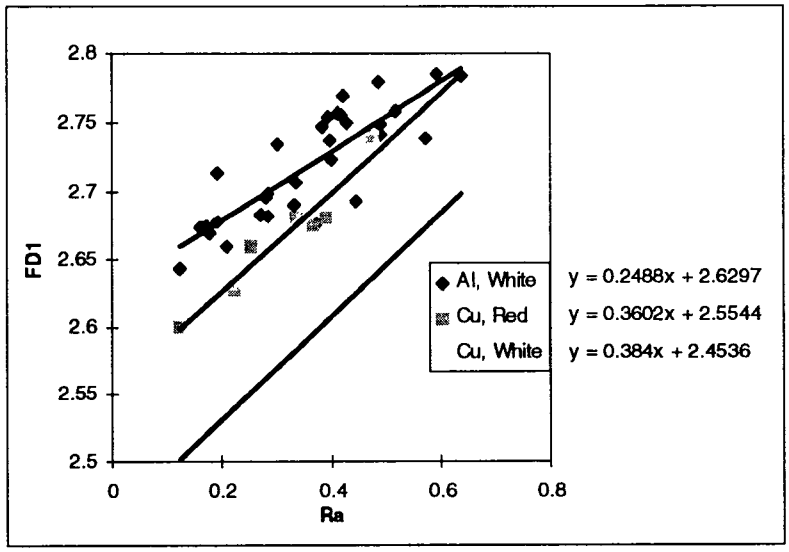

Figure 5.9 Cu and Al with Red and White Filters

Table 5.12· Aluminum Samples with Filter

Table 5-12a Aluminum with White filter

Ra(μm)	0.19	0.3	0.39	0.57	0.85	1.1	1.11
FD	2.71	2.73	2.75	2.74	2.75	2.78	2.78

Table 5.12b Copper with White filter

Ra(μm)	0.12	0.37	0.22	0.25	0.38	0.39	0.48
FD	2.51	2.58	2.53	2.55	2.58	2.62	2.64

Table 5.12c Copper with red filter

Ra(μm)	0.12	0.37	0.22	0.25	0.38	0.39	0.48
FD	2.6	2.675	2.628	2.66	2.68	2.681	2.74

Figure 5.9 shows that the filters can be used to change the slope and intercept of the correlation curve. This can lead to using only one curve and different filters for different materials. Table 5.12 shows the values of some of the points presented in the graphs in Figure 5.9.

5.4.5 Decreased Roughness Range

A new set of samples were machined in order to investigate the correlation of Ra and FD1 over a smaller roughness range. One fixed magnification of the camera should be able to better accommodate a smaller roughness range. The roughness range that will be targeted will be 0.10 μm to 0.75 μm.

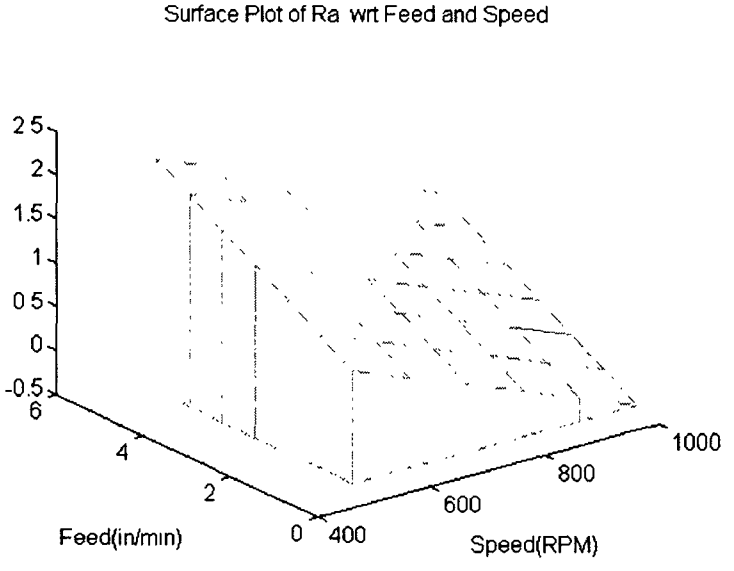

Figure 5.10 Model for Selecting Machining Conditions

In order to create a set of surfaces within this range the machining conditions must be carefully selected. The previous machining conditions can be used as an indicator of the roughness range that can be attained. There are two possible ways to predict the machining conditions. The two methods are conducting a factorial design experiment and generating a surface plot of the previous machining conditions. The surface plot method uses a linear least squares fit for a surface. The x component of the surface is the spindle speed, the y component is the feed and the z component is the roughness average. The previous machining conditions for a two flutes endmill

were used to model the machining conditions for the new samples. A surface plot of this model is shown in Figure 5.10. The model is only used for reference purposes in order to predict a range of machining conditions. The model does not taken several factors into account including tool diameter and tool wear. A new tool with a diameter 5/8 in. is used to machine the surfaces. The machining conditions and roughness values are seen in Table 5.13. A surface plot of the roughness values with respect to the speed and feed is shown in Figure 5.11.

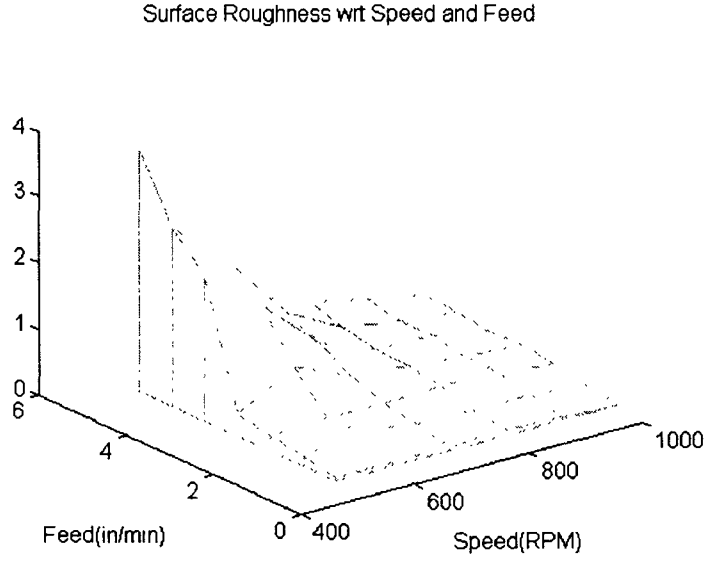

Figure 5.11 Surface Plot of Roughness Values

Table 5.13 Roughness Values

	(μm)	(μm)	(μm)	(μm)	(μm)	(μm)
0.01 m/min	0.18	0.17	0.19	0.21	0.16	0.12
0.03 m/min	0.28	0.42	0.30	0.28	0.27	0.19
0.05 m/min	0.37	0.41	0.39	0.42	0.38	0.28
0.07 m/min	0.45	0.97	0.57	0.49	0.40	0.33
0.09 m/min	2.33	1.66	0.85	0.52	0.49	0.34
0.11 m/min	2.82	2.06	1.10	0.64	0.49	0.40
0.13 m/min	3.80	2.18	1.11	0.78	0.59	0.43

The best conditions for this experiment were not the same as the previous experiment with aluminum. In this experiment the highest magnification factor of 30x proved to have the highest correlation. The best filter was red and the other correlations for magnification equal to 30x can be seen in Table 5.14.

Table 5.14 Correlation Coefficients

	Correlation Coeff. (R)	
	31 Samples	42 Samples
Filter	0.12 - 0.64 μm	0.12 - 3.80 μm
Red	0.8976	0.7970
Blue	0.8725	0.7939
Green	0.8576	0.7642
White	0.8316	0.7587

The correlations were done on two sets of samples of the data. The first correlation was just for roughness values between 0.12 μm and 0.64 μm which consisted of 31 samples, the second correlation was performed on all of the surfaces. Table 5.14 demonstrates that the samples taken in the smaller roughness group have a higher correlation than the entire population. The curve used to fit the 31 samples was a linear equation while the curve used to fit all 42 samples was an exponential equation. Figure 5.12 shows the best correlation obtained from the samples.

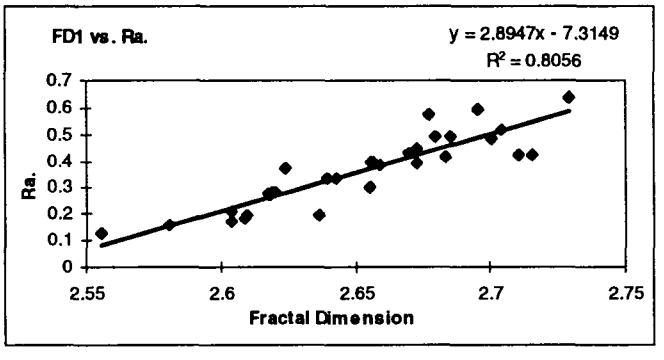

Figure 5.12 Correlation

5.5 Repeatability

In order to test the repeatability of the system 52 samples are examined with the vision system using a magnification of 15x with white diffuser filters. The same 52 samples where then examined with the vision system one day later under the same conditions. The only difference in the tests is the location examined by the vision system between the two experiments. It turned out that the highest absolute error between any sample was 0.020 and the highest relative error was 0.697%. Table 5.15 shows the maximum, the minimum, and the average errors from the experiment.

Table 5.15 Repeatability Error

	Absolute error	Relative Error (%)
Maximum	0.020	0.697
Minimum	0.000	0.000
Average	0.006	0.224

5.6 Alternate Parameters

Several alternate parameters were used in order to determine the surface roughness. Some of the parameters that were calculated from the image data were the mean, variance, skewness, kurtosis, and Ω2, where Ω2 is the mean times the standard deviation divided by 1000. This parameter was developed by Don Devoe. FD1 outperforms all other parameters for characterizing surface roughness from the image data in all tests.

5.7 Velocity Tests

If the vision system is to be successfully adapted to an on-line system then it must be able to capture images at a wide range of machining conditions. The feed of the CNC milling machine is the parameter that will affect the vision systems ability to clearly capture an image. In order to test the capability of the vision system the powerslide was programmed to move at feeds between 0.02 in/min and 80 in/min. The images captured are seen in Figures 5.13 to 5.20. From the images it appears that a feed rate of 10 in/min is where the image begins to blur. The reason for the blur in the image is not a function of the quality of the camera or frame grabber used in the vision system, but rather it is due to an inherent property of NTSC video. This property is called interlaced video[20]. In order to reduce eye strain an odd field of image lines is displayed and then followed by a second field of even image lines. The two fields are then combined to produce the overall image, displayed as one frame.

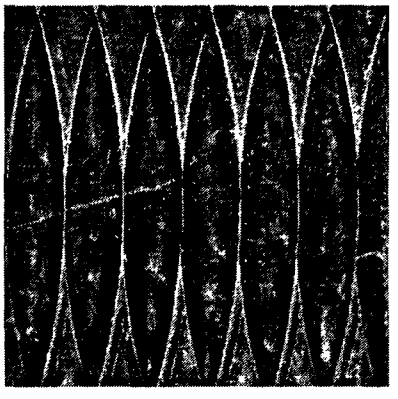

Figure 5.13 Feed = 0.02 in/min

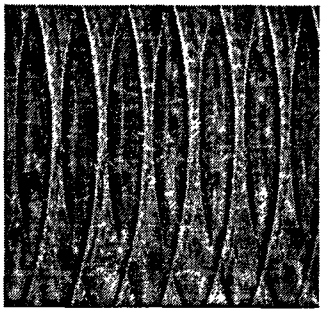

Figure 5.14 Feed = 0.1 in/min

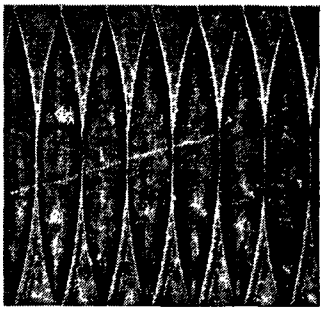

Figure 5.15 Feed = 1.0 in/min

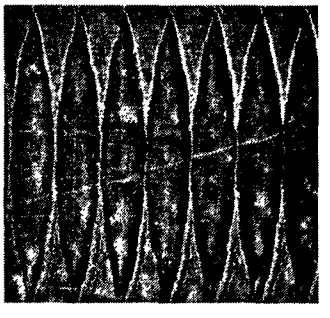

Figure 5.16 Feed = 5.0 in/min

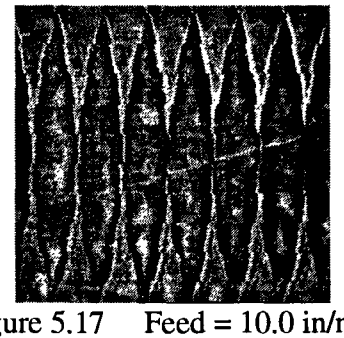

Figure 5.17 Feed = 10.0 in/min

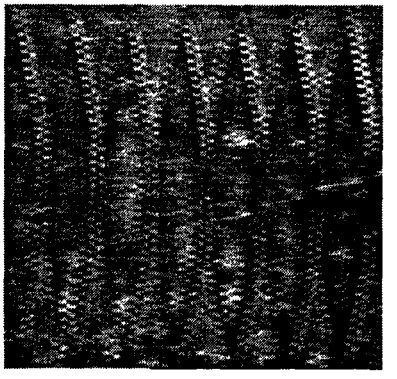

Figure 5.18 Feed = 25.0 in/min

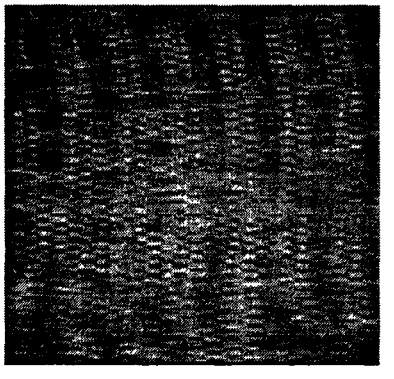

Figure 5.19 Feed = 50 in/min

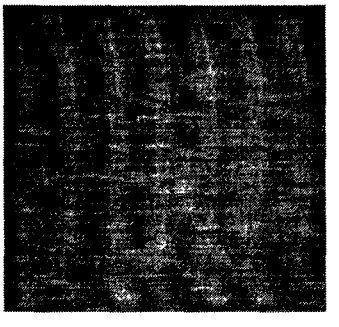

Figure 5.20 Feed = 80 in/min

5.8 Experiments with Lacunarity on Machined Surfaces

5.8.1 Evaluation of Machined Surfaces with Lacunarity

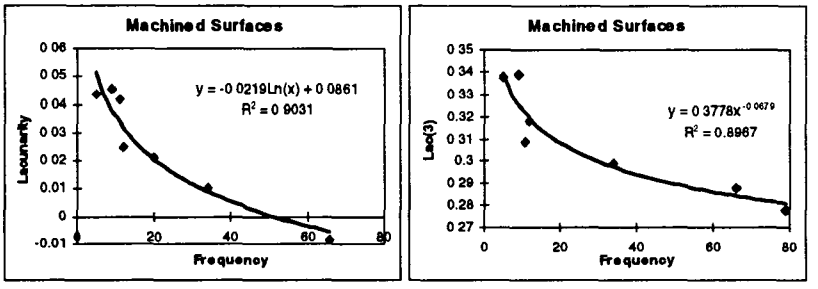

(a) (b)

Figure 5.21 Frequency vs. Lacunarity of Machined Surfaces

It has been found that the lacunarity of a surface is dependent upon both the spatial frequency of a surface and on the amount of noise present on the surface. The next step is to correlate lacunarity to surfaces created with the milling process. The dominant frequency of each surface is determined by taking the power spectrum of 256 profiles of the surface. The dominant frequency is then compared to the lacunarity of the surface in Figures 5.21. Figures 5.22 - 5.28 show a power spectrum and surface profile of the machined surface.

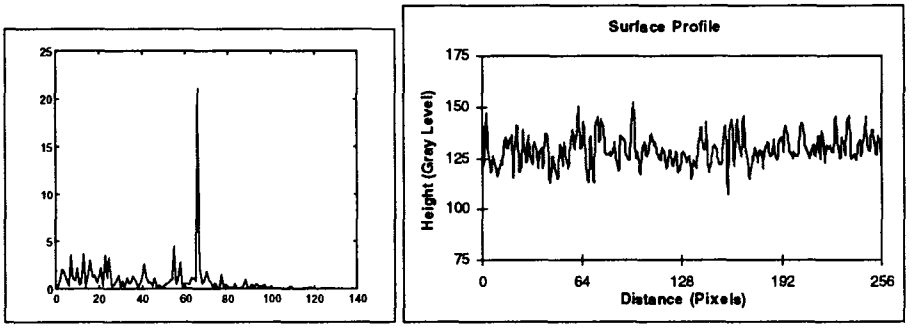

(a) (b)

Figure 5.22 Speed=1000 rpm, Feed=1.2 in/min, Lac=-0.00857, Lac(3)=0.2879

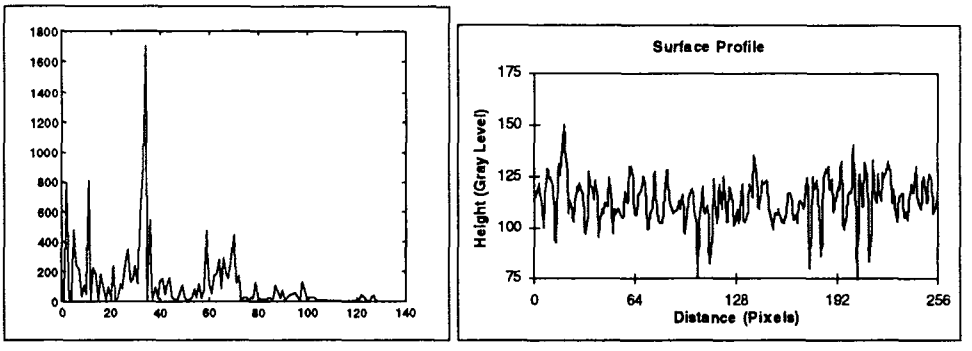

(a) (b)

Figure 5.23 Speed=1000 rpm, Feed=2.4 in/min, Lac=0.010375, Lac(3)=0.2988

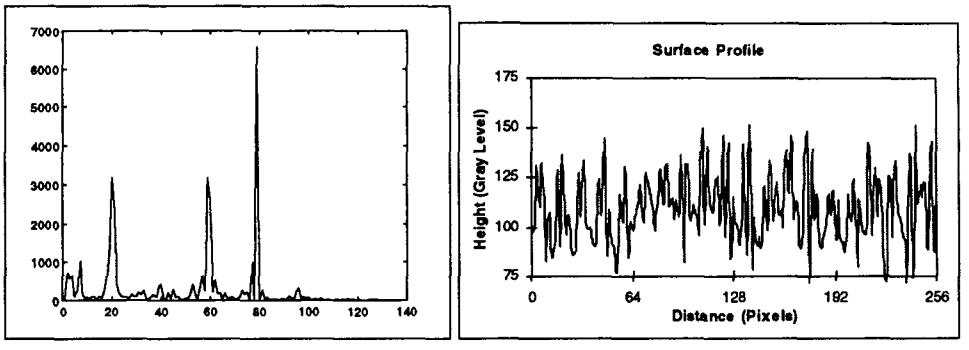

(a) (b)

Figure 5.24 Speed=1000 rpm, Feed=4.0 in/min, Lac=0.02085, Lac(3)=0.2776

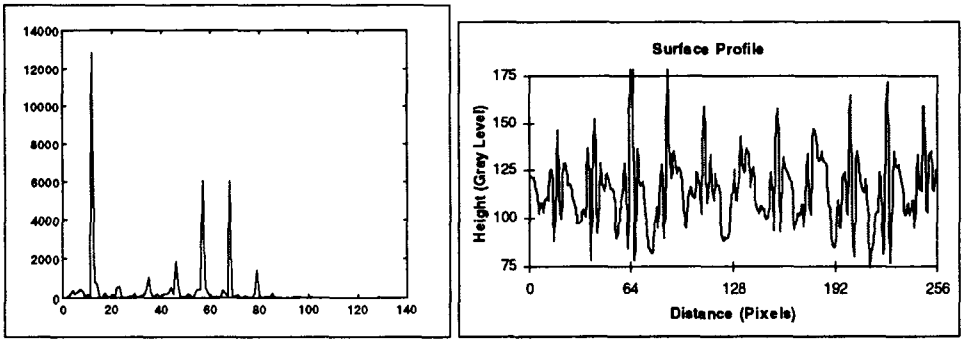

(a) (b)

Figure 5.25 Speed=1000 rpm, Feed=7.0 in/min, Lac=0.0248, Lac(3)=0.3178

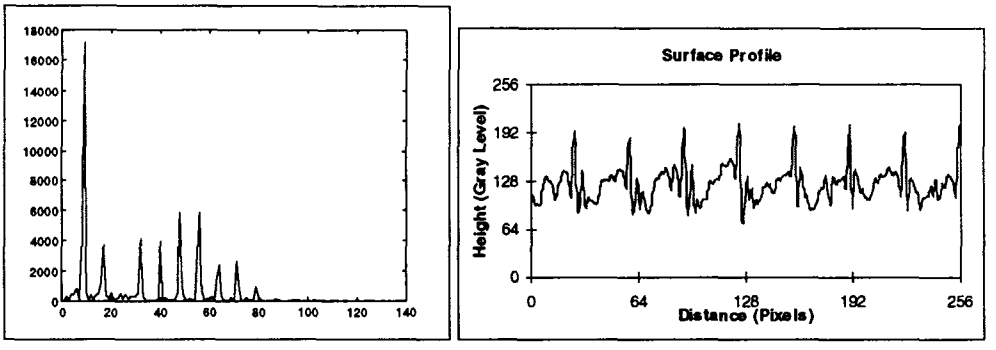

(a) (b)

Figure 5.26 Speed=1000 rpm, Feed=10.0 in/min, Lac=0.0453, Lac(3)=0.3389

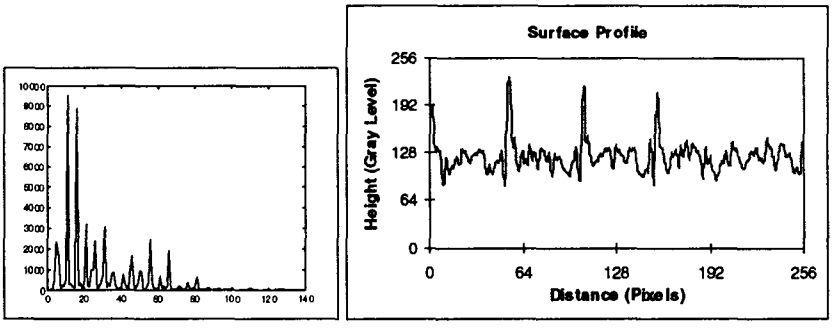

(a) (b)

Figure 5.27 Speed=1000 RPM, Feed=15.7 in/min, Lac=0.0419, Lac(3)=0.3084

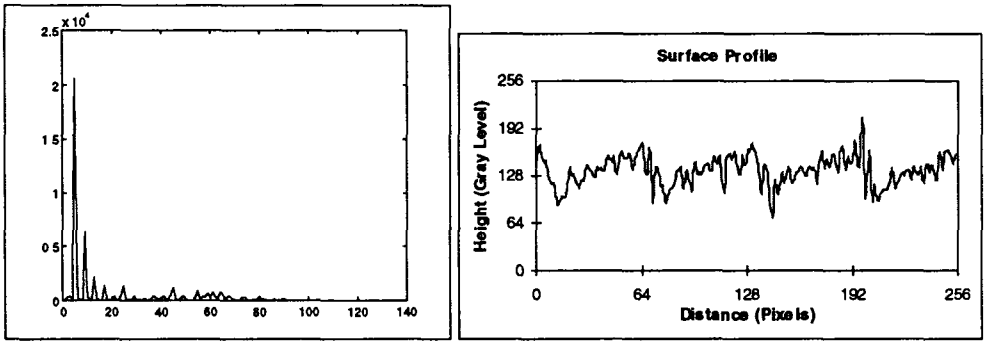

(a) (b)

Figure 5.28 Speed=1000 RPM, Feed=19.7 in/min, Lac=0.04365, Lac(3)=0.3377

5.8.2 Reconstruction of Surfaces Using Fractal Dimension and Lacunarity

In the previous sections experiments have been performed to show the correlation between Ra and FD1 under varying conditions. It has been verified that there is a correlation between the fractal dimension and the surface roughness. Both of these parameters give an insight into the height distribution of a surface. Neither parameter gives an insight into the frequency components of a surface or spatial distribution of the surface. As shown in Chapter 3, the Lacunarity can give insight into the dominant frequency component of a surface. A set of milled surfaces with a distinct frequency component shown by the power spectrum can be differentiated by the lacunarity. When reconstructing a surface with both the fractal dimension and the lacunarity a representation of the surface based on the height and spatial components can be realized. Figures 5.29 and 5.31 show two reconstructed profiles based on the fractal dimension and the lacunarity. Figures 5.30 and 5.32 show the equivalent machined surface with which the Fractal Geometry parameters were extracted. The surfaces were reconstructed using a combination of random noise and a periodic function. As can be seen the reconstructed surfaces do not exactly represent the machined surfaces but they give an insight into the spacing of peaks and valleys in the surface and the height distribution.

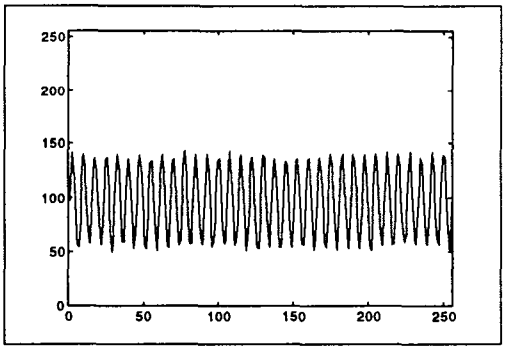

Figure 5.29 Lac = .01375 FD1 = 2.79

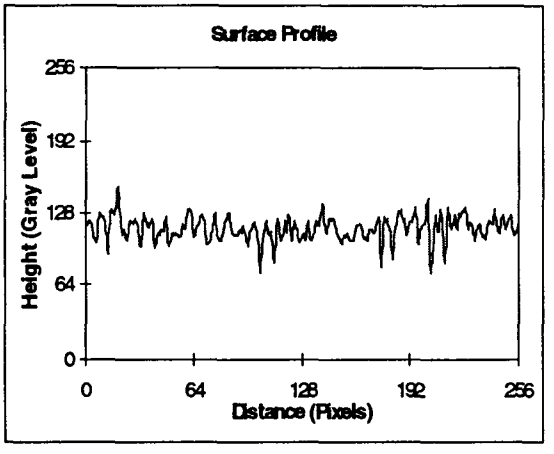

Figure 5.30 1000 rpm, 2.4 in/min

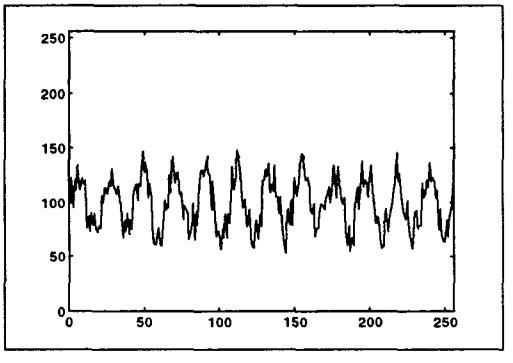

Figure 5.31 Lac = .04485, FD1 = 2.82

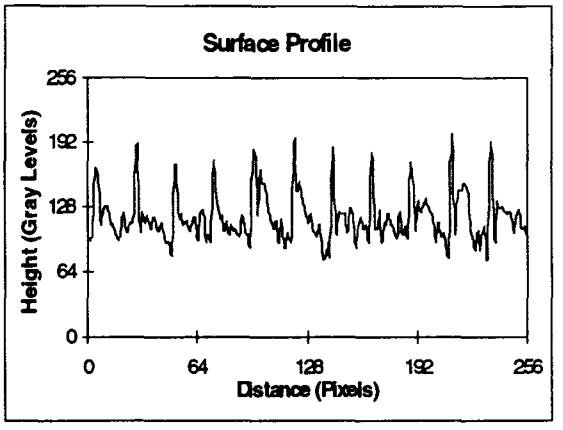

Figure 5.32 1000 rpm, 7.0 in/min

Chapter 6

Conclusions and Future Work

6.1 Conclusions

The main objective of this thesis research is to investigate the effectiveness of optical-based vision systems for surface finish assessment. Main contributions and significant findings are summarized as follows:

1. An appropriate selection of the surface characterization parameters used by the vision system plays a critical role in determining the system effectiveness. Traditionally used parameters, such as roughness average and peak-to-valley, suffer from their limitations in uniquely defining surface texture. The two new parameters in fractal geometry, fractal dimension and lacunarity, represent a unique replacement. Results from this thesis research provide strong evidence through case studies, demonstrating the functionality of each of these two parameters and the combination power of these two parameters in characterizing surface texture.

2. A vision system is designed and built, in which optical devices are employed, to implement the surface finish assessment using fractal geometry. The system employs a CCD camera to capture the image of a machined surface. A computer software tool is developed and implemented to process the image data and extract information of the surface condition using a fractal geometry approach. The vision system's theoretical foundations are based

on the principles of electromagnetic wave scattering, which have been used in a number of commercially available optical surface roughness measurement techniques. Therefore, the developed vision system offers a test bed, which is representative of the current industrial practices.

3. Results presented in this thesis clearly illustrate that the proposed approach applying fractal geometry to characterize the surface texture is more effective for

   (1) The parameter of fractal dimension is a better indicator of surface roughness when applied to images of rough surfaces acquired with the vision system. The parameter of fractal dimension also outperforms calculating the Ra from the image data, the variance, and other optical roughness parameters including $\Omega 1$ and $\Omega 2$ proposed by other researchers.

   (2) The parameter of lacunarity has been found to give insight into the number of gaps in a surface. It can be used to find the dominant frequency in some machined surfaces. When the fractal geometry parameters fractal dimension and lacunarity are combined they can be used to recreate a surface. The reconstruction of the surface with both parameters gives more of an insight into the nature of the surface.

4. There are several factors which have significant effects on the design of optical-based vision systems. These factors include the ambient light, the grazing angle of an external light source, the intensity of an external light source, the orientation of an external light source, the filtering of the external light source, and the magnification of the CCD camera. Results from a systematic investigation of these factors on surface characterization have provided rich information which is useful for designing and redesigning optical-based vision systems.

5. It should be pointed out that the effectiveness of the system in regards to characterizing surfaces created with different machining conditions, different endmills, and different materials is critical in determining the limitations of the system. The system characterizes surfaces irregardless of the machining conditions used, or the endmill used. Utilization of light filters represents an effective means among other alternatives in meeting such needs. Results obtained from this thesis research indicate that an appropriate selection of light filters may replace the need for system calibration when a new type of material is to be machined.

6.2 Future Work

1. Implement the vision system on-line while keeping the features that have been designed into the off-line system. The surface will need to be

illuminated from two perpendicular light sources in order to reduce variations in measurements due to illumination with respect to the feed direction. The intensity of the light sources will need to be bright enough to reduce effects to system parameters due to variations in ambient light. Also the portion of the surface being examined will need to be cleared of debris before measurements are taken. A built in compressed air gun can be incorporated into the camera and lighting apparatus.

2. The system should work in conjunction with the G-Code used to perform machining on the CNC Milling Machine. The system should be able to operate on motion commands from the G-Code and also provide feedback to the Milling Machine from the sensory data obtained from in-process diagnosis. The camera and lighting system will need to follow the direction of feed in order to capture the machined surface. A control system can be designed to rotate the vision system around the spindle. The control system will also be controlled by the G-Code.

3. Surfaces created by other manufacturing processes such as grinding, plating, turning, etc. should be examined with this system. Results obtained can be used to determine the effectiveness of the vision system and its algorithms to a broader range of surfaces. Materials that have ductile surfaces or that are easily damaged by contact surface assessment devices can be assessed using other optical or non-contact methods. These surfaces should then be

examined with the vision system presented in this research to examine any correlation.

4. The current system obtains a three dimensional reconstruction of the surface based on light scattering theory. Another way to obtain a three dimensional representation of the surface could be to use two cameras at different angles to extract depth from points on the surface. A parallel processing unit could be used in order to accommodate two frame grabber cards to analyze the data from both images simultaneously.

Appendix A Experimental Data

Table A1 - Stylus measurements results for aluminum samples

Speed	Feed	Rz 1	Rz 2	Rz 3	Rz AVG.	Ra 1	Ra 2	Ra 3	Ra AVG.
500	0.5	1.10	1.43	1.32	1.283	0.14	0.22	0.18	0.180
	1.25	2.30	1.62	1.54	1.820	0.38	0.23	0.24	0.283
	2	2.33	2.88	2.15	2.453	0.36	0.42	0.34	0.373
	2.75	3.39	3.12	2.34	2.950	0.54	0.47	0.33	0.447
	3.5	9.22	11.76	10.25	10.410	2.15	2.42	2.41	2.327
	4.25	11.58	12.07	12.38	12.010	2.67	2.95	2.83	2.817
	5	13.38	14.80	14.86	14.347	3.64	3.99	3.78	3.803
600	0.5	1.27	1.33	1.21	1.270	0.18	0.17	0.16	0.170
	1.25	2.56	2.72	2.76	2.680	0.43	0.40	0.44	0.423
	2	2.67	2.50	2.90	2.690	0.41	0.39	0.44	0.413
	2.75	4.56	5.63	5.26	5.150	0.89	1.06	0.96	0.970
	3.5	7.33	8.04	7.42	7.597	1.67	1.67	1.65	1.663
	4.25	9.02	8.66	8.67	8.783	2.10	2.05	2.04	2.063
	5	8.52	8.56	8.73	8.603	2.09	2.19	2.26	2.180
700	0.5	1.40	1.45	1.43	1.427	0.19	0.20	0.19	0.193
	1.25	2.58	1.73	1.61	1.973	0.41	0.27	0.23	0.303
	2	2.44	2.24	2.35	2.343	0.39	0.40	0.39	0.393
	2.75	3.10	3.74	3.52	3.453	0.52	0.63	0.57	0.573
	3.5	4.73	4.71	4.76	4.733	0.87	0.83	0.85	0.850
	4.25	6.21	6.07	5.83	6.037	1.13	1.12	1.05	1.100
	5	6.20	5.27	5.89	5.787	1.17	1.04	1.13	1.113
800	0.5	1.50	1.48	1.50	1.493	0.19	0.22	0.22	0.210
	1.25	1.85	2.19	2.14	2.060	0.28	0.29	0.28	0.283
	2	2.69	3.35	3.09	3.043	0.37	0.48	0.41	0.420
	2.75	3.13	3.51	3.59	3.410	0.47	0.51	0.48	0.487
	3.5	3.94	3.63	3.39	3.653	0.57	0.50	0.49	0.520
	4.25	4.50	4.38	4.21	4.363	0.70	0.60	0.62	0.640
	5	4.44	5.68	5.21	5.110	0.72	0.85	0.77	0.780
900	0.5	1.17	1.21	1.29	1.223	0.14	0.16	0.18	0.160
	1.25	1.69	1.87	1.56	1.707	0.27	0.31	0.23	0.270
	2	2.57	2.50	2.45	2.507	0.41	0.38	0.36	0.383
	2.75	2.76	2.98	2.13	2.623	0.41	0.50	0.29	0.400
	3.5	3.26	3.26	3.13	3.217	0.46	0.49	0.52	0.490
	4.25	3.90	3.57	3.53	3.667	0.45	0.50	0.52	0.490
	5	3.19	4.42	3.97	3.860	0.52	0.67	0.59	0.593
s1000	0.5	1.10	1.26	1.05	1.137	0.11	0.14	0.12	0.123
	1.25	1.31	1.47	1.56	1.447	0.18	0.19	0.21	0.193
	2	2.19	2.15	1.95	2.097	0.32	0.26	0.26	0.280
	2.75	2.05	2.67	2.14	2.287	0.29	0.41	0.30	0.333
	3.5	2.06	2.54	2.45	2.350	0.32	0.33	0.36	0.337
	4.25	2.91	2.95	2.74	2.867	0.42	0.40	0.37	0.397
	5	2.69	3.40	3.05	3.047	0.37	0.49	0.43	0.430

Table A2 - Stylus measurements results for copper samples

Speed	Feed	Rz1	Rz2	Rz3	Rz Avg	Ra1	Ra2	Ra3	Ra AVG
500	0.5	1.71	1.61	1.81	1.710	0.21	0.18	0.22	0.203
	1.25	5.08	4.46	3.78	4.440	0.60	0.66	0.37	0.543
	2	2.91	3.73	4.49	3.710	0.40	0.47	0.49	0.453
	2.75	4.75	4.92	5.33	5.000	0.67	0.58	0.66	0.637
	3.5	4.91	6.58	5.21	5.567	0.62	0.77	0.61	0.667
	4.25	5.79	7.79	7.43	7.003	0.74	0.84	0.79	0.790
	5	5.85	7.08	7.29	6.740	0.89	0.86	0.87	0.873
600	0.5	1.85	1.89	2.24	1.993	0.26	0.26	0.28	0.267
	1.25	2.29	2.65	2.68	2.540	0.34	0.35	0.35	0.347
	2	5.54	5.95	4.49	5.327	0.74	0.79	0.65	0.727
	2.75	11.14	9.94	9.54	10.207	1.70	1.35	1.36	1.470
	3.5	2.78	2.96	3.08	2.940	0.37	0.38	0.39	0.380
	4.25	3.30	4.06	4.16	3.840	0.47	0.53	0.54	0.513
	5	4.23	4.63	4.91	4.590	0.60	0.56	0.58	0.580
700	0.5	1.01	1.32	1.46	1.263	0.12	0.16	0.19	0.157
	1.5	2.64	1.63	2.05	2.107	0.29	0.41	0.46	0.387
	3	2.40	2.77	2.93	2.700	0.29	0.31	0.31	0.303
	4	2.74	3.17	2.71	2.873	0.37	0.35	0.35	0.357
	5	2.75	3.12	3.05	2.973	0.38	0.41	0.42	0.403
	6	3.22	3.41	3.58	3.403	0.43	0.45	0.48	0.453
	7	3.84	4.20	4.62	4.220	0.54	0.53	0.51	0.527
800	0.5	2.34	2.35	2.17	2.287	0.26	0.24	0.25	0.250
	1.5	2.05	2.08	3.38	2.503	0.28	0.26	0.40	0.313
	3	2.55	2.90	3.22	2.890	0.31	0.37	0.40	0.360
	4	3.00	2.58	3.47	3.017	0.42	0.35	0.55	0.440
	5	3.92	3.41	3.08	3.470	0.51	0.50	0.43	0.480
	6	3.89	3.56	3.74	3.730	0.49	0.48	0.46	0.477
	7	4.51	4.47	4.15	4.377	0.60	0.55	0.48	0.543
900	0.5	1.40	1.51	1.57	1.493	0.16	0.15	0.16	0.157
	1.5	3.15	3.38	2.00	2.843	0.38	0.45	0.24	0.357
	3	3.47	3.48	3.19	3.380	0.44	0.43	0.40	0.423
	4	3.47	3.64	3.20	3.437	0.43	0.47	0.45	0.450
	5	3.52	3.56	3.68	3.587	0.43	0.42	0.49	0.447
	6	4.43	3.97	4.30	4.233	0.56	0.55	0.58	0.563
	7	4.54	4.36	4.89	4.597	0.52	0.59	0.56	0.557
1000	0.5	2.28	2.26	2.08	2.207	0.31	0.31	0.26	0.293
	1.5	1.64	1.82	1.79	1.750	0.21	0.24	0.23	0.227
	3	2.71	2.99	2.59	2.763	0.31	0.35	0.28	0.313
	4	3.94	3.30	3.79	3.677	0.49	0.37	0.46	0.440
	5	2.94	3.90	3.40	3.413	0.40	0.48	0.50	0.460
	6	3.86	3.80	4.93	4.197	0.51	0.59	0.70	0.600
	7	3.94	4.55	4.58	4.357	0.63	0.67	0.78	0.693

Table A3 - Stylus measurements results for aluminum samples

Speed	Feed	Flutes	Ra (μm)			
(RPM)	(in/min)		Trial 1	Trial 2	Trial 3	Avg.(Ra.)
1000	1.2	2.0	0.43	0.43	0.46	0.44
	2.4	2.0	0.57	0.57	0.59	0.58
	4.0	2.0	0.47	0.54	0.54	0.52
	7.0	2.0	0.92	1.12	1.12	1.05
	10.0	2.0	1.86	2.36	2.26	2.16
	15.7	2.0	4.35	4.4	4.5	4.42
	19.7	2.0	5.2	5.5	5.3	5.33
	1.2	4.0	0.16	0.16	0.16	0.16
	2.4	4.0	0.24	0.28	0.29	0.27
	4.0	4.0	0.45	0.52	0.53	0.50
	7.0	4.0	2.50	2.52	2.36	2.46
	10.0	4.0	3.36	3.02	3.05	3.14
	15.7	4.0	5.30	5.90	5.90	5.70
800	1.2	2.0	0.3	0.36	0.34	0.33
	2.4	2.0	0.39	0.4	0.41	0.40
	4.0	2.0	0.52	0.54	0.52	0.53
	7.0	2.0	1.26	1.62	2.05	1.64
	10.0	2.0	3	3.52	3.63	3.38
	15.7	2.0	5.44	5.9	5.75	5.70
	19.7	2.0	4.94	6.36	6.64	5.98
	1.2	4.0	0.2	0.19	0.19	0.19
	2.4	4.0	0.37	0.4	0.39	0.39
	4.0	4.0	1.46	1.53	1.54	1.51
	7.0	4.0	3.6	3.96	3.93	3.83
	10.0	4.0	4.7	5	4.4	4.70
	15.7	4.0	8.2	6.8	7.5	7.50
600	1.2	2.0	0.19	0.2	0.22	0.20
	2.4	2.0	0.44	0.45	0.45	0.45
	4.0	2.0	1.17	1.12	1.09	1.13
	7.0	2.0	3.36	3.7	3.63	3.56
	10.0	2.0	3.84	4.03	4.1	3.99
	15.7	2.0	5.8	5.3	4.9	5.33
	19.7	2.0	6.3	6	6	6.10
	1.2	4.0	0.34	0.36	0.35	0.35
	2.4	4.0	1.06	1.14	1.98	1.39
	4.0	4.0	2.54	2.66	2.45	2.55
	7.0	4.0	5.6	5.2	5.3	5.37
	10.0	4.0	6.7	6.4	6	6.37
	15.7	4.0	9.2	8.5	7.9	8.53
400	1.2	2.0	1.24	1.3	1	1.18
	2.4	2.0	1.93	1.89	1.56	1.79
	4.0	2.0	2.66	2.77	2.53	2.65
	7.0	2.0	3.49	3.32	3.29	3.37
	10.0	2.0	4.46	4.73	4.3	4.50
	15.7	2.0	6.5	6.8	6.8	6.70
	19.7	2.0	4.9	5.3	5.4	5.20
	1.2	4.0	0.61	0.67	0.68	0.65
	2.4	4.0	2.58	2.64	2.57	2.60
	4.0	4.0	2.84	3.24	3.97	3.35
	7.0	4.0	7.7	7.1	7.1	7.30
	10.0	4.0	7.8	8.6	8.6	8.33
	15.7	4.0	7.8	9.3	9.4	8.83

Table A4 - Repeatability test for samples

Trial1 FD1	Trial2 FD1	Absolute Error	Relative Error (%)
2.797	2.779	0.017	0.618
2.799	2.797	0.002	0.063
2.815	2.797	0.018	0.643
2.819	2.811	0.008	0.290
2.876	2.856	0.020	0.706
2.876	2.862	0.014	0.485
2.911	2.897	0.015	0.500
2.754	2.756	0.002	0.083
2.830	2.820	0.009	0.330
2.781	2.780	0.001	0.036
2.818	2.816	0.003	0.092
2.852	2.843	0.009	0.312
2.877	2.865	0.012	0.407
2.750	2.750	0.001	0.033
2.787	2.781	0.006	0.198
2.802	2.787	0.015	0.529
2.826	2.826	0.001	0.027
2.872	2.872	0.000	0.003
2.892	2.885	0.007	0.244
2.920	2.909	0.010	0.359
2.739	2.739	0.000	0.012
2.793	2.787	0.007	0.242
2.824	2.830	0.006	0.204
2.829	2.831	0.002	0.074
2.853	2.855	0.002	0.074
2.870	2.868	0.002	0.072
2.726	2.729	0.004	0.132
2.788	2.786	0.001	0.050
2.832	2.828	0.004	0.141
2.858	2.853	0.005	0.179
2.922	2.925	0.003	0.106
2.930	2.923	0.007	0.242
2.941	2.940	0.002	0.052
2.787	2.781	0.006	0.215
2.850	2.855	0.005	0.173
2.841	2.836	0.005	0.160
2.872	2.864	0.008	0.288
2.888	2.886	0.002	0.084
2.888	2.882	0.006	0.209
2.829	2.822	0.007	0.258
2.871	2.851	0.020	0.705
2.883	2.886	0.003	0.105
2.845	2.844	0.001	0.042
2.894	2.901	0.007	0.247
2.898	2.896	0.002	0.078
2.904	2.909	0.005	0.163
2.835	2.852	0.017	0.609
2.897	2.887	0.010	0.340
2.876	2.867	0.009	0.317
2.863	2.859	0.004	0.126
2.910	2.911	0.001	0.033
2.896	2.893	0.003	0.098
	Max.	0.020	0.706
	Min.	0.000	0.003
	Avg.	0.006	0.227

Table A5 Aluminum, Magnification = 15x, White Filters, All Four Lights

Speed (RPM)	Feed (in/min)	Flutes	Lac(3)	Lac(5)	Lac(7)	Lac(Slope)	Spatial Frequency	
							1	2
1000	1.2	2	0.2879	0.2690	0.2536	-0.00857	66	66.0
1000	2.4	2	0.2988	0.3784	0.3403	0.01038	34	34.0
1000	4	2	0.2776	0.3583	0.3610	0.02085	79	20.0
1000	7	2	0.3178	0.4440	0.4170	0.02480	12	12.0
1000	10	2	0.3389	0.5360	0.5201	0.04530	9	9.0
1000	15.7	2	0.3084	0.4394	0.4760	0.04190	11	11.0
1000	19.7	2	0.3377	0.4895	0.5123	0.04365	5	5.0
1000	1.2	4	0.2984	0.3051	0.2304	-0.01700	66	66.0
1000	2.4	4	0.2752	0.3233	0.3113	0.00903	66	33.0
1000	4	4	0.2798	0.3591	0.3520	0.01805	40	40.0
1000	7	4	0.3106	0.4665	0.5015	0.04772	12	12.0
1000	10	4	0.3240	0.4799	0.4792	0.03880	9	9.0
1000	15.7	4	0.3160	0.4739	0.5120	0.04900	11	11.0
800	1.2	2	0.3039	0.3327	0.2713	-0.00815	6	53.0
800	2.4	2	0.2725	0.3267	0.3353	0.01570	27	27.0
800	4	2	0.2858	0.3749	0.3307	0.01122	32	16.0
800	7	2	0.3200	0.5060	0.5383	0.05458	10	10.0
800	10	2	0.3186	0.4874	0.5492	0.05765	7	7.0
800	15.7	2	0.2814	0.4430	0.5156	0.05855	9	4.5
800	19.7	2	0.3080	0.4740	0.4798	0.04295	4	4.0
800	1.2	4	0.2765	0.2884	0.2379	-0.00965	53	53.0
800	2.4	4	0.2984	0.3933	0.3671	0.01718	27	27.0
800	4	4	0.3003	0.4043	0.4722	0.04298	17	17.0
800	7	4	0.3448	0.5087	0.6013	0.06413	19	9.5
800	10	4	0.3186	0.4874	0.5492	0.05765	45	5.6
800	15.7	4	0.3114	0.4434	0.5136	0.05055	5	5.0
600	1.2	2	0.2760	0.3143	0.2924	0.00410	6	40.0
600	2.4	2	0.3066	0.3933	0.4011	0.02363	21	21.0
600	4	2	0.2757	0.3684	0.3561	0.02010	36	12.0
600	7	2	0.3255	0.5144	0.6405	0.07875	8	8.0
600	10	2	0.2669	0.3800	0.4312	0.04108	29	29.0
600	15.7	2	0.2891	0.4096	0.4455	0.03910	16	16.0
600	19.7	2	0.2814	0.3996	0.4110	0.03240	6	6.0
600	1.2	4	0.3029	0.3376	0.2745	-0.00710	40	40.0
600	2.4	4	0.2935	0.4138	0.4352	0.03543	21	21.0
600	4	4	0.3460	0.5462	0.5750	0.05725	13	13.0
600	7	4	0.3624	0.6018	0.6565	0.07353	28	7.0
600	10	4	0.3313	0.4822	0.4763	0.03625	20	4.0
600	15.7	4	0.3076	0.4087	0.4011	0.02338	19	6.3
400	1.2	2	0.3204	0.3460	0.3118	-0.00215	4	4.0
400	2.4	2	0.3367	0.3852	0.3899	0.01330	14	14.0
400	4	2	0.3105	0.4391	0.4614	0.03772	9	9.0
400	7	2	0.3383	0.4575	0.4955	0.03930	19	19.0
400	10	2	0.3101	0.4192	0.4692	0.03978	4	4.0
400	15.7	2	0.2888	0.3933	0.4264	0.03440	5	2.5
400	19.7	2	0.3146	0.4489	0.4372	0.03065	4	4.0
400	1.2	4	0.2830	0.3914	0.3673	0.02108	27	27.0
400	2.4	4	0.3169	0.4591	0.5285	0.05290	14	14.0
400	4	4	0.3645	0.5920	0.7239	0.08985	17	8.5
400	7	4	0.3339	0.4707	0.5468	0.05323	10	8.0
400	10	4	0.3065	0.4551	0.5143	0.05195	20	10.0
400	15.7	4	0.3215	0.4885	0.4808	0.03983	9	9.0

Table A6 Copper, Magnification = 20x, White Filters, All Four Lights

Speed (RPM)	Feed (in/min)	Avg	Var	Skewness	Omega2	Ra(Image)	Lac(old)	FD2	FD1	Ra(Stylus) (μm)
500	0.50	103	17.9	-0.1885	0.4349	3.260	0.2001	2.835	2.655	0.203
500	1.25	96	24.5	-0.3460	0.4740	3.862	0.2031	2.823	2.669	0.543
500	2.00	95	23.8	-0.1956	0.4636	3.754	0.1973	2.821	2.659	0.453
500	2.75	92	30.2	-0.3432	0.5068	4.309	0.1997	2.816	2.673	0.637
500	3.50	93	59.1	-0.5689	0.7169	6.223	0.1972	2.818	2.713	0.667
500	4.25	96	54.6	-0.7009	0.7099	5.845	0.1951	2.823	2.726	0.790
500	5.00	97	36.8	-0.9634	0.5894	4.664	0.1987	2.825	2.710	0.873
600	0.50	101	15.5	0.1695	0.3973	3.060	0.1921	2.832	2.662	0.267
600	1.25	102	24.6	0.1725	0.5045	3.997	0.1851	2.834	2.664	0.347
600	2.00	97	17.4	0.2839	0.4043	3.216	0.1821	2.825	2.641	0.727
600	2.75	93	28.8	0.0762	0.4983	4.138	0.1881	2.817	2.672	1.470
600	3.50	97	11.0	0.6168	0.3229	2.586	0.1799	2.825	2.614	0.380
600	4.25	100	14.7	0.4817	0.3818	2.993	0.1854	2.830	2.630	0.513
600	5.00	100	15.5	0.8472	0.3946	3.127	0.1894	2.831	2.607	0.580
700	0.50	106	15.2	-0.2640	0.4146	3.123	0.1872	2.842	2.660	0.157
700	1.25	101	35.1	-0.1532	0.5976	4.595	0.2006	2.832	2.712	0.387
700	2.00	98	25.7	-0.0652	0.4972	4.042	0.2010	2.827	2.668	0.303
700	2.75	96	34.7	0.0908	0.5642	4.657	0.2191	2.823	2.679	0.357
700	3.50	98	36.7	0.3042	0.5944	4.717	0.2108	2.827	2.678	0.403
700	4.25	101	45.1	0.3589	0.6771	5.288	0.2151	2.832	2.703	0.453
700	5.00	102	57.5	0.2635	0.7716	5.910	0.2194	2.834	2.721	0.527
800	0.50	99	28.5	-0.0515	0.5284	4.247	0.2166	2.829	2.680	0.250
800	1.25	97	23.8	-0.0803	0.4757	3.787	0.2026	2.826	2.670	0.313
800	2.00	97	24.8	0.2392	0.4824	3.820	0.2027	2.825	2.652	0.360
800	2.75	103	45.8	0.2591	0.6975	5.303	0.2111	2.836	2.711	0.440
800	3.50	102	60.3	0.7125	0.7921	5.948	0.2154	2.834	2.716	0.480
800	4.25	102	69.8	0.4852	0.8561	6.566	0.2174	2.835	2.728	0.477
800	5.00	102	75.2	0.7474	0.8848	6.485	0.2136	2.834	2.724	0.543
900	0.50	92	49.2	-1.7473	0.6438	4.862	0.2030	2.815	2.738	0.157
900	1.25	94	42.0	-0.3238	0.6081	5.119	0.2151	2.819	2.705	0.357
900	2.00	95	60.3	0.3908	0.7352	6.047	0.2138	2.821	2.691	0.423
900	2.75	94	49.0	0.2095	0.6603	5.432	0.2069	2.820	2.688	0.450
900	3.50	93	48.8	0.6721	0.6500	5.282	0.2025	2.817	2.673	0.447
900	4.25	94	40.0	0.7593	0.5922	4.766	0.1935	2.819	2.661	0.563
900	5.00	94	40.0	0.5337	0.5931	4.932	0.1973	2.819	2.663	0.557
1000	0.50	92	29.5	0.1412	0.4987	4.298	0.2163	2.815	2.646	0.293
1000	1.25	94	115.1	-1.5404	1.0130	7.688	0.2112	2.820	2.777	0.227
1000	2.00	88	26.0	-0.8335	0.4496	3.813	0.2016	2.808	2.628	0.313
1000	2.75	88	22.6	0.5070	0.4198	3.631	0.2053	2.808	2.620	0.440
1000	3.50	91	23.1	0.2897	0.4369	3.755	0.1997	2.813	2.633	0.460
1000	4.25	92	24.4	-0.0567	0.4530	3.941	0.2090	2.815	2.655	0.600
1000	5.00	90	27.5	-0.1306	0.4697	3.995	0.2126	2.811	2.639	0.693

Table A7 Aluminum, Magnification = 20x, White Filters, All Four Lights

Speed (RPM)	Feed (in/min)	Avg	Var	Skewness	Omega2	Ra(Image)	Lac(old)	FD2	FD1	Ra(Stylus) (μm)
500	0.50	84	47.5	-0.1868	0.5770	5.445	0.2143	2.799	2.670	0.180
500	1.25	87	46.0	-0.1733	0.5916	5.377	0.2078	2.806	2.683	0.283
500	2.00	91	45.0	0.0312	0.6106	5.370	0.2123	2.814	2.676	0.373
500	2.75	93	48.3	-0.1436	0.6439	5.518	0.1991	2.817	2.694	0.447
500	3.50	102	109.0	0.6858	1.0616	7.875	0.2025	2.833	2.746	2.327
500	4.25	105	82.1	0.4136	0.9556	6.772	0.2039	2.840	2.756	2.817
500	5.00	110	78.2	0.3684	0.9741	6.837	0.2058	2.848	2.763	3.803
600	0.50	87	50.0	0.0486	0.6120	5.605	0.2186	2.804	2.675	0.170
600	1.25	105	102.3	-0.1303	1.0587	8.168	0.2285	2.839	2.770	0.423
600	2.00	108	57.7	-0.3918	0.8168	5.988	0.2175	2.844	2.757	0.413
600	2.75	105	65.9	-0.3709	0.8509	6.185	0.2065	2.839	2.761	0.970
600	3.50	109	61.4	-0.3162	0.8554	6.163	0.2252	2.846	2.766	1.663
600	4.25	113	66.2	-0.7268	0.9212	6.192	0.2116	2.853	2.790	2.063
600	5.00	114	76.8	-0.4769	0.9963	6.785	0.2250	2.854	2.794	2.180
700	0.50	98	50.5	-0.2185	0.6932	5.601	0.2235	2.826	2.714	0.193
700	1.25	97	67.4	-0.3427	0.7975	6.466	0.2257	2.825	2.735	0.303
700	2.00	98	72.0	-0.7896	0.8292	6.567	0.2127	2.826	2.754	0.393
700	2.75	98	60.9	-0.5901	0.7671	6.106	0.2236	2.827	2.739	0.573
700	3.50	100	75.3	-0.6514	0.8681	6.958	0.2217	2.831	2.748	0.850
700	4.25	106	97.0	-0.5193	1.0438	7.838	0.2253	2.841	2.783	1.100
700	5.00	102	118.7	-0.6682	1.1100	8.796	0.2260	2.834	2.782	1.113
800	0.50	91	29.4	-0.0828	0.4948	4.296	0.2110	2.814	2.660	0.210
800	1.25	95	41.8	-0.3036	0.6158	5.107	0.2032	2.822	2.698	0.283
800	2.00	107	61.4	-0.3093	0.8366	6.284	0.2142	2.842	2.756	0.420
800	2.75	103	84.7	-1.0080	0.9498	7.042	0.2189	2.836	2.779	0.487
800	3.50	106	71.8	-0.0495	0.8959	6.670	0.2174	2.841	2.758	0.520
800	4.25	109	87.7	-0.3583	1.0195	7.378	0.2112	2.846	2.783	0.640
800	5.00	107	100.4	-0.0199	1.0766	7.901	0.2192	2.843	2.777	0.780
900	0.50	83	55.0	-0.0709	0.6189	5.941	0.2138	2.798	2.674	0.160
900	1.25	85	49.8	0.2887	0.6003	5.492	0.2090	2.801	2.683	0.270
900	2.00	96	80.8	-0.5779	0.8652	7.099	0.2112	2.824	2.747	0.383
900	2.75	89	70.1	-0.6169	0.7421	6.444	0.2125	2.809	2.724	0.400
900	3.50	93	88.0	-0.4302	0.8725	7.416	0.2129	2.817	2.742	0.490
900	4.25	98	75.2	-0.5453	0.8524	6.749	0.2222	2.827	2.749	0.490
900	5.00	100	132.6	-0.5346	1.1540	9.057	0.2173	2.831	2.784	0.593
1000	0.50	78	42.6	0.3068	0.5110	5.152	0.2078	2.786	2.643	0.123
1000	1.25	81	67.8	0.1309	0.6670	6.587	0.2168	2.792	2.678	0.193
1000	2.00	86	58.0	-0.1583	0.6588	5.976	0.2139	2.804	2.696	0.280
1000	2.75	85	61.3	-0.0346	0.6619	6.165	0.2131	2.800	2.691	0.333
1000	3.50	91	53.9	-0.2755	0.6648	5.723	0.2112	2.813	2.707	0.337
1000	4.25	94	63.3	-0.4529	0.7508	6.179	0.2142	2.820	2.738	0.397
1000	5.00	98	86.5	-0.3439	0.9088	7.469	0.2165	2.826	2.749	0.430

Table A8 Aluminum, Magnification = 30x, White Filters, All Four Lights

Speed (RPM)	Feed (in/min)	Avg	Var	Skewness	Omega2	Ra(Image)	Lac(old)	FD2	FD1	Ra(Stylus) (μm)
500	0.50	94	57.6	-0.1744	0.7160	6.042	0.2188	2.820	2.710	0.180
500	1.25	98	60.7	-0.2951	0.7660	6.172	0.2139	2.827	2.727	0.283
500	2.00	102	58.6	-0.2027	0.7821	6.046	0.2132	2.834	2.725	0.373
500	2.75	107	82.5	-0.1842	0.9709	7.263	0.2140	2.843	2.768	0.447
500	3.50	115	162.5	0.7560	1.4599	9.519	0.2095	2.855	2.808	2.327
500	4.25	117	103.0	0.5513	1.1858	7.607	0.2044	2.859	2.800	2.817
500	5.00	122	109.0	0.3913	1.2715	8.177	0.2074	2.866	2.812	3.803
600	0.50	95	64.6	-0.0419	0.7639	6.356	0.2160	2.821	2.717	0.170
600	1.25	117	143.1	-0.2461	1.4045	9.647	0.2292	2.859	2.828	0.423
600	2.00	120	90.2	-0.3530	1.1384	7.562	0.2296	2.863	2.819	0.413
600	2.75	121	106.7	-0.2247	1.2458	7.687	0.2126	2.864	2.835	0.970
600	3.50	123	95.6	-0.1298	1.2043	7.683	0.2202	2.868	2.828	1.663
600	4.25	126	100.8	-0.4796	1.2626	7.637	0.2176	2.872	2.847	2.063
600	5.00	126	116.3	-0.2767	1.3551	8.317	0.2139	2.872	2.856	2.180
700	0.50	107	73.5	-0.2219	0.9131	6.628	0.2118	2.842	2.765	0.193
700	1.25	105	107.6	-0.2892	1.0929	8.187	0.2332	2.840	2.783	0.303
700	2.00	107	100.8	-0.7578	1.0744	7.884	0.2188	2.843	2.786	0.393
700	2.75	111	95.1	-0.4439	1.0846	7.519	0.2208	2.850	2.800	0.573
700	3.50	113	124.2	-0.4022	1.2623	8.851	0.2132	2.853	2.810	0.850
700	4.25	119	132.1	-0.1910	1.3658	9.077	0.2106	2.862	2.836	1.100
700	5.00	113	165.0	-0.5428	1.4505	10.187	0.2218	2.852	2.828	1.113
800	0.50	101	66.4	-0.0937	0.8208	6.468	0.2253	2.832	2.743	0.210
800	1.25	107	48.3	-0.2296	0.7414	5.375	0.2081	2.842	2.743	0.283
800	2.00	120	98.3	-0.1097	1.1900	8.033	0.2084	2.863	2.816	0.420
800	2.75	116	89.3	-0.5554	1.0998	7.409	0.2171	2.858	2.814	0.487
800	3.50	120	122.0	0.2771	1.3284	8.641	0.2250	2.864	2.822	0.520
800	4.25	122	135.7	-0.0258	1.4162	9.172	0.2236	2.866	2.845	0.640
800	5.00	119	132.9	0.0186	1.3673	9.104	0.2258	2.861	2.829	0.780
900	0.50	94	55.9	-0.3450	0.7017	5.892	0.2301	2.819	2.718	0.160
900	1.25	93	56.6	-0.0646	0.7031	5.958	0.2071	2.818	2.701	0.270
900	2.00	108	113.1	-0.4818	1.1463	8.405	0.2221	2.844	2.799	0.383
900	2.75	100	88.6	-0.4616	0.9442	7.493	0.2118	2.831	2.764	0.400
900	3.50	104	124.6	-0.3716	1.1616	8.792	0.2072	2.838	2.785	0.490
900	4.25	108	104.5	-0.8013	1.1017	7.776	0.2102	2.844	2.798	0.490
900	5.00	112	129.8	-0.4145	1.2792	9.237	0.2194	2.851	2.811	0.593
1000	0.50	87	50.5	-0.1792	0.6208	5.631	0.2032	2.806	2.691	0.123
1000	1.25	91	84.4	-0.2333	0.8385	7.294	0.2169	2.814	2.724	0.193
1000	2.00	96	54.2	-0.1393	0.7080	5.861	0.2210	2.823	2.708	0.280
1000	2.75	94	77.7	-0.5022	0.8273	6.882	0.2146	2.819	2.734	0.333
1000	3.50	101	70.2	-0.4162	0.8441	6.622	0.2180	2.832	2.749	0.337
1000	4.25	104	95.1	-0.2429	1.0177	7.660	0.2117	2.838	2.767	0.397
1000	5.00	108	87.1	-0.2965	1.0104	7.321	0.2099	2.845	2.779	0.430

Table A9 Aluminum, Magnification = 20x, Red Filters, All Four Lights

Speed (RPM)	Feed (in/min)	Avg	Var	Skewness	Omega2	Ra(Image)	Lac(old)	FD2	FD1	Ra(Stylus) (μm)
500	0.50	60	56.8	0.2930	0.4516	5.986	0.2072	2.738	2.620	0.180
500	1.25	67	61.6	0.3011	0.5266	6.255	0.2092	2.758	2.638	0.283
500	2.00	66	56.5	0.2285	0.4980	6.019	0.2092	2.756	2.622	0.373
500	2.75	65	109.6	0.1448	0.6807	8.407	0.2060	2.753	2.662	0.447
500	3.50	77	160.1	0.9560	0.9739	9.449	0.2056	2.783	2.690	2.327
500	4.25	82	121.5	0.6521	0.8987	8.294	0.2055	2.794	2.700	2.817
500	5.00	84	126.1	0.5806	0.9421	8.625	0.2057	2.799	2.713	3.803
600	0.50	63	22.9	0.0667	0.3036	3.818	0.1703	2.748	2.557	0.170
600	1.25	85	18.0	-0.6559	0.3616	3.337	0.1711	2.802	2.610	0.423
600	2.00	85	20.3	0.6544	0.3852	3.572	0.1734	2.802	2.625	0.413
600	2.75	85	30.3	0.4233	0.4674	4.207	0.1765	2.801	2.659	0.970
600	3.50	87	36.6	0.1854	0.5281	4.953	0.1766	2.806	2.649	1.663
600	4.25	90	35.8	0.1129	0.5379	4.777	0.1720	2.811	2.663	2.063
600	5.00	86	53.3	-0.3758	0.6265	5.725	0.1743	2.803	2.696	2.180
700	0.50	74	46.0	0.3183	0.5007	5.333	0.2099	2.776	2.629	0.193
700	1.25	71	63.8	-0.0743	0.5651	6.360	0.2108	2.768	2.651	0.303
700	2.00	75	69.4	-0.3889	0.6210	6.574	0.2077	2.778	2.687	0.393
700	2.75	76	77.8	-0.0416	0.6676	7.078	0.2154	2.780	2.680	0.573
700	3.50	79	96.9	-0.1334	0.7815	7.928	0.2188	2.789	2.694	0.850
700	4.25	84	92.0	0.0110	0.8092	7.700	0.2225	2.800	2.701	1.100
700	5.00	79	113.8	-0.3108	0.8434	8.400	0.2118	2.788	2.701	1.113
800	0.50	70	44.0	0.3249	0.4661	5.243	0.2188	2.767	2.624	0.210
800	1.25	71	44.2	0.1164	0.4712	5.242	0.2013	2.768	2.645	0.283
800	2.00	85	102.2	0.1386	0.8633	8.349	0.2070	2.802	2.698	0.420
800	2.75	83	83.2	-0.3828	0.7570	7.194	0.2184	2.797	2.706	0.487
800	3.50	86	105.3	0.7883	0.8861	7.789	0.2173	2.804	2.706	0.520
800	4.25	87	96.6	0.1196	0.8593	7.878	0.2215	2.806	2.715	0.640
800	5.00	83	109.7	0.1576	0.8714	8.508	0.2127	2.797	2.712	0.780
900	0.50	60	36.4	0.6372	0.3616	4.665	0.2043	2.738	2.578	0.160
900	1.25	62	49.4	0.3397	0.4383	5.528	0.2092	2.745	2.605	0.270
900	2.00	75	90.7	0.0101	0.7155	7.615	0.2191	2.779	2.682	0.383
900	2.75	67	72.8	0.1292	0.5741	6.744	0.2003	2.759	2.652	0.400
900	3.50	73	92.3	-0.2814	0.6972	7.649	0.2212	2.773	2.692	0.490
900	4.25	77	97.8	-0.3612	0.7596	7.447	0.2113	2.783	2.711	0.490
900	5.00	76	145.0	-0.0011	0.9123	9.680	0.2180	2.780	2.712	0.593
1000	0.50	52	35.2	0.6527	0.3106	4.701	0.1983	2.714	2.564	0.123
1000	1.25	62	54.9	0.2939	0.4559	5.902	0.2109	2.743	2.621	0.193
1000	2.00	65	47.3	0.4268	0.4453	5.476	0.2105	2.752	2.614	0.280
1000	2.75	61	58.7	0.2167	0.4635	6.085	0.2055	2.740	2.618	0.333
1000	3.50	70	66.1	-0.0550	0.5663	6.442	0.2128	2.765	2.660	0.337
1000	4.25	73	84.3	0.0663	0.6681	7.115	0.2095	2.773	2.679	0.397
1000	5.00	75	71.5	-0.0413	0.6373	6.738	0.2036	2.779	2.672	0.430

Table A10 Aluminum, Magnification = 30x, Red Filters, All Four Lights

Speed (RPM)	Feed (in/min)	Avg	Var	Skewness	Omega2	Ra(Image)	Lac(old)	FD2	FD1	Ra(Stylus) (μm)
500	0.50	61	56.4	0.1384	0.4592	6.003	0.2017	2.742	2.609	0.180
500	1.25	66	44.1	-0.0368	0.4389	5.273	0.2047	2.756	2.620	0.283
500	2.00	67	47.2	0.1207	0.4620	5.433	0.2028	2.759	2.624	0.373
500	2.75	75	73.4	0.0958	0.6405	6.905	0.2004	2.778	2.673	0.447
500	3.50	79	98.3	0.8462	0.7841	7.289	0.2031	2.788	2.680	2.327
500	4.25	83	85.5	0.2607	0.7656	7.030	0.2022	2.796	2.704	2.817
500	5.00	81	117.7	0.2016	0.8782	8.334	0.2110	2.792	2.714	3.803
600	0.50	64	40.2	0.1520	0.4043	5.002	0.2047	2.749	2.604	0.170
600	1.25	80	158.6	0.3165	1.0123	10.299	0.2182	2.791	2.710	0.423
600	2.00	86	65.8	0.1757	0.6968	6.406	0.2226	2.803	2.683	0.413
600	2.75	83	101.7	-0.0701	0.8399	7.701	0.2217	2.798	2.713	0.970
600	3.50	88	113.1	0.3893	0.9386	8.254	0.2311	2.808	2.721	1.663
600	4.25	89	81.0	0.4025	0.8043	6.926	0.2139	2.810	2.708	2.063
600	5.00	90	99.2	-0.0608	0.8929	7.680	0.2130	2.811	2.722	2.180
700	0.50	72	47.8	0.0776	0.4995	5.405	0.2081	2.772	2.637	0.193
700	1.25	71	64.0	-0.1777	0.5642	6.336	0.2159	2.768	2.655	0.303
700	2.00	70	82.2	-0.4634	0.6336	7.249	0.2005	2.766	2.673	0.393
700	2.75	75	71.2	-0.1545	0.6352	6.681	0.2251	2.779	2.677	0.573
700	3.50	76	86.2	-0.4389	0.7028	7.430	0.2144	2.780	2.686	0.850
700	4.25	81	88.0	-0.4965	0.7633	7.438	0.2185	2.793	2.708	1.100
700	5.00	77	118.6	0.0408	0.8336	8.617	0.2181	2.782	2.702	1.113
800	0.50	67	40.4	0.1869	0.4260	5.065	0.2116	2.758	2.604	0.210
800	1.25	71	42.5	0.0833	0.4605	5.198	0.1998	2.768	2.619	0.283
800	2.00	85	131.9	0.0555	0.9755	9.450	0.2032	2.801	2.715	0.420
800	2.75	80	73.3	-0.7008	0.6874	6.716	0.2088	2.791	2.700	0.487
800	3.50	83	112.6	0.7996	0.8782	7.863	0.2063	2.796	2.704	0.520
800	4.25	86	132.9	0.2483	0.9874	9.048	0.2183	2.803	2.729	0.640
800	5.00	82	123.7	0.1032	0.9074	8.882	0.2114	2.794	2.710	0.780
900	0.50	58	39.6	0.1221	0.3635	5.041	0.2078	2.731	2.581	0.160
900	1.25	63	47.1	-0.0580	0.4312	5.434	0.2076	2.747	2.618	0.270
900	2.00	72	66.4	-0.0467	0.5900	6.461	0.2104	2.772	2.659	0.383
900	2.75	65	81.9	-0.1678	0.5884	7.157	0.2005	2.753	2.657	0.400
900	3.50	71	83.5	-0.1041	0.6468	7.260	0.2140	2.768	2.679	0.490
900	4.25	75	83.8	-0.2851	0.6864	7.139	0.2113	2.779	2.686	0.490
900	5.00	74	132.3	0.1852	0.8554	9.146	0.2123	2.777	2.695	0.593
1000	0.50	54	38.4	0.6712	0.3352	4.787	0.1992	2.720	2.556	0.123
1000	1.25	58	63.7	0.4878	0.4635	6.237	0.2085	2.732	2.609	0.193
1000	2.00	64	52.8	0.1118	0.4619	5.785	0.2122	2.749	2.618	0.280
1000	2.75	64	57.6	-0.0019	0.4884	5.956	0.2108	2.751	2.640	0.333
1000	3.50	69	56.3	-0.1687	0.5187	5.843	0.2068	2.764	2.643	0.337
1000	4.25	73	52.6	-0.3085	0.5330	5.684	0.2090	2.775	2.656	0.397
1000	5.00	75	87.7	0.0405	0.7028	7.529	0.2060	2.779	2.670	0.430

Table A11 Copper, Magnification = 20x, Red Filters, All Four Lights

Speed (RPM)	Feed (in/min)	Avg	Var	Skewness	Omega2	Ra(Image)	Lac(old)	FD2	FD1	Ra(Stylus) (μm)
500	0.50	91	30.3	0.6171	0.4985	4.329	0.2082	2.813	2.641	0.203
500	1.25	83	37.8	-0.0289	0.5078	4.777	0.2053	2.796	2.657	0.543
500	2.00	82	48.5	0.1335	0.5696	5.551	0.2117	2.794	2.664	0.453
500	2.75	79	55.6	0.2034	0.5886	5.938	0.2122	2.788	2.658	0.637
500	3.50	79	96.6	-0.3678	0.7735	8.026	0.2065	2.787	2.698	0.667
500	4.25	82	103.4	-0.6223	0.8339	8.137	0.2029	2.795	2.721	0.790
500	5.00	83	75.0	-0.7628	0.7207	6.647	0.2121	2.797	2.712	0.873
600	0.50	89	21.6	-0.0511	0.4118	3.658	0.1848	2.809	2.623	0.267
600	1.25	89	19.3	0.7228	0.3923	3.415	0.1842	2.810	2.622	0.347
600	2.00	87	19.0	1.0120	0.3787	3.280	0.2566	2.805	2.622	0.727
600	2.75	85	50.2	-0.3124	0.5993	5.475	0.1879	2.800	2.691	1.470
600	3.50	86	13.8	1.6460	0.3205	2.917	0.1701	2.804	2.566	0.380
600	4.25	87	16.1	1.2596	0.3477	3.149	0.1789	2.805	2.574	0.513
600	5.00	88	19.0	1.3650	0.3845	3.382	0.1869	2.808	2.589	0.580
700	0.50	96	20.6	0.7815	0.4352	3.558	0.1840	2.823	2.637	0.157
700	1.25	90	22.4	0.6200	0.4278	3.831	0.1713	2.812	2.611	0.387
700	2.00	88	15.1	1.3725	0.3433	3.053	0.1698	2.808	2.589	0.303
700	2.75	85	22.6	0.6101	0.4055	3.862	0.1665	2.802	2.611	0.357
700	3.50	88	14.6	1.6121	0.3360	3.000	0.1703	2.807	2.568	0.403
700	4.25	90	24.7	0.6382	0.4488	3.968	0.1662	2.812	2.636	0.453
700	5.00	86	18.2	1.3111	0.3683	3.290	0.1632	2.804	2.600	0.527
800	0.50	86	21.4	1.1100	0.3989	3.692	0.1737	2.804	2.584	0.250
800	1.25	85	17.0	0.9300	0.3508	3.184	0.1638	2.801	2.607	0.313
800	2.00	86	17.9	1.1078	0.3658	3.192	0.1616	2.804	2.614	0.360
800	2.75	95	25.4	0.8750	0.4808	3.961	0.1688	2.822	2.640	0.440
800	3.50	96	28.9	0.9480	0.5145	4.252	0.1683	2.823	2.633	0.480
800	4.25	92	35.5	0.3014	0.5471	4.753	0.1672	2.815	2.658	0.477
800	5.00	91	33.8	0.9300	0.5273	4.552	0.1651	2.813	2.631	0.543
900	0.50	84	26.8	-1.3878	0.4365	3.674	0.1710	2.800	2.620	0.157
900	1.25	83	15.1	1.4737	0.3243	3.030	0.1686	2.798	2.580	0.357
900	2.00	81	30.3	0.8960	0.4472	4.281	0.1675	2.793	2.612	0.423
900	2.75	84	24.6	0.6782	0.4152	3.922	0.1693	2.798	2.612	0.450
900	3.50	79	25.0	1.2383	0.3958	3.880	0.1626	2.788	2.579	0.447
900	4.25	84	28.8	1.0858	0.4530	4.161	0.1675	2.800	2.610	0.563
900	5.00	85	29.5	1.0350	0.4643	4.245	0.1649	2.802	2.613	0.557
1000	0.50	81	26.4	0.7532	0.4171	4.028	0.1876	2.793	2.621	0.293
1000	1.25	87	26.5	-0.3556	0.4460	3.874	0.1896	2.805	2.660	0.227
1000	2.00	78	20.9	1.0508	0.3580	3.581	0.1775	2.786	2.592	0.313
1000	2.75	77	14.9	1.5687	0.2964	2.994	0.1717	2.783	2.568	0.440
1000	3.50	79	14.4	1.9147	0.3011	2.954	0.1741	2.788	2.547	0.460
1000	4.25	80	11.9	1.8970	0.2749	2.725	0.1686	2.789	2.555	0.600
1000	5.00	77	14.7	1.8058	0.2955	2.966	0.1726	2.784	2.558	0.693

Table A12 Copper, Magnification = 30x, Red Filters, All Four Lights

Speed (RPM)	Feed (in/min)	Avg	Var	Skewness	Omega2	Ra(Image)	Lac(old)	FD2	FD1	Ra(Stylus) (μm)
500	0.50	92	31.7	0.0346	0.5175	4.504	0.2133	2.815	2.658	0.203
500	1.25	82	40.7	-0.1029	0.5248	5.014	0.2067	2.795	2.653	0.543
500	2.00	82	47.6	-0.1290	0.5682	5.426	0.2034	2.796	2.671	0.453
500	2.75	80	55.5	-0.2136	0.5926	5.878	0.2105	2.789	2.678	0.637
500	3.50	77	100.9	-0.5199	0.7780	8.190	0.2021	2.784	2.703	0.667
500	4.25	84	75.4	-0.5932	0.7297	6.706	0.2103	2.799	2.713	0.790
500	5.00	81	93.4	-0.8748	0.7870	7.491	0.2092	2.793	2.725	0.873
600	0.50	88	49.6	-0.2909	0.6186	5.368	0.2054	2.807	2.695	0.267
600	1.25	90	37.8	0.2047	0.5552	4.885	0.2104	2.812	2.659	0.347
600	2.00	86	55.4	-0.0466	0.6373	5.627	0.2083	2.802	2.700	0.727
600	2.75	81	98.7	-0.1156	0.8033	7.611	0.2139	2.792	2.709	1.470
600	3.50	86	33.3	0.4185	0.4949	4.467	0.2141	2.803	2.641	0.380
600	4.25	86	32.3	-0.3846	0.4913	4.172	0.2053	2.804	2.638	0.513
600	5.00	88	40.4	0.8173	0.5593	4.767	0.2141	2.807	2.649	0.580
700	0.50	86	37.4	-0.3482	0.5273	4.743	0.2056	2.804	2.646	0.157
700	1.25	88	44.1	-0.0190	0.5817	5.211	0.1975	2.807	2.679	0.387
700	2.00	87	31.8	0.2209	0.4921	4.443	0.2095	2.806	2.640	0.303
700	2.75	85	41.8	0.1954	0.5470	5.094	0.2151	2.800	2.655	0.357
700	3.50	87	41.9	0.1245	0.5628	5.123	0.2074	2.805	2.664	0.403
700	4.25	89	67.1	0.4033	0.7297	6.388	0.2122	2.810	2.694	0.453
700	5.00	88	52.7	0.6789	0.6395	5.566	0.2060	2.808	2.659	0.527
800	0.50	82	41.8	0.0176	0.5290	5.105	0.2103	2.794	2.648	0.250
800	1.25	83	40.4	0.2181	0.5290	4.972	0.2095	2.797	2.648	0.313
800	2.00	86	43.9	0.3713	0.5690	5.128	0.2064	2.803	2.660	0.360
800	2.75	92	102.3	0.7152	0.9256	7.555	0.2161	2.814	2.721	0.440
800	3.50	93	58.6	0.8675	0.7099	5.780	0.2148	2.817	2.678	0.480
800	4.25	90	70.3	0.5397	0.7542	6.490	0.2129	2.811	2.695	0.477
800	5.00	89	51.1	0.6714	0.6382	5.523	0.2134	2.810	2.664	0.543
900	0.50	87	21.7	0.1113	0.4062	3.707	0.2051	2.806	2.616	0.157
900	1.25	85	61.0	-0.0450	0.6604	6.002	0.2173	2.800	2.691	0.357
900	2.00	81	66.3	0.4265	0.6565	6.314	0.2176	2.792	2.668	0.423
900	2.75	84	78.9	0.5138	0.7442	6.874	0.2154	2.799	2.684	0.450
900	3.50	79	81.3	0.9112	0.7108	6.677	0.2263	2.788	2.671	0.447
900	4.25	82	75.9	0.4116	0.7111	6.664	0.2123	2.794	2.690	0.563
900	5.00	83	78.0	0.2985	0.7287	6.596	0.2240	2.796	2.685	0.557
1000	0.50	79	29.4	0.2116	0.4274	4.274	0.2091	2.787	2.611	0.293
1000	1.25	84	33.2	-0.4981	0.4821	4.402	0.2175	2.798	2.669	0.227
1000	2.00	76	34.6	0.0178	0.4442	4.585	0.2082	2.780	2.630	0.313
1000	2.75	75	33.2	0.0220	0.4323	4.469	0.2097	2.779	2.633	0.440
1000	3.50	77	31.5	0.5535	0.4339	4.373	0.2073	2.784	2.603	0.460
1000	4.25	78	29.6	0.2667	0.4250	4.267	0.2113	2.786	2.613	0.600
1000	5.00	75	33.9	0.2465	0.4393	4.536	0.2026	2.780	2.620	0.693

Table A13 Aluminum, Magnification = 20x, Green Filters, All Four Lights

Speed (RPM)	Feed (in/min)	Avg	Var	Skewness	Omega2	Ra(Image)	Lac(old)	FD2	FD1	Ra(Stylus) (μm)
500	0.50	106	92.9	-0.0412	1.0266	7.443	0.2215	2.842	2.774	0.180
500	1.25	116	89.0	0.0780	1.0896	7.395	0.2173	2.856	2.794	0.283
500	2.00	118	109.8	0.1978	1.2319	8.027	0.2145	2.860	2.801	0.373
500	2.75	121	206.4	1.2120	1.7321	10.964	0.2139	2.864	2.838	0.447
500	3.50	136	265.1	1.5052	2.2115	11.545	0.2067	2.886	2.885	2.327
500	4.25	135	288.5	1.2930	2.2894	12.412	0.2138	2.884	2.887	2.817
500	5.00	136	314.1	0.6153	2.4118	13.661	0.2184	2.886	2.906	3.803
600	0.50	103	124.2	0.1149	1.1495	8.874	0.2255	2.836	2.767	0.170
600	1.25	134	278.9	0.0191	2.2322	13.261	0.2383	2.883	2.902	0.423
600	2.00	137	222.4	0.0109	2.0473	11.433	0.2265	2.888	2.911	0.413
600	2.75	140	372.3	0.3179	2.7061	14.345	0.2360	2.891	2.933	0.970
600	3.50	143	391.7	0.3768	2.8345	15.153	0.2069	2.895	2.944	1.663
600	4.25	143	231.1	0.1516	2.1753	11.621	0.2274	2.895	2.931	2.063
600	5.00	141	313.3	-0.0973	2.4996	13.647	0.2218	2.893	2.934	2.180
700	0.50	110	122.6	-0.1804	1.2207	8.688	0.2263	2.848	2.807	0.193
700	1.25	107	152.7	-0.3456	1.3275	9.480	0.2325	2.843	2.805	0.303
700	2.00	114	153.7	-0.5511	1.4123	9.647	0.2256	2.854	2.826	0.393
700	2.75	117	153.6	-0.1706	1.4494	9.419	0.2213	2.859	2.833	0.573
700	3.50	122	217.3	0.1449	1.8031	11.679	0.2200	2.867	2.852	0.850
700	4.25	125	205.4	-0.0207	1.7886	11.022	0.2265	2.870	2.864	1.100
700	5.00	124	286.7	0.0690	2.0916	12.811	0.2288	2.869	2.873	1.113
800	0.50	110	83.9	-0.0671	1.0080	7.124	0.2298	2.848	2.778	0.210
800	1.25	117	91.9	0.2650	1.1172	7.291	0.2196	2.858	2.802	0.283
800	2.00	135	292.4	0.3321	2.3071	13.842	0.2197	2.884	2.898	0.420
800	2.75	132	220.3	-0.5370	1.9653	11.467	0.2195	2.881	2.899	0.487
800	3.50	139	422.0	0.8259	2.8565	15.345	0.2347	2.890	2.926	0.520
800	4.25	137	352.3	0.1275	2.5728	14.862	0.2315	2.887	2.918	0.640
800	5.00	133	305.2	0.2820	2.3301	13.922	0.2306	2.882	2.899	0.780
900	0.50	101	86.8	-0.2307	0.9364	7.329	0.2318	2.831	2.756	0.160
900	1.25	106	102.0	0.0732	1.0656	7.742	0.2160	2.840	2.776	0.270
900	2.00	122	207.5	0.0933	1.7554	11.288	0.2174	2.866	2.854	0.383
900	2.75	115	173.3	-0.0430	1.5080	10.036	0.2220	2.855	2.825	0.400
900	3.50	118	218.1	-0.0681	1.7466	11.427	0.2238	2.861	2.846	0.490
900	4.25	121	236.6	-0.7684	1.8628	11.452	0.2294	2.865	2.869	0.490
900	5.00	123	401.8	0.0106	2.4610	15.859	0.2314	2.867	2.877	0.593
1000	0.50	96	64.6	0.1497	0.7677	6.292	0.2149	2.822	2.715	0.123
1000	1.25	98	98.4	0.0749	0.9704	7.827	0.2158	2.827	2.746	0.193
1000	2.00	105	89.7	0.0168	0.9957	7.416	0.2198	2.840	2.764	0.280
1000	2.75	103	125.8	-0.2665	1.1574	8.684	0.2208	2.836	2.786	0.333
1000	3.50	112	123.4	-0.1671	1.2477	8.570	0.2286	2.851	2.808	0.337
1000	4.25	113	162.2	-0.2229	1.4433	9.742	0.2386	2.853	2.817	0.397
1000	5.00	121	148.2	0.0615	1.4701	9.420	0.2223	2.864	2.840	0.430

Table A14 Aluminum, Magnification = 30x, Green Filters, All Four Lights

Speed (RPM)	Feed (in/min)	Avg	Var	Skewness	Omega2	Ra(Image)	Lac(old)	FD2	FD1	Ra(Stylus) (μm)
500	0.50	95	91.7	-0.1090	0.9083	7.500	0.2218	2.821	2.742	0.180
500	1.25	101	88.1	-0.1740	0.9481	7.207	0.2203	2.832	2.755	0.283
500	2.00	102	97.5	0.1716	1.0102	7.666	0.2169	2.835	2.761	0.373
500	2.75	111	136.2	0.1732	1.2978	9.184	0.2186	2.850	2.800	0.447
500	3.50	118	305.7	1.4645	2.0692	12.542	0.2166	2.861	2.836	2.327
500	4.25	120	196.6	0.5545	1.6799	10.356	0.2232	2.863	2.842	2.817
500	5.00	119	242.7	0.6395	1.8473	11.763	0.2162	2.861	2.835	3.803
600	0.50	99	76.0	-0.1329	0.8654	6.806	0.2216	2.829	2.747	0.170
600	1.25	116	345.8	0.4619	2.1483	14.746	0.2418	2.857	2.844	0.423
600	2.00	126	166.8	-0.0441	1.6279	10.064	0.2321	2.872	2.859	0.413
600	2.75	129	281.8	0.3159	2.1656	12.254	0.2292	2.876	2.891	0.970
600	3.50	130	312.0	0.5174	2.2933	13.415	0.2349	2.878	2.885	1.663
600	4.25	133	225.1	0.4884	1.9919	11.152	0.2331	2.882	2.890	2.063
600	5.00	131	246.5	0.0282	2.0596	12.009	0.2239	2.879	2.889	2.180
700	0.50	107	105.5	-0.3546	1.1020	7.792	0.2197	2.843	2.788	0.193
700	1.25	107	162.6	-0.3518	1.3597	10.053	0.2262	2.842	2.801	0.303
700	2.00	107	149.4	-0.6388	1.3041	9.329	0.2175	2.842	2.804	0.393
700	2.75	116	155.8	-0.2421	1.4467	9.470	0.2080	2.857	2.840	0.573
700	3.50	115	190.1	-0.3745	1.5923	10.933	0.2264	2.856	2.830	0.850
700	4.25	120	215.5	-0.4552	1.7603	11.438	0.2353	2.863	2.856	1.100
700	5.00	113	250.9	0.0835	1.7884	12.257	0.2297	2.852	2.835	1.113
800	0.50	101	74.6	-0.1285	0.8742	6.737	0.2301	2.833	2.742	0.210
800	1.25	104	72.7	0.1018	0.8870	6.668	0.2204	2.838	2.743	0.283
800	2.00	128	310.6	0.5123	2.2533	14.283	0.2267	2.875	2.870	0.420
800	2.75	123	163.7	-0.5828	1.5674	10.027	0.2300	2.867	2.858	0.487
800	3.50	124	260.3	0.7148	1.9936	12.054	0.2264	2.869	2.863	0.520
800	4.25	127	376.2	0.6147	2.4643	15.062	0.2292	2.874	2.883	0.640
800	5.00	120	278.2	0.2575	1.9994	13.342	0.2245	2.863	2.852	0.780
900	0.50	93	80.8	0.1924	0.8343	7.100	0.2261	2.817	2.715	0.160
900	1.25	98	71.7	-0.0724	0.8325	6.661	0.2206	2.827	2.734	0.270
900	2.00	112	160.1	-0.0979	1.4151	9.857	0.2198	2.851	2.817	0.383
900	2.75	106	142.7	-0.2758	1.2627	9.186	0.2226	2.841	2.795	0.400
900	3.50	109	162.0	-0.0911	1.3865	9.815	0.2180	2.846	2.806	0.490
900	4.25	112	194.5	-0.2005	1.5573	10.841	0.2315	2.850	2.826	0.490
900	5.00	112	291.7	0.4432	1.9078	13.316	0.2277	2.850	2.824	0.593
1000	0.50	88	69.3	0.1894	0.7294	6.458	0.2197	2.807	2.687	0.123
1000	1.25	92	123.8	0.1512	1.0287	8.627	0.2240	2.816	2.742	0.193
1000	2.00	100	111.9	-0.1789	1.0527	8.334	0.2269	2.830	2.762	0.280
1000	2.75	103	114.6	-0.2192	1.1006	8.307	0.2272	2.835	2.777	0.333
1000	3.50	106	131.7	-0.3579	1.2219	8.852	0.2313	2.842	2.790	0.337
1000	4.25	110	122.2	-0.3508	1.2115	8.445	0.2306	2.847	2.797	0.397
1000	5.00	113	195.1	0.0394	1.5736	11.250	0.2210	2.852	2.816	0.430

Table A15 Copper, Magnification = 20x, Green Filters, All Four Lights

Speed (RPM)	Feed (in/min)	Avg	Var	Skewness	Omega2	Ra(Image)	Lac(old)	FD2	FD1	Ra(Stylus) (μm)
500	0.50	107	44.0	0.1522	0.7104	5.175	0.2195	2.843	2.725	0.203
500	1.25	98	49.6	-0.2605	0.6921	5.502	0.2215	2.827	2.714	0.543
500	2.00	98	48.1	-0.0467	0.6811	5.425	0.2104	2.827	2.714	0.453
500	2.75	95	63.4	0.0686	0.7587	6.258	0.2122	2.822	2.712	0.637
500	3.50	93	104.9	-0.3837	0.9477	8.315	0.2086	2.816	2.743	0.667
500	4.25	97	106.1	-0.5771	0.9992	8.146	0.2149	2.825	2.765	0.790
500	5.00	98	82.3	-0.6341	0.8856	7.074	0.2131	2.826	2.757	0.873
600	0.50	106	18.3	-0.0030	0.4510	3.333	0.1842	2.840	2.661	0.267
600	1.25	106	33.2	0.3100	0.6116	4.594	0.1760	2.841	2.693	0.347
600	2.00	104	27.3	0.0272	0.5456	4.055	0.1775	2.838	2.702	0.727
600	2.75	100	57.0	-0.4368	0.7572	5.903	0.1804	2.831	2.733	1.470
600	3.50	103	14.7	-0.0603	0.3955	3.053	0.1714	2.836	2.616	0.380
600	4.25	102	15.3	-0.3278	0.3976	3.103	0.1758	2.833	2.636	0.513
600	5.00	103	23.5	0.7243	0.4985	3.736	0.1806	2.835	2.641	0.580
700	0.50	113	23.7	-0.0437	0.5493	3.913	0.1717	2.852	2.701	0.157
700	1.25	104	18.7	-0.2091	0.4516	3.486	0.1687	2.838	2.656	0.387
700	2.00	103	15.2	0.2530	0.4012	3.055	0.1689	2.835	2.606	0.303
700	2.75	100	22.4	-0.0334	0.4754	3.833	0.1685	2.831	2.643	0.357
700	3.50	103	20.5	0.0623	0.4676	3.592	0.1809	2.837	2.637	0.403
700	4.25	107	27.8	0.2657	0.5653	4.226	0.1918	2.843	2.688	0.453
700	5.00	105	27.3	0.3987	0.5504	4.092	0.1657	2.840	2.670	0.527
800	0.50	103	18.6	0.1709	0.4436	3.474	0.1689	2.835	2.625	0.250
800	1.25	100	20.5	-0.1419	0.4517	3.572	0.1644	2.830	2.657	0.313
800	2.00	101	17.3	0.5777	0.4218	3.121	0.1633	2.833	2.629	0.360
800	2.75	111	29.1	0.4240	0.5984	4.283	0.1661	2.849	2.683	0.440
800	3.50	111	37.4	0.7031	0.6779	4.802	0.1664	2.849	2.682	0.480
800	4.25	108	49.7	0.0000	0.7578	5.563	0.1631	2.844	2.729	0.477
800	5.00	107	37.1	0.4179	0.6501	4.876	0.1615	2.842	2.680	0.543
900	0.50	97	19.2	-1.2484	0.4263	3.256	0.1671	2.825	2.667	0.157
900	1.25	99	17.3	0.0382	0.4098	3.319	0.2214	2.828	2.623	0.357
900	2.00	98	33.8	0.5376	0.5714	4.579	0.1662	2.827	2.659	0.423
900	2.75	101	33.9	0.3300	0.5905	4.623	0.1654	2.833	2.670	0.450
900	3.50	94	22.0	0.6057	0.4433	3.617	0.1672	2.820	2.610	0.447
900	4.25	101	35.5	0.9339	0.6018	4.473	0.1657	2.832	2.666	0.563
900	5.00	101	44.9	1.4581	0.6775	4.973	0.1620	2.833	2.667	0.557
1000	0.50	92	20.9	-0.6729	0.4200	3.455	0.1631	2.815	2.658	0.293
1000	1.25	101	38.1	-2.7425	0.6232	3.946	0.1671	2.832	2.782	0.227
1000	2.00	92	15.9	-0.3328	0.3683	3.115	0.1605	2.816	2.617	0.313
1000	2.75	92	10.5	-0.3641	0.2968	2.541	0.1604	2.815	2.588	0.440
1000	3.50	93	12.1	0.0158	0.3229	2.785	0.1663	2.817	2.574	0.460
1000	4.25	92	12.2	-0.4929	0.3227	2.810	0.1601	2.816	2.600	0.600
1000	5.00	89	12.1	0.0236	0.3110	2.723	0.1635	2.810	2.577	0.693

Table A16 Copper, Magnification = 30x, Green Filters, All Four Lights

Speed (RPM)	Feed (in/min)	Avg	Var	Skewness	Omega2	Ra(Image)	Lac(old)	FD2	FD1	Ra(Stylus) (μm)
500	0.50	100	37.5	-0.1888	0.6149	4.792	0.2168	2.831	2.707	0.203
500	1.25	91	45.7	-0.1921	0.6127	5.272	0.2127	2.813	2.680	0.543
500	2.00	91	60.0	-0.2330	0.7078	6.088	0.2075	2.814	2.708	0.453
500	2.75	88	66.0	0.0395	0.7146	6.321	0.2165	2.807	2.696	0.637
500	3.50	87	119.4	-0.4805	0.9538	8.891	0.2176	2.806	2.732	0.667
500	4.25	93	95.4	-0.3232	0.9114	7.393	0.2177	2.818	2.748	0.790
500	5.00	92	99.3	-0.9362	0.9205	7.422	0.2129	2.816	2.757	0.873
600	0.50	97	42.9	-0.5637	0.6329	4.915	0.2130	2.824	2.719	0.267
600	1.25	100	48.1	0.1197	0.6917	5.449	0.2127	2.830	2.699	0.347
600	2.00	95	92.4	-0.1514	0.9151	7.241	0.2170	2.822	2.749	0.727
600	2.75	90	128.9	-0.0080	1.0218	8.677	0.2194	2.811	2.746	1.470
600	3.50	96	42.8	0.5935	0.6280	5.029	0.2220	2.823	2.681	0.380
600	4.25	96	57.8	1.0776	0.7315	5.307	0.2130	2.823	2.683	0.513
600	5.00	97	68.1	1.3718	0.8030	5.980	0.2180	2.826	2.697	0.580
700	0.50	102	61.2	0.2354	0.7983	6.320	0.2233	2.834	2.716	0.157
700	1.25	99	59.4	-0.2806	0.7602	6.118	0.2100	2.828	2.731	0.387
700	2.00	97	43.6	0.0371	0.6379	5.226	0.2123	2.824	2.680	0.303
700	2.75	96	62.8	0.3727	0.7609	6.156	0.2275	2.823	2.706	0.357
700	3.50	98	62.0	0.2917	0.7707	6.088	0.2212	2.827	2.710	0.403
700	4.25	101	127.0	0.6612	1.1376	8.703	0.2217	2.832	2.750	0.453
700	5.00	102	109.6	0.5619	1.0700	7.844	0.2321	2.834	2.755	0.527
800	0.50	95	68.0	0.1555	0.7803	6.409	0.2255	2.821	2.719	0.250
800	1.25	91	34.0	0.1584	0.5292	4.613	0.2201	2.813	2.654	0.313
800	2.00	97	69.8	0.5018	0.8078	6.324	0.2215	2.824	2.712	0.360
800	2.75	106	147.1	0.8460	1.2871	8.793	0.2265	2.841	2.776	0.440
800	3.50	105	100.3	1.0117	1.0526	7.422	0.2138	2.839	2.747	0.480
800	4.25	102	90.9	0.6204	0.9701	7.246	0.2275	2.834	2.746	0.477
800	5.00	101	96.7	0.9250	0.9913	7.369	0.2254	2.832	2.738	0.543
900	0.50	97	26.8	0.0820	0.5003	4.054	0.2098	2.824	2.660	0.157
900	1.25	96	60.9	-0.0195	0.7471	6.054	0.2041	2.823	2.717	0.357
900	2.00	94	61.4	0.5286	0.7337	6.083	0.2025	2.819	2.689	0.423
900	2.75	98	101.6	0.8732	0.9911	7.737	0.2036	2.827	2.721	0.450
900	3.50	92	71.8	0.7263	0.7829	6.405	0.2040	2.816	2.698	0.447
900	4.25	95	58.0	0.8134	0.7211	5.755	0.2046	2.821	2.700	0.563
900	5.00	96	57.5	0.4882	0.7260	5.753	0.2106	2.823	2.687	0.557
1000	0.50	87	37.8	0.2960	0.5365	4.761	0.2116	2.806	2.658	0.293
1000	1.25	97	34.4	-0.3362	0.5668	4.453	0.2106	2.824	2.679	0.227
1000	2.00	88	33.6	0.0426	0.5080	4.471	0.1981	2.807	2.654	0.313
1000	2.75	87	27.4	0.0098	0.4553	3.970	0.1904	2.805	2.656	0.440
1000	3.50	89	38.0	0.4788	0.5490	4.746	0.2147	2.810	2.653	0.460
1000	4.25	89	39.6	0.0899	0.5631	4.956	0.2155	2.810	2.667	0.600
1000	5.00	87	43.9	0.2505	0.5766	5.005	0.2129	2.805	2.673	0.693

Table A17 Copper, Magnification = 20x, Blue Filters, All Four Lights

Speed (RPM)	Feed (in/min)	Avg	Var	Skewness	Omega2	Ra(Image)	Lac(old)	FD2	FD1	Ra(Stylus) (μm)
500	0.50	62	11.9	-0.1127	0.2136	2.691	0.1837	2.744	2.515	0.203
500	1.25	55	13.7	-0.0339	0.2056	2.927	0.1799	2.724	2.526	0.543
500	2.00	55	15.0	-0.0763	0.2115	3.068	0.1843	2.721	2.526	0.453
500	2.75	52	23.0	-0.0171	0.2495	3.743	0.1814	2.713	2.550	0.637
500	3.50	50	39.9	0.3174	0.3171	4.993	0.1795	2.706	2.569	0.667
500	4.25	54	33.5	-0.3755	0.3141	4.603	0.1794	2.720	2.586	0.790
500	5.00	55	28.3	-0.7749	0.2928	4.196	0.1782	2.723	2.586	0.873
600	0.50	60	9.4	-0.4711	0.1829	2.361	0.1847	2.737	2.524	0.267
600	1.25	59	13.1	0.4155	0.2151	2.888	0.1804	2.736	2.482	0.347
600	2.00	55	10.4	0.1505	0.1784	2.507	0.1814	2.723	2.507	0.727
600	2.75	51	19.0	-0.2524	0.2234	3.453	0.1760	2.710	2.540	1.470
600	3.50	56	9.2	0.3192	0.1697	2.424	0.1738	2.725	2.464	0.380
600	4.25	57	9.6	0.3471	0.1759	2.495	0.1765	2.728	2.462	0.513
600	5.00	58	13.6	0.9715	0.2135	2.824	0.1791	2.732	2.470	0.580
700	0.50	64	7.5	0.2991	0.1770	2.194	0.1823	2.751	2.475	0.157
700	1.25	58	12.9	0.1207	0.2095	2.851	0.1757	2.733	2.499	0.387
700	2.00	56	9.7	0.3043	0.1760	2.476	0.1742	2.727	2.477	0.303
700	2.75	54	15.3	0.4574	0.2095	3.134	0.1742	2.718	2.492	0.357
700	3.50	56	13.1	0.5302	0.2034	2.852	0.1744	2.726	2.471	0.403
700	4.25	60	22.3	0.3879	0.2837	3.783	0.1793	2.738	2.530	0.453
700	5.00	59	18.4	0.5420	0.2511	3.373	0.1787	2.734	2.520	0.527
800	0.50	56	12.7	0.2326	0.2012	2.821	0.1884	2.727	2.495	0.250
800	1.25	57	8.6	0.4145	0.1672	2.320	0.1739	2.729	2.466	0.313
800	2.00	56	12.8	0.7317	0.1991	2.788	0.1775	2.725	2.461	0.360
800	2.75	60	27.8	0.5854	0.3166	3.990	0.1799	2.738	2.556	0.440
800	3.50	59	27.9	0.5438	0.3139	4.103	0.1804	2.737	2.548	0.480
800	4.25	59	28.6	0.3984	0.3182	4.208	0.1827	2.737	2.561	0.477
800	5.00	58	28.0	0.6729	0.3056	4.164	0.1862	2.731	2.535	0.543
900	0.50	53	28.6	-1.5544	0.2843	3.786	0.1810	2.717	2.613	0.157
900	1.25	53	10.9	0.3847	0.1757	2.570	0.1805	2.717	2.486	0.357
900	2.00	54	24.3	0.6643	0.2669	3.854	0.1841	2.720	2.519	0.423
900	2.75	56	27.1	0.6309	0.2906	4.055	0.1884	2.725	2.532	0.450
900	3.50	51	13.3	0.4179	0.1867	2.853	0.1754	2.710	2.499	0.447
900	4.25	57	25.4	0.9580	0.2855	3.837	0.1828	2.728	2.531	0.563
900	5.00	58	27.7	0.9690	0.3054	4.042	0.1872	2.732	2.526	0.557
1000	0.50	51	14.8	0.2677	0.1966	3.049	0.1804	2.709	2.495	0.293
1000	1.25	58	12.1	-0.5647	0.2006	2.681	0.1845	2.731	2.533	0.227
1000	2.00	48	10.5	0.1576	0.1566	2.476	0.1749	2.699	2.477	0.313
1000	2.75	48	5.9	0.6369	0.1178	1.927	0.1744	2.700	2.412	0.440
1000	3.50	50	7.6	0.6336	0.1365	2.180	0.1717	2.704	2.444	0.460
1000	4.25	51	8.3	0.1167	0.1468	2.306	0.1744	2.708	2.452	0.600
1000	5.00	49	8.6	0.6920	0.1441	2.278	0.1759	2.702	2.433	0.693

Table A18 Copper, Magnification = 30x, Blue Filters, All Four Lights

Speed (RPM)	Feed (in/min)	Avg	Var	Skewness	Omega2	Ra(Image)	Lac(old)	FD2	FD1	Ra(Stylus) (μm)
500	0.50	52	8.7	1.7561	0.1529	2.286	0.1819	2.712	2.432	0.203
500	1.25	47	11.4	1.3234	0.1572	2.608	0.1750	2.693	2.479	0.543
500	2.00	47	9.5	1.8338	0.1441	2.369	0.1739	2.694	2.465	0.453
500	2.75	44	15.0	0.7511	0.1699	2.971	0.1778	2.682	2.507	0.637
500	3.50	43	27.7	-0.4195	0.2247	4.235	0.1794	2.677	2.538	0.667
500	4.25	48	20.1	0.0736	0.2144	3.464	0.1772	2.697	2.539	0.790
500	5.00	46	30.0	-1.0666	0.2543	4.224	0.1770	2.692	2.579	0.873
600	0.50	52	11.6	0.0355	0.1786	2.710	0.1825	2.714	2.487	0.267
600	1.25	53	8.6	0.1849	0.1549	2.367	0.1770	2.715	2.453	0.347
600	2.00	49	11.6	-0.0949	0.1681	2.635	0.1766	2.703	2.510	0.727
600	2.75	45	15.5	0.1268	0.1780	3.098	0.1787	2.687	2.500	1.470
600	3.50	49	7.1	0.5257	0.1314	2.112	0.1730	2.703	2.438	0.380
600	4.25	51	9.8	1.7309	0.1593	2.222	0.1768	2.709	2.454	0.513
600	5.00	51	10.3	1.2442	0.1649	2.409	0.1828	2.710	2.444	0.580
700	0.50	56	8.5	0.2177	0.1635	2.352	0.1869	2.727	2.451	0.157
700	1.25	52	11.5	-0.1529	0.1767	2.668	0.1765	2.713	2.497	0.387
700	2.00	51	7.1	0.6530	0.1361	2.074	0.1722	2.709	2.432	0.303
700	2.75	49	12.2	0.5696	0.1707	2.773	0.1727	2.701	2.448	0.357
700	3.50	52	11.7	0.3607	0.1791	2.706	0.1749	2.713	2.465	0.403
700	4.25	56	14.5	0.4334	0.2142	3.032	0.1725	2.727	2.493	0.453
700	5.00	55	13.4	0.5988	0.2006	2.850	0.1735	2.722	2.481	0.527
800	0.50	44	4.7	0.5489	0.0948	1.710	0.1659	2.682	2.389	0.250
800	1.25	49	6.7	-1.7193	0.1259	1.762	0.1634	2.700	2.511	0.313
800	2.00	48	6.4	0.7017	0.1229	1.991	0.1615	2.700	2.414	0.360
800	2.75	52	14.6	0.3488	0.1992	3.083	0.1651	2.713	2.480	0.440
800	3.50	51	9.4	0.5608	0.1555	2.429	0.1666	2.708	2.429	0.480
800	4.25	53	17.2	0.3111	0.2195	3.345	0.1660	2.716	2.496	0.477
800	5.00	52	13.5	0.3254	0.1922	2.973	0.1704	2.714	2.485	0.543
900	0.50	49	6.3	1.2150	0.1244	1.910	0.1754	2.703	2.414	0.157
900	1.25	50	9.4	0.2785	0.1524	2.481	0.1752	2.704	2.445	0.357
900	2.00	51	19.3	0.5203	0.2243	3.429	0.1778	2.709	2.494	0.423
900	2.75	51	15.3	0.4003	0.1998	3.114	0.1715	2.709	2.495	0.450
900	3.50	48	13.3	0.8148	0.1737	2.846	0.1712	2.697	2.461	0.447
900	4.25	51	14.7	0.6781	0.1963	2.984	0.1718	2.710	2.482	0.563
900	5.00	53	17.8	0.5802	0.2222	3.341	0.1706	2.715	2.491	0.557
1000	0.50	46	13.9	0.2538	0.1721	2.877	0.1790	2.691	2.502	0.293
1000	1.25	54	9.9	-2.1149	0.1682	2.172	0.1752	2.718	2.473	0.227
1000	2.00	46	7.1	0.0662	0.1211	2.072	0.1683	2.689	2.455	0.313
1000	2.75	44	6.8	0.2734	0.1142	2.063	0.1683	2.682	2.415	0.440
1000	3.50	45	6.3	0.4952	0.1143	2.008	0.1678	2.688	2.409	0.460
1000	4.25	48	7.3	-0.0799	0.1282	2.188	0.1687	2.696	2.439	0.600
1000	5.00	45	5.9	0.1079	0.1095	1.915	0.1692	2.687	2.424	0.693

Table A19 Aluminum, Magnification = 20x, Blue Filters, All Four Lights

Speed (RPM)	Feed (in/min)	Avg	Var	Skewness	Omega2	Ra(Image)	Lac(old)	FD2	FD1	Ra(Stylus) (μm)
500	0.50	63	24.4	0.0623	0.3139	3.931	0.1966	2.749	2.570	0.180
500	1.25	70	24.9	0.0468	0.3493	4.003	0.1913	2.766	2.579	0.283
500	2.00	71	22.5	0.0283	0.3367	3.835	0.1958	2.769	2.582	0.373
500	2.75	68	42.8	0.1727	0.4464	5.305	0.1930	2.762	2.610	0.447
500	3.50	82	55.5	0.5190	0.6087	5.754	0.1885	2.794	2.656	2.327
500	4.25	84	55.1	0.6676	0.6228	5.608	0.1968	2.799	2.655	2.817
500	5.00	85	80.6	0.1067	0.7612	7.143	0.1951	2.801	2.699	3.803
600	0.50	62	28.1	0.3485	0.3276	4.204	0.1977	2.744	2.558	0.170
600	1.25	80	30.2	0.2369	0.4389	4.427	0.2039	2.790	2.603	0.423
600	2.00	80	26.3	0.1174	0.4099	4.012	0.2039	2.790	2.616	0.413
600	2.75	81	46.9	0.5764	0.5553	5.167	0.2020	2.793	2.649	0.970
600	3.50	86	50.7	0.4734	0.6148	5.687	0.2075	2.804	2.648	1.663
600	4.25	86	36.6	-0.0971	0.5211	4.779	0.1988	2.804	2.663	2.063
600	5.00	87	44.1	-0.2875	0.5750	5.168	0.1968	2.804	2.683	2.180
700	0.50	76	24.2	0.1083	0.3737	3.899	0.1992	2.781	2.595	0.193
700	1.25	74	28.8	0.0850	0.3965	4.301	0.2051	2.776	2.600	0.303
700	2.00	77	31.8	-0.7858	0.4315	4.391	0.1934	2.782	2.657	0.393
700	2.75	77	38.2	-0.0584	0.4734	5.006	0.2010	2.782	2.625	0.573
700	3.50	81	56.8	-0.2907	0.6073	6.006	0.2114	2.792	2.660	0.850
700	4.25	86	44.6	-0.2729	0.5731	5.411	0.2027	2.803	2.675	1.100
700	5.00	81	63.7	-0.4183	0.6505	6.423	0.2058	2.794	2.688	1.113
800	0.50	71	20.2	0.1660	0.3197	3.584	0.2034	2.769	2.570	0.210
800	1.25	75	19.6	-0.2030	0.3300	3.519	0.1940	2.777	2.585	0.283
800	2.00	84	47.6	0.0266	0.5765	5.642	0.1900	2.798	2.651	0.420
800	2.75	80	27.5	-0.4462	0.4183	4.212	0.1960	2.790	2.633	0.487
800	3.50	85	31.3	0.5310	0.4759	4.369	0.1959	2.801	2.619	0.520
800	4.25	86	28.6	-0.2230	0.4618	4.241	0.1972	2.804	2.647	0.640
800	5.00	85	33.1	0.1703	0.4877	4.657	0.1877	2.801	2.626	0.780
900	0.50	64	20.8	-0.0151	0.2921	3.657	0.1951	2.750	2.554	0.160
900	1.25	67	23.2	0.1525	0.3226	3.826	0.1980	2.758	2.572	0.270
900	2.00	78	40.2	-0.1651	0.4926	5.084	0.1981	2.785	2.637	0.383
900	2.75	71	36.7	0.0716	0.4293	4.749	0.1984	2.768	2.612	0.400
900	3.50	74	48.0	-0.2077	0.5145	5.515	0.2015	2.777	2.649	0.490
900	4.25	78	38.8	-0.6494	0.4881	4.840	0.1997	2.787	2.667	0.490
900	5.00	81	59.4	0.0740	0.6227	6.148	0.1955	2.792	2.669	0.593
1000	0.50	61	27.2	0.2746	0.3161	4.115	0.1894	2.740	2.565	0.123
1000	1.25	64	31.1	0.0569	0.3581	4.505	0.2009	2.751	2.580	0.193
1000	2.00	69	29.2	-0.1852	0.3735	4.318	0.2005	2.764	2.591	0.280
1000	2.75	63	42.1	-0.0169	0.4078	5.143	0.1958	2.747	2.602	0.333
1000	3.50	71	31.2	0.0859	0.3942	4.461	0.1956	2.768	2.588	0.337
1000	4.25	74	40.8	-0.0427	0.4754	5.104	0.1933	2.777	2.627	0.397
1000	5.00	76	41.7	-0.1038	0.4901	5.134	0.1896	2.781	2.642	0.430

Table A20 Aluminum, Magnification = 30x, Blue Filters, All Four Lights

Speed (RPM)	Feed (in/min)	Avg	Var	Skewness	Omega2	Ra(Image)	Lac(old)	FD2	FD1	Ra(Stylus) (μm)
500	0.50	59	20.9	0.0475	0.2712	3.621	0.1975	2.737	2.547	0.180
500	1.25	66	27.1	0.0948	0.3454	4.150	0.1880	2.756	2.586	0.283
500	2.00	67	21.8	-0.0047	0.3118	3.833	0.1869	2.757	2.555	0.373
500	2.75	65	45.9	0.2065	0.4430	5.545	0.1883	2.754	2.594	0.447
500	3.50	76	65.6	0.6235	0.6178	6.273	0.1888	2.782	2.646	2.327
500	4.25	78	54.6	0.4547	0.5770	5.724	0.1870	2.786	2.641	2.817
500	5.00	77	64.3	0.1923	0.6202	6.332	0.1908	2.784	2.657	3.803
600	0.50	62	20.4	0.0339	0.2816	3.585	0.1904	2.745	2.554	0.170
600	1.25	75	58.4	0.0911	0.5756	6.176	0.2048	2.779	2.645	0.423
600	2.00	80	21.4	-0.1191	0.3726	3.684	0.1965	2.791	2.612	0.413
600	2.75	80	36.2	0.0651	0.4790	4.565	0.1955	2.789	2.658	0.970
600	3.50	82	34.6	0.2978	0.4828	4.677	0.2023	2.795	2.611	1.663
600	4.25	86	34.3	-0.1686	0.5048	4.542	0.2000	2.804	2.663	2.063
600	5.00	83	40.4	-0.4363	0.5303	4.914	0.1953	2.798	2.666	2.180
700	0.50	70	24.3	0.1474	0.3440	3.859	0.2016	2.766	2.577	0.193
700	1.25	71	24.8	0.0807	0.3516	4.001	0.2028	2.768	2.587	0.303
700	2.00	68	34.9	-0.5858	0.4046	4.607	0.2071	2.762	2.636	0.393
700	2.75	73	36.2	0.0228	0.4366	4.776	0.2114	2.773	2.614	0.573
700	3.50	74	47.0	-0.3888	0.5079	5.495	0.1938	2.776	2.639	0.850
700	4.25	78	42.3	-0.3204	0.5106	5.222	0.1990	2.787	2.646	1.100
700	5.00	74	65.6	-0.2911	0.5964	6.678	0.1997	2.775	2.663	1.113
800	0.50	65	20.6	0.0666	0.2930	3.647	0.2072	2.751	2.547	0.210
800	1.25	70	18.1	0.0238	0.2961	3.357	0.1923	2.765	2.559	0.283
800	2.00	81	51.1	0.3076	0.5791	5.741	0.1882	2.793	2.640	0.420
800	2.75	75	28.3	-0.2079	0.4014	4.195	0.1957	2.780	2.610	0.487
800	3.50	81	40.8	0.8788	0.5167	4.755	0.2114	2.792	2.629	0.520
800	4.25	82	39.0	-0.1000	0.5144	5.039	0.2029	2.795	2.655	0.640
800	5.00	79	40.3	0.0109	0.5023	5.137	0.1928	2.788	2.635	0.780
900	0.50	58	22.2	0.1374	0.2734	3.767	0.1963	2.732	2.540	0.160
900	1.25	62	20.4	0.1172	0.2784	3.597	0.1912	2.743	2.555	0.270
900	2.00	71	42.3	-0.0965	0.4633	5.208	0.1894	2.769	2.626	0.383
900	2.75	65	36.2	-0.0791	0.3897	4.807	0.2002	2.752	2.606	0.400
900	3.50	68	56.0	-0.0374	0.5071	5.979	0.2059	2.760	2.637	0.490
900	4.25	72	45.4	-0.4726	0.4864	5.296	0.1982	2.772	2.651	0.490
900	5.00	72	85.7	0.0755	0.6692	7.341	0.2031	2.772	2.670	0.593
1000	0.50	53	21.5	0.4507	0.2454	3.671	0.1841	2.716	2.513	0.123
1000	1.25	56	28.6	0.2110	0.2979	4.339	0.1932	2.725	2.542	0.193
1000	2.00	64	29.6	0.1031	0.3494	4.385	0.1919	2.750	2.579	0.280
1000	2.75	61	28.3	0.0467	0.3247	4.234	0.1930	2.742	2.571	0.333
1000	3.50	67	24.5	0.1276	0.3295	3.913	0.1984	2.757	2.578	0.337
1000	4.25	70	33.5	-0.0932	0.4052	4.622	0.1969	2.766	2.602	0.397
1000	5.00	71	34.3	0.0564	0.4157	4.691	0.1930	2.769	2.593	0.430

Table A21 Aluminum, Magnification = 30x, White Filters, Back and Right Lights

Speed (RPM)	Feed (in/min)	Flutes	Avg	Var	Skewness	Omega2	Ra(Image)	Lac(old)	FD2	FD1	Ra(Stylus) (µm)
1000	1.2	2	63	89.2	0.5672	0.5996	7.482	0.2029	2.749	2.632	0.440
1000	2.4	2	59	85.7	0.6669	0.5506	7.105	0.2107	2.737	2.623	0.577
1000	4.0	2	58	123.6	1.1346	0.6417	8.290	0.2083	2.731	2.627	0.517
1000	7.0	2	64	142.9	0.3849	0.7677	9.622	0.2011	2.751	2.661	1.053
1000	10.0	2	66	317.0	2.2082	1.1794	11.666	0.1884	2.756	2.661	2.160
1000	15.7	2	73	84.1	-0.7346	0.6730	7.328	0.1871	2.775	2.693	4.417
1000	19.7	2	77	252.1	2.0998	1.2206	10.776	0.1820	2.783	2.699	5.333
1000	1.2	4	70	37.6	0.0226	0.4321	4.834	0.2240	2.767	2.608	0.160
1000	2.4	4	61	65.6	-0.1234	0.4927	6.568	0.2148	2.741	2.628	0.270
1000	4.0	4	62	85.8	0.1286	0.5708	7.770	0.2040	2.743	2.628	0.500
1000	7.0	4	62	271.9	2.5632	1.0284	10.570	0.2036	2.745	2.647	2.460
1000	10.0	4	66	87.3	0.0046	0.6133	7.672	0.2060	2.755	2.651	3.143
1000	15.7	4	66	499.4	2.3746	1.4696	14.365	0.1977	2.755	2.681	5.700
800	1.2	2	50	82.8	0.9530	0.4564	7.197	0.1997	2.706	2.568	0.333
800	2.4	2	53	103.9	0.6012	0.5386	8.296	0.1897	2.715	2.596	0.400
800	4.0	2	54	97.6	0.8996	0.5293	7.622	0.2011	2.718	2.603	0.527
800	7.0	2	58	199.8	0.3197	0.8188	11.995	0.2040	2.732	2.646	1.643
800	10.0	2	62	652.4	1.9876	1.5780	17.634	0.2023	2.744	2.680	3.383
800	15.7	2	73	214.4	0.0899	1.0667	11.781	0.2110	2.773	2.709	5.697
800	19.7	2	73	439.5	2.0738	1.5261	13.987	0.2129	2.773	2.706	5.980
800	1.2	4	54	76.8	0.5204	0.4773	6.836	0.2013	2.721	2.604	0.193
800	2.4	4	55	156.2	0.4829	0.6916	10.155	0.2132	2.724	2.637	0.387
800	4.0	4	60	262.9	0.1553	0.9676	13.938	0.2096	2.737	2.671	1.510
800	7.0	4	59	519.2	2.4514	1.3411	14.384	0.2037	2.735	2.657	3.830
800	10.0	4	63	151.3	0.3484	0.7774	9.499	0.2159	2.748	2.673	4.700
800	15.7	4	61	580.7	2.7395	1.4678	15.448	0.1994	2.741	2.657	7.500
600	1.2	2	48	48.2	0.2895	0.3334	5.460	0.2027	2.698	2.571	0.203
600	2.4	2	51	104.4	0.0854	0.5238	8.523	0.2009	2.710	2.616	0.447
600	4.0	2	55	135.3	0.6497	0.6375	9.067	0.2044	2.722	2.633	1.127
600	7.0	2	65	255.6	0.2003	1.0337	13.708	0.2099	2.752	2.686	3.563
600	10.0	2	70	420.5	1.8769	1.4269	14.188	0.1968	2.765	2.701	3.990
600	15.7	2	81	158.2	0.5399	1.0236	9.908	0.2102	2.793	2.708	5.333
600	19.7	2	83	451.9	1.6104	1.7540	16.010	0.1991	2.796	2.724	6.100
600	1.2	4	57	105.2	0.6564	0.5838	8.244	0.2008	2.729	2.613	0.350
600	2.4	4	59	338.8	1.3437	1.0899	13.407	0.2018	2.736	2.660	1.393
600	4.0	4	67	213.2	-0.1699	0.9727	12.351	0.2138	2.757	2.698	2.550
600	7.0	4	66	416.8	2.8101	1.3444	11.612	0.1981	2.755	2.673	5.367
600	10.0	4	71	248.1	1.1396	1.1211	11.712	0.2100	2.769	2.703	6.367
600	15.7	4	69	640.6	2.1956	1.7398	16.550	0.2036	2.763	2.692	8.533
400	1.2	2	75	81.5	1.1876	0.6763	6.918	0.2083	2.778	2.632	1.180
400	2.4	2	75	83.3	0.5288	0.6828	7.258	0.2082	2.778	2.654	1.793
400	4.0	2	70	286.2	1.9190	1.1794	11.815	0.2003	2.765	2.672	2.653
400	7.0	2	72	89.5	0.2036	0.6798	7.549	0.2009	2.771	2.661	3.367
400	10.0	2	69	373.3	2.0463	1.3376	13.510	0.2080	2.764	2.687	4.497
400	15.7	2	81	103.3	0.2014	0.8195	8.106	0.2023	2.792	2.698	6.700
400	19.7	2	76	214.3	1.1270	1.1155	11.031	0.2018	2.781	2.699	5.200
400	1.2	4	71	102.2	-0.0849	0.7219	8.270	0.2009	2.770	2.674	0.653
400	2.4	4	68	350.4	2.2697	1.2710	11.993	0.2012	2.761	2.673	2.597
400	4.0	4	75	292.3	0.8205	1.2757	13.595	0.1950	2.778	2.705	3.350
400	7.0	4	71	215.2	3.0456	1.0378	8.275	0.1897	2.768	2.644	7.300
400	10.0	4	76	210.6	0.9041	1.1032	10.361	0.1850	2.781	2.714	8.333
400	15.7	4	70	451.0	2.6159	1.4868	12.790	0.1796	2.766	2.688	8.833

Table A22 Aluminum, Magnification = 15x, White Filters, Back and Right Lights

Speed (RPM)	Feed (in/min)	Flutes	Avg	Var	Skewness	Omega2	Ra(Image)	Lac(old)	FD2	FD1	Ra(Stylus) (µm)
1000	1.2	2	85	51.3	0.2121	0.6055	5.515	0.2241	2.800	2.677	0.440
1000	2.4	2	79	73.3	0.0290	0.6785	6.613	0.2291	2.789	2.681	0.577
1000	4.0	2	76	122.2	0.2179	0.8428	8.486	0.2210	2.782	2.695	0.517
1000	7.0	2	79	135.0	-0.0035	0.9122	9.682	0.2130	2.787	2.697	1.053
1000	10.0	2	81	338.8	1.8533	1.4971	12.342	0.2123	2.793	2.721	2.160
1000	15.7	2	91	102.6	-0.6734	0.9189	8.169	0.2060	2.813	2.743	4.417
1000	19.7	2	98	276.8	1.9846	1.6280	11.240	0.2037	2.827	2.770	5.333
1000	1.2	4	82	36.3	0.2917	0.4953	4.687	0.2088	2.795	2.635	0.160
1000	2.4	4	78	75.4	-0.1617	0.6743	6.940	0.2205	2.785	2.680	0.270
1000	4.0	4	78	55.4	0.1554	0.5799	5.870	0.2171	2.786	2.656	0.500
1000	7.0	4	85	94.8	-0.1652	0.8298	8.027	0.2248	2.802	2.708	2.460
1000	10.0	4	87	226.0	1.7684	1.3068	10.353	0.2328	2.805	2.716	3.143
1000	15.7	4	103	133.4	0.0453	1.1865	8.982	0.2212	2.835	2.780	5.700
800	1.2	2	69	84.3	0.5303	0.6348	7.236	0.2261	2.764	2.643	0.333
800	2.4	2	72	96.5	0.3492	0.7031	7.935	0.2169	2.770	2.658	0.400
800	4.0	2	67	87.6	0.2822	0.6266	7.580	0.2193	2.758	2.643	0.527
800	7.0	2	74	254.5	0.0724	1.1777	13.811	0.2135	2.776	2.708	1.643
800	10.0	2	75	588.3	1.8904	1.8236	16.595	0.2091	2.779	2.716	3.383
800	15.7	2	91	222.7	-0.3274	1.3594	12.036	0.2156	2.814	2.762	5.697
800	19.7	2	96	345.4	1.9387	1.7814	12.274	0.2047	2.823	2.768	5.980
800	1.2	4	68	79.4	0.3360	0.6078	6.976	0.2208	2.761	2.648	0.193
800	2.4	4	66	149.5	0.4628	0.8036	9.850	0.2139	2.755	2.662	0.387
800	4.0	4	72	339.3	1.0407	1.3275	13.672	0.2321	2.771	2.718	1.510
800	7.0	4	84	202.5	-0.4554	1.1981	11.381	0.2207	2.799	2.747	3.830
800	10.0	4	83	477.0	2.4458	1.8075	13.276	0.2230	2.796	2.743	4.700
800	15.7	4	101	167.5	0.0451	1.3127	10.198	0.2278	2.833	2.779	7.500
600	1.2	2	65	57.0	0.1326	0.4899	6.004	0.2156	2.753	2.624	0.203
600	2.4	2	67	113.8	0.0020	0.7184	8.762	0.2104	2.759	2.664	0.447
600	4.0	2	74	138.3	0.0669	0.8758	9.415	0.2107	2.777	2.696	1.127
600	7.0	2	82	278.8	-0.1135	1.3700	14.405	0.2144	2.795	2.742	3.563
600	10.0	2	88	408.0	1.6902	1.7821	14.133	0.2096	2.808	2.752	3.990
600	15.7	2	101	145.7	0.5174	1.2196	9.413	0.2190	2.832	2.760	5.333
600	19.7	2	105	277.0	1.2791	1.7548	12.784	0.2141	2.840	2.787	6.100
600	1.2	4	71	85.1	0.0749	0.6540	7.492	0.2084	2.768	2.658	0.350
600	2.4	4	76	261.8	-0.4115	1.2313	13.542	0.2137	2.781	2.733	1.393
600	4.0	4	78	352.4	1.6478	1.4629	12.564	0.2098	2.786	2.722	2.550
600	7.0	4	90	173.3	-0.8917	1.1893	10.114	0.2106	2.812	2.766	5.367
600	10.0	4	88	529.3	2.5437	2.0153	14.227	0.2170	2.807	2.734	6.367
600	15.7	4	102	158.5	-0.1219	1.2818	9.955	0.2238	2.834	2.781	8.533
400	1.2	2	96	70.1	0.5477	0.8035	6.637	0.2141	2.823	2.698	1.180
400	2.4	2	92	60.2	0.4990	0.7166	6.081	0.2164	2.816	2.691	1.793
400	4.0	2	88	247.3	1.8304	1.3766	10.865	0.2104	2.806	2.715	2.653
400	7.0	2	88	95.9	-0.2733	0.8641	7.769	0.2212	2.808	2.725	3.367
400	10.0	2	87	342.9	2.0866	1.6130	12.636	0.2137	2.806	2.731	4.497
400	15.7	2	101	84.1	0.0954	0.9273	7.174	0.2169	2.833	2.746	6.700
400	19.7	2	101	166.3	1.5126	1.3018	9.247	0.2089	2.832	2.755	5.200
400	1.2	4	82	203.1	0.0626	1.1735	11.549	0.2087	2.795	2.737	0.653
400	2.4	4	92	137.2	-0.6340	1.0786	9.339	0.2167	2.816	2.761	2.597
400	4.0	4	84	566.9	2.1961	1.9901	14.454	0.2291	2.798	2.747	3.350
400	7.0	4	97	75.5	-0.9274	0.8470	6.574	0.2112	2.826	2.760	7.300
400	10.0	4	94	487.9	2.8069	2.0667	12.773	0.2215	2.818	2.764	8.333
400	15.7	4	106	108.7	-0.6206	1.1041	7.980	0.2168	2.841	2.787	8.833

Table A21 Aluminum, Magnification = 30x, White Filters, Back and Right Lights

Speed (RPM)	Feed (in/min)	Flutes	Avg	Var	Skewness	Omega2	Ra(Image)	Lac(old)	FD2	FD1	Ra(Stylus) (µm)
1000	1.2	2	63	89.2	0.5672	0.5996	7.482	0.2029	2.749	2.632	0.440
1000	2.4	2	59	85.7	0.6669	0.5506	7.105	0.2107	2.737	2.623	0.577
1000	4.0	2	58	123.6	1.1346	0.6417	8.290	0.2083	2.731	2.627	0.517
1000	7.0	2	64	142.9	0.3849	0.7677	9.622	0.2011	2.751	2.661	1.053
1000	10.0	2	66	317.0	2.2082	1.1794	11.666	0.1884	2.756	2.661	2.160
1000	15.7	2	73	84.1	-0.7346	0.6730	7.328	0.1871	2.775	2.693	4.417
1000	19.7	2	77	252.1	2.0998	1.2206	10.776	0.1820	2.783	2.699	5.333
1000	1.2	4	70	37.6	0.0226	0.4321	4.834	0.2240	2.767	2.608	0.160
1000	2.4	4	61	65.6	-0.1234	0.4927	6.568	0.2148	2.741	2.628	0.270
1000	4.0	4	62	85.8	0.1286	0.5708	7.770	0.2040	2.743	2.628	0.500
1000	7.0	4	62	271.9	2.5632	1.0284	10.570	0.2036	2.745	2.647	2.460
1000	10.0	4	66	87.3	0.0046	0.6133	7.672	0.2060	2.755	2.651	3.143
1000	15.7	4	66	499.4	2.3746	1.4696	14.365	0.1977	2.755	2.681	5.700
800	1.2	2	50	82.8	0.9530	0.4564	7.197	0.1997	2.706	2.568	0.333
800	2.4	2	53	103.9	0.6012	0.5386	8.296	0.1897	2.715	2.596	0.400
800	4.0	2	54	97.6	0.8996	0.5293	7.622	0.2011	2.718	2.603	0.527
800	7.0	2	58	199.8	0.3197	0.8188	11.995	0.2040	2.732	2.646	1.643
800	10.0	2	62	652.4	1.9876	1.5780	17.634	0.2023	2.744	2.680	3.383
800	15.7	2	73	214.4	0.0899	1.0667	11.781	0.2110	2.773	2.709	5.697
800	19.7	2	73	439.5	2.0738	1.5261	13.987	0.2129	2.773	2.706	5.980
800	1.2	4	54	76.8	0.5204	0.4773	6.836	0.2013	2.721	2.604	0.193
800	2.4	4	55	156.2	0.4829	0.6916	10.155	0.2132	2.724	2.637	0.387
800	4.0	4	60	262.9	0.1553	0.9676	13.938	0.2096	2.737	2.671	1.510
800	7.0	4	59	519.2	2.4514	1.3411	14.384	0.2037	2.735	2.657	3.830
800	10.0	4	63	151.3	0.3484	0.7774	9.499	0.2159	2.748	2.673	4.700
800	15.7	4	61	580.7	2.7395	1.4678	15.448	0.1994	2.741	2.657	7.500
600	1.2	2	48	48.2	0.2895	0.3334	5.460	0.2027	2.698	2.571	0.203
600	2.4	2	51	104.4	0.0854	0.5238	8.523	0.2009	2.710	2.616	0.447
600	4.0	2	55	135.3	0.6497	0.6375	9.067	0.2044	2.722	2.633	1.127
600	7.0	2	65	255.6	0.2003	1.0337	13.708	0.2099	2.752	2.686	3.563
600	10.0	2	70	420.5	1.8769	1.4269	14.188	0.1968	2.765	2.701	3.990
600	15.7	2	81	158.2	0.5399	1.0236	9.908	0.2102	2.793	2.708	5.333
600	19.7	2	83	451.9	1.6104	1.7540	16.010	0.1991	2.796	2.724	6.100
600	1.2	4	57	105.2	0.6564	0.5838	8.244	0.2008	2.729	2.613	0.350
600	2.4	4	59	338.8	1.3437	1.0899	13.407	0.2018	2.736	2.660	1.393
600	4.0	4	67	213.2	-0.1699	0.9727	12.351	0.2138	2.757	2.698	2.550
600	7.0	4	66	416.8	2.8101	1.3444	11.612	0.1981	2.755	2.673	5.367
600	10.0	4	71	248.1	1.1396	1.1211	11.712	0.2100	2.769	2.703	6.367
600	15.7	4	69	640.6	2.1956	1.7398	16.550	0.2036	2.763	2.692	8.533
400	1.2	2	75	81.5	1.1876	0.6763	6.918	0.2083	2.778	2.632	1.180
400	2.4	2	75	83.3	0.5288	0.6828	7.258	0.2082	2.778	2.654	1.793
400	4.0	2	70	286.2	1.9190	1.1794	11.815	0.2003	2.765	2.672	2.653
400	7.0	2	72	89.5	0.2036	0.6798	7.549	0.2009	2.771	2.661	3.367
400	10.0	2	69	373.3	2.0463	1.3376	13.510	0.2080	2.764	2.687	4.497
400	15.7	2	81	103.3	0.2014	0.8195	8.106	0.2023	2.792	2.698	6.700
400	19.7	2	76	214.3	1.1270	1.1155	11.031	0.2018	2.781	2.699	5.200
400	1.2	4	71	102.2	-0.0849	0.7219	8.270	0.2009	2.770	2.674	0.653
400	2.4	4	68	350.4	2.2697	1.2710	11.993	0.2012	2.761	2.673	2.597
400	4.0	4	75	292.3	0.8205	1.2757	13.595	0.1950	2.778	2.705	3.350
400	7.0	4	71	215.2	3.0456	1.0378	8.275	0.1897	2.768	2.644	7.300
400	10.0	4	76	210.6	0.9041	1.1032	10.361	0.1850	2.781	2.714	8.333
400	15.7	4	70	451.0	2.6159	1.4868	12.790	0.1796	2.766	2.688	8.833

Table A22 Aluminum, Magnification = 15x, White Filters, Back and Right Lights

Speed (RPM)	Feed (in/min)	Flutes	Avg	Var	Skewness	Omega2	Ra(Image)	Lac(old)	FD2	FD1	Ra(Stylus) (μm)
1000	1.2	2	85	51.3	0.2121	0.6055	5.515	0.2241	2.800	2.677	0.440
1000	2.4	2	79	73.3	0.0290	0.6785	6.613	0.2291	2.789	2.681	0.577
1000	4.0	2	76	122.2	0.2179	0.8428	8.486	0.2210	2.782	2.695	0.517
1000	7.0	2	79	135.0	-0.0035	0.9122	9.682	0.2130	2.787	2.697	1.053
1000	10.0	2	81	338.8	1.8533	1.4971	12.342	0.2123	2.793	2.721	2.160
1000	15.7	2	91	102.6	-0.6734	0.9189	8.169	0.2060	2.813	2.743	4.417
1000	19.7	2	98	276.8	1.9846	1.6280	11.240	0.2037	2.827	2.770	5.333
1000	1.2	4	82	36.3	0.2917	0.4953	4.687	0.2088	2.795	2.635	0.160
1000	2.4	4	78	75.4	-0.1617	0.6743	6.940	0.2205	2.785	2.680	0.270
1000	4.0	4	78	55.4	0.1554	0.5799	5.870	0.2171	2.786	2.656	0.500
1000	7.0	4	85	94.8	-0.1652	0.8298	8.027	0.2248	2.802	2.708	2.460
1000	10.0	4	87	226.0	1.7684	1.3068	10.353	0.2328	2.805	2.716	3.143
1000	15.7	4	103	133.4	0.0453	1.1865	8.982	0.2212	2.835	2.780	5.700
800	1.2	2	69	84.3	0.5303	0.6348	7.236	0.2261	2.764	2.643	0.333
800	2.4	2	72	96.5	0.3492	0.7031	7.935	0.2169	2.770	2.658	0.400
800	4.0	2	67	87.6	0.2822	0.6266	7.580	0.2193	2.758	2.643	0.527
800	7.0	2	74	254.5	0.0724	1.1777	13.811	0.2135	2.776	2.708	1.643
800	10.0	2	75	588.3	1.8904	1.8236	16.595	0.2091	2.779	2.716	3.383
800	15.7	2	91	222.7	-0.3274	1.3594	12.036	0.2156	2.814	2.762	5.697
800	19.7	2	96	345.4	1.9387	1.7814	12.274	0.2047	2.823	2.768	5.980
800	1.2	4	68	79.4	0.3360	0.6078	6.976	0.2208	2.761	2.648	0.193
800	2.4	4	66	149.5	0.4628	0.8036	9.850	0.2139	2.755	2.662	0.387
800	4.0	4	72	339.3	1.0407	1.3275	13.672	0.2321	2.771	2.718	1.510
800	7.0	4	84	202.5	-0.4554	1.1981	11.381	0.2207	2.799	2.747	3.830
800	10.0	4	83	477.0	2.4458	1.8075	13.276	0.2230	2.796	2.743	4.700
800	15.7	4	101	167.5	0.0451	1.3127	10.198	0.2278	2.833	2.779	7.500
600	1.2	2	65	57.0	0.1326	0.4899	6.004	0.2156	2.753	2.624	0.203
600	2.4	2	67	113.8	0.0020	0.7184	8.762	0.2104	2.759	2.664	0.447
600	4.0	2	74	138.3	0.0669	0.8758	9.415	0.2107	2.777	2.696	1.127
600	7.0	2	82	278.8	-0.1135	1.3700	14.405	0.2144	2.795	2.742	3.563
600	10.0	2	88	408.0	1.6902	1.7821	14.133	0.2096	2.808	2.752	3.990
600	15.7	2	101	145.7	0.5174	1.2196	9.413	0.2190	2.832	2.760	5.333
600	19.7	2	105	277.0	1.2791	1.7548	12.784	0.2141	2.840	2.787	6.100
600	1.2	4	71	85.1	0.0749	0.6540	7.492	0.2084	2.768	2.658	0.350
600	2.4	4	76	261.8	-0.4115	1.2313	13.542	0.2137	2.781	2.733	1.393
600	4.0	4	78	352.4	1.6478	1.4629	12.564	0.2098	2.786	2.722	2.550
600	7.0	4	90	173.3	-0.8917	1.1893	10.114	0.2106	2.812	2.766	5.367
600	10.0	4	88	529.3	2.5437	2.0153	14.227	0.2170	2.807	2.734	6.367
600	15.7	4	102	158.5	-0.1219	1.2818	9.955	0.2238	2.834	2.781	8.533
400	1.2	2	96	70.1	0.5477	0.8035	6.637	0.2141	2.823	2.698	1.180
400	2.4	2	92	60.2	0.4990	0.7166	6.081	0.2164	2.816	2.691	1.793
400	4.0	2	88	247.3	1.8304	1.3766	10.865	0.2104	2.806	2.715	2.653
400	7.0	2	88	95.9	-0.2733	0.8641	7.769	0.2212	2.808	2.725	3.367
400	10.0	2	87	342.9	2.0866	1.6130	12.636	0.2137	2.806	2.731	4.497
400	15.7	2	101	84.1	0.0954	0.9273	7.174	0.2169	2.833	2.746	6.700
400	19.7	2	101	166.3	1.5126	1.3018	9.247	0.2089	2.832	2.755	5.200
400	1.2	4	82	203.1	0.0626	1.1735	11.549	0.2087	2.795	2.737	0.653
400	2.4	4	92	137.2	-0.6340	1.0786	9.339	0.2167	2.816	2.761	2.597
400	4.0	4	84	566.9	2.1961	1.9901	14.454	0.2291	2.798	2.747	3.350
400	7.0	4	97	75.5	-0.9274	0.8470	6.574	0.2112	2.826	2.760	7.300
400	10.0	4	94	487.9	2.8069	2.0667	12.773	0.2215	2.818	2.764	8.333
400	15.7	4	106	108.7	-0.6206	1.1041	7.980	0.2168	2.841	2.787	8.833

Table A21 Aluminum, Magnification = 30x, White Filters, Back and Right Lights

Speed (RPM)	Feed (in/min)	Flutes	Avg	Var	Skewness	Omega2	Ra(Image)	Lac(old)	FD2	FD1	Ra(Stylus) (µm)
1000	1.2	2	63	89.2	0.5672	0.5996	7.482	0.2029	2.749	2.632	0.440
1000	2.4	2	59	85.7	0.6669	0.5506	7.105	0.2107	2.737	2.623	0.577
1000	4.0	2	58	123.6	1.1346	0.6417	8.290	0.2083	2.731	2.627	0.517
1000	7.0	2	64	142.9	0.3849	0.7677	9.622	0.2011	2.751	2.661	1.053
1000	10.0	2	66	317.0	2.2082	1.1794	11.666	0.1884	2.756	2.661	2.160
1000	15.7	2	73	84.1	-0.7346	0.6730	7.328	0.1871	2.775	2.693	4.417
1000	19.7	2	77	252.1	2.0998	1.2206	10.776	0.1820	2.783	2.699	5.333
1000	1.2	4	70	37.6	0.0226	0.4321	4.834	0.2240	2.767	2.608	0.160
1000	2.4	4	61	65.6	-0.1234	0.4927	6.568	0.2148	2.741	2.628	0.270
1000	4.0	4	62	85.8	0.1286	0.5708	7.770	0.2040	2.743	2.628	0.500
1000	7.0	4	62	271.9	2.5632	1.0284	10.570	0.2036	2.745	2.647	2.460
1000	10.0	4	66	87.3	0.0046	0.6133	7.672	0.2060	2.755	2.651	3.143
1000	15.7	4	66	499.4	2.3746	1.4696	14.365	0.1977	2.755	2.681	5.700
800	1.2	2	50	82.8	0.9530	0.4564	7.197	0.1997	2.706	2.568	0.333
800	2.4	2	53	103.9	0.6012	0.5386	8.296	0.1897	2.715	2.596	0.400
800	4.0	2	54	97.6	0.8996	0.5293	7.622	0.2011	2.718	2.603	0.527
800	7.0	2	58	199.8	0.3197	0.8188	11.995	0.2040	2.732	2.646	1.643
800	10.0	2	62	652.4	1.9876	1.5780	17.634	0.2023	2.744	2.680	3.383
800	15.7	2	73	214.4	0.0899	1.0667	11.781	0.2110	2.773	2.709	5.697
800	19.7	2	73	439.5	2.0738	1.5261	13.987	0.2129	2.773	2.706	5.980
800	1.2	4	54	76.8	0.5204	0.4773	6.836	0.2013	2.721	2.604	0.193
800	2.4	4	55	156.2	0.4829	0.6916	10.155	0.2132	2.724	2.637	0.387
800	4.0	4	60	262.9	0.1553	0.9676	13.938	0.2096	2.737	2.671	1.510
800	7.0	4	59	519.2	2.4514	1.3411	14.384	0.2037	2.735	2.657	3.830
800	10.0	4	63	151.3	0.3484	0.7774	9.499	0.2159	2.748	2.673	4.700
800	15.7	4	61	580.7	2.7395	1.4678	15.448	0.1994	2.741	2.657	7.500
600	1.2	2	48	48.2	0.2895	0.3334	5.460	0.2027	2.698	2.571	0.203
600	2.4	2	51	104.4	0.0854	0.5238	8.523	0.2009	2.710	2.616	0.447
600	4.0	2	55	135.3	0.6497	0.6375	9.067	0.2044	2.722	2.633	1.127
600	7.0	2	65	255.6	0.2003	1.0337	13.708	0.2099	2.752	2.686	3.563
600	10.0	2	70	420.5	1.8769	1.4269	14.188	0.1968	2.765	2.701	3.990
600	15.7	2	81	158.2	0.5399	1.0236	9.908	0.2102	2.793	2.708	5.333
600	19.7	2	83	451.9	1.6104	1.7540	16.010	0.1991	2.796	2.724	6.100
600	1.2	4	57	105.2	0.6564	0.5838	8.244	0.2008	2.729	2.613	0.350
600	2.4	4	59	338.8	1.3437	1.0899	13.407	0.2018	2.736	2.660	1.393
600	4.0	4	67	213.2	-0.1699	0.9727	12.351	0.2138	2.757	2.698	2.550
600	7.0	4	66	416.8	2.8101	1.3444	11.612	0.1981	2.755	2.673	5.367
600	10.0	4	71	248.1	1.1396	1.1211	11.712	0.2100	2.769	2.703	6.367
600	15.7	4	69	640.6	2.1956	1.7398	16.550	0.2036	2.763	2.692	8.533
400	1.2	2	75	81.5	1.1876	0.6763	6.918	0.2083	2.778	2.632	1.180
400	2.4	2	75	83.3	0.5288	0.6828	7.258	0.2082	2.778	2.654	1.793
400	4.0	2	70	286.2	1.9190	1.1794	11.815	0.2003	2.765	2.672	2.653
400	7.0	2	72	89.5	0.2036	0.6798	7.549	0.2009	2.771	2.661	3.367
400	10.0	2	69	373.3	2.0463	1.3376	13.510	0.2080	2.764	2.687	4.497
400	15.7	2	81	103.3	0.2014	0.8195	8.106	0.2023	2.792	2.698	6.700
400	19.7	2	76	214.3	1.1270	1.1155	11.031	0.2018	2.781	2.699	5.200
400	1.2	4	71	102.2	-0.0849	0.7219	8.270	0.2009	2.770	2.674	0.653
400	2.4	4	68	350.4	2.2697	1.2710	11.993	0.2012	2.761	2.673	2.597
400	4.0	4	75	292.3	0.8205	1.2757	13.595	0.1950	2.778	2.705	3.350
400	7.0	4	71	215.2	3.0456	1.0378	8.275	0.1897	2.768	2.644	7.300
400	10.0	4	76	210.6	0.9041	1.1032	10.361	0.1850	2.781	2.714	8.333
400	15.7	4	70	451.0	2.6159	1.4868	12.790	0.1796	2.766	2.688	8.833

Table A22 Aluminum, Magnification = 15x, White Filters, Back and Right Lights

Speed (RPM)	Feed (in/min)	Flutes	Avg	Var	Skewness	Omega2	Ra(Image)	Lac(old)	FD2	FD1	Ra(Stylus) (µm)
1000	1.2	2	85	51.3	0.2121	0.6055	5.515	0.2241	2.800	2.677	0.440
1000	2.4	2	79	73.3	0.0290	0.6785	6.613	0.2291	2.789	2.681	0.577
1000	4.0	2	76	122.2	0.2179	0.8428	8.486	0.2210	2.782	2.695	0.517
1000	7.0	2	79	135.0	-0.0035	0.9122	9.682	0.2130	2.787	2.697	1.053
1000	10.0	2	81	338.8	1.8533	1.4971	12.342	0.2123	2.793	2.721	2.160
1000	15.7	2	91	102.6	-0.6734	0.9189	8.169	0.2060	2.813	2.743	4.417
1000	19.7	2	98	276.8	1.9846	1.6280	11.240	0.2037	2.827	2.770	5.333
1000	1.2	4	82	36.3	0.2917	0.4953	4.687	0.2088	2.795	2.635	0.160
1000	2.4	4	78	75.4	-0.1617	0.6743	6.940	0.2205	2.785	2.680	0.270
1000	4.0	4	78	55.4	0.1554	0.5799	5.870	0.2171	2.786	2.656	0.500
1000	7.0	4	85	94.8	-0.1652	0.8298	8.027	0.2248	2.802	2.708	2.460
1000	10.0	4	87	226.0	1.7684	1.3068	10.353	0.2328	2.805	2.716	3.143
1000	15.7	4	103	133.4	0.0453	1.1865	8.982	0.2212	2.835	2.780	5.700
800	1.2	2	69	84.3	0.5303	0.6348	7.236	0.2261	2.764	2.643	0.333
800	2.4	2	72	96.5	0.3492	0.7031	7.935	0.2169	2.770	2.658	0.400
800	4.0	2	67	87.6	0.2822	0.6266	7.580	0.2193	2.758	2.643	0.527
800	7.0	2	74	254.5	0.0724	1.1777	13.811	0.2135	2.776	2.708	1.643
800	10.0	2	75	588.3	1.8904	1.8236	16.595	0.2091	2.779	2.716	3.383
800	15.7	2	91	222.7	-0.3274	1.3594	12.036	0.2156	2.814	2.762	5.697
800	19.7	2	96	345.4	1.9387	1.7814	12.274	0.2047	2.823	2.768	5.980
800	1.2	4	68	79.4	0.3360	0.6078	6.976	0.2208	2.761	2.648	0.193
800	2.4	4	66	149.5	0.4628	0.8036	9.850	0.2139	2.755	2.662	0.387
800	4.0	4	72	339.3	1.0407	1.3275	13.672	0.2321	2.771	2.718	1.510
800	7.0	4	84	202.5	-0.4554	1.1981	11.381	0.2207	2.799	2.747	3.830
800	10.0	4	83	477.0	2.4458	1.8075	13.276	0.2230	2.796	2.743	4.700
800	15.7	4	101	167.5	0.0451	1.3127	10.198	0.2278	2.833	2.779	7.500
600	1.2	2	65	57.0	0.1326	0.4899	6.004	0.2156	2.753	2.624	0.203
600	2.4	2	67	113.8	0.0020	0.7184	8.762	0.2104	2.759	2.664	0.447
600	4.0	2	74	138.3	0.0669	0.8758	9.415	0.2107	2.777	2.696	1.127
600	7.0	2	82	278.8	-0.1135	1.3700	14.405	0.2144	2.795	2.742	3.563
600	10.0	2	88	408.0	1.6902	1.7821	14.133	0.2096	2.808	2.752	3.990
600	15.7	2	101	145.7	0.5174	1.2196	9.413	0.2190	2.832	2.760	5.333
600	19.7	2	105	277.0	1.2791	1.7548	12.784	0.2141	2.840	2.787	6.100
600	1.2	4	71	85.1	0.0749	0.6540	7.492	0.2084	2.768	2.658	0.350
600	2.4	4	76	261.8	-0.4115	1.2313	13.542	0.2137	2.781	2.733	1.393
600	4.0	4	78	352.4	1.6478	1.4629	12.564	0.2098	2.786	2.722	2.550
600	7.0	4	90	173.3	-0.8917	1.1893	10.114	0.2106	2.812	2.766	5.367
600	10.0	4	88	529.3	2.5437	2.0153	14.227	0.2170	2.807	2.734	6.367
600	15.7	4	102	158.5	-0.1219	1.2818	9.955	0.2238	2.834	2.781	8.533
400	1.2	2	96	70.1	0.5477	0.8035	6.637	0.2141	2.823	2.698	1.180
400	2.4	2	92	60.2	0.4990	0.7166	6.081	0.2164	2.816	2.691	1.793
400	4.0	2	88	247.3	1.8304	1.3766	10.865	0.2104	2.806	2.715	2.653
400	7.0	2	88	95.9	-0.2733	0.8641	7.769	0.2212	2.808	2.725	3.367
400	10.0	2	87	342.9	2.0866	1.6130	12.636	0.2137	2.806	2.731	4.497
400	15.7	2	101	84.1	0.0954	0.9273	7.174	0.2169	2.833	2.746	6.700
400	19.7	2	101	166.3	1.5126	1.3018	9.247	0.2089	2.832	2.755	5.200
400	1.2	4	82	203.1	0.0626	1.1735	11.549	0.2087	2.795	2.737	0.653
400	2.4	4	92	137.2	-0.6340	1.0786	9.339	0.2167	2.816	2.761	2.597
400	4.0	4	84	566.9	2.1961	1.9901	14.454	0.2291	2.798	2.747	3.350
400	7.0	4	97	75.5	-0.9274	0.8470	6.574	0.2112	2.826	2.760	7.300
400	10.0	4	94	487.9	2.8069	2.0667	12.773	0.2215	2.818	2.764	8.333
400	15.7	4	106	108.7	-0.6206	1.1041	7.980	0.2168	2.841	2.787	8.833

Table A23 Aluminum, Magnification = 7.5x, White Filters, Back and Right Lights

Speed (RPM)	Feed (in/min)	Flutes	Avg	Var	Skewness	Omega2	Ra(Image)	Lac(old)	FD2	FD1	Ra(Stylus) (µm)
1000	1.2	2	98	30.9	0.2332	0.5473	4.421	0.2229	2.828	2.663	0.440
1000	2.4	2	88	50.1	0.0461	0.6220	5.562	0.2207	2.807	2.682	0.577
1000	4.0	2	84	45.5	-0.2103	0.5677	5.259	0.2080	2.799	2.680	0.517
1000	7.0	2	84	89.0	-0.2355	0.7932	7.775	0.2100	2.799	2.698	1.053
1000	10.0	2	86	167.0	0.7061	1.1161	9.788	0.2008	2.804	2.726	2.160
1000	15.7	2	102	111.9	-0.5287	1.0763	8.470	0.2179	2.834	2.777	4.417
1000	19.7	2	111	163.8	0.5396	1.4159	9.528	0.2198	2.849	2.807	5.333
1000	1.2	4	91	26.1	0.0639	0.4641	4.033	0.1988	2.813	2.645	0.160
1000	2.4	4	86	35.6	-0.1311	0.5109	4.730	0.2298	2.802	2.657	0.270
1000	4.0	4	84	32.0	0.0826	0.4739	4.484	0.2293	2.799	2.635	0.500
1000	7.0	4	93	59.3	-0.0401	0.7126	6.270	0.2231	2.816	2.699	2.460
1000	10.0	4	98	115.2	0.8629	1.0548	7.972	0.2215	2.827	2.733	3.143
1000	15.7	4	122	130.7	-0.0773	1.3909	9.152	0.2280	2.866	2.836	5.700
800	1.2	2	78	32.9	0.7453	0.4470	4.497	0.2192	2.785	2.610	0.333
800	2.4	2	81	57.3	0.0441	0.6097	6.053	0.2253	2.791	2.674	0.400
800	4.0	2	76	60.8	-0.0364	0.5909	6.287	0.2198	2.780	2.663	0.527
800	7.0	2	80	193.0	-0.0097	1.1151	11.689	0.2109	2.791	2.722	1.643
800	10.0	2	83	283.2	1.0961	1.3904	12.708	0.2214	2.796	2.725	3.383
800	15.7	2	103	162.8	-0.4171	1.3156	10.315	0.2181	2.836	2.789	5.697
800	19.7	2	113	224.5	0.5758	1.6957	11.100	0.2272	2.853	2.819	5.980
800	1.2	4	77	47.4	0.6161	0.5274	5.392	0.2209	2.782	2.633	0.193
800	2.4	4	76	134.8	0.1577	0.8865	9.389	0.2264	2.782	2.700	0.387
800	4.0	4	78	172.3	-0.2154	1.0290	10.407	0.2144	2.787	2.734	1.510
800	7.0	4	95	164.8	-0.4560	1.2237	10.311	0.2171	2.822	2.774	3.830
800	10.0	4	96	199.7	0.6033	1.3561	9.775	0.2196	2.823	2.772	4.700
800	15.7	4	108	121.0	0.0085	1.1872	8.862	0.2232	2.844	2.785	7.500
600	1.2	2	79	48.1	0.1105	0.5506	5.351	0.2375	2.789	2.663	0.203
600	2.4	2	78	89.9	-0.1388	0.7362	7.724	0.2084	2.785	2.685	0.447
600	4.0	2	85	85.2	-0.3297	0.7837	7.215	0.2253	2.801	2.715	1.127
600	7.0	2	88	208.5	-0.1566	1.2650	12.441	0.2116	2.807	2.745	3.563
600	10.0	2	92	188.7	0.6876	1.2686	10.176	0.2263	2.816	2.757	3.990
600	15.7	2	112	104.1	-0.1425	1.1380	8.046	0.2218	2.850	2.786	5.333
600	19.7	2	120	203.9	0.9228	1.7104	11.097	0.2242	2.863	2.826	6.100
600	1.2	4	79	45.7	0.4444	0.5314	5.353	0.2432	2.787	2.639	0.350
600	2.4	4	85	191.7	-0.1772	1.1765	11.500	0.1964	2.801	2.743	1.393
600	4.0	4	82	190.0	0.1223	1.1336	10.384	0.2184	2.795	2.740	2.550
600	7.0	4	97	117.1	-0.8395	1.0524	8.182	0.2179	2.825	2.770	5.367
600	10.0	4	97	271.6	0.7947	1.6065	11.023	0.2165	2.826	2.790	6.367
600	15.7	4	121	203.3	-0.1190	1.7262	11.315	0.2186	2.865	2.854	8.533
400	1.2	2	104	32.7	0.4129	0.5931	4.579	0.2155	2.837	2.681	1.180
400	2.4	2	100	30.0	0.3093	0.5479	4.345	0.2180	2.830	2.683	1.793
400	4.0	2	93	86.4	1.0636	0.8658	7.151	0.2312	2.818	2.683	2.653
400	7.0	2	93	51.3	0.0763	0.6638	5.684	0.2176	2.817	2.694	3.367
400	10.0	2	93	142.1	1.5021	1.1079	8.524	0.2210	2.817	2.716	4.497
400	15.7	2	110	80.0	0.0912	0.9853	7.015	0.2109	2.848	2.775	6.700
400	19.7	2	114	107.0	0.8624	1.1802	7.605	0.2205	2.854	2.776	5.200
400	1.2	4	93	124.1	-0.7548	1.0330	8.773	0.2285	2.817	2.765	0.653
400	2.4	4	99	107.0	-0.4004	1.0205	8.444	0.2072	2.828	2.761	2.597
400	4.0	4	87	239.1	0.8718	1.3467	10.831	0.2194	2.806	2.752	3.350
400	7.0	4	101	57.9	-0.5676	0.7667	5.804	0.2107	2.832	2.749	7.300
400	10.0	4	103	231.5	1.8165	1.5617	9.831	0.2185	2.835	2.776	8.333
400	15.7	4	112	91.9	-0.2538	1.0743	7.316	0.2203	2.851	2.785	8.833

Table A24 Aluminum, Magnification = 7.5x, White Filters, Back Light

Speed (RPM)	Feed (in/min)	Flutes	Avg	Var	Skewness	Omega2	Ra(Image)	Lac(old)	FD2	FD1	Ra(Stylus) (μm)
1000	1.2	2	95	41.3	0.2046	0.6128	5.123	0.2284	2.822	2.683	0.440
1000	2.4	2	89	83.3	-0.0323	0.8088	7.156	0.2314	2.809	2.714	0.577
1000	4.0	2	83	101.0	0.2362	0.8344	7.806	0.2601	2.797	2.706	0.517
1000	7.0	2	90	180.8	0.1745	1.2092	11.081	0.2236	2.811	2.741	1.053
1000	10.0	2	88	644.4	1.4741	2.2265	17.159	0.2391	2.807	2.782	2.160
1000	15.7	2	98	187.8	-0.3750	1.3413	11.116	0.2238	2.827	2.782	4.417
1000	19.7	2	101	653.3	2.0361	2.5907	17.234	0.2250	2.833	2.798	5.333
1000	1.2	4	91	41.3	-0.2735	0.5846	5.160	0.2129	2.813	2.683	0.160
1000	2.4	4	87	63.3	-0.2475	0.6885	6.369	0.2335	2.804	2.696	0.270
1000	4.0	4	90	68.9	0.0936	0.7439	6.572	0.2387	2.811	2.698	0.500
1000	7.0	4	96	154.9	-0.3046	1.1900	10.230	0.2197	2.822	2.763	2.460
1000	10.0	4	92	486.0	1.4233	2.0241	15.798	0.2196	2.815	2.766	3.143
1000	15.7	4	113	212.1	-0.3130	1.6519	11.498	0.2233	2.853	2.835	5.700
800	1.2	2	76	49.8	0.3274	0.5365	5.582	0.2327	2.781	2.636	0.333
800	2.4	2	79	119.1	0.1079	0.8595	8.778	0.2299	2.787	2.699	0.400
800	4.0	2	74	99.4	0.1466	0.7416	8.010	0.2260	2.777	2.681	0.527
800	7.0	2	86	283.0	0.1159	1.4408	13.961	0.2296	2.803	2.755	1.643
800	10.0	2	82	1013.6	1.8938	2.6107	21.927	0.2284	2.795	2.762	3.383
800	15.7	2	100	331.0	-0.1545	1.8199	14.857	0.2345	2.831	2.804	5.697
800	19.7	2	102	786.2	1.9096	2.8599	19.077	0.2277	2.834	2.809	5.980
800	1.2	4	75	50.5	0.2691	0.5350	5.662	0.2236	2.779	2.636	0.193
800	2.4	4	73	206.1	0.1784	1.0459	11.732	0.2320	2.773	2.709	0.387
800	4.0	4	83	522.1	0.3271	1.8911	17.333	0.2384	2.796	2.780	1.510
800	7.0	4	98	288.0	-0.6762	1.6566	13.929	0.2159	2.826	2.802	3.830
800	10.0	4	86	938.2	1.7898	2.6327	21.155	0.2260	2.803	2.774	4.700
800	15.7	4	113	268.0	0.3554	1.8566	12.561	0.2282	2.853	2.831	7.500
600	1.2	2	83	48.7	0.0840	0.5815	5.484	0.2323	2.798	2.665	0.203
600	2.4	2	76	158.1	0.1128	0.9602	10.244	0.2188	2.782	2.704	0.447
600	4.0	2	84	151.0	-0.0062	1.0303	9.879	0.2367	2.799	2.733	1.127
600	7.0	2	94	348.2	-0.0013	1.7463	15.775	0.2239	2.819	2.780	3.563
600	10.0	2	98	766.4	1.2463	2.6992	20.267	0.2289	2.826	2.809	3.990
600	15.7	2	109	318.6	0.5006	1.9492	13.966	0.2259	2.846	2.810	5.333
600	19.7	2	109	770.7	1.0562	3.0363	21.103	0.2243	2.847	2.843	6.100
600	1.2	4	80	56.1	0.1865	0.6017	5.902	0.2375	2.791	2.665	0.350
600	2.4	4	84	315.4	-0.0003	1.4939	14.843	0.2253	2.799	2.755	1.393
600	4.0	4	88	583.2	0.8710	2.1257	17.170	0.2306	2.807	2.786	2.550
600	7.0	4	105	214.5	-0.6941	1.5306	11.554	0.2125	2.838	2.812	5.367
600	10.0	4	93	1057.9	2.1121	3.0175	20.614	0.2212	2.817	2.797	6.367
600	15.7	4	111	323.9	0.1715	2.0033	14.022	0.2200	2.850	2.833	8.533
400	1.2	2	105	171.7	-0.0934	1.3767	10.570	0.2266	2.839	2.791	1.180
400	2.4	2	99	131.3	0.0671	1.1321	9.241	0.2297	2.828	2.761	1.793
400	4.0	2	95	465.8	1.3929	2.0397	15.951	0.2363	2.820	2.772	2.653
400	7.0	2	102	184.8	0.0485	1.3881	10.677	0.2243	2.834	2.789	3.367
400	10.0	2	96	818.1	1.6819	2.7469	20.162	0.2270	2.823	2.805	4.497
400	15.7	2	107	223.8	0.1575	1.6082	12.149	0.2216	2.844	2.806	6.700
400	19.7	2	106	377.9	1.3241	2.0595	14.028	0.2262	2.841	2.805	5.200
400	1.2	4	93	322.5	-0.4032	1.6684	14.576	0.2328	2.817	2.792	0.653
400	2.4	4	102	245.5	-0.2160	1.6027	12.725	0.2166	2.835	2.801	2.597
400	4.0	4	94	943.0	1.5704	2.8832	20.519	0.2266	2.819	2.804	3.350
400	7.0	4	110	194.2	-0.7289	1.5324	10.581	0.2201	2.848	2.826	7.300
400	10.0	4	100	922.5	2.8282	3.0514	17.585	0.2199	2.831	2.791	8.333
400	15.7	4	115	190.3	-0.5913	1.5890	10.525	0.2137	2.856	2.836	8.833

Table A25 Aluminum, Magnification = 7.5x, White Filters, Right Light

Speed (RPM)	Feed (in/min)	Flutes	Avg	Var	Skewness	Omega2	Ra(Image)	Lac(old)	FD2	FD1	Ra(Stylus) (µm)
1000	1.2	2	92	31.4	1.4146	0.5131	4.227	0.2157	2.814	2.643	0.440
1000	2.4	2	83	55.4	1.6637	0.6172	5.422	0.2226	2.797	2.661	0.577
1000	4.0	2	84	48.8	0.4158	0.5889	5.405	0.2109	2.800	2.668	0.517
1000	7.0	2	85	78.9	0.6104	0.7555	6.742	0.2159	2.801	2.695	1.053
1000	10.0	2	91	168.0	0.3696	1.1807	10.407	0.2119	2.814	2.741	2.160
1000	15.7	2	96	117.7	0.5657	1.0362	7.932	0.2142	2.822	2.747	4.417
1000	19.7	2	105	136.4	-0.0419	1.2285	8.969	0.2220	2.840	2.792	5.333
1000	1.2	4	93	41.9	2.4876	0.6020	4.398	0.2082	2.817	2.652	0.160
1000	2.4	4	86	68.1	2.2577	0.7092	5.635	0.2321	2.803	2.661	0.270
1000	4.0	4	84	46.4	0.8899	0.5754	5.163	0.2148	2.800	2.644	0.500
1000	7.0	4	88	92.4	0.9257	0.8438	7.474	0.2174	2.807	2.681	2.460
1000	10.0	4	95	74.7	0.4151	0.8228	6.582	0.2171	2.822	2.718	3.143
1000	15.7	4	102	156.7	1.2514	1.2799	9.165	0.2210	2.834	2.750	5.700
800	1.2	2	72	43.3	2.6577	0.4725	4.659	0.2143	2.771	2.593	0.333
800	2.4	2	78	48.1	0.7900	0.5379	5.273	0.2114	2.785	2.644	0.400
800	4.0	2	78	53.2	0.2328	0.5713	5.741	0.2155	2.786	2.660	0.527
800	7.0	2	81	249.5	1.2866	1.2769	12.145	0.2128	2.792	2.713	1.643
800	10.0	2	87	247.4	0.7862	1.3697	12.248	0.2170	2.806	2.734	3.383
800	15.7	2	94	153.2	0.9381	1.1680	8.945	0.2126	2.820	2.747	5.697
800	19.7	2	103	162.9	0.1153	1.3170	9.986	0.2161	2.836	2.786	5.980
800	1.2	4	78	63.6	1.6073	0.6230	5.899	0.2216	2.786	2.633	0.193
800	2.4	4	79	142.0	0.7606	0.9390	8.986	0.2267	2.788	2.704	0.387
800	4.0	4	81	186.2	-0.0221	1.0991	11.087	0.2084	2.791	2.730	1.510
800	7.0	4	87	158.8	0.7258	1.0922	9.524	0.2151	2.805	2.732	3.830
800	10.0	4	92	131.7	-0.1875	1.0549	8.544	0.2214	2.815	2.764	4.700
800	15.7	4	98	265.0	1.8829	1.5897	11.068	0.2221	2.826	2.749	7.500
600	1.2	2	67	45.7	2.2020	0.4515	4.854	0.2102	2.758	2.592	0.203
600	2.4	2	74	63.8	0.7587	0.5938	6.026	0.2055	2.777	2.650	0.447
600	4.0	2	83	92.3	0.3379	0.8009	7.407	0.2192	2.798	2.704	1.127
600	7.0	2	87	251.8	0.5527	1.3766	13.010	0.2151	2.805	2.732	3.563
600	10.0	2	97	84.3	0.1419	0.8877	6.842	0.2260	2.824	2.746	3.990
600	15.7	2	104	153.1	1.0113	1.2816	9.065	0.2186	2.837	2.770	5.333
600	19.7	2	109	200.3	1.5284	1.5487	10.144	0.2228	2.847	2.779	6.100
600	1.2	4	80	51.3	0.5694	0.5728	5.528	0.2427	2.790	2.646	0.350
600	2.4	4	85	196.3	0.3289	1.1913	11.145	0.2286	2.801	2.740	1.393
600	4.0	4	84	157.6	-0.0118	1.0579	9.881	0.2170	2.800	2.735	2.550
600	7.0	4	90	163.8	0.3525	1.1495	9.560	0.2055	2.811	2.751	5.367
600	10.0	4	94	162.1	0.3654	1.1909	9.138	0.2171	2.818	2.764	6.367
600	15.7	4	101	196.4	1.3931	1.4083	9.786	0.2143	2.831	2.765	8.533
400	1.2	2	103	25.5	1.4226	0.5206	3.798	0.2101	2.836	2.659	1.180
400	2.4	2	108	45.1	0.7756	0.7219	5.075	0.2172	2.844	2.721	1.793
400	4.0	2	99	47.0	0.6653	0.6803	5.161	0.2195	2.829	2.709	2.653
400	7.0	2	94	99.6	1.2251	0.9397	7.355	0.2139	2.820	2.721	3.367
400	10.0	2	93	93.1	0.8805	0.8939	7.238	0.2160	2.817	2.719	4.497
400	15.7	2	108	149.0	1.3666	1.3123	8.843	0.2193	2.844	2.773	6.700
400	19.7	2	105	120.4	1.9215	1.1533	7.782	0.2083	2.839	2.747	5.200
400	1.2	4	93	105.4	-0.4685	0.9574	7.976	0.2226	2.818	2.752	0.653
400	2.4	4	96	143.6	0.4602	1.1464	9.353	0.2210	2.822	2.748	2.597
400	4.0	4	88	181.4	0.1573	1.1864	10.098	0.2185	2.808	2.748	3.350
400	7.0	4	96	109.3	1.3685	0.9990	7.353	0.2066	2.822	2.721	7.300
400	10.0	4	98	159.6	0.8896	1.2391	9.108	0.2197	2.827	2.756	8.333
400	15.7	4	106	188.4	1.2528	1.4487	9.793	0.2093	2.840	2.776	8.833

Table A26 Aluminum, Magnification = 15x, White Filters, Right Light

Speed (RPM)	Feed (in/min)	Flutes	Avg	Var	Skewness	Omega2	Ra(Image)	Lac(old)	FD2	FD1	Ra(Stylus) (μm)
1000	1.2	2	61	36.8	1.9986	0.3722	4.384	0.2171	2.742	2.575	0.440
1000	2.4	2	54	49.0	1.0080	0.3780	5.254	0.2080	2.719	2.575	0.577
1000	4.0	2	53	47.7	0.3223	0.3676	5.413	0.2153	2.717	2.592	0.517
1000	7.0	2	54	92.1	0.9473	0.5166	7.249	0.2048	2.719	2.598	1.053
1000	10.0	2	60	174.8	0.5768	0.7886	10.735	0.1966	2.737	2.648	2.160
1000	15.7	2	64	91.3	1.0694	0.6107	6.694	0.2015	2.750	2.636	4.417
1000	19.7	2	72	114.2	0.2033	0.7674	8.037	0.2058	2.771	2.691	5.333
1000	1.2	4	60	29.4	2.5193	0.3251	3.694	0.2007	2.738	2.529	0.160
1000	2.4	4	54	65.5	1.9802	0.4392	5.706	0.2135	2.720	2.587	0.270
1000	4.0	4	54	51.7	1.4873	0.3899	5.389	0.2030	2.720	2.557	0.500
1000	7.0	4	58	101.1	1.3539	0.5802	7.627	0.2129	2.731	2.589	2.460
1000	10.0	4	62	75.8	1.4366	0.5426	6.387	0.2019	2.745	2.605	3.143
1000	15.7	4	70	148.2	1.4385	0.8497	8.936	0.2051	2.766	2.649	5.700
800	1.2	2	43	33.9	2.4206	0.2526	4.038	0.2085	2.680	2.499	0.333
800	2.4	2	52	41.4	1.0344	0.3338	4.796	0.2089	2.712	2.559	0.400
800	4.0	2	48	52.4	0.6901	0.3456	5.873	0.2050	2.697	2.538	0.527
800	7.0	2	51	198.7	0.9032	0.7135	11.343	0.2079	2.708	2.611	1.643
800	10.0	2	55	204.3	0.8776	0.7807	11.112	0.2086	2.721	2.632	3.383
800	15.7	2	62	138.0	0.9026	0.7326	8.529	0.2091	2.745	2.658	5.697
800	19.7	2	70	130.4	-0.0484	0.8023	8.989	0.2055	2.767	2.685	5.980
800	1.2	4	49	49.8	1.7285	0.3492	5.197	0.2032	2.704	2.550	0.193
800	2.4	4	51	99.5	1.2767	0.5079	7.496	0.2012	2.709	2.585	0.387
800	4.0	4	52	143.4	0.6033	0.6220	10.112	0.2010	2.712	2.609	1.510
800	7.0	4	56	147.3	1.3389	0.6783	8.781	0.2102	2.726	2.624	3.830
800	10.0	4	60	116.1	1.6558	0.6500	7.545	0.2093	2.739	2.624	4.700
800	15.7	4	65	147.4	1.7069	0.7890	8.275	0.2099	2.753	2.645	7.500
600	1.2	2	40	25.1	2.2072	0.2026	3.601	0.1940	2.667	2.494	0.203
600	2.4	2	46	55.0	1.2236	0.3434	5.525	0.1960	2.692	2.570	0.447
600	4.0	2	53	91.9	0.7318	0.5038	7.560	0.2036	2.714	2.601	1.127
600	7.0	2	56	236.0	0.8363	0.8639	12.386	0.2049	2.727	2.638	3.563
600	10.0	2	62	86.7	0.2342	0.5796	7.127	0.2093	2.745	2.646	3.990
600	15.7	2	70	122.2	1.3063	0.7685	8.310	0.2085	2.765	2.653	5.333
600	19.7	2	76	132.8	1.3618	0.8772	8.509	0.2065	2.781	2.666	6.100
600	1.2	4	50	53.5	0.8410	0.3683	5.700	0.2004	2.707	2.560	0.350
600	2.4	4	54	143.4	0.1594	0.6450	9.841	0.2102	2.719	2.637	1.393
600	4.0	4	53	114.6	0.4272	0.5726	8.604	0.2050	2.718	2.616	2.550
600	7.0	4	61	159.7	1.0212	0.7666	9.248	0.2001	2.740	2.660	5.367
600	10.0	4	64	119.8	0.8962	0.6996	8.244	0.2041	2.750	2.642	6.367
600	15.7	4	69	142.6	1.4759	0.8181	8.387	0.2072	2.762	2.650	8.533
400	1.2	2	71	17.0	1.3674	0.2912	3.063	0.1915	2.768	2.532	1.180
400	2.4	2	74	31.8	0.8314	0.4186	4.262	0.1968	2.777	2.593	1.793
400	4.0	2	68	44.3	0.7357	0.4525	4.895	0.2004	2.761	2.624	2.653
400	7.0	2	64	88.4	1.1302	0.6026	7.126	0.2014	2.750	2.623	3.367
400	10.0	2	64	80.0	0.5001	0.5744	6.789	0.2051	2.751	2.638	4.497
400	15.7	2	74	101.1	1.2539	0.7489	7.246	0.2135	2.777	2.658	6.700
400	19.7	2	76	91.5	0.7091	0.7315	7.145	0.2031	2.782	2.656	5.200
400	1.2	4	61	71.9	-0.0699	0.5153	7.011	0.1891	2.741	2.628	0.653
400	2.4	4	64	115.6	0.7036	0.6930	8.404	0.1978	2.751	2.640	2.597
400	4.0	4	60	153.4	0.6581	0.7381	9.774	0.2010	2.737	2.642	3.350
400	7.0	4	66	75.9	1.1902	0.5727	6.336	0.1924	2.755	2.616	7.300
400	10.0	4	67	123.1	0.8640	0.7406	8.127	0.2003	2.758	2.659	8.333
400	15.7	4	74	141.3	0.8502	0.8785	8.877	0.2006	2.776	2.683	8.833

Table A27 Aluminum, Magnification = 15x, White Filters, Back Light

Speed (RPM)	Feed (in/min)	Flutes	Avg	Var	Skewness	Omega2	Ra(Image)	Lac(old)	FD2	FD1	Ra(Stylus) (µm)
1000	1.2	2	85	47.3	0.1611	0.5818	5.370	0.2152	2.800	2.663	0.440
1000	2.4	2	80	99.1	0.3446	0.7989	7.800	0.2039	2.791	2.690	0.577
1000	4.0	2	76	212.9	0.5175	1.1119	11.156	0.2139	2.781	2.719	0.517
1000	7.0	2	83	240.4	0.2114	1.2896	12.758	0.2103	2.797	2.736	1.053
1000	10.0	2	83	1021.0	2.4400	2.6390	18.942	0.2189	2.796	2.772	2.160
1000	15.7	2	91	268.7	-0.4205	1.4898	13.433	0.2179	2.813	2.774	4.417
1000	19.7	2	90	717.6	2.6120	2.4143	17.489	0.2199	2.812	2.762	5.333
1000	1.2	4	88	37.5	-0.0460	0.5419	4.810	0.2183	2.808	2.664	0.160
1000	2.4	4	83	93.6	0.1133	0.7997	7.802	0.2201	2.796	2.692	0.270
1000	4.0	4	84	104.7	0.2316	0.8630	8.106	0.2200	2.800	2.701	0.500
1000	7.0	4	91	187.7	-0.3080	1.2476	11.648	0.2147	2.814	2.752	2.460
1000	10.0	4	87	612.1	2.2120	2.1612	16.389	0.2078	2.806	2.750	3.143
1000	15.7	4	100	238.0	0.5146	1.5494	11.148	0.2274	2.831	2.796	5.700
800	1.2	2	71	152.8	0.2323	0.8766	10.039	0.2248	2.768	2.690	0.333
800	2.4	2	77	176.7	0.5155	1.0275	10.637	0.2125	2.784	2.702	0.400
800	4.0	2	71	148.6	0.6026	0.8638	9.396	0.2086	2.768	2.680	0.527
800	7.0	2	82	395.0	0.0916	1.6251	16.563	0.2151	2.794	2.758	1.643
800	10.0	2	79	1643.4	2.5178	3.2188	25.211	0.2162	2.789	2.744	3.383
800	15.7	2	94	601.4	0.2902	2.3131	19.493	0.2273	2.820	2.801	5.697
800	19.7	2	90	1043.7	2.3717	2.9104	21.703	0.2230	2.812	2.774	5.980
800	1.2	4	68	69.9	0.2281	0.5710	6.702	0.2085	2.762	2.642	0.193
800	2.4	4	70	197.8	0.4463	0.9839	11.418	0.2015	2.766	2.683	0.387
800	4.0	4	78	601.4	1.5516	1.9110	17.685	0.2241	2.786	2.737	1.510
800	7.0	4	92	302.0	-0.8712	1.5987	14.375	0.2085	2.815	2.788	3.830
800	10.0	4	82	1126.4	2.7825	2.7387	20.822	0.2163	2.794	2.750	4.700
800	15.7	4	99	238.6	2.1774	1.5223	10.843	0.2200	2.828	2.780	7.500
600	1.2	2	72	68.9	0.2005	0.5976	6.492	0.2087	2.771	2.655	0.203
600	2.4	2	70	184.8	-0.0275	0.9464	11.537	0.2076	2.765	2.690	0.447
600	4.0	2	77	278.2	0.4317	1.2776	13.220	0.2179	2.782	2.724	1.127
600	7.0	2	90	441.9	0.0335	1.8889	17.765	0.2232	2.811	2.777	3.563
600	10.0	2	96	1070.5	1.7729	3.1264	22.864	0.2290	2.822	2.795	3.990
600	15.7	2	104	557.1	0.9152	2.4604	18.213	0.2257	2.838	2.814	5.333
600	19.7	2	103	1103.7	1.7197	3.4258	23.853	0.2209	2.836	2.817	6.100
600	1.2	4	73	125.8	0.1771	0.8239	9.120	0.2187	2.775	2.684	0.350
600	2.4	4	80	382.5	-0.2876	1.5745	16.333	0.2123	2.791	2.758	1.393
600	4.0	4	86	745.9	2.1286	2.3394	17.572	0.2280	2.803	2.769	2.550
600	7.0	4	101	295.4	-0.8779	1.7298	13.214	0.2258	2.832	2.816	5.367
600	10.0	4	90	1509.3	2.7496	3.4778	23.169	0.2157	2.811	2.767	6.367
600	15.7	4	102	211.0	-0.4538	1.4759	11.560	0.2230	2.833	2.802	8.533
400	1.2	2	101	200.3	0.4428	1.4309	11.448	0.2181	2.832	2.769	1.180
400	2.4	2	97	171.0	0.4359	1.2653	10.702	0.2157	2.825	2.747	1.793
400	4.0	2	93	915.3	1.9305	2.8255	21.391	0.2189	2.818	2.774	2.653
400	7.0	2	97	247.0	0.1239	1.5236	12.628	0.2133	2.825	2.785	3.367
400	10.0	2	93	1149.2	2.1794	3.1489	22.884	0.2170	2.817	2.783	4.497
400	15.7	2	103	309.2	0.4370	1.8158	14.184	0.2196	2.836	2.798	6.700
400	19.7	2	97	684.4	1.7135	2.5301	18.409	0.2316	2.824	2.795	5.200
400	1.2	4	90	243.8	0.2751	1.4048	12.604	0.2084	2.811	2.756	0.653
400	2.4	4	101	225.5	-0.3798	1.5223	12.287	0.2046	2.833	2.800	2.597
400	4.0	4	95	1204.6	2.5763	3.2991	20.868	0.2143	2.821	2.789	3.350
400	7.0	4	112	177.2	-0.6972	1.4950	10.208	0.2029	2.851	2.834	7.300
400	10.0	4	100	1320.7	2.8005	3.6482	21.270	0.2131	2.831	2.800	8.333
400	15.7	4	105	202.7	-0.0845	1.4957	10.610	0.2145	2.839	2.808	8.833

Table A28 Aluminum, Magnification = 15x, Green Filters, All Four Lights

Speed (RPM)	Feed (in/min)	Flutes	Avg	Var	Skewness	Omega2	Ra(Image)	Lac(old)	FD2	FD1	Ra(Stylus) (µm)
1000	1.2	2	107	62.2	0.0963	0.8424	6.251	0.2014	2.842	2.744	0.440
1000	2.4	2	97	106.4	0.0421	1.0036	8.149	0.2180	2.826	2.751	0.577
1000	4.0	2	100	260.0	0.3758	1.6082	12.481	0.2177	2.830	2.790	0.517
1000	7.0	2	106	330.6	1.9778	1.9226	12.064	0.2237	2.841	2.792	1.053
1000	10.0	2	104	482.6	1.4617	2.2951	15.611	0.2212	2.838	2.811	2.160
1000	15.7	2	107	344.5	1.8662	1.9897	12.140	0.2176	2.843	2.807	4.417
1000	19.7	2	115	640.5	1.5100	2.9039	17.939	0.2191	2.855	2.852	5.333
1000	1.2	4	106	52.6	-0.0062	0.7676	5.696	0.2141	2.841	2.741	0.160
1000	2.4	4	98	86.2	-0.3668	0.9095	7.357	0.1889	2.827	2.751	0.270
1000	4.0	4	99	124.6	-0.3015	1.1008	8.927	0.2085	2.828	2.768	0.500
1000	7.0	4	105	620.3	2.5116	2.6045	15.380	0.2270	2.839	2.812	2.460
1000	10.0	4	104	347.6	2.4158	1.9435	11.817	0.2176	2.838	2.793	3.143
1000	15.7	4	106	751.7	2.9674	2.9060	15.780	0.2260	2.841	2.805	5.700
800	1.2	2	85	153.5	0.2020	1.0584	9.766	0.2208	2.802	2.728	0.333
800	2.4	2	88	171.0	0.3602	1.1549	10.485	0.2155	2.808	2.739	0.400
800	4.0	2	86	222.8	0.2366	1.2901	12.033	0.2218	2.804	2.741	0.527
800	7.0	2	98	458.6	1.3955	2.0954	15.886	0.2207	2.827	2.787	1.643
800	10.0	2	100	591.8	1.6139	2.4333	17.182	0.2182	2.831	2.800	3.383
800	15.7	2	109	535.2	1.9756	2.5149	15.670	0.2192	2.846	2.820	5.697
800	19.7	2	111	368.2	1.1150	2.1388	13.705	0.2059	2.850	2.837	5.980
800	1.2	4	90	117.3	-0.0842	0.9720	8.619	0.2100	2.811	2.736	0.193
800	2.4	4	84	260.0	0.3100	1.3614	13.154	0.2259	2.800	2.743	0.387
800	4.0	4	95	597.1	0.7702	2.3218	19.242	0.2254	2.821	2.794	1.510
800	7.0	4	101	620.4	2.0278	2.5198	16.212	0.2212	2.833	2.811	3.830
800	10.0	4	101	718.8	3.1558	2.7160	14.802	0.2199	2.833	2.795	4.700
800	15.7	4	105	904.1	2.9800	3.1426	17.456	0.2201	2.838	2.807	7.500
600	1.2	2	85	100.8	0.0632	0.8562	7.892	0.2177	2.802	2.718	0.203
600	2.4	2	83	131.6	-0.1913	0.9479	9.153	0.2134	2.796	2.721	0.447
600	4.0	2	95	176.2	-0.1977	1.2554	10.632	0.2110	2.820	2.770	1.127
600	7.0	2	109	626.8	1.8735	2.7353	17.107	0.2084	2.846	2.823	3.563
600	10.0	2	122	575.1	1.4405	2.9324	16.656	0.2210	2.867	2.872	3.990
600	15.7	2	116	464.3	1.6161	2.4900	15.561	0.2289	2.857	2.842	5.333
600	19.7	2	121	809.9	1.9201	3.4443	19.044	0.2177	2.865	2.860	6.100
600	1.2	4	89	136.9	0.1332	1.0471	9.502	0.2050	2.810	2.730	0.350
600	2.4	4	98	446.5	0.4328	2.0668	16.819	0.2146	2.826	2.796	1.393
600	4.0	4	104	713.9	2.1664	2.7801	17.009	0.2207	2.838	2.820	2.550
600	7.0	4	118	965.0	2.2869	3.6763	18.622	0.2128	2.861	2.861	5.367
600	10.0	4	114	1011.3	2.4279	3.6299	19.598	0.2201	2.854	2.846	6.367
600	15.7	4	108	963.9	2.7882	3.3531	18.081	0.2332	2.844	2.820	8.533
400	1.2	2	116	104.9	0.7647	1.1915	7.632	0.2206	2.858	2.790	1.180
400	2.4	2	113	159.5	2.3700	1.4310	8.182	0.2273	2.853	2.786	1.793
400	4.0	2	116	410.5	2.4167	2.3564	13.026	0.2261	2.858	2.830	2.653
400	7.0	2	113	348.1	2.0729	2.1173	12.325	0.2153	2.853	2.821	3.367
400	10.0	2	116	643.5	2.0547	2.9384	16.163	0.2202	2.857	2.835	4.497
400	15.7	2	116	490.5	2.3557	2.5628	13.866	0.2119	2.857	2.839	6.700
400	19.7	2	116	380.7	1.2543	2.2616	13.914	0.2233	2.857	2.840	5.200
400	1.2	4	109	220.3	-0.3235	1.6216	11.708	0.2119	2.846	2.823	0.653
400	2.4	4	114	671.2	2.1124	2.9525	16.927	0.2238	2.854	2.842	2.597
400	4.0	4	122	1317.4	1.7186	4.4289	25.001	0.2180	2.866	2.877	3.350
400	7.0	4	122	412.2	2.5582	2.4755	12.538	0.2140	2.866	2.850	7.300
400	10.0	4	123	1465.4	2.2098	4.6974	24.458	0.2046	2.867	2.867	8.333
400	15.7	4	112	804.6	3.2899	3.1846	15.320	0.2059	2.851	2.820	8.833

Table A29 Aluminum, Magnification = 15x, Red Filters, All Four Lights

Speed (RPM)	Feed (in/min)	Flutes	Avg	Var	Skewness	Omega2	Ra(Image)	Lac(old)	FD2	FD1	Ra(Stylus) (μm)
1000	1.2	2	67	41.2	0.1575	0.4309	5.150	0.1914	2.759	2.606	0.440
1000	2.4	2	60	66.3	0.4490	0.4910	6.396	0.1991	2.739	2.616	0.577
1000	4.0	2	61	145.7	0.4863	0.7386	9.628	0.2047	2.742	2.654	0.517
1000	7.0	2	62	185.0	1.2836	0.8483	9.878	0.2065	2.745	2.658	1.053
1000	10.0	2	65	239.2	0.9300	1.0088	11.611	0.2047	2.753	2.686	2.160
1000	15.7	2	68	167.4	0.8092	0.8759	9.381	0.1972	2.760	2.689	4.417
1000	19.7	2	71	250.5	0.3320	1.1248	12.568	0.1991	2.769	2.716	5.333
1000	1.2	4	68	25.6	-0.1685	0.3453	4.025	0.1951	2.762	2.590	0.160
1000	2.4	4	61	56.6	-0.2099	0.4627	6.093	0.1925	2.743	2.627	0.270
1000	4.0	4	57	63.7	0.0722	0.4570	6.341	0.2008	2.730	2.609	0.500
1000	7.0	4	62	283.6	2.4303	1.0419	10.705	0.2061	2.744	2.659	2.460
1000	10.0	4	66	153.9	1.4619	0.8133	8.890	0.2051	2.754	2.666	3.143
1000	15.7	4	67	292.9	2.5204	1.1468	10.842	0.2086	2.758	2.672	5.700
800	1.2	2	50	56.1	0.7457	0.3709	5.888	0.2132	2.704	2.560	0.333
800	2.4	2	56	98.3	0.4503	0.5551	7.948	0.2030	2.726	2.618	0.400
800	4.0	2	51	112.0	0.4885	0.5399	8.624	0.2054	2.709	2.601	0.527
800	7.0	2	57	311.3	0.8598	1.0118	14.035	0.2017	2.730	2.665	1.643
800	10.0	2	64	308.2	1.0430	1.1173	13.082	0.2071	2.749	2.691	3.383
800	15.7	2	68	239.0	0.9058	1.0588	11.758	0.2123	2.762	2.698	5.697
800	19.7	2	73	225.6	-0.0412	1.0994	11.736	0.2039	2.774	2.724	5.980
800	1.2	4	51	73.2	0.2284	0.4395	6.885	0.2062	2.710	2.597	0.193
800	2.4	4	51	130.8	0.4165	0.5851	9.383	0.2090	2.710	2.615	0.387
800	4.0	4	56	308.8	0.7134	0.9884	14.267	0.2120	2.727	2.662	1.510
800	7.0	4	60	244.9	1.5002	0.9454	10.866	0.2077	2.740	2.668	3.830
800	10.0	4	65	239.1	2.2324	1.0116	9.909	0.2080	2.754	2.679	4.700
800	15.7	4	67	415.5	2.6887	1.3649	12.195	0.2056	2.758	2.685	7.500
600	1.2	2	50	54.8	0.2386	0.3666	5.920	0.2008	2.704	2.579	0.203
600	2.4	2	48	85.5	-0.0547	0.4466	7.543	0.2026	2.699	2.604	0.447
600	4.0	2	57	121.4	-0.1329	0.6247	9.071	0.1983	2.728	2.647	1.127
600	7.0	2	65	295.9	1.0513	1.1236	12.976	0.2022	2.754	2.686	3.563
600	10.0	2	79	154.2	0.3344	0.9867	9.180	0.1859	2.789	2.720	3.990
600	15.7	2	77	195.7	1.4699	1.0795	10.240	0.2110	2.784	2.697	5.333
600	19.7	2	80	241.9	1.5862	1.2502	10.984	0.1967	2.791	2.710	6.100
600	1.2	4	54	78.8	0.2617	0.4802	7.228	0.1986	2.720	2.608	0.350
600	2.4	4	60	268.7	0.5141	0.9774	13.156	0.2048	2.737	2.671	1.393
600	4.0	4	61	328.1	1.6465	1.1126	12.644	0.2057	2.743	2.678	2.550
600	7.0	4	70	383.2	1.7372	1.3612	12.700	0.2070	2.765	2.714	5.367
600	10.0	4	72	490.9	1.7009	1.6003	15.217	0.2084	2.772	2.719	6.367
600	15.7	4	69	288.2	2.6694	1.1789	10.346	0.2107	2.765	2.688	8.533
400	1.2	2	75	38.0	0.5099	0.4623	4.777	0.2010	2.779	2.615	1.180
400	2.4	2	74	79.6	2.3943	0.6624	5.880	0.2049	2.777	2.642	1.793
400	4.0	2	74	164.6	1.9221	0.9551	8.691	0.2031	2.777	2.676	2.653
400	7.0	2	70	145.2	1.4810	0.8434	8.500	0.2058	2.766	2.674	3.367
400	10.0	2	74	230.0	1.7821	1.1182	10.123	0.2029	2.776	2.700	4.497
400	15.7	2	75	146.1	1.6458	0.9097	8.397	0.2086	2.779	2.677	6.700
400	19.7	2	73	144.7	0.7820	0.8818	9.180	0.1941	2.774	2.688	5.200
400	1.2	4	71	86.8	-0.1859	0.6580	7.443	0.2032	2.768	2.678	0.653
400	2.4	4	74	239.3	1.4950	1.1422	10.829	0.2086	2.776	2.700	2.597
400	4.0	4	71	551.9	1.6765	1.6645	16.389	0.2066	2.768	2.708	3.350
400	7.0	4	75	174.7	2.2693	0.9913	8.338	0.2086	2.779	2.686	7.300
400	10.0	4	77	500.8	2.4690	1.7152	13.538	0.2049	2.783	2.718	8.333
400	15.7	4	72	358.9	3.2759	1.3713	10.727	0.2029	2.772	2.686	8.833

Table A30 Aluminum, Magnification = 15x, Blue Filters, All Four Lights

Speed (RPM)	Feed (in/min)	Flutes	Avg	Var	Skewness	Omega2	Ra(Image)	Lac(old)	FD2	FD1	Ra(Stylus) (µm)
1000	1.2	2	107	60.4	-0.1479	0.8278	6.165	0.2281	2.842	2.748	0.440
1000	2.4	2	104	66.3	1.5922	0.8478	5.821	0.2160	2.838	2.744	0.577
1000	4.0	2	102	111.9	0.1043	1.0799	8.423	0.2257	2.834	2.764	0.517
1000	7.0	2	106	148.3	0.9320	1.2878	9.074	0.2157	2.841	2.768	1.053
1000	10.0	2	110	319.9	1.2677	1.9749	12.694	0.2248	2.848	2.814	2.160
1000	15.7	2	114	231.8	1.5872	1.7292	10.061	0.2103	2.853	2.816	4.417
1000	19.7	2	117	334.5	1.0684	2.1421	13.382	0.2144	2.859	2.846	5.333
1000	1.2	4	107	25.7	0.0014	0.5429	3.970	0.2107	2.843	2.708	0.160
1000	2.4	4	102	62.7	-0.3450	0.8055	6.140	0.2178	2.834	2.746	0.270
1000	4.0	4	99	49.6	-0.0773	0.6962	5.637	0.2132	2.828	2.705	0.500
1000	7.0	4	104	157.4	1.7794	1.3105	8.822	0.2148	2.838	2.747	2.460
1000	10.0	4	113	154.4	1.7363	1.3987	8.515	0.2077	2.852	2.779	3.143
1000	15.7	4	114	488.6	2.7231	2.5164	13.472	0.2088	2.854	2.811	5.700
800	1.2	2	90	52.5	0.1533	0.6487	5.677	0.2224	2.811	2.684	0.333
800	2.4	2	93	87.9	0.0124	0.8732	7.564	0.2148	2.818	2.729	0.400
800	4.0	2	95	101.7	-0.0713	0.9544	8.275	0.2155	2.821	2.735	0.527
800	7.0	2	98	242.0	0.9408	1.5203	11.745	0.2110	2.826	2.766	1.643
800	10.0	2	108	358.5	0.9459	2.0408	14.131	0.2070	2.844	2.810	3.383
800	15.7	2	114	283.5	1.3547	1.9119	11.835	0.2142	2.853	2.822	5.697
800	19.7	2	119	243.7	0.6231	1.8518	11.364	0.2151	2.861	2.845	5.980
800	1.2	4	95	54.1	-0.2329	0.6961	5.821	0.2090	2.821	2.706	0.193
800	2.4	4	91	148.1	0.4276	1.1103	9.525	0.2194	2.814	2.738	0.387
800	4.0	4	96	268.4	0.3329	1.5731	13.477	0.2249	2.823	2.772	1.510
800	7.0	4	102	267.2	1.7931	1.6656	10.849	0.2170	2.834	2.775	3.830
800	10.0	4	109	346.9	2.2108	2.0380	11.305	0.2319	2.847	2.806	4.700
800	15.7	4	112	522.0	2.8869	2.5493	13.212	0.2157	2.850	2.806	7.500
600	1.2	2	90	58.6	-0.2270	0.6903	5.948	0.2064	2.812	2.704	0.203
600	2.4	2	89	105.5	0.1061	0.9190	8.252	0.2065	2.810	2.725	0.447
600	4.0	2	101	130.7	-0.3798	1.1575	9.346	0.2132	2.833	2.774	1.127
600	7.0	2	106	394.0	1.5105	2.0981	14.328	0.2027	2.840	2.798	3.563
600	10.0	2	123	307.9	1.1201	2.1510	12.783	0.2177	2.867	2.858	3.990
600	15.7	2	124	257.8	1.4060	1.9854	11.819	0.2216	2.869	2.843	5.333
600	19.7	2	126	431.8	1.8677	2.6139	14.117	0.2159	2.872	2.867	6.100
600	1.2	4	93	78.9	-0.0254	0.8295	7.138	0.2108	2.818	2.720	0.350
600	2.4	4	102	254.1	-0.2190	1.6201	12.801	0.2170	2.833	2.799	1.393
600	4.0	4	106	279.3	0.9531	1.7638	11.688	0.2148	2.840	2.805	2.550
600	7.0	4	110	521.2	2.1294	2.5117	13.664	0.2123	2.848	2.824	5.367
600	10.0	4	118	500.3	2.5299	2.6295	13.454	0.2074	2.860	2.829	6.367
600	15.7	4	116	603.8	2.9943	2.8470	13.647	0.2200	2.857	2.827	8.533
400	1.2	2	118	42.5	0.1914	0.7705	5.023	0.2176	2.861	2.746	1.180
400	2.4	2	115	72.9	1.7931	0.9836	5.804	0.2087	2.856	2.760	1.793
400	4.0	2	116	105.1	1.6242	1.1877	7.092	0.2055	2.857	2.780	2.653
400	7.0	2	112	203.7	2.3320	1.6053	9.186	0.2118	2.852	2.783	3.367
400	10.0	2	116	246.0	2.0002	1.8247	10.391	0.2088	2.858	2.821	4.497
400	15.7	2	121	206.5	2.3311	1.7379	9.305	0.2092	2.865	2.814	6.700
400	19.7	2	120	228.9	1.7392	1.8154	10.296	0.2138	2.863	2.828	5.200
400	1.2	4	107	165.5	-0.2908	1.3775	10.504	0.2023	2.843	2.804	0.653
400	2.4	4	118	271.8	1.5553	1.9422	11.269	0.2154	2.860	2.830	2.597
400	4.0	4	116	802.8	1.6455	3.2795	18.788	0.2176	2.857	2.859	3.350
400	7.0	4	123	369.6	2.6435	2.3582	11.576	0.2069	2.867	2.836	7.300
400	10.0	4	126	950.8	2.3944	3.8737	18.429	0.2185	2.872	2.874	8.333
400	15.7	4	118	536.0	3.3602	2.7311	12.417	0.2058	2.860	2.831	8.833

Table A30 Aluminum, Magnification = 15x, White 10-90 Filters, All Four Lights

Speed (RPM)	Feed (in/min)	Flutes	Avg	Var	Skewness	Omega2	Ra(Image)	Lac(old)	FD2	FD1	Ra(Stylus) (µm)
1000	1.2	2	118	54.9	-0.2513	0.8768	5.805	0.2189	2.861	2.779	0.440
1000	2.4	2	108	141.1	-0.1335	1.2773	9.091	0.2229	2.844	2.797	0.577
1000	4.0	2	103	251.0	0.2299	1.6387	12.800	0.2305	2.837	2.797	0.517
1000	7.0	2	104	420.7	0.5345	2.1319	16.156	0.2333	2.837	2.811	1.053
1000	10.0	2	115	718.3	1.0266	3.0921	19.938	0.2193	2.856	2.856	2.160
1000	15.7	2	119	590.0	1.5577	2.8847	16.195	0.2276	2.861	2.862	4.417
1000	19.7	2	128	619.1	0.7389	3.1915	18.454	0.2293	2.875	2.897	5.333
1000	1.2	4	107	55.8	-0.1896	0.7979	5.886	0.2271	2.842	2.756	0.160
1000	2.4	4	107	212.9	-0.7139	1.5579	11.577	0.2363	2.842	2.820	0.270
1000	4.0	4	102	134.3	-0.1873	1.1780	9.129	0.2305	2.833	2.780	0.500
1000	7.0	4	108	402.0	1.3961	2.1718	14.173	0.2342	2.845	2.816	2.460
1000	10.0	4	117	390.4	1.4231	2.3188	13.512	0.2434	2.859	2.843	3.143
1000	15.7	4	123	648.4	1.8999	3.1264	17.034	0.2366	2.867	2.865	5.700
800	1.2	2	97	95.9	0.0317	0.9453	7.580	0.2401	2.824	2.750	0.333
800	2.4	2	99	182.1	-0.0985	1.3317	10.925	0.2305	2.828	2.781	0.400
800	4.0	2	99	246.6	0.0759	1.5523	12.799	0.2245	2.828	2.787	0.527
800	7.0	2	107	650.2	0.8019	2.7195	19.808	0.2268	2.842	2.826	1.643
800	10.0	2	119	912.9	1.0903	3.6062	21.578	0.2311	2.862	2.872	3.383
800	15.7	2	125	672.7	0.9195	3.2439	19.107	0.2346	2.871	2.885	5.697
800	19.7	2	132	554.1	0.3084	3.1147	17.345	0.2175	2.881	2.909	5.980
800	1.2	4	90	130.8	-0.0205	1.0242	8.967	0.2234	2.811	2.739	0.193
800	2.4	4	100	212.8	0.0560	1.4539	11.704	0.2330	2.830	2.787	0.387
800	4.0	4	105	440.9	-0.1610	2.2101	17.208	0.2287	2.840	2.830	1.510
800	7.0	4	110	391.8	1.0667	2.1748	13.568	0.2248	2.847	2.831	3.830
800	10.0	4	121	375.0	1.7687	2.3469	11.976	0.2308	2.865	2.855	4.700
800	15.7	4	125	459.8	2.0426	2.6826	13.655	0.2262	2.871	2.868	7.500
600	1.2	2	93	78.2	-0.2144	0.8184	6.911	0.2100	2.817	2.729	0.203
600	2.4	2	98	172.8	-0.5436	1.2900	10.579	0.2178	2.827	2.786	0.447
600	4.0	2	108	303.1	-0.3567	1.8763	14.045	0.2217	2.844	2.828	1.127
600	7.0	2	115	675.6	0.8496	2.9935	19.918	0.2216	2.856	2.853	3.563
600	10.0	2	137	556.0	0.6730	3.2214	17.371	0.2319	2.887	2.925	3.990
600	15.7	2	139	431.0	0.9562	2.8928	15.866	0.2324	2.890	2.923	5.333
600	19.7	2	143	500.5	1.2358	3.2077	16.228	0.2332	2.895	2.940	6.100
600	1.2	4	102	171.9	-0.0529	1.3351	10.521	0.2199	2.834	2.781	0.350
600	2.4	4	113	503.4	-0.3272	2.5303	17.972	0.2270	2.852	2.855	1.393
600	4.0	4	109	440.5	0.2569	2.2954	15.394	0.2223	2.847	2.836	2.550
600	7.0	4	118	581.1	1.2650	2.8417	15.801	0.2180	2.860	2.864	5.367
600	10.0	4	125	747.9	1.4517	3.4297	18.176	0.2211	2.871	2.886	6.367
600	15.7	4	126	678.6	1.9686	3.2808	16.511	0.2305	2.872	2.882	8.533
400	1.2	2	135	39.8	0.4381	0.8534	4.852	0.2030	2.885	2.822	1.180
400	2.4	2	134	84.5	0.8178	1.2285	6.714	0.2102	2.883	2.851	1.793
400	4.0	2	132	255.5	1.2124	2.1121	11.048	0.2160	2.881	2.886	2.653
400	7.0	2	123	249.4	1.6333	1.9469	10.752	0.2192	2.868	2.844	3.367
400	10.0	2	132	407.0	1.1706	2.6648	13.779	0.2237	2.881	2.901	4.497
400	15.7	2	132	425.2	1.3849	2.7247	14.165	0.2232	2.881	2.896	6.700
400	19.7	2	133	414.3	0.3901	2.7095	15.588	0.2300	2.882	2.909	5.200
400	1.2	4	116	274.7	-0.4814	1.9169	13.379	0.2075	2.857	2.852	0.653
400	2.4	4	130	260.1	0.1982	2.1044	12.440	0.2113	2.878	2.887	2.597
400	4.0	4	119	700.8	1.1662	3.1453	18.692	0.2169	2.862	2.867	3.350
400	7.0	4	124	358.0	1.7820	2.3467	12.312	0.2098	2.869	2.859	7.300
400	10.0	4	134	860.8	1.6458	3.9213	18.752	0.2236	2.883	2.911	8.333
400	15.7	4	131	649.1	2.1425	3.3445	15.697	0.2179	2.880	2.893	8.833

Appendix B

Hardware Specifications

(1) CCD Camera

Manufacturer	Sony
Model	SSC-M350 monochrome CCD video camera
Specifications	1/2" Inter-line transfer type monochrome CCD
Resolution	510 (horizontal) x 492 (vertical)
Automatic gain control	switched off
Video out	NTSC

(2) Frame Grabber Card

Manufacturer	Imagenation
Model	CX100
Specifications	NTSC, monochrome interlaced
Resolution	512 (horizontal) x 486 (vertical)
Frame grab speed	1/30 second
Aspect ratio	1:1 (square pixels)

Appendix C

Surface Assessment Devices

Non-Optical Devices

Laser Profilometry

A laser beam is directed onto the surface at near-normal incidence and stepped along by incremental distances d, the diameter of the beam. At each step the angle of reflection θ of the returned beam is measured by autocollimation. There are many sources of measurement uncertainty, such as beam direction fluctuation due to thermal drift and air turbulence, which limit the instrumental accuracy[31]. This method of analyzing the surface only takes into account a profile.

Microscopy

In conventional microscopy a compromise exists between the resolution and the depth of the image. Conventional optical microscopes are not suitable for the study of surface topography. Electron microscopy has a higher resolution and depth of field than does the optical microscopy method. The two types of electron microscopy are transmission electron microscopy and reflection electron microscopy. TEM requires a specimen that is less than 1 μm thick. In order to investigate the specimen without destroying it a replica is made of the surface and this causes several difficulties.

The second method of electron microscopy is REM and in this method electrons are scattered from the surface and strike a collector which generates an electrical signal. From the signal the surface can be reconstructed. Another form of electron microscopy is SEM in which scattered electrons are produced by a beam of finely focused electrons that scan the surface in a raster pattern. The disadvantage of all these methods is that a small specimen is necessary and a destructive method is required to measure larger specimens. The specimen must be conductive or a fine coating can be applied to make the specimen electrically conductive. The photogrammetric method was described by Matsuno. The method requires viewing the image from two different angles off the main beam. The surface height can be determined by evaluating the height difference as a stereoscopic pair using a photogrammetric plotter[7].

Comparative Techniques

The reliability of these devices is limited to a given class of surface topography. Comparative devices are relatively inexpensive and are quick to apply. One comparative method is a friction test where a tactile test is performed to measure the average slope. Electrostatic techniques are employed by using two metal plates to form a capacitor. The capacitance is given by:

$$C = \frac{K\varepsilon_a A}{t_a} \qquad \text{(C.1)}$$

Where C is the capacitance, t_a is the thickness of the air gap between the plates, A is the area of the smaller plane, ε_a is the permittivity of air and K is a constant. A free electrode is passed over a rough surface and the capacitance is measured. The value t_a provides the value for surface roughness assessment.

A pneumatic method which uses air gauging can assess the flow of air through a gap between a specimen surface and an open ended nozzle placed facing down on it.

The inductance of a coil varies as its separation from a magnetic material is changed. The specimen must be magnetic and deviations in the homogeneous nature of the material may affect the readings[Z7].

Optical Devices

Three Dimensional Optical Profilometer

This device uses a Michelson interferometer that is capable of a lateral resolution of 0.4 μm and a vertical resolution as small as 0.1 nm. This optical profiler consists of a microscope, an interferometer, a detector array, interface electronics, and a computer[30]. It is not feasible to use this device for in-process or on-line surface monitoring due to the current system interface.

Non-Parameteric Optical Techniques

A Foucault knife probe takes a point source of light from an image and as the object is moved the knife will interrupt part of the light beam. The speed is about 10 minutes to take a profile of 1mm long (or 6mm per hour). The results are inaccurate for a slope of over 15^0.

Another method is the defect focus method where an image of a point source used as the exploration spot is focused in the plane of the sample surface. As the specimen is moved its surface roughness leads to a defect of focus. The spot size variation is proportional to the defect of focus.

Light sectioning is a non-destructive analogue of the process of taper sectioning where a microscope is used to examine a section cut through a specimen at a shallow angle to magnify height variations.

Intensity feedback uses an optical device which records surface roughness by monitoring the intensity of a spot of light reflected from a surface.

Interference microscopy uses two slightly inclined glass plates that are illuminated by a coherent monochromatic light source, a series of parallel light and dark bands will be visible when viewed from above. If the bottom plate is a reflective specimen then the top plate will form a reference plane for the specimen. The interference between the light beams from the surface will generate a contour pattern of the surface irregularities[8].

Parameteric Optical Techniques

Three basic optical phenomena are used to assess the surface topography. They are speckle, scattering, and polarization.

Measurement of roughness using scattered beams can be classified according to the component of the beam that is recorded.

1. Specular beam
2. Diffuse beam
3. Total scatter
4. Angular distribution

When a collimated beam of light is reflected from a plane conduction surface, all the light remains in a collimated beam known as the specular beam. If the surface is rough, light is scattered into a distribution of angles. In general as the roughness increases less light is scattered along the specular direction.

As surface roughness increases, the pattern of the scattered radiation tends to become more diffuse. Measuring the total intensity of diffusely scattered light, a technique known as the total integrated scatter method has been used to assess the roughness of surfaces with an R_q of up to .01μm.

The angular distribution of light scattered from a rough surface directly maps the power spectral density of light scattered from a rough surface. The advantage of angular distribution measurements over other forms of scatter measurement is that they supply spatial data as well as height information about surface roughness[8].

When a rough surface is illuminated by coherent light, random patterns of bright and dark regions can be observed in the reflected beam. This phenomenon is known as speckle. The spatial distribution and contrast of speckle patterns is dependent upon the roughness. There are three main types of speckle measurement:

1. monochromatic speckle contrast
2. polychromatic speckle contrast
3. speckle pattern correlation

Appendix D

Windows C++ Vision Program

D.1 Demo.cpp

```
//demo.cpp
#include <windows.h>
#include <stdio.h>
#include <string.h>
#include <ctype.h>
#include <dos.h>
#include <direct.h>
#include <limits.h>
#include <stdlib.h>
#include <commdlg.h>
#include "\app\image\cx100\wcx.h"
#include "demo.h"

 /*---------------------------------------------------------------------
       This button structure is used to create the function buttons as child
       windows. There are other ways to do this. We figured this would be the
       best way to do it for our example.
       ---------------------------------------------------------------------*/
typedef struct tagBUTTON {
 HWND hwnd;
 long style;
 char *text;
 int id;
} BUTTON;

 /*---------------------------------------------------------------------
 These values are used to control the processing of the WM_COMMAND message.
       ---------------------------------------------------------------------*/
#define ID_ACQUIRE   101
#define ID_STOP      102
#define ID_WRITE     103
#define ID_READ      104
#define ID_EXIT      105
#define ID_INC                  106
#define ID_DEC                  107
#define ID_IDLE          108
```

```
BUTTON Functions[] = {
 {NULL, BS_PUSHBUTTON, "Acquire   ", ID_ACQUIRE},
 {NULL, BS_PUSHBUTTON, "Stop      ", ID_STOP},
 {NULL, BS_PUSHBUTTON, "Write File", ID_WRITE},
 {NULL, BS_PUSHBUTTON, "Read File ", ID_READ},
 {NULL, BS_PUSHBUTTON, "Increase  ", ID_INC },
 {NULL, BS_PUSHBUTTON, "Decrease  ", ID_DEC },
 {NULL, BS_PUSHBUTTON, "Idle Graph", ID_IDLE},
 {NULL, BS_PUSHBUTTON, "Exit      ", ID_EXIT},
};

 /*------------------------------------------------------------------------
 Palette and line buffer control variables. Information is moved from the
 frame grabber in a buffer, linedata[], which has a bunch of Windows GDI
 stuff attached to it so it can be used with Windows bitblit functions.
 convert[] is an array used for palette remapping, which gets done
 explicitly by paletteview() rather than internally by the Windows GDI
        ------------------------------------------------------------------------*/
static unsigned char convert[256];
static HBITMAP hline;
static HDC linecontext,windowcontext;
static unsigned char linedata[640];
static HPALETTE hpalette;
static float ToleranceRate=1, Tolerance=0 ;
static unsigned long int number=0;
static float fMean=0,
FraDim=0,Lacunarity=0,fVar=0,fAverage=0,fLac=0,omega2=0, slope=0;
static float fnormdev = 0, Ra = 0, fskew = 0;

int display_surface(HWND );
unsigned long int  display_histogram(
HWND,PAINTSTRUCT*);//,HDC,PAINTSTRUCT* );
int display_data(HWND,HDC,PAINTSTRUCT*);
//int display_data(HWND hWnd);
LRESULT FAR PASCAL _export WndProc(HWND ,UINT ,WPARAM
,LPARAM );
void ReadFile(HWND);
void WriteFile(HWND);
void InitializeFileSave(HWND);
void cleanupview(HWND);
void setupview(HWND);
void paletteview(HWND);
void redrawview(HWND,PAINTSTRUCT *);
```

```
int Do_Cal(HWND);//, float&, float&, float&, float&, unsigned long int&, float&,
float&, float&,float&, float&);

 /* text data for drawing text */
static TEXTMETRIC tm;                   /* text metric structure */
static short    cxChar,                 /* average character width */
                                        cxCaps,                 /* capital
height */
                                        cyChar;                 /*
character height */

static int SCALE=0;
static int ButtonHeight, ButtonWidth;
static int viewoffset;

static char szAppName[] = "Video" ;
static char *WriteErr = "Stop acquiring an image before writing a file";
static char *ReadErr = "Stop acquiring an image before reading a file";

/*------------------------------< file data >------------------------------*/
static OPENFILENAME rfn,sfn;
static char szFilterSel[] = "Binary files (*.bin)\0*.bin\0\
All Files (*.*)\0*.*\0";

//#define MAXPATH 128
#define MAXDIR  66
#define MAXEXT  5
static char szReadFileName[MAXPATH];
static char szSaveFileName[MAXPATH];
static char szReadFileTitle[MAXPATH];
static char szSaveFileTitle[MAXPATH];
static char szReadFileDir[MAXDIR]="";
static char szSaveFileDir[MAXDIR]="";
static char szReadExt[MAXEXT]="bin";
static char szSaveExt[MAXEXT]="bin";

static int acquiring, G_idle;

/*****************************************************************
***********
 * Name:        WinMain                                    *
 * Description:  Main window program and message processing loop.        *
```

```
**********************************************************************
**********/
int PASCAL WinMain(HANDLE hInstance, HANDLE hPrevInstance,
                   LPSTR lpszCmdParam, int nCmdShow)
{
HWND   hwnd;
MSG    msg;
WNDCLASS  wndclass;
LPSTR err;

 /*-------------------------------------------------------------------
 initialize the library and reset The CX100 to put it in a known state
 -------------------------------------------------------------------*/
 err = init_library();
 if(err != NULL) {
        MessageBox(0, err, szAppName, MB_ICONSTOP);
        return(0);
 }
 reset_cx();
 acquiring = TRUE;
 G_idle = TRUE;

 /* if no previous instance, register window class */

 memset(&wndclass,0,sizeof(wndclass));       /* clear stack variable */
 memset(&msg,0,sizeof(msg));

 if(!hPrevInstance) {
        wndclass.style         = CS_HREDRAW | CS_VREDRAW;
        wndclass.lpfnWndProc   = WndProc;
        wndclass.cbClsExtra    = 0;
        wndclass.cbWndExtra    = 0;
        wndclass.hInstance     = hInstance;
        wndclass.hIcon         = NULL;
        wndclass.hCursor       = LoadCursor (NULL, IDC_ARROW);
        wndclass.hbrBackground = GetStockObject (WHITE_BRUSH);
        wndclass.lpszMenuName  = NULL;
        wndclass.lpszClassName = szAppName;

        RegisterClass (&wndclass);
 }
```

```
/* create window */

hwnd = CreateWindow (szAppName,              // window class name
                "ADML",  // window caption
                WS_OVERLAPPEDWINDOW,                 // window style
                CW_USEDEFAULT,                  // initial x position
                CW_USEDEFAULT,                  // initial y position
                CW_USEDEFAULT,                  // initial x size
                CW_USEDEFAULT,                  // initial y size
                NULL,                          // parent window handle
                NULL,                          // window menu handle
                hInstance,                     // program instance handle
                NULL);                          // creation parameters

/* display window and generate WM_CREATE and WM_PAINT messages */

InitializeFileSave(hwnd);
ShowWindow(hwnd, nCmdShow);
UpdateWindow(hwnd);

/* message processing loop */

while(1) {
        while(PeekMessage(&msg, NULL, 0, 0,PM_REMOVE)) {
                if(msg.message == WM_QUIT)
                  break;
                TranslateMessage(&msg);
                DispatchMessage(&msg);
        }
        if(msg.message == WM_QUIT)
                break;
        if(acquiring) {
                grab();
         //     redrawview(hwnd,NULL);
                Do_Cal(hwnd);
                if (G_idle) display_histogram(hwnd,NULL);
                display_surface(hwnd);
        }
}
exit_library();
return msg.wParam;
}
```

```
/*****************************************************************
***********
 * Name:       WndProc                                    *
 * Description:  Main window procedure.                        *

*****************************************************************
**********/
LRESULT FAR PASCAL _export  WndProc(HWND hwnd, UINT message,
WPARAM wParam, LPARAM lParam)
{
static int i;
static RECT rect;
static HDC hdc;
static PAINTSTRUCT    ps;
static int Width, Height;
static LPSTR err;
static char st[80];

 switch (message) {

        case WM_CREATE:
                hdc = GetDC (hwnd);
                SelectObject(hdc, GetStockObject(SYSTEM_FONT));
                GetTextMetrics (hdc, &tm);
                cxChar = tm.tmAveCharWidth;
                cxCaps = (tm.tmPitchAndFamily & 1 ? 3 : 2) * cxChar / 2;
                cyChar = tm.tmHeight + tm.tmExternalLeading;
                ReleaseDC (hwnd, hdc);
                Width = 1080; //640;
                Height = 770;  //480;
                ButtonHeight = 4*cyChar/3;
                viewoffset=ButtonHeight;
                ButtonWidth =1080/8;

        SetWindowPos(hwnd,NULL,0,0,Width,Height,SWP_SHOWWINDOW);

                /*-------------------------------------------------------------
                create 5 function buttons as child windows
                 -------------------------------------------------------------*/
                for(i=0; i<8; i++) {
                 Functions[i].hwnd = CreateWindow("button", Functions[i].text,
                        WS_CHILD | WS_VISIBLE | Functions[i].style,
                        ButtonWidth*i, 0,
```

```
                ButtonWidth, ButtonHeight,
                hwnd, Functions[i].id,
                ((LPCREATESTRUCT)lParam)->hInstance, NULL);
        }
        setupview(hwnd);
        paletteview(hwnd);
 //  display_histogram(hwnd);
 //     display_surface(hwnd);
        return 0L;

 case WM_SIZE:
        return 0L;

 case WM_PALETTECHANGED:
  // display_surface(hwnd);
  // display_histogram(hwnd);
        paletteview(hwnd);
        return 0L;

 case WM_PAINT:
        hdc=BeginPaint(hwnd,&ps);

        //display_surface(hwnd);
        EndPaint(hwnd,&ps);
        if(!acquiring)
        {
        if (!G_idle) display_histogram(hwnd,&ps);
        redrawview(hwnd,&ps);
        }
        return 0L;

 case WM_ACTIVATE:
        if(lParam >> 16) {
          SCALE=4;
          viewoffset=0;
        }
        else {
          SCALE=0;
          viewoffset=ButtonHeight;
        }
        Do_Cal(hwnd);
 //     display_histogram(hwnd);
        //display_surface(hwnd);
```

```
            //paletteview(hwnd);
            break;

        case WM_COMMAND:
            switch(wParam) {
             default:
             break;

             case ID_ACQUIRE:
                    acquiring = TRUE;
                    G_idle = TRUE;
                    InvalidateRect(hwnd,NULL,FALSE);
                    break;

             case ID_STOP:
                    acquiring = FALSE;
                    G_idle = FALSE;
                    break;

             case ID_IDLE:
                    G_idle = FALSE;
                    break;

             case ID_WRITE:
                    if(acquiring) {
                           MessageBox(hwnd, WriteErr, szAppName,
MB_OK);
                    }
                    else {
                           WriteFile(hwnd);
                    }
                    break;

             case ID_INC:
                           if(ToleranceRate<4)
                                  ToleranceRate +=0.5;
                           break;

             case ID_DEC:
                           if(ToleranceRate >0.5)
                                  ToleranceRate -=0.5;
                           break;
```

```
                case ID_READ:
                        if(acquiring) {
                                MessageBox(hwnd, ReadErr, szAppName, MB_OK);
                        }
                        else {
                                ReadFile(hwnd);
                                InvalidateRect(hwnd,NULL,FALSE);
                        }
                        break;

                case ID_EXIT:
                        SendMessage(hwnd, WM_DESTROY, 0, 0L);
                        break;

                }
                return 0L;

        case WM_DESTROY:
                cleanupview(hwnd);
                PostQuitMessage(0);
                return 0L;
 }
 return(DefWindowProc(hwnd, message, wParam, lParam));
}
/*****************************************************************
***********
 * Name:        setupview                                  *

*****************************************************************
**********
 | Constructing a grayscale palette, arranged in order of importance. If you |
 | take the first 2^n entries, you get a palette which provides a 2^n tone   |
 | grayscale stretching from black to white. This is done because there is   |
 | no guarantee that Windows will let us have all the colors we ask for.     |

*****************************************************************
**********/
void setupview(HWND handle)
{
struct mypalette {
  WORD version;
  WORD number;
```

```
 PALETTEENTRY palette[256];
} pal;

int i,j,c;

 for(i=0; i<256; i++) {
        c=0;
        for(j=0; j<8; j++)
                if(i & (1<<j))
                  c|=(0x80>>j);
        pal.palette[i].peRed=c;
        pal.palette[i].peGreen=c;
        pal.palette[i].peBlue=c;
        pal.palette[i].peFlags=0;
 }
 pal.version=0x300;
 pal.number=256;
 hpalette=CreatePalette((LOGPALETTE far *)&pal);
 hline=CreateBitmap(640,1,1,8,(LPSTR)linedata);
}
/*************************************************************************
***********
 * Name:        paletteview                                    *

*************************************************************************
**********
 | This function manually remaps the palette.  This must be done because we  |
 | are constructing a bitmap directly, rather than drawing to it, so we need |
 | to know the actual palette rather than just Windows' virtual palettes. We |
 | get the mapping by using Windows to write a grayscale, then reading it    |
 | back as a bitmap.  This tells us what to put in a bitmap in order to have |
 | Windows render it as a grayscale.                                         |

*************************************************************************
**********/
void paletteview(HWND handle)
{
int i;

 windowcontext=GetDC(handle);
 SelectPalette(windowcontext,hpalette,0);
 RealizePalette(windowcontext);
 linecontext=CreateCompatibleDC(windowcontext);
```

```
 SelectObject(linecontext,hline);
 SelectPalette(linecontext,hpalette,0);
 RealizePalette(linecontext);

 for(i=0; i<256; i++)
        SetPixel(linecontext,i,0,PALETTERGB(i,i,i));

 GetBitmapBits(hline,256,(LPSTR)convert);

 ReleaseDC(handle,windowcontext);
 DeleteDC(linecontext);
}

/*****************************************************************
***********
 * Name:      redrawview                                    *

*****************************************************************
**********/
void redrawview(HWND handle,PAINTSTRUCT *ps)
{
int x,y;

 windowcontext = GetDC(handle);
 linecontext = CreateCompatibleDC(windowcontext);
 SelectObject(linecontext,hline);

 ram_on();
 for(y=0; y<(480>>SCALE); y++) {
        set_page(y>>(7-SCALE));
        for(x=0; x<(512>>SCALE); x++)
               linedata[x]=convert[videoram[(x<<SCALE)+(y<<(SCALE+9))]];
        SetBitmapBits(hline,512,(LPSTR)linedata);
        StretchBlt(windowcontext,0,y+viewoffset,440>>SCALE,1,
               linecontext,40,0,440>>SCALE,1,SRCCOPY);
 }
 ram_off();
 display_data(handle,windowcontext, ps);
 //display_histogram(handle,windowcontext,ps);
 ReleaseDC(handle,windowcontext);
 DeleteDC(linecontext);
}
```

```
/*****************************************************************
***********
 * Name:        cleanupview                                      *

*****************************************************************
**********/
void cleanupview(HWND handle)
{
 DeleteObject(hline);
}
/*****************************************************************
***********
 * Name:        ReadFile                                         *

*****************************************************************
**********/
void ReadFile(HWND hwnd)
{
int i, j, hFile;
HCURSOR hCursor;

 if(GetOpenFileName(&rfn)) {
        hFile = _lopen(rfn.lpstrFile, OF_READWRITE);
        hCursor = SetCursor(LoadCursor(NULL, IDC_WAIT));
        ShowCursor(TRUE);
        read_file_to_ram(hFile);
        ShowCursor(FALSE);
        SetCursor(hCursor);
        _lclose(hFile);
        lstrcpy((LPSTR)szReadFileDir,(LPSTR)szReadFileName);
        j = lstrlen((LPSTR)szReadFileDir);
        for(i=j; i>0; --i) {
                if(szReadFileDir[i] != '\\') {
                  szReadFileDir[i] = '\0';
                }
                else {
                  if(szReadFileDir[i-1] != ':')
                        szReadFileDir[i] = '\0';
                  break;
                }
        }
        lstrcpy((LPSTR)szReadFileName,(LPSTR)szReadFileTitle);
 }
```

```
 else {
  }
}
/*****************************************************************
***********
 * Name:        WriteFile                                        *

*****************************************************************
**********/
void WriteFile(HWND hwnd)
{
int i, j, hFile, ret;
OFSTRUCT ofs;
HCURSOR hCursor;
static char *szWriteError = \
"An error was encountered writing data to the file.\n\
The file is incomplete and the data is invalid.";
static char *szComplete = \
"The file was written successfully.";

 if(GetSaveFileName(&sfn)) {
        hFile = OpenFile(sfn.lpstrFile, &ofs, OF_CREATE | OF_WRITE);
        if(hFile == -1) {
                MessageBox(hwnd, "Cannot open file", szAppName, MB_OK);
                return;
        }
        hCursor = SetCursor(LoadCursor(NULL, IDC_WAIT));
        ShowCursor(TRUE);
        ret = write_ram_to_file(hFile);
        ShowCursor(FALSE);
        SetCursor(hCursor);
        _lclose(hFile);
        if(ret != 0) {
                MessageBox(hwnd, szWriteError, szAppName, MB_OK);
        }
        else {
                MessageBox(hwnd, szComplete, szAppName, MB_OK);
                lstrcpy((LPSTR)szSaveFileName,(LPSTR)szSaveFileTitle);
                lstrcpy((LPSTR)szSaveFileDir,(LPSTR)ofs.szPathName);
                j = lstrlen((LPSTR)szSaveFileDir);
                for(i=j; i>0; --i) {
                  if(szSaveFileDir[i] != '\\') {
                        szSaveFileDir[i] = '\0';
```

```
                }
                else {
                        if(szSaveFileDir[i-1] != ':')
                                szSaveFileDir[i] = '\0';
                        break;
                }
               }
        }
 }
}
/*****************************************************************
***********
 * Name:        InitializeFileSave                                *
 * Description:  Initialize the file open/save structures              *

*****************************************************************
**********/
void InitializeFileSave(HWND hwnd)
{
 rfn.lpstrTitle = "Read an Image from a File";
 rfn.Flags = OFN_PATHMUSTEXIST | OFN_FILEMUSTEXIST;
 rfn.lStructSize = sizeof(OPENFILENAME);
 rfn.hwndOwner = hwnd;
 rfn.lpstrFilter = szFilterSel;
 rfn.nMaxCustFilter = 0;
 rfn.nFilterIndex = 1l;
 rfn.nMaxFile = MAXPATH;
 rfn.nMaxFileTitle = MAXPATH;
 rfn.lpstrFile = szReadFileName;
 rfn.lpstrInitialDir = szReadFileDir;
 rfn.lpstrFileTitle = szReadFileTitle;
 rfn.lpstrDefExt = szReadExt;

 sfn.lpstrTitle = "Save Image in File";
 sfn.Flags = OFN_OVERWRITEPROMPT | OFN_HIDEREADONLY;
 sfn.lStructSize = sizeof(OPENFILENAME);
 sfn.hwndOwner = hwnd;
 sfn.lpstrFilter = szFilterSel;
 sfn.nMaxCustFilter = 0;
 sfn.nFilterIndex = 1l;
 sfn.nMaxFile = MAXPATH;
 sfn.nMaxFileTitle = MAXPATH;
 sfn.lpstrFile = szSaveFileName;
```

```
 sfn.lpstrInitialDir = szSaveFileDir;
 sfn.lpstrFileTitle = szSaveFileTitle;
 sfn.lpstrDefExt = szSaveExt;
}

int Do_Cal(HWND hwnd)//, float &fra_dim , float &lacunarity, float &fVar, float
&fRoughAvg, unsigned long int &number, float &fLac, float &omega2, float
&slope, float &tolerance, float &fMean)
{
        static unsigned long int xStart = 130, yStart = 130, Length = 256, Width =
256;

        int histogram[256]={0};
        unsigned long int sum, limit=Length*Width ;
        DWORD dlen;
        HANDLE hbuf;
        BYTE huge *buf=0;
        LPSTR err;

        dlen = 512l * 512l;
        if(status(LOW_RESOLUTION))
                dlen = 256l * 256l;
//-----------------------------------------------------------------------
// Allocate a buffer big enough for the whole video RAM
// -----------------------------------------------------------------------
        hbuf = GlobalAlloc( GMEM_FIXED, dlen);
        if(hbuf == NULL)
        {
                MessageBox(hwnd, "Cannot allocate buffer", "display", MB_OK);
                return 0;
        }
        buf = GlobalLock(hbuf);
        grab();
        get_rectangle(hbuf,xStart,yStart,Length,Width);


        get_histogram(buf,limit,histogram);
        sum=get_sum(buf,limit);

        Lacunarity=Get_Lacunarity(buf,Length, Width);

        FraDim=FDim3(sum,ifqmin(histogram),ifqmax(histogram));
```

```
        fMean = sum/pow(Length,2);
        fVar = get_var(buf,fMean, limit);
        fLac = (fVar+pow(fMean,2)-pow(fMean,2))/pow(fMean,2); //?????

        fAverage =  get_mean_rou(buf,fMean,limit);
        float fStdev=pow(fVar,0.5);
  fskew = get_skew(buf,fMean,fVar,limit);
        omega2=fMean*fStdev/1000;
        Ra = (-.9968*pow(omega2,3))+(4.4755*pow(omega2,2))-
(3.6281*omega2)+1.1483;
  fnormdev = Deviation(histogram, fMean, fVar);
        slope = get_slope(buf,Length);
        Tolerance = fMean + ToleranceRate *fStdev;

        GlobalUnlock(hbuf);
        GlobalFree(hbuf);
        return 1;
}

int display_data(HWND hWnd, HDC hDC, PAINTSTRUCT *ps)
{
                int tmp=strlen("Fractal Dimemson:"), sig=4, i = 470;
                char str[25];
                HBRUSH hBrush;

          //    hBrush = CreateSolidBrush(RGB(100,100,120));
                hBrush = CreateSolidBrush(RGB(255,255,255));
                SelectObject(hDC, hBrush);
                Rectangle(hDC,0,505,440,770);

                SetTextColor(hDC, RGB(0, 100, 190));

                TextOut( hDC, 50, i+40, "Fractal Dimemson:", tmp);
                TextOut( hDC, 220,i+40, "=", 1) ;
                gcvt(FraDim,sig,str);
                TextOut(hDC,240, i+40, str , strlen(str));

                TextOut( hDC, 50, i+60, "Lacunarity:     ", tmp);
                TextOut( hDC, 220, i+60, "=", 1) ;
                gcvt(Lacunarity,sig, str);
                TextOut(hDC, 240, i+60, str , strlen(str));

                TextOut( hDC, 50, i+80, "fVar:          ", tmp);
```

```
TextOut( hDC, 220, i+80, "=", 1) ;
gcvt(fVar,sig, str);
TextOut(hDC, 240, i+80, str , strlen(str));

TextOut( hDC, 50, i+100, "fRoughAvg:      ", tmp);
TextOut( hDC, 220, i+100, "=", 1) ;
gcvt(fAverage,sig, str);
TextOut(hDC, 240, i+100, str , strlen(str));

TextOut( hDC,  50, i+120, "fLac:          ", tmp);
TextOut( hDC, 220, i+120, "=", 1) ;
gcvt(fLac,sig, str);
TextOut(hDC, 240, i+120, str , strlen(str));

TextOut( hDC,  50,i+140, "Omega2:         ", tmp);
TextOut( hDC, 220,i+140, "=", 1) ;
gcvt(omega2,sig, str);
TextOut(hDC, 240,i+140, str , strlen(str));

TextOut( hDC,  50,i+160, "Slope:          ", tmp);
TextOut( hDC, 220,i+160, "=", 1) ;
gcvt(slope,sig, str);
TextOut(hDC, 240,i+160, str , strlen(str));

TextOut( hDC,  50,i+180, "Ra(micrometers):      ", tmp);
TextOut( hDC, 220,i+180, "=", 1) ;
gcvt(Ra,2, str);
TextOut(hDC, 240,i+180, str , strlen(str));

TextOut( hDC,  50,i+200, "Tolerance:      ", tmp);
TextOut( hDC, 220,i+200, "=", 1) ;
gcvt(Tolerance,sig, str);
TextOut(hDC, 240,i+200, str , strlen(str));

TextOut( hDC,  50,i+220, "Skewness:       ", tmp);
TextOut( hDC, 220,i+220, "=", 1) ;
gcvt(fskew,sig, str);
TextOut(hDC, 240,i+220, str , strlen(str));

TextOut( hDC,  50,i+240, "Norm Dev:       ", tmp);
TextOut( hDC, 220,i+240, "=", 1) ;
gcvt(fnormdev,sig, str);
TextOut(hDC, 240,i+240, str , strlen(str));
```

```
            DeleteObject(hBrush);

}

unsigned long int  display_histogram( HWND hWnd,PAINTSTRUCT *ps )//,HDC
hDC, PAINTSTRUCT *ps)
{
        static HDC hDC;
        //static PAINTSTRUCT ps;
        HPEN hPen,hPenDash,hPenGreen;
        HBRUSH hBrush;
        int index=0, i=0, row=0, col=0, bottom=200, work[255]={0};
        int histogram[256]={0} ;

        static unsigned long int xStart = 130, yStart = 112, Length = 256, Width =
256;
        DWORD dlen;
        HANDLE hbuf;
        BYTE huge *buf=0;
        LPSTR err;
        unsigned long int L_index, sum, limit=Length*Width ;

        dlen = 512l * 512l;
        if(status(LOW_RESOLUTION))
                dlen = 256l * 256l;
 //---------------------------------------------------------------------
 // Allocate a buffer big enough for the whole video RAM
 // ---------------------------------------------------------------------
        hbuf = GlobalAlloc( GMEM_FIXED, dlen);
        if(hbuf == NULL)
        {
                MessageBox(hWnd, "Cannot allocate buffer", "display", MB_OK);
                return 0;
        }
        buf = GlobalLock(hbuf);
        grab();
        get_rectangle(hbuf,xStart,yStart,Length,Width);

        get_histogram(buf,limit,histogram);
        hDC=GetDC(hWnd);
        //hDC = BeginPaint(hWnd, &ps);
        hPen = CreatePen(PS_SOLID,3,RGB(255,0,0) );
        hPenDash=CreatePen(PS_DASH,1,RGB(0,0,255));
```

```
        hBrush = CreateSolidBrush(RGB(123,45,100));
        //hBrush = CreateSolidBrush(RGB(255,255,255));
/*
        SelectObject(hDC, hBrush);
        Rectangle(hDC,440,viewoffset,1080,770);


        SetViewportOrg(hDC, 690, 480);
        SelectObject(hDC,hPen);
        for (index=0; index<=255; index++)
                {
                MoveTo(hDC,index, bottom);
                LineTo(hDC,index ,bottom-histogram[index]/40);
                }

        MoveTo(hDC,0,80);
        LineTo(hDC,0,bottom);
        MoveTo(hDC, 0, bottom);
        LineTo(hDC, index+4, bottom);

        TextOut(hDC, 0,bottom+4, "(0,0)", 5);
        TextOut(hDC, index,bottom+4, "(255,0)",7);
        TextOut(hDC, -10,40,"(0,4800)",8);

*/
        hPenGreen = CreatePen(PS_SOLID,1,RGB(0,250,0) );


        SetViewportOrg(hDC, 500,250);
        SelectObject(hDC,hPenGreen);

        for (L_index=0; L_index<Length*Width; L_index +=256)
        {
                for (int i=0; i<=255 ; i++)
                {
                        work[i]=buf[L_index+i];
                };

                int col = (L_index/256); int row=(L_index/256);
                i = 0;
                MoveTo(hDC, i+row,col-work[i]);
                for (i=0; i<255; i+=15 )
```

```
                {
        //      LineTo(hDC,i+row,col-100);
                if (work[i]>(fMean+Tolerance))
                        SelectObject(hDC,hPenDash);
                else
                        SelectObject(hDC,hPenGreen);
                LineTo(hDC,i+row,col-work[i]);
                };
        };

        SetViewportOrg(hDC,500,120);
        SelectObject(hDC, hPenDash);
        MoveTo(hDC,0,0);
        LineTo(hDC,215,0);
        LineTo(hDC,255+255,255);
        MoveTo(hDC,0,0);
        LineTo(hDC,255,255);
        LineTo(hDC,255+255,255);



        GlobalUnlock(hbuf);
        GlobalFree(hbuf);
        DeleteObject(hPen);
        DeleteObject(hPenDash);
        DeleteObject(hBrush);
        DeleteObject(hPenGreen);
        ReleaseDC(hWnd,hDC);

}


int display_surface(HWND hWnd)
{
        HDC hDC;
        PAINTSTRUCT ps;
        HPEN hPen;
        int work[255]={0};

        static unsigned long int xStart = 130, yStart = 130, Length = 256, Width =
256;
        DWORD dlen;
        HANDLE hbuf;
```

```
        BYTE huge *buf=0;
        LPSTR err;
        unsigned long int index=0, limit=Length*Width ;

        dlen = 512l * 512l;
        if(status(LOW_RESOLUTION))
                dlen = 256l * 256l;
//-----------------------------------------------------------------------
// Allocate a buffer big enough for the whole video RAM
// -----------------------------------------------------------------------
        hbuf = GlobalAlloc( GMEM_FIXED, dlen);
        if(hbuf == NULL)
        {
                MessageBox(hWnd, "Cannot allocate buffer", "display", MB_OK);
                return 0;
        }
        buf = GlobalLock(hbuf);
        grab();
        get_rectangle(hbuf,xStart,yStart,Length,Width);

        hDC = BeginPaint(hWnd, &ps);
        hPen = CreatePen(PS_SOLID,1,RGB(0,255,0) );
        SetViewportOrg(hDC, 50, 50);//640,30);
        SelectObject(hDC,hPen);

        for (index=0; index<Length*Width; index +=256)
        {
                for (int i=0; i<=255 ; i++)
                {
                        work[i]=buf[index+i];
                };

                int col = 120+(2*index/256); int row=(index/256);
                i = 0;
                MoveTo(hDC, i+row,col-work[i]);
                for (i=0; i<=255; i++)
                {
                LineTo(hDC,2*i+row,col-work[i]);
                };
        };

        GlobalUnlock(hbuf);
        GlobalFree(hbuf);
```

```
        DeleteObject(hPen);
        ReleaseDC(hWnd,hDC);
        EndPaint(hWnd, &ps);
}
```

D.2 Demo.h

```
// demo.h
#include <math.h>

LRESULT FAR PASCAL _export WindowFunc (HWND      hWnd,
                                                                UINT
message,

WPARAM    wParam,

LPARAM    lParam);


unsigned long int get_sum(BYTE huge *buf, unsigned long int limit)
{
        unsigned long int sum = 0;
        for ( unsigned long int i=1; i<= limit; i++)
                sum += buf[i];
        return sum;
}


//int* get_histogram(BYTE huge *buf, unsigned long int limit)
int get_histogram(BYTE huge *buf, unsigned long int limit, int gram[256] )
{
        gram[256]=0;
        unsigned long int i=0;
        for (i; i<limit; i++)
                ++gram[buf[i]];
}

int ifqmin(int *iHistogram){
        int ifreqmin = 0;
        for (int iCnt4 = 0; iCnt4 <= 255; iCnt4++){
                if (iHistogram[iCnt4] >= 100){
                        ifreqmin = iCnt4;
                        break;
                }
```

```
        }
        return ifreqmin;
}

// Find relevant frequency max
int ifqmax(int *iHistogram){
        int ifreqmax = 0;
        for (int iCnt4 = 255; iCnt4 >= 0; iCnt4--){
                if (iHistogram[iCnt4] >= 100){
                        ifreqmax = iCnt4;
                        break;
                }
        }
        return ifreqmax;
}

//Calculate deviation between surface and equivalent Gaussian surface
float Deviation(int *iHistogram, float mean, float fVar)
{
        float gdiff = 0;
        for (int x = 0; x <=255; x++){
                float gauss = 65536*(1/(pow((fVar*2*3.14159),0.5)))*exp((-
0.5)*(pow(((x-mean)/pow(fVar,.5)),2)));// the function.
                gdiff += abs(gauss-iHistogram[x]);
        }
        return (gdiff/255);
}

float FDim3(unsigned long int fSum, int ifreqmin, int ifreqmax){
        float fFracDim3 = 0.0f;
        fFracDim3 = (log10(fSum-(256.0f*256.0f*ifreqmin)))/(log10(256.0f-
ifreqmin));
        return fFracDim3;
}

float Get_Lacunarity(BYTE huge *buf, unsigned long int Length, unsigned long int
Width)
{
        unsigned long int  fSum = 0, ulSumTot = 0;
        float flamdaA = 0.0f, flamdaB = 0.0f;
        unsigned long int ulCountOne = 0;
        float flacA = 0.0f, flacC = 0.0f, flacB = 0.0f;
```

```
// Lacunarity using 3x3 box without ANY!!!!!! overlap

        fSum = get_sum(buf, Length*Length);
        for(unsigned long int iCntA = Length+1; iCntA < Length*(Length-1); iCntA
+= Length*3)
        {
                for(unsigned long int iCnt2 = iCntA ;iCnt2 <= (iCntA + Length-4);
iCnt2 += 3)
                {
                        ulCountOne += 1;
                        for (unsigned long int iVal = Length-1; iVal <= Length+1;
iVal++)
                                if (buf[iCnt2] <= buf[iCnt2-iVal])ulCountOne++;

                        if (buf[iCnt2] <= buf[iCnt2-1])ulCountOne++;
                        if (buf[iCnt2] <= buf[iCnt2+1])ulCountOne++;

                        for (iVal = Length-1; iVal <= Length+1; iVal++)
                                if (buf[iCnt2] <= buf[iCnt2+iVal])ulCountOne++;

                        flamdaA += ulCountOne/9.F;
                        flamdaB += pow((1.0f-(ulCountOne/9.F)),2);
                        ulCountOne = 0;
                        ulSumTot++;
                }
        } // end of lacunarity 3x3 without ANY!!!!! overlap

        flacA = flamdaA/((float)ulSumTot);
        flacB = flamdaB/((float)ulSumTot); //Mandelbrot
        flacC = (flacA-
(fSum/(256.F*256.F*256.0f)))/(flacA+(fSum/(256.F*256.F*256.0f))); // KCC
        return flacB;
}

float get_var(BYTE huge *buf, float mean, unsigned long int limit)
{
        float fVar=0;
        for (unsigned long int i =0; i<=limit; i++)
                fVar +=pow(buf[i]- mean, 2)/limit;
        return fVar;
}

float get_mean_rou(BYTE huge *buf, float mean, unsigned long int limit)
```

```
{
        float roughtness =0;
        for (unsigned long int i=0; i<=limit; i++)
                roughtness +=(fabs(buf[i]-mean));
        return (roughtness/limit);
}

float get_skew(BYTE huge *buf, float mean, float fVar, unsigned long int limit)
{
        float skew =0;
        for (unsigned long int i=0; i<=limit; i++)
                skew +=(pow((buf[i]-mean),3))/(pow(fVar,1.5));
        return (skew/limit);
}

int get_box(BYTE huge *buf, int **box, unsigned long int col, unsigned long int
row, unsigned long int size, int length)
{
        unsigned long int index =0, i , j, tmp2;
        //box={};
        for(i=0; i<size; i++ )
                for (j=0; j<size; j++)
                  {
                  unsigned long int tmp=(row+i)*length+(col+j);
                  int tmp1 = buf[(row+i)*length+(col+j)];
                  box[i][j]=buf[(row+i)*length+(col+j)];
                  buf[(row+i)*length+(col+j)];
                        }
}

int get_num_box(int **box,int size)
{
        int fMax =0, fMin=255, i,j;
        for (i =0; i<=size-1; i++)
                for ( j=0; j<=size-1; j++)
                        {
                                fMax=(box[i][j]>fMax) ? box[i][j] : fMax;
                                fMin=(box[i][j]<fMin) ? box[i][j] : fMin;
                        }
        return ((fMax/size)-(fMin/size) +1);
}

float get_slope(BYTE huge *buf, unsigned long int Length)
```

```
{
        int **box;
        unsigned long int iNumBox[5]={0}, i, j,  size, index=0;
        float fXmatrix[2][5]={{0.80, 0.50, 0.20, -0.10,-0.40},

{0.66438562,0.33219281,0.00,-0.33219281,-0.66438562}};
        float fYmatrix[5]={0}, fFDmatrix[2]={0};


        for(size=2; size<=32; size *=2)
        {
                box = (int**)malloc(sizeof(int*)*size);
                for (i=0; i<size; i++)
                        box[i] = (int*)malloc(sizeof(int)*size);

                        for (i=0; i<Length; i+=size)
                        for (j=0; j<Length; j+=size)
                        {
                        get_box(buf, box,i,j,size,Length);

                                iNumBox[index] += get_num_box(box,size);
                        }

                for (i=0; i<size; i++)
                        free(box[i]);// = (int*)malloc(sizeof(int)*size);
                free(box);
                index++;
        }

        unsigned long int tmp=0;

        for (index=0; index< 5; index++)
        {
                tmp = iNumBox[index];
                fYmatrix[index]= log10(iNumBox[index]);
        }

        for (index=0; index<5; index++)
                fFDmatrix[0] += fXmatrix[0][index]*fYmatrix[index];
        for (index=0; index<5; index++)
                fFDmatrix[1] += fXmatrix[1][index]*fYmatrix[index];

         return fFDmatrix[1];
```

```
}
```

D.3 Demo.def

```
;
;       Program 01 ---- DEMO.DEF
;

NAME   DEMO

DESCRIPTION 'Windows Program'

EXETYPE WINDOWS


CODE DISCARDABLE  PRELOAD
DATA MOVEABLE   MULTIPLE    PRELOAD

HEAPSIZE   1024
STACKSIZE  5120
```

References

[1] Jansson P., Deconvolution: With Applications in Spectroscopy, academic Press, New York, 1984.

[2] Gilsinn, T. Vorburger et al., "Optical Techniques for Industrial Inspection, Vol. 665, 1986.

[3] "Surface Texture (Surface Roughness, Waviness, and Lay)," ANSI/ASME B46.1-1985, American Society of Mechanical Engineers, 1985

[4] Kalpakjian S., "Manufacturing Processes for Engineering Materials," Addison-Wesley, 1992

[5] Jacobs P. F., Stereolithography and Other RP&M Technologies, ASME Press, New York, 1996

[6] Thomas T. R., Ed., "Rough Surfaces," Longman, London, p13, 1982

[7] Sherington I, Smith E. H., "Modern Measurement Techniques in Surface Metrology Part1; Stylus Instruments, Electron Microscopy and Non-Optical Comparators," Wear Journal Vol. 125, 271-288, 1988

[8] Sherington I, Smith E. H., "Modern Measurement Techniques in Surface Metrology Part II; Optical Instruments," Wear Journal Vol. 125, 289-308, 1988

[9] Song J. F., Vorburger T. V., "Surface Texture," Metals Handbook Vol. 18, 1992

[10] Peitgen H., Jurgens H., Saupe D., Fractals for the Classroom, an Introduction to Fractals and Chaos, Springer-Verlag, New York, 1992.

[11] Stout K. J., "Three Dimenisonal Surface Topography; Measurement, Interpretation and Applications," Penton Press, 1994

[12] Larry S. Liebovitch and Tiber Toth, "A Fast Algorithm to Determine Fractal Dimension by Box Counting", Physics Letters A, Volume 141, n8.9, 1989.

[13] Kaye B. H., "A Random Walk Through Fractals; Fractals in the Mining Industry," VCH Publishers, 1989

[14] Peitgen H. O., Saupe D, "The Science of Fractal Images," Springer-Verlag, New York, 1988

[15] Majumdar A., Tien C. L., "Fractal Characterization and Simulation of Rough Surfaces," Wear, 136(1990) 313-327

[16] Twersky V., *On the Scattering and Reflection of Electromagnetic Waves by Rough Surfaces,* Trans. I.R.E. AP-5, 81-90, 1957.

[17] Rice S.O., *Reflection of Electromagnetic Waves From Slightly Rough Surfaces,* Comm. Pure Appl. Math. 4, 351-378, 1951.

[18] Beckman P., Spizzichino A., "The Scattering of Electromagnetic Waves From Rough Surfaces," Ocford:Pergamon, 1963.

[19] Vorburger T., Raja J., "Surface Finish Metrology," NISTIR-4088, U. S. Dept. of Commerce, 1990.

[20] DeVoe D., 1993, "Optical Area Based Surface Quality Assessment for In-Process Measurement", Masters Thesis, University of Maryland, College Park

[21] Jung M. J., Zhang G, "Implementation of an On-Line Surface Monitoring System Roughness Using Image Processing," CIRP Proceedings, 1995

[22] Gopalakrishnan S., "Development of a Prototype System for On-Line Monitoring of Surface Roughness Using Fractal Geometry", Masters Thesis, University of Maryland, College Park

[23] Keller, Chen, Crownover, "Texture Description and Segmentation through Fractal Geometry," Computer Vision, Graphics, and Image Processing, p153-158, 1989

[24] Voss, R. F., Random Fractals: Characterization and Measurement, Physical Scripta T13 (1986) 27-32

[25] Devor R.E., Chang T. H., Sutherland J. W., "Statistical Quality Design and Control," Macmillan Publishing Co., New York, 1992

[26] Snedecor, W., "Statistical Methods", Iowa State University Press, Iowa, 1989

[27] Thuman A., Lighting Efficiency Applications, 1992, The Fairmont Press, Inc.

[28] Awock G. J., "Applied Image Processing", McGraw-Hill Inc., New York, 1996

[29] Vandenberg S., Osborne C. F., "Digital image processing techniques, fractal dimensionality and scale-space applied to surface roughness," Wear, 159 (1992) 17-30

[30] Bhushan, B., et al, A New Three-Dimensional Non-Contact Digital Optical Profiler.

[31] Ennos, A. E., Virdee, M. S., Precision Measurement of Surface Form by Laser Profilometry.